Towards adipose tissue-derived stromal cells-based therapy for diabetic retinopathy

Hajmousa, Ghazaleh

Towards adipose tissue-derived stromal cells-based therapy for diabetic retinopathy

Ghazaleh Hajmousa

Hajmousa, Ghazaleh
Towards adipose tissue-derived stromal cells-based therapy for diabetic retinopathy

university of groningen

Towards adipose tissue-derived stromal cells-based therapy for diabetic retinopathy

PhD thesis

to obtain the degree of PhD at the
University of Groningen
on the authority of the
Rector Magnificus Prof. E. Sterken
and in accordance with
the decision by the College of Deans.

This thesis will be defended in public on

Wednesday 17 October 2018 at 12.45 hours

by

Ghazaleh Hajmousa

born on 16 September 1983
in Tehran, Iran

Supervisor
Prof. M.C. Harmsen

Co-supervisor
Dr. G. Krenning

Assessment Committee
Prof. J.L. Hillebrands
Prof. R.O. Schlingemann
Prof. M. Schmidt

Paranymphs

Linda Brouwer

Ena Sokol

Contents

GENERAL INTRODUCTION

Adipose tissue derived stromal cells for treatment of diabetic retinopathy; the best or the last choice?

CHAPTER 01

1. Diabetes

Diabetes mellitus (DM) is a developing issue around the world. This cutting-edge plague is one of the world's oldest sicknesses, specified in authentic records of ancient civilizations, for example, those found in old Egypt, Persian Empire, and India [1-3]. The International Diabetes Federation estimates that ~415 million individuals over the globe were experiencing diabetes in 2015 and about 642 million individuals are assessed to be diabetic by 2040 [4]. Mortality identified with DM and its complexities results in 3.8 million passings yearly, representing 6% of the overall mortality [5]. Lately, records propose the overall prevalence of diabetes is 9.2% in females and 9.8% in males [6].

There are two primary types of diabetes, type 1 (T1DM) and type 2 (T2DM), in spite of the fact that diabetes may likewise happen during pregnancy and under different conditions, for example, medication or compound poisonous quality, endocrinopathies and in a relationship with insulin disregluation and pancreatic exocrine infections [7]. The increased fasting levels of glucose, named hyperglycemia, is the major indicative parameter that is found in the two kinds of diabetes [8, 9] which can be caused by constant or relative insulin inadequacy [10].

T1DM is 100% insulin dependence, and in T2DM, upwards of half of patients expect insulin to control hyperglycemia [8]. T1DM is caused by autoimmune ablation of pancreatic beta cells inside the islets of Langerhans, which abrogates insulin production and affects associated metabolic entanglements [11]. Various hereditary determinants of T1DM, for example, alleles of the real histocompatibility locus (HLA) at the HLA-DRB1, DQB1 loci [12], and

HLA-B*39 locus [13] represent 40% – half of the familial grouping of this issue. T2DM represents about 90% of all analyzed cases [14]. what's more, is related to both fringe insulin protection and hindered insulin discharge. The most sensitive tissues respect to instigated insulin incorporates skeletal muscle, liver, and fat tissue by reason of the particular necessities for glucose take-up and digestion. The confirmations recommend that mitochondria assume a part of the two procedures [15].

2. Complications of Diabetes

Diabetes is a noteworthy reason for mortality and (co)morbidity due to its vascular complications. Vascular dysfunction is a causative factor in the etiology of essential optional difficulties of DM which are gathered under "microvascular sickness" (because of harm to small blood vessels) and "macrovascular inflammation" (because of harm to the arteries). Microvascular entanglements incorporate eye ailment named "retinopathy," kidney ailment as "nephropathy," and neural damage or "neuropathy". The major macrovascular entanglements incorporate quickened cardiovascular inflammation causing myocardial infarction and cerebrovascular disease showing as strokes [16-23]. The danger of the difficulties in T1DM as indicated by the Diabetes Control and Complications Cohort (DCCT) and Epidemiology of Diabetes Interventions and Complications (EDIC) [24] are 47% for retinopathy, 17% for nephropathy, and 14% for cardiovascular illness. For T2DM, there are more constrained information [25]. Contrasted to people without complications, the risk of retinopathy was related to ~1.7-fold expanded hazard for cardiovascular occurrence and more than two-fold expanded hazard for coronary events in T2DM [26].

3. Diabetic Retinopathy

Diabetic retinopathy (DR) influences around 33% of all people who experience the disease effects of DM [27]. The longer the patient has diabetes, the higher the possibility of contracting DR [25]. Half of the patients with T1DM show features of retinopathy within 10– 15 years after diagnosis. This increments to 75– 95% following 15 years and 100% following 30 years. 60% of patients with T2DM show signs of retinopathy within 16 years [28]. DR has two overlapping phases i.e. non-proliferative diabetic retinopathy (NPDR) and proliferative diabetic retinopathy (PDR) [29, 30]. Diabetics with NPDR, generally have normal visual acuity. The most punctual clinical indications of NPDR are microaneurysms and retinal hemorrhaging. Improvement of cotton-wool spots, venous bleeding and intraretinal microvascular abnormalities are signs of progressive capillary profusion [31].

The severity of DR ranges from non-proliferative and pre-proliferative to all the more extremely proliferative, in which the anomalous development of new vessels occurs [32]. The new vessels are fragile and very permeable. They pass through the optic disc and develop along the surface of the retina and into the scaffold of the back hyaloid face. The vessels themselves do not disable vision, yet are disturbed effortlessly by vitreous traction and hemorrhage into the vitreous cavity [31, 33].

This procedure of the disease with neovascularization and accumulation of liquid and protein inside the retina, is termed diabetic macular edema (DME), and significantly contributes to the visual weakness. In more serious cases, bleeding may occur with related contorting of the retinal structure including improvement of a fibro-vascular membrane which can, therefore, prompt retinal detachment [34]. Though in T1DM the fundamental vision

undermining retinal issue has all the hallmarks of PDR, in T2DM there is a higher frequency of macular edema [35].

As indicated by the World health organization, DR represents around 5% of worldwide visual impairment among grown-ups matured 20–74 years [36].

4. Current Treatment of DR

The beginning stage of retinopathy, most of the time goes unnoticed as it does not have noteworthy pathological signs. In any case, advanced retinopathy is sought after of treatment. Currently, there is no technique to prevent or treat DR and accessible methods have just restricted accomplishment in controlling its overwhelming outcomes*.*

4.1. Primary Prevention

Hypertension, hyperglycemia, and diabetes term are the major risk factor for DR, in particular their combined occurrence [9, 37]. The early phases of the retinopathy can be alleviated by control of blood glucose levels [38, 39], blood pressure, and lipids [39-41]. Tight glucose and blood pressure control can postpone the beginning of retinopathy by means of suppression of its progression [37]. Importantly, application of glycemic control can cause brief declines, generally because of the advancement of small arteriolar infarctions which result in the cotton wool spots. Specifically, patients merit cautious observation previously and at 3-month to month interims after practice of intensified control for no less than 1 year [42]. In animal models of diabetes, exogenous insulin treatment may retard

development of both micro and macrovascular diabetic co-morbidities [43, 44].

4.2. Secondary Prevention

Treatment to restrain advanced phases of retinopathy essentially manages vascular changes primarily. Current methods incorporate laser and vitrectomy, anti-angiogenesis treatments joined with steroids, and anti-inflammation drugs. Laser photocoagulation and vitrectomy have enhanced the personal satisfaction for patients with DR and the danger of serious visual misfortune by 50 – 60% [37]. This includes focal laser photocoagulation for areas of focal blood retinal barrier (BRB) breakdown in diabetes, grid photocoagulation for DME, and scatter photocoagulation as a prophylaxis in contradiction of neovascularization in PDR [45]. Pan retinal photocoagulation (PRP) therapy may get its impact by diminishing the host of angiogenic and permeability factors that have accumulated in the photoreceptor layer of the retina [46]. A few endeavors have been made to modify laser procedures to diminish their side-effects, for example, diminished visual sharpness, peripheral field misfortune, and compounding of macular edema [47]. This process likewise affects night vision and requires repeated treatment [48-50]. Late studies have demonstrated that antiangiogenic methods joined with laser treatment, result in preferable visual outcomes over laser alone [51]. It has been demonstrated that people with PDR have elevated levels of intravitreal vascular endothelial growth factor (VEGF), and that laser photocoagulation treatment altogether decreases these levels [51, 52].

Presently, blocking VEGF can keep the improvement of PDR in murine models [53]. There are three principle components by which anti-angiogenesis specialists are utilized for the treatment of PDR: (a) Inhibition of VEGF through direct binding; (b) Inhibition of VEGF

signaling; and (c) Inhibition of VEGF synthesis. Pegaptanib, Bevacizumab, Ranibizumab, and VEGF Trap are utilized for the management of PDR by sterically hindering of VEGF isomers through direct binding [54]. The issue with block of VEGF isomers is in reality the reduction of physiologic revascularization, which is imperative in avoiding exacerbated PDR [55]. A considerable part of intraocular anti-VEGF could diffuse into the systemic circulation [56-58]. Anti-VEGF treatment requires repeated intravitreal infusions for quite a while with conceivable inconveniences [50].

In addition, hypertension (because of the expanded vasoconstriction) and proteinuria (because of glomerular dysfunction) are the most widely recognized symptoms of fundamental VEGF block [59]. Vitreous hemorrhage, tractional retinal detachment (TRD) [60], endophthalmitis, cataract, and potential loss of neural retinal cells [61] may likewise seem separated from nearby side-effects of Anti-VEGF treatment. Twisting of the eye amid intravitreal infusion with conceivable interference of the vitreous in the sclera, may bring about vitreoretinal traction [62]. Steroids strongly inhibit angiogenesis, proliferation, apoptosis, and inflammation. In the eye the impact of most steroids is temporary, demanding repeated or nonstop administration to keep up the supportive impact [63].

5. Pathology of DR

It is amply acknowledged that DR builds up first by vascular cell dysfunction and apoptosis, pericyte loss, thickening of the basement membrane (BM), and compromised BRB permeability [64]. The expression "pericyte ghosts" alludes to pericytes which left pockets in the BM and vanished from the capillary wall [65]. Pericyte dropout

in the diabetic retinal vasculature is identified by the existence of ghosts as seen in transmission electron microscopy micrographs [66]. Pericytes harbor anti-apoptotic support for the endothelium [67], in this way, the loss of pericytes in DR might be lenient for endothelial cells (EC) development [49].

EC are additionally lost in DR, bringing about acellular capillaries that comprise exclusively of BM sleeves. BM thickening originates from gathering and lessened corruption of BM modules. The synthesis of BM is as yet not fully understood, in any case it is realized that collagen type IV, fibronectin, laminin, and heparan sulfate proteoglycan are included [68-70]. The associations of these portions are expanded by hyperglycemic conditions. Hyperglycemia enhances fibronectin, collagen IV, and laminin gene expression [71-73].

In diabetes, the vascular BM achieves a thickness that is often a few times more than the ordinary vascular BM [74, 75]. One of the early events in DR is the modification of the BRB which increases the permeability of vessels. The barrier function of retinal EC is also affected, because gap junction intercellular communication (GJIC) are reduced in number and function, as a result of changed connexin expression in various tissues [76]. GJIC are essential for the intercellular transport of various small molecules and ions, for example, ATP, Na+, and K+ that are fundamental for cell viability [77]. Also, onset and development of DR correlates with the diminished GJIC in the retina. Interestingly, retinal EC are more prone to dysfunction caused by oxidative stress than other EC types a result of which is increased permeability [78]. Hyperglycemia induces increased plasma levels of tumor necrosis factor alpha (TNF-α), interleukin (IL)-6, and IL-8 [79]. Increased leukostasis, cytokines, and growth factors direct the breakdown of the BRB in diabetes [80-82]. Specifically, the proliferative phase is portrayed by the

formation of new defective vessels spreading without normal configuration i.e. pericyte coverage, on the retinal surface which may lead to fibrosis, and tractional retinal detachment [83].

6. Animal models of DR

Animal models are suitable to replicate specific phases or processes of the onset and development of human disease such as diabetes and DR. This allows to dissect the pathophysiology and assess treatment modalities prior to clinical trials. There have been several animal species and strains examined to model human DR, including mice, rats and monkeys [84]. Mammalian models build up the beginning stages of retinopathy, which incorporates degeneration of retinal vessels. Also, degeneration of retinal neuronal cells in diabetic mice [85] and rats [86]. The most regularly utilized diabetes models are instigated by chemical toxins, for example, streptozotocin (STZ) or alloxan which destruct the insulin-producing beta cells in the islands of Langerhans in the pancreas. Thus, both chemicals induce T1DM more than insulin resistance-based T2DM [87]. Be that as it may, toxin-incited diabetes in mice is highly strain-variable as a result of strain-subordinate protection from STZ [88].

Preretinal neovascularization is not found in any rodent animal model, probably because of their short lifespan. This has brought about the development of various nondiabetic models of retinal complications where neovascularization is counted as the secondary complication, for example, hypoxia-induced models like oxygen-induced retinopathy (OIR) also known as retinopathy of premature (ROP) in newborn mice[89], or models with overexpression of VEGF [90] and insulin-like growth factor I (IGF-I) [91] in the eye. Rodent pups have an immature retinal vasculature at birth [92].

Therefore, development of the intraretinal vasculature happens postnatally in mice which can be seen and controlled tentatively [93].

6.1. OIR mouse model

Mouse model of OIR, is a standout amongst the most generally utilized animal models with in excess of 15,000 publications since it was first distributed in 1994 [94]. In a word, neonatal mice are presented to 75% oxygen from postnatal (P) day 7 until P12 and came back to room air (21% oxygen) from P12 to P17. Amid the primary hyperoxic stage, retinal vessels constrict to control oxygen levels [95]. What's more, immature vessels of the central retina relapse prompting a central zone of vaso-obliteration (VO). On return to room air at P12, the VO retinal area turns hypoxic and a huge upregulation of HIF-1α-dependent proangiogenic pathways ensues. From P17 on, neovessels begin to relapse, until at P25 [96, 97].

6.2. Ins2Akita mouse model

The Mody4 locus on chromosome 7 has a mutation in the insulin 2 gene, now alluded to as the Ins2Akita allele. This mutation induces protein changes, prompting its collection in the endoplasmic reticulum of pancreatic β cells and leads to β-cell apoptosis. Heterozygous mice with this mutation develop increased hypoinsulinemia and hyperglycemia during their life span and thus represent a rodent model for human diabetes. The various studies bolster the utilization of the Ins2Akita mouse as a suitable model of early stage of DR [98].

6.3. Akimba mouse model

The Akimba is another basic experimental model which is a cross between the hyperglycemic Akita mouse and the Kimba mouse (overexpresses human VEGF in photoreceptor cells of the retina). The merger of these two makes a mouse with hallmarks of PDR, such as neovascularization and retinal edema [99, 100]. The outcomes from animal model studies must be taken with alert, recalling the impediments of these models with general reference back to the human state, which is basic for characterizing the significance of these discoveries.

7. Pericyte

Pericytes were depicted by Charles-Marie Benjamin Rouget in 1873 for the first time as cells with contractile properties that envelop capillary EC [64]. Pericytes are particular perivascular cells [101], derived from the vascular smooth muscle lineage. Pericytes of the capillaries are connected to the abluminal side of EC [102]. Pericytes share a BM with the EC and straightforwardly interaction these through gaps in the BM. These heterologous peg-and-socket contacts include tight and gap junctions [103, 104]. Pericytes express mesenchymal markers such as neuron-glial antigen 2 (NG2), regulator of G-protein signaling 5 (RGS5), N-Cadherin (CDH2), Platelet-derived growth factor receptor beta (PDGFRβ) and CD146 and lack hematopoietic markers such as CD45 or CD34. Despite the fact that pericytes share numerous markers with smooth muscle cells (SMC), they can be recognized from SMC by expanded PDGFRβ and diminished alpha smooth muscle actin (αSMA). In vivo, the typical way to distinguish pericytes remains

their morphology and anatomical restriction [105]. In fact, the operational definition of a pericyte is a matrix-embedded cell that surrounds small arterioles and capillaries. The highest density of pericytes i.e. pericyte to EC ratio is in neural tissues, particularly the retina, perhaps because of its high metabolic action and its prerequisite of a tightly-controlled blood retinal barrier (BRB).

The pericyte to EC ratio in retina is 1:1. This is as opposed to the skeletal muscles where the pericyte to EC ratio is approximately 1:10 [64, 102]. This extraordinary quantity of pericytes in retina, may mirror their commitment to the BRB, in which they are proposed to constitute a guardian and sentinel cellular layer [106].

8. Pericyte Function

Pericytes are contractile cells that assist to control local perfusion [107]. Pericytes contract when exposed to hyperoxia [108], ATP, endothelin1, angiotensin 2 [109] and they relax upon exposure to nitric oxide (NO) [110], CO_2 [111] and adenosine [112].

They are likewise known to keep up the integrity of the BRB by prompting the zonula occludens-1 (ZO-1) and occludin expression between EC under normoxia and reversing the occludin decrease that happens under hypoxia [113]. Pericytes support the stabilization, remodeling, and maturation of vessels. Moreover, pericytes are in charge of providing an anti-angiogenic and anti-inflammatory environment for EC and actually cause endothelial quiescence [114]. The construction of the BRB relies on the connection of the vascular EC with pericytes and glial cells in the so-called neurovascular unit or NVU [115].

Procedures supporting angiogenesis organized by the principle physical or paracrine communications amongst EC and pericytes. This connection is controlled by the crosstalk between a few ligands/receptors, the principle of which is specified in Table.1 modified from [116].

Ligand/receptor	Consequence	Ref
Ang1/Tie2	Vessel stabilization	[117]
TGFβ/ALK-1/5	EC proliferation and migration (ALK-1)	[118]
	Vessel maturation (ALK-5)	
PDGF-BB/PDGFR-β	Pericyte recruitment and proliferation	[119]
	Vessel stabilization	[117]
VEGFA/VEGFR2	EC survival	[114]
	Vessel stabilization	[114]
	Angiogenesis sprouting	[120]
N-Cadherin/N-Cadherin	Pericyte recruitment	[121]
	Vessel maturation	
Jagged1/Notch	Vessel maturation and stabilization	[122]
	Angiogenesis sprouting	

Table. 1. The principle communications between EC and pericytes amongst angiogenesis [116].

9. Pericytes in DR

Pericytes are associated with the pathogenesis of the DR [123]. Studies on retinal vessels uncovered that the loss of pericytes is the principal morphological conversion in a diabetic retina. EC in this way vanish, giving rise to acellular vessels, which are obviously not functional and non-perfused [124, 125]. The reason for pericyte apoptosis in DR is not understood to date. Some conceivable mechanisms relate pericyte apoptosis with prolonged oxidative stress [126] followed by nuclear factor-kappa B (NF-κB) activation. Hyperglycemia activates NF-κB in retinal pericytes which activates apoptotic pathways [127].

Apoptosis may occur independent of NF-κB. Downstream of the hyperglycemia-induced PKC activation and expanded the protein tyrosine phosphate called Src homology-2 domain– containing phosphatase-1 (SHP1) expression, dephosphorylates activated PDGFRβ. Downregulation of the pericyte's PDGF signaling suppresses survival signals in these cells [128]. Interruption of PDGFB/PDGFRβ signaling has been proposed a part in of the pericyte apoptosis [49]. Angiopoietin-1 (Ang-1) is additionally one pericyte-delivered factor that is essential for the pericyte's balancing function [129]. Ang-1 exerts anti-inflammatory and anti-apoptotic properties, and loss of Ang-1 increases expression of angiopoietin-2 (Ang-2) [130]. Angiopoitin-2 (Ang-2) is an antagonist of Ang-1 by hindering the Ang-1 induced-autophosphorylation of Tie-2 [131], which can meddle with Tie-2 receptor signaling, which causes the reduced survival of EC and pericytes [132, 133]. While Ang-2 induces neovascularization, Ang-1 supports vascular maturation, thus both molecules require to be well-balanced under normal physiology [134].

The angiopoietin/Tie-2 signaling has a critical part in the pathogenesis of PDR [132, 135]. Ang-2 injection into the retina of wild type mice causes pericyte loss [136]. Cytokines, for example, TNF-α cause pericyte apoptosis and restraint of TNF-α inhibited pericyte ghost appearance caused by T1DM and T2DM [137].

Chronic hyperglycemic exposure for 2-12 days broadly raised IL-1β , NF-κB, VEGF, TNF-α, transforming growth factor beta (TGF β), and intercellular adhesion molecule-1 (ICAM-1) gene expression and protein concentration in retinal pericytes, and these changes continued even after reclamation to normalglycemia [138]. VEGF is another pivotal factor associated with the breakdown of the BRB and increased permeability of the retinal vessels [139]. Peroxisome proliferator-activated receptor-gamma (PPAR-γ) agonists can inhibit VEGF signaling. Blocking of tyrosine kinase action can bring about remarkable suppression of the VEGF-induced neovascularization [140].

Downmodulation of pathological neovascularization in DR, is a therapeutic goal [141, 142]. Pericytes from diabetic patients have an alteration in the secretion of pro-angiogenic factors, like VEGF [143]. Likewise, mitochondria in pericytes are influenced by hyperglycemia which disturbed mitochondrial network. Changes in mitochondrial metabolism and morphology underlies pericyte apoptosis [144]. The prevention of the earliest events in the pathogenesis of DR, for instance, pericyte loss, will keep the ensuing improvement of DR.

10. EC in DR

Hyperglycemia-induced reactive oxygen species (ROS) is the best-known critical factor in diabetic vascular complications. NADPH oxidases (NOX) are the main producer of ROS in the vessels. Under hyperglycemia, stimulation of mitochondrial uncoupling protein 2 (UCP2) diminishes the mitochondrial membrane potential which leads to a lowered release of ROS and protection of EC [145]. Hyperglycemia causes mitochondrial fragmentation and membrane potential heterogeneity in rodent retinal EC. Bioenergetics analysess shows that hyperglycemia causes a higher extracellular acidification and a lower steady state and maximal oxygen consumption under in these retinal EC [146]. Human umbilical vein endothelial cells (HUVEC) under hyperglycemia also had elevated ROS formation and upregulated vascular adhesion molecule-1 (VCAM1) expression [147].

Upregulation of ICAM-1 on retinal EC has been shown in diabetes by others too [148]. Also in human microvascular endothelial cell lines such as EA.hy926, hyperglycemia induces ROS both by activated NOX and a dysfunctional mitochondrial respiratory chain [149].

Moreover, hyperglycemically challenged HUVEC and EA.hy926 cells had a misbalance between oxidative stress and nitric oxide-cyclic guanosine monophosphate (NO-cGMP) pathway i.e. uncoupled endothelial nitric oxide synthase (eNOS) activity. In spite of the fact that, in hyperglycemic condition EA.hy926 cells showed more proliferation [150].

Toll-like receptors (TLRs) are pathogen-associated molecular pattern receptors (PAMPs), broadly expressed by several cell types, which a part of the native immune response [151, 152]. Toll-like receptors

signal via myeloid differentiation primary response 88 (MyD88) and NF-κB and upregulate pro-inflammatory mediators. In fact, TLRs are regulated by NF-κB and thus sensitive to hyperglycemically-induced ROS. TLR2 and TLR4 mRNA and protein expression in human microvascular retinal endothelial cells (HMVREC) is increased under hyperglycemia.

Additionally, increased NF-κB, MyD88 and non-MyD88 pathways and monocyte adhesion are shown in this condition. Noteworthy, altered TLR2 and TLR4 expression can be treated by antioxidant which is followed by downstream inflammatory markers [153].

Hyperglycemia significantly elevated NO and prostaglandin E2 (PGE2) in bovine retinal endothelial cells (BREC) [154]. Reduced expression of connexin 43 [155], occludin (through the activation of VEGF and IGF-1) [156] and ZO-1 [157] levels caused of hyperglycemia in the retinal EC may lead to the increased BRB breakdown.

11. The main contributors of DR

11.1.　　　Impaired Glucose Metabolism

A considerable collection of evidence from in vivo and in vitro studies offer four biochemical irregularities in the development of micro and macro-vascular complexities in DM as demonstrated by: (a) increased polyol pathway flux [158, 159]; (b) hyperactivation of isoform(s) of protein kinase C (PKC) [160, 161]; (c) increased oxidative stress [162]; and (d) increased deposit of advanced glycation end-products (AGEs) [163-166]. These apparently irrelevant pathways share a single factor: overproduction of mitochondrial superoxides. These metabolic pathways are related to excessive ROS [167]. Aldose reductase (AR) is the main compound and the first step in the polyol pathway. In a hyperglycemic condition, AR inhibits nicotinamide adenine dinucleotide phosphate (NADPH)-dependent conversion of glucose to sorbitol. The second step of the pathway is oxidation of sorbitol to fructose by the sorbitol dehydrogenase enzyme. Generating the intracellular antioxidant glutathione (GSH) depends on NADPH consumption. Consequently, a decline in the accessibility of NADPH impairs intracellular oxidative stress. An increased enzymatic activity of AR by hyperglycemia worsens the state of DR [163, 168]. Thus, inhibition of AR may limit progress of DR [169, 170]. AGEs and its receptor, RAGE, can also induce oxidative stress and ROS [171]. Similar to AR, the inhibition AGE and RAGE signaling offers therapeutic prospects to treat DR [172, 173]. Hyperglycemia induces accumulation of glyceraldehyde-3 phosphate which additionally causes the ROS overproduction and stimulates the collection of poly(ADP-ribose) polymerase-1 (PARP), which triggers the PKC pathway activation followed by increased deposition of

AGEs [174]. Taken together, these pathways initiate DR through ROS-induced vascular permeability and ischemia [168, 175, 176].

11.2.   Oxidative Stress

The imbalance between the generation of ROS and the capacity to scavenge ROS by endogenous antioxidants states is called oxidative stress. The retina is profoundly vulnerable to oxidative stress-induced damage. Neural tissue, in particular the retina, has the highest oxygen consumption in the body [177], thus this high oxygen demand of the retina likely generates ROS if not properly controlled [178].

Superoxide anion ($O2\bullet-$), perhydroxyl radical (hydroperoxyl radical, HO_2) and hydroxyl radical ($OH\bullet$) are relevant ROS. Superoxide is formed non-enzymatically via mitochondrial respiration or by the enzymatic oxygen decline of NOX. Superoxide is enzymatically converted into hydrogen peroxide (H2O2) via superoxide dismutase (SOD) or non-enzymatically to H_2O_2 and single oxygen [179]. Oxidation of the guanidine gathering of L-arginine by the nitric oxide synthase (NOS) produces NO.

NO as a free radical react with superoxide and create an oxidant named peroxynitrite (ONOO), one of the reactive nitrogen species (RNS) [180]. The enzymatic antioxidants, for example, manganese superoxide dismutase (MnSOD), copper/zinc superoxide dismutase (Cu/Zn SOD), catalase, and glutathione peroxidase (GPx) and nonenzymatic antioxidants like ascorbic acid (vitamin C), α-tocopherol (vitamin E), GSH, and β-carotene can proficiently scavenge ROS. Superoxide can be converted to H_2O_2 by MnSOD and Cu/Zn SOD, which is then effectively converted to water by GPx or catalase [181].

The ROS overproduction can disturb the normal capacity of cells by damaging the lipids, proteins and DNA of the cells. Intracellularly, ROS can damage mitochondria by opening the mitochondrial membrane permeability transition pores (PTPs), which may leads to additional ROS production [182]. Releasing of ROS-induced Cytochrome-c, further prompting apoptosis in the cells [183, 184].

11.3. Mitochondrial Dysfunction

In the diabetic retina before histopathology signs can be recognized, dysfunctional mitochondria, damaged DNA (mtDNA) and increases apoptotic cells are seen. The fact that is showing the role of mitochondria in the development of DR [185-187]. The typical shape of mitochondria in the cells is tubular, and balanced between mitochondrial fission and fusion dedicates mitochondrial shape [188]. Mitochondrial function is additionally controlled by cycle of fusion and fission, and changes in shape and mitochondrial structure are considered as a sign of dysfunctional mitochondria [189]. Mitochondrial fission is associated with apoptosis and mitochondrial fusion with inhibition of apoptosis. Hyperglycemia-induced ROS causes mitochondrial fragmentation [190, 191].

Oxidative phosphorylation is the basic function of mitochondria through its five enzyme complexes, assigned as complex I, II, III, IV and ATP synthase. In 1966, for the first time, mitochondria were reported as the ROS generators. NADH dehydrogenase at complex I, and the interface amongst co-enzyme Q and complex III are principle culprits that generate superoxide in mitochondria [192]. Dysfunctional mitochondria cause low respiration rate and formation of superoxide [193-196]. Under physiological conditions, electron exchange through complexes I, III and IV expels protons outwards into the intermembrane space, creating a proton gradient that drives

ATP synthase as protons go back through the inner membrane into the matrix. Interestingly, in diabetic cells under hyperglycemic conditions, there is more oxidation of glucose-derived pyruvate in the tricarboxylic acid (TCA) cycle (oxidative phosphorylation), which increases the flux of NADH and $FADH_2$ (electron donors) into the electron transport chain. The mitochondrial membrane's potential increases till the point when a critical threshold is reached. At this point, electron exchange inside complex III is blocked, making the electrons go down to coenzyme Q, which gives the electrons each one in turn to molecular oxygen, subsequently creating superoxide [197].

Thenoyltrifluoroacetone (TTFA, complex II inhibitor) and carbonyl cyanide m-chlorophenylhydrazone (CCCP, an uncoupler), totally prevent the impact of hyperglycemia. Overexpression of mitochondrial antioxidants, uncoupling protein-1 (UCP1) and MnSOD, likewise prevent the hyperglycemia impact [198, 199]. Mitochondrial dysfunction induces the oxidation of unsaturated fat, bringing about expanded intracellular fatty acyl-CoA and diacylglycerol content which leads to PKC inhibition [200]. Damaged oxidative phosphorylation [201]; disabled ATP synthesis [202]; reduced density of mitochondria; expanded intracellular lipids with diminished glucose metabolism [203]; and reduced TCA-cycle substrate oxidation [204] are observed in T2DM. The function of antioxidants, such as SOD, glutathione reductase, glutathione peroxidase, and catalase to scavenge ROS and maintain a proper redox homeostasis, are compromised in the diabetic retina [205].

Vitamin C, vitamin E, and β-carotene control the redox homeostasis and are also compromised by hyperglycemia [206]. Moreover, inside the retinal mitochondria, reduced activity of complex III is reported in diabetic rodents [207]. In spite of the fact that mitochondrial

dysfunction might be the main indicator of the disease, the loss of ATP generation is likely adding to apoptosis in the later phases of DR [208, 209].

11.4.   Inflammation

The previous sections hinted already that hyperglycemia activates NF-κB signaling and renders the retina in a pro-inflammatory state; therefore DR is a chronic inflammation. Interestingly, as early as in 1964, it was noticed that diabetics with rheumatoid arthritis who took high dose aspirin (a cyclooxygenase inhibitor), showed a reduction in severity of PDR [210].

Inflammation is composed by several factors that include release of pro-inflammatory cytokines, chemokines, and upregulation of adhesion molecules. Inflammation is a first line activated defense and a reaction to damage that connects leukocytes and the endothelium and conducts leukocyte migration towards damaged area. Inflammation has advantageous effects on an acute damage, however can have negative impacts if chronically [211]. The immune system boosts a repair response of damaged tissue which includes the eradication of unwanted pathogens or removal of undesirable molecules. Endothelium and immune cells, but also a host of other tissue cells, are equipped with pathogen and damage-associated molecular pattern (PAMP resp. DAMP) receptors. These include the before mentioned TLRs and the receptor for AGE (RAGE). Activation of pattern recognition receptors causes pro-inflammatory activation and induces expression of pro-inflammatory proteins [212].

The expression of a host of pro-inflammatory proteins is controlled through the activation of pro-inflammatory transcription factors, including NF-κB, p38 MAPkinase, and TAK1 and sustains a feed

forward loop of synthesis of cytokines, chemokines, and inflammatory molecules [212]. Leukocytes bind to ICAM-1 on the surface of endothelium during inflammation. ICAM-1 is upregulated by VEGF, PARP, dyslipidemia and oxidative stress via NF-κB [148]. Upregulated expression of E-Selectin, ICAM-1 and VCAM-1 is also detected in diabetic retinal vasculature [213]. ICAM-1, VCAM-1 and E-selectins assist recruitment of leukocytes and enable their infiltration into the damaged tissue [214]. Blockade of ICAM-1 may prevent or reduce the disruption breakdown of the BRB, as well as prevent capillary occlusion and EC damage in DR [148, 215].

Expression of ICAM-1 is promoted by VEGF in EC. This leads to leukocyte activation and cytokine release, along these lines generating additional VEGF and amplification of the inflammatory reaction. Suppression of retinal leukostasis and BRB breakdown has shown followed by particular blockade of endogenous VEGF in diabetes [216]. In retinas of diabetic mice the activity of caspase-1 is increased. Caspase-1, also known as IL-1 converting enzyme (ICE), generates IL-1β from its precursor. IL-1β activity is mediated by binding to IL-1R1 on the cell surface [217, 218]. The increased level of the cytokines TNF-α, IL-1β [219], IL-6 [220] and the chemokine (C-C motif) ligand 2 (CCL2) [221], CCL5 [222], C-X-C motif chemokine 8 (CXCL8), CXCL10, CXCL12 is reported in the serum and vitreous samples from DR patients [222-224]. This shows that during DR, local chronic inflammation exists. Additionally, expression of NF-κB is higher than ordinary in retinal membranes of patients with PDR [225]. Endothelial damage and even loss may associate with inflammation in DR via CCL2 that activates PKCα/ζ-mediated phosphorylation and translocation of ZO-1, ZO-2, occludin and claudin-5 which causes disruption of endothelial tight junctions and loss of the BRB barrier [226]. Remarkably, CXCL8 causes loss of membrane expression of VE-cadherin through phosphatidylinositol

3-kinases/Rac/p21 activated kinase signaling which increases endothelial permeability [227]. Prostanoids such as prostaglandins (PG) and thromboxane A2 (TXA2) are generated as part of the arachidonic acid (AA) pathway by plasma membrane bound phospholipases (PLAs). Pivotal enzymes in PG synthesis is the cyclooxygenase 1 and 2 (COX) and prostaglandin G/H synthase [228].

In healthy tissues the production of prostaglandin is low, however this increases promptly during onset of acute inflammation and promotes the recruitment of leukocytes among others. In contrast to COX-1 which is expressed in a majority of cells, COX-2 is induced by inflammatory stimuli, hormones and growth factors. COX-2 is the main source of prostanoids during inflammation [229]. Both COX-2 expression and extensive generation of prostaglandins occurs in retinas of diabetic animals. Similarly, COX-2 was shown in vascular EC in fibrovascular epiretinal membranes from patients in late phase DR [230].

PGE2 synthesis in diabetic rat retinas was fundamentally abrogated by celecoxib (a specific COX-2 inhibitor) but not by a COX-1 inhibitor [231], which suggests that COX-2 is responsible for the increased retinal prostaglandin generation in diabetes. The COX enzymes are targeted by non-steroidal anti-inflammatory drugs (NSAIDs), for example, aspirin and salicylate [232]. While parenchymal cells are generally pro-inflammatory activated by PGE2, the function of immune cells including lymphocytes and macrophages is suppressed by PGE2. Thus PGE2 is both pro-inflammatory and anti-inflammatory. This double role of PGE2 in tweaking the inflammation has been seen in various medical complications [233]. The cyclooxygenase/prostaglandin pathway is a common pathway in both neovascularization and inflammation [234]. Also, various

chemokines serve a double-role i.e. as leukocyte attractant and as angiogenic mediator on EC [235]. IL-1α, IL-1β, IL-6, TNF-α, and more pro-inflammatory cytokines invoke vascularization directly by targeting EC or indirectly by prompting leukocytes and EC to create additional proangiogenic mediators [236-238].

12. Stem Cells

Stem cell (SC) [239] have two main properties: self-renewal and differentiation [240]. Preferably, stem cells which are applied for regenerative therapies ought should fulfill the following criteria: (a) available a high numbers, depending on the application from thousands to even millions; (b) can be collected by a minimally invasive procedure; (c) can be differentiated along different lineages, and (d) can be safely and efficiently administered to the patient [241]. Embryonic stem cells are the most versatile stem cells and capable to differentiate to all cells of the body. However, primarily ethical, legal and political concerns, render embryonic stem cells unsuitable for large-scale clinical applications [242, 243]. Hematopoietic stem cells (HSCs) have been used in experimental therapies for tissue repair for many decades, yet HSCs remain hard to isolate and have low yields in general [244].

Induced pluripotent stem cells (iPSC) are exceptionally encouraging, yet current procedures to generate iPSC virus or vector free are in their infancy and restrict clinical use [245, 246]. Endogenous stem cells derived from adult tissues such as brain, gut, lung, liver, adipose tissue and bone marrow [247], in general have the ability to self-renew and differentiate into numerous cell types [248, 249].

13. Mesenchymal Stem Cells

Mesenchymal stem cells (MSC), also called multipotent mesenchymal stromal cells, are present in the connective tissue of every postnatal organ and tissue [250]. MSC have been isolated from adipose tissue [251], umbilical cord blood [252], dura mater [253], cartilage [254], compact bone [255], tonsil [256], synovial membrane [257], skin [258], hair [259], placenta [260] and dental pulp [261]. MSC, first distinguished in 1966 in the investigations of Friedenstein and Petrakova [262], these bone-forming cells were isolated from bone marrow of rats. To date, according to international society for cellular therapy (ISCT), MSC are characterized by the following three criteria [263]: (a) MSC adhere to plastic. MSC after isolation attach to plastic and expand in serum containing medium without extra prerequisites growth factors or cytokines;

(b) MSC express variable levels of following molecules. CD44, CD90, CD166 (vascular cell adhesion molecule), CD54/CD102 (intracellular adhesion molecule), CD105 (SH2), CD73 (SH3/4), stromal antigen 1, and CD49 [263, 264]. Contrariwise, MSC do not express of surface markers of hematopoietic cells (i.e. CD14, CD45, and CD11a), EC marker (i.e. CD31) and erythrocytes marker (i.e. glycophorin An) [265]. MSC express very low levels of cell-surface HLA class I molecules and the absence expression of HLA class II, CD40, CD80 and CD86 in these cells leading to reduced activation of immune reactions [266]. The absence of major histocompatibility complex II (MHCII) (encoded by HLA gene) expression in MSC marks them a reasonable choice for allogeneic transplantation [267, 268]. (c) MSC has differentiation potential: MSC can be differentiated into the trilineage comprising adipocytes, osteoblasts and chondrocytes in vitro [269, 270]. The efficacy of MSC in vivo has been credited to

various mechanisms counting differentiation to other cell lineage, release of paracrine factors to change microenvironment, balancing oxidative stress and immunomodulatory capacity [271].

In 2005, international society for cellular therapy (ISCT) proposed that cells depicted as mesenchymal stem cells should be rephrase to multipotent mesenchymal stromal cells because most MSC types lack the capacity to self-renew, at least in vitro. As per the ISCT, the term mesenchymal stem cells ought to be held just for subpopulations with particular highlights of stem cells [272].

14. Immuno-modulating Properties *of MSC*

The therapeutic efficacy of MSC has been shown in different inflammatory studies in three distinctive methodologies: (a) expressing the interleukin (IL)-1 receptor antagonist; (b) making a negative feedback loop where pro-inflammatory cytokines like TNF-α from local macrophages cause MSC to secrete the anti-inflammatory TNF-α stimulated gene/protein 6 (TSG-6). The TSG-6 at that point decreases NF-κB pathway and tweaks the inflammation; (c) making a negative feedback loop whereby damage-associated molecular patterns (DAMPs) or pathogen-associated molecular patterns (PAMPs), NO, lipopolysaccharide and TNF-α from local macrophages cause MSC to emit PGE2. The PGE2 changes macrophages to an anti-inflammatory, so-called M2, phenotype that secretes IL-10 as well as anti-inflammatory TGFß, IP10, and PGE2 [273]. MSC require inflammatory activation such as by cytokines secreted by immune cells, to acquire. TNF-α, interferon (IFN)γ and IL1β appear to play a key role in this activation [274, 275]. Therefore, the inflammatory condition and the immunological status of administered therapeutic MSC are important and require optimization to reach optimal clinical

efficacy. Immunosuppressive impact of MSC can be in two ways: (a) cell contact mechanisms (i.e. through Jagged1-Notch1) [276]; (b) paracrine impact via PGE2, indoleamine 2,3-dioxygenase (IDO) [277], IL-6, IL-10 [278], hepatocyte growth factor (HGF) [279], TGFβ1 [280], TSG6 [281], NO [282] and heme oxygenase-1 (HO-1) [283].

MSC suppress production of cytokine and T-cell proliferation [282, 284]. MSC-derived IL-6 constitutively polarizes macrophages towards the M2 phenotype [285]. This polarization is also accomplished via MSC-derived IDO and PGE2. MSC that do not secrete IL-6, drive polarization of macrophages towards the pro-inflammatory M1 phenotype, which expresses IFNγ, TNF-α, and CD40L [286]. Promoted polarization of M2 by MSC, associates with a high expression of the mannose receptor CD206, increased production of IL-10 and a reduced production of pro-inflammatory cytokines and reduced phagocytic activity [287].

The expression of co-stimulatory molecule CD86 and MHCII on macrophages is reduced by MSC thus diminishing their stimulatory potency of the adaptive immune system [288]. MSC suppress mast cells by their constitutive release of PGE2 upon pro-inflammatory COX-2 upregulation [289] and suppress expression of TNF-α and IL-6 in activated macrophages [288]. The inhibition of natural killer cells (NK) is through IDO expression by MSC [290] which coincides with suppression of NK activating receptors [291]. MSC repress proliferation of B cells by arrest at the G0/G1 check point, without induction of apoptosis [292-294]. Preventing the allogeneic skin grafts rejection [295], ameliorating graft-versus-host disease (GvHD) [296], experimental autoimmune encephalomyelitis [297], collagen-induced arthritis [298], sepsis [299] and colitis [300, 301] are all reported after applying MSC.

15. Adipose Tissue

Adipose tissue, in mammals, has been grouped into: white adipose tissue (WAT), the storage of energy with adipokine secretory capacity which is morphologically described by the extensive lipid vacuoles in vivo. (b) brown adipose tissue (BAT), particular for energy consumption in fatty acids metabolism and providing heat [302] which is morphologically described by the small lipid vacuoles in vivo. BAT is closely associated with skeletal muscle as opposed to WAT that is found as visceral fat and subcutaneous fat depots [303, 304]. Of note, there is a sub-type adipocyte called Beige adipocytes (distinguished as brown/white), with the possibility of energy storage and express UCP1, however this type is related to WAT [305]. WAT and BAT derives from various precursor cell populations. Finally, perivascular adipose tissue (PVAT) is found around large arteries and important for blood pressure regulation [306]. The phenotype of PVAT is intermediate between WAT and BAT. In adipogenesis, PPARγ heterodimerizes with retinoid X receptor (RXR) and drives the development of differentiated adipocytes by regulation of downstream target gene expression. The CCAAT/enhancer-binding proteins (C/EBP) family (α, β, δ) participate in adipogenesis in a feedback loop to control the expression of PPARγ [307, 308]. Progenitor cells of skeletal muscle i.e. satellite cells, can also differentiate into either muscle cells or BAT, but not WAT [304]. Adipocytes' main endocrine function is the production of fat-derived systemic mediators such as adipokines, e.g. adiponectin, leptin, and resistin, but also retinol binding protein 4 (RBP4) and pro-inflammatory TNFα, that together maintain a balanced systemic metabolism [309]. This endocrine capacity is maintained by both WAT and BAT.

16. Adipose tissue-derived stromal cells (ASC)

Several of names have been used to denote the plastic adherent cell population isolated from fat tissue after collagenase digestion. Adipose tissue-derived Stem/Stromal Cells (ASC); Adipose-Derived Adult Stem/Stromal (ADAS) Cells, Adipose-Derived Stromal Cells (ASC), Adipose Stromal Cells (ASC), Adipose Mesenchymal Stem Cells (AdMSC), Lipoblast, Pericyte, Pre-Adipocyte, Processed Lipoaspirate (PLA) Cells have all been used to distinguish the same cell population [310]. A current definition from the 2004 meeting of the International Fat Applied Technology Society (IFATS) has settled on the expression "adipose tissue-derived stem cells" (ASC) [311].

However, because self-renewal has not been conclusively confirmed and, in concurrence with the announcement of ISCT [272], we use the term "stromal" instead of "stem". First time, Zuk and his colleagues recognized ASC in 2001; they characterized the stem cell qualities of ASC by their capacity to differentiate into other mesenchymal lineages [312].

ASC can be easily isolated from WAT [313]. A ubiquitous amount of ASC can be isolated from lipoaspirates, the waste result of liposuction operations. About 300mL of lipoaspirates may yield 1×10^7 to 6×10^8 cells. Besides, ASC reach senescence upon prolonged passaging in vitro but (in general) can be cultured longer compared to bone marrow mesenchymal stem cells (BM-MSC) [314-316]. ASC are a promising choice for cell therapy. ASC can be harvested, propagated and handled effectively with relatively mild procedures. ASC have a pluripotency capacity equivalent to BM-MSC and the

harvesting process from donors i.e. lipoaspiration, requires just local anesthesia and a short recovery time [317].

ASC are characterized by their capacity to adhere to plastic as all the MSC; ASC express certain cell surface markers, i.e.CD73, CD90 and CD105 whereas lacking the expression of CD34 and CD45; There have been references that affirm specific markers like CD49d, CD105, CD44 and CD29 are reliably upregulated in ASC culture [270, 318-320]. Noteworthy, surface expression of CD49d, as known as integrin α4β1 or VLA, decreases in ASC culture significantly [312, 321]. At last, ASC require not be cultured long period of times to get desired number of cells to accomplish what is called as therapeutic threshold [310, 316, 322-324].

17. ASC Isolation

In 1960, Rodbell and colleagues, established the first method to isolate cells from adipose tissue [325]. Briefly, the rat fat pads were minced and washed to get rid of mixed hematopoietic cells. The minced tissues were incubated with collagenase and centrifuged. Subsequently the floating population of mature adipocytes was separated from the pelleted so-called stromal vascular fraction (SVF). The last step comprised plating the SVF to select for the plastic adherent population which was presumed to contain pre-adipocytes. The liposuction aspiration procedure has no effect on the viability of isolated cells [326-328]. Virtually all presently used methods are adjusted from the Rodbell technique.

The SVF derived from fat tissue is a mixed population of stroma i.e. vascular cells (EC, SMC, pericytes) and fibroblasts, as well as immune cells (macrophages and lymphocytes) and preadipocytes as known as ASC [329, 330]. The superficial location of fat tissue makes it visually

accessible and can be removed from a donor without serious harm [331].

Worldwide survey published in 2002 demonstrates that in the vicinity of 1994 and 2000 zero mortality was reported in 66,570 liposuction operations (serious adverse event rate of 0.068%) [332]. In comparison, lipoaspirates and bone marrow aspirates respectively, contain 2% and 0.002% MSC [333].

The fat tissue from abdomen area has the higher ASC yield than the hip/thigh, albeit no distinction in differentiation capacity between the two origins were found [334].

18. ASC vs. MSC

In 2001, Gronthos and colleagues showed that ASC express CD105, CD106, CD166 and CD44 which are considered as MSC markers. Plus the expression of perivascular cell marker, CD146 [323]. In the meantime, Zuk stated that ASC and MSC have similar ability to differentiate into adipogenic, osteogenic, chondrogenic and myogenic cells [312, 321].

Additionally, similar gene expression table and proliferation rates have been documented for MSC and ASC [335, 336].

19. ASC vs. BM-MSC

ASC and BM-MSC are both stromal cells with the capacity to adhere to plastic. Also, their growth kinetics, cell senescence, gene transduction efficiency have been exhibited in a similar pattern

[337], as well as their gene transcription and cell surface marker expression [324]. Fat tissue, as opposed to bone marrow, is regularly removed in cosmetic operations with negligible risk to the patient. From this tissue, 200,000 – 290,000 cells/g of tissue [338] or 404,000 cells/ml of lipoaspirate [314] can be isolated, which this reality makes fat tissue a bottomless and available source of stem cells. It is difficult to state accurately what volume of tissue will be needed until characterized treatment parameters.

20. ASC vs SVF

The presence of endothelial precursor cells alongside the ASC in SVF is the one and only advantage of SVF over ASC. The inconvenience of SVF usage is that the quantity of cells that can be applied for cell therapy is constrained to what can be removed from the patient. On the other hand, purified ASC have a broadened time of cell culture which implies that the cells can be cultured up to far more prominent numbers than initial isolated cell number [353]. The heterogenous mixture of cells in SVF, renders this less suitable for e.g. intraocular use: the advantage of cultured cells such as ASC, is that these have a significantly lower degree of heterogeneity than SVF, albeit not absent.

21. ASC vs. Pericytes

ASC have been shown to have phenotypic and functional resemblance to pericytes [339, 340]. Pericytes and ASC are of mesenchymal origin, and harbor a similar potency to differentiate into muscle cells, osteoblasts, chondrocytes, and adipocytes [341-343].

Surface markers including NG2, PDGFR α and β, and N-cadherin are shared between ASC and pericytes [344]. ASC have a pericytic property to self-assemble into vascular network in co-culture with EC [345-347]. On monolayers of ASC, EC form branching networks with a degree of similarity to the sprouting networks form by EC suspensions on matrigel [348]. Injection of ASC-derived pericytes after TGF-β1 treatment, could coordinate into abluminal areas around retinal capillaries in DR models, which is a significant pericyte characteristic [349] and suggesting ASC could serve to substitute pericytes [350].

ASC joined vascular system in murine model of oxygen-induced retinopathy (OIR) and maintain their pericytic phenotype for at least two months after injection [349]. ASC diminish the capillary loss by 79% in the Akimba mouse model with DR [351]. ASC promoted re-endothelialization via Ang-1 secretion in a time-dependent manner [352]. The unchanged vessel stabilizing properties of ASC in hyperglycemia indicate that ASC are able to maintain fate and function in the hostile diabetic condition while retinal pericytes cannot [345].

22. ASC in Cell Therapy

Initially, the aim of clinical application of ASC was their capacity to differentiate into different cell lineages which are important to the field of regenerative medicine. This includes tissue engineering of bone and cartilage, which is the constructive action of ASC. Injected human ASC into immunosuppressed mice differentiated into numerous organs, i.e. bone marrow, brain, thymus, heart, liver, and lung [354] proposing that ASC can possibly use to repair numerous

organs. The systemic distribution of ASC by means of intravenous, intraperitoneal, intra-arterial, or intracardial injection depends on the native homing of ASC to the damaged site. Expression of cytokine and chemokine receptors on ASC cell surface, empower them to move to the damaged tissue. MSC culturing brings about adjustments of their cell surface receptors expression, i.e. the C-X-C chemokine receptor compose 4 (CXCR4), which are fundamental for homing after injection [355]. For this purpose, CXCR4 expression can be instigated by cytokine cocktail in culture, which has been appeared to boost the MSC homing capability [356]. Besides, culturing ASC under hypoxia can expand expression of CXCR4 and in this way improve the ASC relocation [357]. Accumulation of ASC after intravenous injection principally in the lungs and also in the liver, heart, and brain has been demonstrated [353]. Extra quantity of injected ASC could rapid cell aggregates, which may cause pulmonary emboli, infarctions and disturb the bloodstream in the patients after cell injection [358].

In contrast, in the past decade, the instructive action of ASC has been appreciated and thoroughly investigated. This constructive action is mediated through the secretion of a plethora of biologically active molecules that instruct receiving, target cells. As mentioned in earlier paragraphs, these paracrine factors may re-educate immune cells. ASC have been used widely in cardiac stem cell therapy primarily for their instructive capacity [359].

23. ASC Differentiation

ASC have exhibited a various versatility, including differentiation into adipo- [312, 321], osteo- [360, 361], chondro- [362, 363], myo- [364], cardiomyo- [365, 366], endothelial [367], hepato- [368], neuro- [369-373], epithelial [374] and haematopoietic [375] lineages.

23.1.   ASC Differentiation to Contractile smooth muscle cells

ASC differentiation into smooth muscle cells (SMC) may offer elective treatment for diseases that include SMC pathology, i.e. gastrointestinal disease, urinary incontinence, cardiovascular complications, bladder dysfunction, hypertension and asthma [376, 377].

The identified markers for contractile SMC incorporate smooth muscle α-actin (αSMA), caldesmon, SM22α, calponin, smooth muscle myosin heavy chain (SM-MHC) and smoothelin. ASC can possibly differentiate into functional SMC. Preconditioning of ASC with Angiotensin 2 upregulated the expression of smooth muscles particular genes and furthermore inspired the TGF-β1 production and induced activation by phosphorylation of Smad2 [378]. Additionally, precondition the cells with PDGF and TGF-β1, upgrade the SMC phenotype in ASC [379].

23.2.   ASC Differentiation to Osteoblasts

The osteogenic capability of ASC has been reported in numerous in vitro studies [360, 361]. In 2003, a study gave the primary confirmation of in vivo bone formation subsequent in vitro differentiation of ASC into osteocytes [361]. One year later in 2004, a 7-year-old young girl with calvarial bone resorption was treated with

bone graft from the ilium supplemented with ASC. Figured tomography indicated re-ossification of the defect regions [380]. In another study ASC formed into mineralised woven bone following a month when stacked on a hardening injectable bone substitute (HIBS) biomaterial and injected subcutaneously into nude mice [381]. Conditioned medium of ASC contained HGF and matrix metalloproteinases which invigorated osteoblast proliferation and differentiation via an extracellular ERK/JNK signaling kinase and its transducer, the Smad transcription factor [382].

23.3.   ASC Differentiation to Myofibroblasts

In the presence of TGF-β1, mesenchymal cells as well as ASC [383] differentiate into myofibroblasts. These profoundly contractile cells are portrayed by increased of the extracellular network (ECM) proteins (i.e. collagen type1 and fibronectin), higher expression of αSMA and robust stress fibers [384]. It should be noted, that the difference between SMC, pericytes, myofibroblasts and even cultured ASC/MSC might be more semantic than factual: in culture these cell types share several markers that are often considered to be specific for each of these cell types. Until extensive 'omics' comparisons are performed the verdict remains inconclusive. Most likely, local tissue microenvironmental conditions dictate the (final) fate and function of these mesenchymal like cell types.

23.4.   ASC Differentiation to Cardiomyocytes

ASC may be an encouraging source for cardiovascular therapeutics [365, 366]. Mice ASC could differentiate into cardiomyocytes with high effectiveness. These discoveries depended on morphology and electrophysical parameters [385]. It should be mentioned that differentiation of ASC into cardiomyocytes is rather inefficient, while other MSC types such as cardiac precursor/stem cells (CPC/CSC) are

by far more efficient to generate large(r) numbes of cardiomyocytes that are required to treat the consequences of myocardial infarction.

23.5.   ASC differentiation to Chondrocytes

Regeneration of damaged cartilage by applying ASC could have huge medical and economic advantages. The hyaline cartilage has a low inborn regenerative ability and currently there is no regenerative treatment accessible for cartilage. In one study, the preconditioning of mouse ASC under hypoxia advances the chondrogenic capability of the cells that should be considered in further studies [386].

24. ASC in Vascular Network Formation

The role of ASC in angiogenesis/vasculogenesis surpasses the secretion of VEGF or other pro-angiogenic factors alone, in fact, some investigators claim that ASC differentiate into EC [311]. In angiogenesis, proliferation and migration of EC from existing vasculature generates new microvessels. These microvessels have a basic impact in the damaged tissue regeneration [387]. Hypoxia is a boost for the onset and progression of angiogenesis which is regulated via hypoxia-inducible factors (HIFs) [388].

The term of vasculogenesis, on the other hand, alludes to the vascular formation by recruitment, aggregation and differentiation of endothelial progenitor cells into vascular plexi [387].

Vessel formation is directed by growth factors signaling, i.e. VEGF, VEGF receptor 1 (VEGFR1/FLT1), VEGFR2 (KDR/FLK1), fibroblast growth factor (FGF), TGF-β1, angiopoietin-1/2 and Tie-2 [389]. ASC-derived VEGF, HGF and TGF-β1 have been reported in cultured

medium [390]. ASC are claimed to differentiate to both endothelial [367, 391, 392] and perivascular cells [101, 393, 394] although endothelial differentiation is questioned by several groups including by us. ASC can stabilize and support EC that form vascular structures by means of direct cell-cell contact guided by ASC-derived paracrine cues [348]. Injection of ASC in a hind limb ischemia model showed higher capillary density and perfusion in limbs, which this result confirms the angiogenic capability of ASC [390, 392].

Recently, our lab showed that the genetic knockdown of NOTCH2 in ASC (SH-NOTCH2) inhibits formation of vascular networks by HUVEC both on monolayers of ASC and in organotypical 3-dimentional co-cultures [395].

25. ASC in Soft Tissue Implantation and Wound Healing

ASC in STZ diabetic rats and obese diabetic (db/db) mice could augment healing full-thickness skin wounds [396, 397]. Conditioned medium from TNF-α-induced ASC accelerated wound repair and upregulated angiogenesis in a skin wound model [398]. ASC endorse wound healing via both differentiation (construction) and paracrine effects (instruction) [399]. Preconditioning of ASC by hypoxia enhances their wound-healing potential by stimulating the angiogenesis plus migration and deposition of collagen by dermal fibroblasts. The augmented wound healing effect of ASC is partly mediated via the secretion of VEGF and bFGF [400].

26. ASC in Ischemic Injuries

Injection of ASC into the myocardium following infarcts in a murine, enhanced cardiovascular recovery [401]. Enhanced recovery capacity is accredited to the ASCs' secretion of VEGF, FGF2 and stromal cell derived factor 1 alpha (SDF1α) which was followed by recruitment of bone marrow-derived endothelial progenitor cells to the ischemic damage area [402]. Transplantation of ASC which were preconditioned under hypoxia likewise enhances recuperation from hindlimb ischemia in murine models [403]. In general, ASC are cultured under normoxia (21% oxygen). Despite that, physiologically, ASC present at lower oxygen pressures, which is no more than a few percent in injured areas, in particular after ischemia [404]. ASC under hypoxia maintain their multipotency, proliferate more with less apoptosis [405]. Interestingly, ROS generation by hypoxia is high but increased the proliferation and viability of ASC [400, 406]. Rehman and his colleagues showed higher production of VEGF and HGF under hypoxia, that have been appeared to be in charge of the upgraded regenerative capability of ASC in ischemia models [407].

27. ASC in DR

The way that ASC share phenotypic markers and therapeutic properties with perivascular pericytes, makes them an alternative choice in the treatment of DR from the viewpoint of vascular stabilization and replacement of lost pericytes [408]. ASC particularly upregulated retinal EC survival under hyperglycemic conditions. In co-cultures with EC, ASC support vascular network formation and differentiate into pericytes [347, 348]. The direct cell-cell contact

between MSC and EC prompts pericyte phenotype in MSC with high expression αSMA and CD146 [348, 409].

One of the difficulties for ASC-therapy in DR is their secretion of proangiogenic growth factors i.e. VEGF and HGF [407], which may unfavorably stimulate retina for proliferative changes. MSC that are preconditioned toward the 'receiving' i.e. damaged microenvironment, appeared to alter their paracrine factors that may tweak between pro-angiogenic to anti-angiogenic state [410-412].

Hyperglycemia- induced Oxidative stress induces ASC apoptosis [345]. ASC with constitutive expression of antioxidant enzymes modulate oxidative stress efficiently [413] and stimulate recovery of damaged tissue by secretion of growth factors [414]. Intense increase in intracellular ROS activates tyrosine kinases (receptor-type or non-receptor-type) in ASC. First of them, PDGFRβ get phosphorylated, trailed by the phosphorylation of PI3K/Akt/mammalian targets in rapamycin (mTOR) and ERK1/2 pathway [406]. At that point, activation of these pathways hinders the degradation of hypoxia-inducible factor-1 alpha (HIF-1α) via propyl-hydroxylation of the von Hippel Lindau tumor suppressor protein (pVHL). All these lead to increased levels of cytosolic HIF-1α in ASC [400]. The collected HIF-1α translocates to the nucleus. After binding to hypoxia-responsive elements (HRE) in the nucleus, it regulates the transcription of its target genes. Among these, VEGF gene is upregulated bringing about more VEGF secretion [400, 407, 415]. Injection of ASC in the murine models with T2DM ameliorated hyperglycemia in 2 weeks and kept up for about six weeks. In the meantime, plasma concentrations of insulin and C-peptide were improved [416].

ASC can incorporate with retinal vasculature in various murine models of retinal vasculopathy, adjusting both pericyte morphology and pericyte markers, and protect the retina from diabetic capillary damage [349]. Additionally, ASC by suppressing inflammation and apoptosis, ameliorate neurodegeneration to improve visual capacity in the STZ-rat model [347]. Diabetic ASC are more prone to cellular senescence and apoptosis than non-diabetic ASC [417]. Hyperglycemia abrogates osteogenic and chondrogenic capability of ASC, however improves their adipogenic capacity. ASC under hyperglycemia have less proliferation in vitro [417] which is also shown in ASC from STZ-diabetic mice [418].

ASCs' ability for regeneration and wound healing is diminished under diabetic condition because of reduced secretion of HGF, VEGFA, and IGF [418]. Diabetic ASC have a higher level of apoptosis than healthy ASC [419].

28. ASC in Inflammatory diseases

Immunomodulatory and immunosuppressive impact of ASC was shown in an in vitro study [318] in 2005; it is demonstrated that ASC did not cause alloreactivity and could suppress lymphocyte response [420] and virtually block inflammatory cytokines production [421]. The immunosuppressive impact of ASC has been reliably seen in all following studies after that [268, 422-425]. While it stays disputable whether cell to cell contact is required for immunosuppressive impact [420, 426-430]. ASC suppress T-cell proliferation via secretion of IFN-γ/ IDO and PGE2 [422, 430]. Noteworthy, inhibition of PGE2 and IDO effectively ended these effects [431]. Expression of Jagged 1 by ASC adds to the T-cell proliferation suppression by means of its

activation of the Notch receptor and resulting hindrance of the NF-κB pathway [429]. Intravenous injection of human ASC to a mouse model of lupus erythematosis enhanced survival rate [432]. Comparable results were seen in a murine model of clinical arthritis [298, 421]. The co-implantation of ASC enhanced the engraftment of pancreatic β-islets in diabetic mice, by upgrading vascularization and lessening immune cell infiltration [433, 434]. It has been proposed that co-culture of ASC with highly inflammatory chondrocytes, down-regulate the outflow of inflammatory molecules while no impact was shown once chondrocytes had low or moderate levels of inflammation [435]. This is additionally confirmed by the study that showed the protective ASC was just seen in the osteoarthritis model once high synovial inflammation was available [436]. The paracrine effect of ASC is the major of their beneficial impacts in cell therapy which can be replaced by cell-free conditioned medium to avoid following tissue injuries from ASC transplantation [407, 437, 438].

29. Conditioned Medium of ASC

Application of ASC-conditioned medium (ASC-Cme) can be an alternative option to transplant of ASC in growth factor-based therapies. Cultured ASC, at early passages, secrete HGF, VEGF, TGF-β1, IGF1, macrophage colony-stimulating factor (CSF1), stromal cell-derived factor 1 (SDF1/CXCL12) [407], PDGF, super oxide dismutase [414], basic fibroblast growth factor (bFGF), TNF-α, IL-6, IL-7, IL-8, IL-11, adiponectin, angiotensin, cathepsin D, pentraxin, pregnancy zone protein and retinol-binding protein [407, 439, 440]. All these factors can be collected in ASC-Cme by using standardized and reproducible conventions [399]. The secretion of nerve growth factor has been shown by ASC as well [441]. Part of the beneficial impacts of ASC in promoting angiogenesis and preventing the apoptosis is associated with to the secretion of these soluble factors [401].

The destiny of injected cells and their secretion activity obviously depend upon the host microenvironment. Under inflammatory conditions, the immunosuppressive ability of ASC is enhanced, while their differentiation ability is stable [426, 427]. Secreted growth factors such as VEGF, HGF and bFGF by ASC promote angiogenesis, EC proliferation, and migration of stromal progenitor cell into the developing vessels and promote neovascularization via the mobilization of bone marrow-derived endothelial precursors [407, 442]. Senescence induced by IL-1β, i.e. senescence-related β-galactosidase activity can be downregulated, at least in part, by ASC-Cme. Likewise, the morphological changes with increased formation of actin stress fibers are modulated by ASC-Cme. Chondrocytes under ASC-Cme showed less oxidative stress, less mitogen-activated protein kinases and the lower expression of caveolin-1 and p21. The

impacts of ASC-Cme were identified within p53 acetylation which depends on increased Sirtuin 1 expression [296, 443].

Preferentially, ASC-Cme should be serum-free for clinical applications. However, serum is required for appropriate cell proliferation and impacts ASC expansion ex vivo. In addition, prolonged exposure to serum-free conditions causes oxidative stress and apoptosis in any cell type including ASC. The proliferation of rat BM-MSC in low-serum medium is lower than in high-serum medium. Conversely, human ASC under low-serum conditions (LASC) demonstrate practically identical growth to human BM-MSC under high-serum medium [444, 445]. The suppression of T cell proliferation by human LASC has been shown in vitro which is more effective than human ASC under high-serum conditions (HASC), regardless of the similar capacity of both cell types in differentiating into the mesenchymal cell [445].

Consequently, LASC- immunomodulatory function may have incredible potential in cell therapy. Outstandingly, LASC polarized macrophages into CD163+ immune-regulatory cells via the production of IL-10 more effectively than HASC [446]. Moreover, ASC-Cme boosted the activity of ROS scavengers i.e. superoxide dismutase and glutathione peroxidase in fibroblasts and keratinocytes [414]. All things considered, these outcomes show that ASC-Cme display as an antioxidant and anti-apoptotic mediator, which assumes a key part in cell protection.

30. Challenges of ASC-therapy

ASC isolated from human lipoaspirates vary in phenotype and purity among various investigations. The heterogeneous populations of cells after different isolations, making it doubtful if ASC separated from other cell types in the population, themselves, are in charge of resulted beneficial effects. The pro- angiogenic properties of ASC bring up the issue of the connection of these cells with advancing tumor formation. Although the administration of MSC into human has been stated no tumor formation upon two years follow up [447].

Up until now, clinical trials around the globe do not show the tumorigenicity of MSC-based treatment represent a notable risk. Should be noted, couple of conflicting investigations have been distributed, with a few reports exhibiting that ASC could advance tumor formation [448]. The quickly developing ASC-based therapy faces new additional challenges, including how finest to transport and stock living cells without harming their therapeutic capacity. Transportation and delivery techniques for stem cells are not generally concurred on. Presently, stem cell must freeze in a procedure known as cryopreservation [449, 450]. Frozen cells are costly to transport, as they should be kept frozen. Moreover, they are difficult to utilize at their destination as facilities to defrost and culture the cells are required. Applying the potential advantages of ASC in tissue engineering and cell-based therapies obliges effective methodology of maintenance and transportation of ASC with custody of their multi-potentiality and therapeutic capability.

OUTLINE OF THE THESIS

Diabetic retinopathy is the main reason for new instances of visual deficiency among grown-ups [27]. During the initial two decades of development of DM, about all patients with T1DM and >60% of patients with T2DM have DR [27, 28]. The current treatments for DR are successful at modulate a significant part of the progression of the disease and decrease loss of vision, yet these do not restore lost vision and their side effects cannot be ignored [45, 46]. Because these therapies are directed for preventing vision loss and DR can be asymptomatic, it is necessary to distinguish and treat patients in the early phase of the disease, before the onset of PDR. To accomplish this objective, cell-based therapies are attractive to both prevent the vascular complications and to augment recovery of debilitated retina, as shown by recent studies [408].

Perivascular coordination of ASC-derived pericytes has been shown in retinal vasculature. Administration of ASC reduced both vascular leakage and apoptosis in retinal vessels [340, 345, 349, 350]. Additionally, the immune modulatory effect of ASC could also play a role in modulating the DR-induced inflammation [451-453]. ASC demonstrate guarantee as potential treatment for DR, albeit that basic research is essential to better found clinical trials. The goal of this thesis is to achieve the optimal objects before applying the ASC-based therapy in DR. Although, diabetic retinal cells experience hyperglycemic condition and oxidative stress-induced apoptosis [168, 175, 176], ASC-derived pericytes onto the diabetic retinal vasculature remains unclear. We showed the impact of HG on ASC in vitro and established if the HG condition may affect the ASC's ability

to support vascular network formation and their pericytic capacity (Chapter 2).

In the diabetic retina, before histopathology signs can be perceived, dysfunctional mitochondria and increments apoptosis are shown [185-187]. It is therefore relevant to demonstrate the role of mitochondria in the advancement of DR. For this reason, we investigated the assessment of energy metabolic changes in hyperglycemically challenged ASC in detail. Our techniques gave broad data to assess bioenergetic changes in ASC before and after culturing under HG condition which may help to evaluate all the possible changes of the ASC after injecting to the diabetic environment in ASC-based treatment for DR (Chapter 3).

DR is a chronic inflammation [211]. This inflammation is composed by several factors that include release of pro-inflammatory cytokines, chemokines, and upregulation of adhesion molecules in the retina, serum, and vitreous samples from DR patients [222-224]. An immunomodulatory and immunosuppressive impact of ASC was shown in recent studies [318], while it remains unclear whether cell to cell contact is required for the immunosuppressive impact of ASC in diabetes [420, 426-430]. We investigated the double role of ASC in promoting the vascular network formation in contact with EC in vivo after intravitreal injection of ASC into the ROP mice model and its paracrine immunomodulatory effect on retinal endothelial cells under HG-induced inflammatory status. MSC ought to be actuated by inflammatory mediators (i.e. cytokines) to apply their immunomodulatory properties [39]. Along these lines, the inflammatory status of the ASC in the time of injection is essential to get the best clinical results. We examined the effects of different time-points of pre-culturing of ASC under HG condition to obtain the

optimal ASC-conditioned medium with the minimum pro-inflammatory impact and maximum anti-inflammatory and pro-angiogenic effects on HG-induced EC (Chapter 4).

Whereas a significant part of the studies centers around how cells can be isolated, expanded and transplanted, only minor thought has been given to how these cells can be maintained and transported to their clinical destination. Hypothermic storing of cells in their own particular culture medium proposes a fascinating alternative to skip the negative effects of liquid nitrogen cryopreservation or other protection techniques. We assessed the efficacy of a new pharmacologic compound, SUL-109, that shields ASC during cell preservation from hypothermic apoptosis without influencing their multi-potency capability. We introduced the new compound which would speak to a genuine advance change in how ASC can be delivered (Chapter 5).

Taking everything into account, in our discussion part, the consequences of all chapters are discussed and their future ramifications are explained (Chapter 6).

This thesis shows in a comprehensive fashion the restorative translational extension of adipose tissue-derived stromal cells-based therapy for diabetic retinopathy to state both supporting retinal vascular structure and inflammatory modulation.

References

1. Ahmed, A.M., *History of diabetes mellitus*. Saudi Medical Journal, 2002. 23(4): p. 373-378.

2. Eknoyan, G. and J. Nagy, *A history of diabetes mellitus or how a disease of the kidneys evolved into a kidney disease*. Advances in Chronic Kidney Disease, 2005. 12(2): p. 223-229.

3. Forbes, J.M. and M.E. Cooper, *Mechanisms of diabetic complications*. Physiol Rev, 2013. 93(1): p. 137-88.

4. Ogurtsova, K., et al., *IDF Diabetes Atlas: Global estimates for the prevalence of diabetes for 2015 and 2040*. Diabetes Research and Clinical Practice, 2017. 128: p. 40-50.

5. Adamiec-Mroczek, J., J. Oficjalska-Mlynczak, and M. Misiuk-Hojlo, *Proliferative diabetic retinopathy-The influence of diabetes control on the activation of the intraocular molecule system.* Diabetes Research and Clinical Practice, 2009. 84(1): p. 46-50.

6. Danaei, G., et al., *National, regional, and global trends in fasting plasma glucose and diabetes prevalence since 1980: systematic analysis of health examination surveys and epidemiological studies with 370 country-years and 2.7 million participants.* Lancet, 2011. 378(9785): p. 31-40.

7. *American diabetes association: Clinical practice recommendations 1997 - Introduction.* Diabetes Care, 1997. 20: p. S1-S1.

8. Shamoon, H., et al., *The Effect of Intensive Treatment of Diabetes on the Development and Progression of Long-Term Complications in Insulin-Dependent Diabetes-Mellitus*. New England Journal of Medicine, 1993. 329(14): p. 977-986.

9. Turner, R.C., et al., *Intensive blood-glucose control with sulphonylureas or insulin compared with conventional treatment and risk of complications in patients with type 2 diabetes (UKPDS 33).* Lancet, 1998. 352(9131): p. 837-853.

10. Mathis, D., L. Vence, and C. Benoist, *beta-cell death during progression to diabetes*. Nature, 2001. 414(6865): p. 792-798.

11. Davies, J.L., et al., *A Genome-Wide Search for Human Type-1 Diabetes Susceptibility Genes*. Nature, 1994. 371(6493): p. 130-136.

12. Nejentsev, S., et al., *Localization of type 1 diabetes susceptibility to the MHC class I genes HLA-B and HLA-A*. Nature, 2007. 450(7171): p. 887-U19.

13. Hyttinen, V., et al., *Genetic liability of type 1 diabetes and the onset age among 22,650 young Finnish twin pairs - A nationwide follow-up study*. Diabetes, 2003. 52(4): p. 1052-1055.

14. Associat, A.D., *Diagnosis and classification of diabetes mellitus*. Diabetes Care, 2008. 31: p. S55-S60.

15. Kahn, S.E., et al., *Quantification of the Relationship between Insulin Sensitivity and Beta-Cell Function in Human-Subjects - Evidence for a Hyperbolic Function.* Diabetes, 1993. 42(11): p. 1663-1672.

16. Beckman, J.A., M.A. Creager, and P. Libby, *Diabetes and atherosclerosis - Epidemiology, pathophysiology, and management*. Jama-Journal of the American Medical Association, 2002. 287(19): p. 2570-2581.

17. Burrows, N.R., et al., *Incidence of end-stage renal disease among persons with diabetes - United States, 1990-2002* (Reprinted from MMWR, vol 54, pg 1097-1100, 2005). Jama-Journal of the American Medical Association, 2005. 294(23): p. 2962-2963.

18. Congdon, N.G., D.S. Friedman, and T. Lietman, *Important causes of visual impairment in the world today*. Jama-Journal of the American Medical Association, 2003. 290(15): p. 2057-2060.

19. Edwards, M.S., et al., *Associations between retinal microvascular abnormalities and declining renal function in the elderly population: The Cardiovascular Health Study.* American Journal of Kidney Diseases, 2005. 46(2): p. 214-224.

20. Falanga, V., *Wound healing and its impairment in the diabetic foot*. Lancet, 2005. 366(9498): p. 1736-1743.

21. Grosso, A., et al., *Hypertensive retinopathy revisited: some answers, more questions.* British Journal of Ophthalmology, 2005. 89(12): p. 1646-1654.

22. Jeerakathil, T., et al., *Short-term risk for stroke is doubled in persons with newly treated type 2 diabetes compared with persons without diabetes - A population-based cohort study*. Stroke, 2007. 38(6): p. 1739-1743.

23. Wong, T.Y., et al., *Retinal microvascular abnormalities and renal dysfunction: The Atherosclerosis Risk in Communities Study*. Journal of the American Society of Nephrology, 2004. 15(9): p. 2469-2476.

24. Nathan, D.M., et al., *Modern-Day Clinical Course of Type 1 Diabetes Mellitus After30 Years' Duration The Diabetes Control and Complications Trial/Epidemiology of Diabetes Interventions and Complications and Pittsburgh Epidemiology of Diabetes Complications Experience (1983-2005).* Archives of Internal Medicine, 2009. 169(14): p. 1307-1316.

25. Chan, J.C.N., et al., *Renin angiotensin aldosterone system blockade and renal disease in patients with type 2 diabetes - An Asian perspective from the RENAAL study.* Diabetes Care, 2004. 27(4): p. 874-879.

26. Rosenson, R.S., P. Fioretto, and P.M. Dodson, *Does microvascular disease predict macrovascular events in type 2 diabetes?* Atherosclerosis, 2011. 218(1): p. 13-18.

27. Kempen, J.H., et al., *The prevalence of diabetic retinopathy among adults in the United States.* Archives of Ophthalmology, 2004. 122(4): p. 552-563.

28. Klein, R., et al., *The Wisconsin Epidemiologic-Study of Diabetic-Retinopathy .15. The Long-Term Incidence of Macular Edema.* Ophthalmology, 1995. 102(1): p. 7-16.

29. Chen, J., et al., *Suppression of Retinal Neovascularization by Erythropoietin siRNA in a Mouse Model of Proliferative Retinopathy*. Investigative Ophthalmology & Visual Science, 2009. 50(3): p. 1329-1335.

30. Cheung, N., P. Mitchell, and T.Y. Wong, *Diabetic retinopathy*. Lancet, 2010. 376(9735): p. 124-136.

31. Crawford, T.N., et al*., Diabetic retinopathy and angiogenesis*. Curr Diabetes Rev, 2009. 5(1): p. 8-13.

32. Harding, S., *Extracts from "concise clinical evidence". Diabetic retinopathy*. BMJ, 2003. 326(7397): p. 1023-5.

32. Mohamed, Q., M.C. Gillies, and T.Y. Wong, *Management of diabetic retinopathy: a systematic review*. JAMA, 2007. 298(8): p. 902-16.

34. Frank, R.N., *Diabetic retinopathy*. N Engl J Med, 2004. 350(1): p. 48-58.

35. Klein, R., et al., *The Wisconsin Epidemiologic Study of Diabetic Retinopathy: XXII the twenty-five-year progression of retinopathy in persons with type 1 diabetes.* Ophthalmology, 2008. 115(11): p. 1859-68.

36. Gustavsson, C., C.D. Agardh, and E. Agardh, *Profile of intraocular tumour necrosis factor-alpha and interleukin-6 in diabetic subjects with different degrees of diabetic retinopathy*. Acta Ophthalmol, 2013. 91(5): p. 445-52.

37. Diabetes, C., et al., *The effect of intensive treatment of diabetes on the development and progression of long-term complications in insulin-dependent diabetes mellitus.* N Engl J Med, 1993. 329(14): p. 977-86.

38. *Effect of intensive diabetes treatment on the development and progression of long-term complications in adolescents with insulin-dependent diabetes mellitus: Diabetes Control and Complications Trial. Diabetes Control and Complications Trial Research Group.* J Pediatr, 1994. 125(2): p. 177-88.

39. *Tight blood pressure control and risk of macrovascular and microvascular complications in type 2 diabetes: UKPDS 38. UK Prospective Diabetes Study Group*. BMJ, 1998. 317(7160): p. 703-13.

40. Chaturvedi, N., et al., *Effect of lisinopril on progression of retinopathy in normotensive people with type 1 diabetes. The EUCLID Study Group. EURODIAB Controlled Trial of Lisinopril in Insulin-Dependent Diabetes Mellitus.* Lancet, 1998. 351(9095): p. 28-31.

41. Mauer, M., et al., *Renal and retinal effects of enalapril and losartan in type 1 diabetes.* N Engl J Med, 2009. 361(1): p. 40-51.

42. *Early worsening of diabetic retinopathy in the Diabetes Control and Complications Trial.* Arch Ophthalmol, 1998. 116(7): p. 874-86.

43. Takimoto, C., et al., *Candesartan and insulin reduce renal sympathetic nerve activity in hypertensive type 1 diabetic rats*. Hypertens Res, 2008. 31(10): p. 1941-51.

44. Wu, X., et al., *Combined MMF and insulin therapy prevents renal injury in experimental diabetic rats.* Cytokine, 2006. 36(5-6): p. 229-36.

45. Dobree, J.H., *Simple diabetic retinopathy. Evolution of the lesions and therapeutic considerations*. Br J Ophthalmol, 1970. 54(1): p. 1-10.

46. Wilson, D.J., et al., *Macular grid photocoagulation. An experimental study on the primate retina.* Arch Ophthalmol, 1988. 106(1): p. 100-5.

47. Diabetic Retinopathy Clinical Research, N., et al., *Observational study of the development of diabetic macular edema following panretinal (scatter) photocoagulation given in 1 or 4 sittings*. Arch Ophthalmol, 2009. 127(2): p. 132-40.

48. Gardner, T.W., et al., *New insights into the pathophysiology of diabetic retinopathy: potential cell-specific therapeutic targets*. Diabetes Technol Ther, 2000. 2(4): p. 601-8.

49. Hammes, H.P., et al., *Pericytes and the pathogenesis of diabetic retinopathy*. Diabetes, 2002. 51(10): p. 3107-12.

50. Heng, L.Z., et al., *Diabetic retinopathy: pathogenesis, clinical grading, management and future developments*. Diabet Med, 2013. 30(6): p. 640-50.

51. Aiello, L.P., et al., *Vascular endothelial growth factor in ocular fluid of patients with diabetic retinopathy and other retinal disorders*. N Engl J Med, 1994. 331(22): p. 1480-7.

52. Aiello, L.M. and J. Cavallerano, *Diabetic retinopathy*. Curr Ther Endocrinol Metab, 1994. 5: p. 436-46.

53. Robinson, G.S., et al., *Oligodeoxynucleotides inhibit retinal neovascularization in a murine model of proliferative retinopathy*. Proc Natl Acad Sci U S A, 1996. 93(10): p. 4851-6.

54. Al-Latayfeh, M., et al., *Antiangiogenic therapy for ischemic retinopathies.* Cold Spring Harb Perspect Med, 2012. 2(6): p. a006411.

55. Ishida, S., et al., *VEGF164-mediated inflammation is required for pathological, but not physiological, ischemia-induced retinal neovascularization*. J Exp Med, 2003. 198(3): p. 483-9.

56. Bakri, S.J., et al., *Pharmacokinetics of intravitreal ranibizumab* (Lucentis). Ophthalmology, 2007. 114(12): p. 2179-82.

57. Drolet, D.W., et al., *Pharmacokinetics and safety of an anti-vascular endothelial growth factor aptamer (NX1838) following injection into the vitreous humor of rhesus monkeys*. Pharm Res, 2000. 17(12): p. 1503-10.

58. Gaudreault, J., et al., *Preclinical pharmacokinetics of Ranibizumab (rhuFabV2) after a single intravitreal administration.* Invest Ophthalmol Vis Sci, 2005. 46(2): p. 726-33.

59. Zhu, X., et al., *Risks of proteinuria and hypertension with bevacizumab, an antibody against vascular endothelial growth factor: systematic review and meta-analysis*. Am J Kidney Dis, 2007. 49(2): p. 186-93.

60. Torres-Soriano, M.E., et al., *Tractional retinal detachment after intravitreal injection of bevacizumab in proliferative diabetic retinopathy.* Retin Cases Brief Rep, 2009. 3(1): p. 70-3.

61. Simo, R. and C. Hernandez, *Intravitreous anti-VEGF for diabetic retinopathy: hopes and fears for a new therapeutic strategy*. Diabetologia, 2008. 51(9): p. 1574-80.

62. Tranos, P., et al., *Progression of diabetic tractional retinal detachment following single injection of intravitreal Avastin*. Eye (Lond), 2008. 22(6): p. 862.

63. Cunningham, M.A., J.L. Edelman, and S. Kaushal, *Intravitreal steroids for macular edema: the past, the present, and the future.* Surv Ophthalmol, 2008. 53(2): p. 139-49.

64. Armulik, A., G. Genove, and C. Betsholtz, *Pericytes: developmental, physiological, and pathological perspectives, problems, and promises*. Dev Cell, 2011. 21(2): p. 193-215.

65. Robison, W.G., Jr., et al., *Degenerated intramural pericytes ('ghost cells') in the retinal capillaries of diabetic rats.* Curr Eye Res, 1991. 10(4): p. 339-50.

66. Cogan, D.G., D. Toussaint, and T. Kuwabara, *Retinal vascular patterns. IV. Diabetic retinopathy*. Arch Ophthalmol, 1961. 66: p. 366-78.

67. Gao, W., et al., *High glucose concentrations alter hypoxia-induced control of vascular smooth muscle cell growth via a HIF-1alpha-dependent pathway*. J Mol Cell Cardiol, 2007. 42(3): p. 609-19.

68. Das, A., et al., *Increases in collagen type IV and laminin in galactose-induced retinal capillary basement membrane thickening--prevention by an aldose reductase inhibitor*. Exp Eye Res, 1990. 50(3): p. 269-80.

69. Das, A., et al., *Ultrastructural localization of extracellular matrix components in human retinal vessels and Bruch's membrane*. Arch Ophthalmol, 1990. 108(3): p. 421-9.

70. Jerdan, J.A. and B.M. Glaser, *Retinal microvessel extracellular matrix: an immunofluorescent study*. Invest Ophthalmol Vis Sci, 1986. 27(2): p. 194-203.

71. Cagliero, E., et al., *Characteristics and mechanisms of high-glucose-induced overexpression of basement membrane components in cultured human endothelial cells*. Diabetes, 1991. 40(1): p. 102-10.

72. Roy, S., E. Cagliero, and M. Lorenzi, *Fibronectin overexpression in retinal microvessels of patients with diabetes*. Invest Ophthalmol Vis Sci, 1996. 37(2): p. 258-66.

73. Roy, S. and M. Lorenzi, *Early biosynthetic changes in the diabetic-like retinopathy of galactose-fed rats*. Diabetologia, 1996. 39(6): p. 735-8.

74. Poladia, D.P., et al., *Innervation and connexin isoform expression during diabetes-related bladder dysfunction: early structural vs. neuronal remodelling*. Acta Diabetol, 2005. 42(3): p. 147-52.

75. Siperstein, M.D., R.H. Unger, and L.L. Madison, *Studies of muscle capillary basement membranes in normal subjects, diabetic, and prediabetic patients*. J Clin Invest, 1968. 47(9): p. 1973-99.

76. Dagli, M.L. and F.J. Hernandez-Blazquez, *Roles of gap junctions and connexins in non-neoplastic pathological processes in which cell proliferation is involved*. J Membr Biol, 2007. 218(1-3): p. 79-91.

77. Inoguchi, T., et al., *Altered gap junction activity in cardiovascular tissues of diabetes*. Med Electron Microsc, 2001. 34(2): p. 86-91.

78. Grammas, P. and M. Riden, *Retinal endothelial cells are more susceptible to oxidative stress and increased permeability than brain-derived endothelial cells*. Microvasc Res, 2003. 65(1): p. 18-23.

79. Esposito, K., et al., *Inflammatory cytokine concentrations are acutely increased by hyperglycemia in humans: role of oxidative stress.* Circulation, 2002. 106(16): p. 2067-72.

80. Antonetti, D.A., et al., *Molecular mechanisms of vascular permeability in diabetic retinopathy.* Semin Ophthalmol, 1999. 14(4): p. 240-8.

81. Harhaj, N.S., et al., *VEGF activation of protein kinase C stimulates occludin phosphorylation and contributes to endothelial permeability*. Invest Ophthalmol Vis Sci, 2006. 47(11): p. 5106-15.

82. Joussen, A.M., et al., *Leukocyte-mediated endothelial cell injury and death in the diabetic retina*. Am J Pathol, 2001. 158(1): p. 147-52.

83. Cunha-Vaz, J.G., *Pathophysiology of diabetic retinopathy.* Br J Ophthalmol, 1978. 62(6): p. 351-5.

84. Engerman, R.L. and T.S. Kern, *Retinopathy in animal models of diabetes*. Diabetes Metab Rev, 1995. 11(2): p. 109-20.

85. Barber, A.J., et al., *Neural apoptosis in the retina during experimental and human diabetes. Early onset and effect of insulin.* J Clin Invest, 1998. 102(4): p. 783-91.

86. Barber, A.J., et al., *The Ins2Akita mouse as a model of early retinal complications in diabetes.* Invest Ophthalmol Vis Sci, 2005. 46(6): p. 2210-8.

87. Bansal, R., N. Ahmad, and J.R. Kidwai, *Alloxan-glucose interaction: effect on incorporation of 14C-leucine into pancreatic islets of rat*. Acta Diabetol Lat, 1980. 17(2): p. 135-43.

88. Rossini, A.A., et al., *Genetic influence of the streptozotocin-induced insulitis and hyperglycemia.* Diabetes, 1977. 26(10): p. 916-20.

89. Madan, A. and J.S. Penn, *Animal models of oxygen-induced retinopathy*. Front Biosci, 2003. 8: p. d1030-43.

90. Ohno-Matsui, K., et al., *Inducible expression of vascular endothelial growth factor in adult mice causes severe proliferative retinopathy and retinal detachment.* Am J Pathol, 2002. 160(2): p. 711-9.

91. Ruberte, J., et al., *Increased ocular levels of IGF-1 in transgenic mice lead to diabetes-like eye disease*. J Clin Invest, 2004. 113(8): p. 1149-57.

92. Gyllensten, L.J. and B.E. Hellstrom, *Experimental approach to the pathogenesis of retrolental fibroplasia. I. Changes of the eye induced by exposure of newborn mice to concentrated oxygen*. Acta Paediatr Suppl, 1954. 43(100): p. 131-48.

93. Dorrell, M.I. and M. Friedlander, *Mechanisms of endothelial cell guidance and vascular patterning in the developing mouse retina*. Prog Retin Eye Res, 2006. 25(3): p. 277-95.

94. Smith, L.E., et al., *Oxygen-induced retinopathy in the mouse*. Invest Ophthalmol Vis Sci, 1994. 35(1): p. 101-11.

95. Wangsa-Wirawan, N.D. and R.A. Linsenmeier, *Retinal oxygen: fundamental and clinical aspects.* Arch Ophthalmol, 2003. 121(4): p. 547-57.

96. Pierce, E.A., et al., *Vascular endothelial growth factor/vascular permeability factor expression in a mouse model of retinal neovascularization.* Proc Natl Acad Sci U S A, 1995. 92(3): p. 905-9.

97. Smith, L.E., et al., *Regulation of vascular endothelial growth factor-dependent retinal neovascularization by insulin-like growth factor-1 receptor.* Nat Med, 1999. 5(12): p. 1390-5.

98. Yoshioka, M., et al., *A novel locus, Mody4, distal to D7Mit189 on chromosome 7 determines early-onset NIDDM in nonobese C57BL/6 (Akita) mutant mice*. Diabetes, 1997. 46(5): p. 887-94.

99. Han, Z., et al., *Retinal angiogenesis in the Ins2(Akita) mouse model of diabetic retinopathy*. Invest Ophthalmol Vis Sci, 2013. 54(1): p. 574-84.

100. Rakoczy, E.P., et al., *Characterization of a mouse model of hyperglycemia and retinal neovascularization*. Am J Pathol, 2010. 177(5): p. 2659-70.

101. Crisan, M., et al., *A perivascular origin for mesenchymal stem cells in multiple human organs.* Cell Stem Cell, 2008. 3(3): p. 301-13.

102. Sims, D.E., *The pericyte--a review.* Tissue Cell, 1986. 18(2): p. 153-74.

103. Cuevas, P., et al., *Pericyte endothelial gap junctions in human cerebral capillaries.* Anat Embryol (Berl), 1984. 170(2): p. 155-9.

104. Tilton, R.G., C. Kilo, and J.R. Williamson, *Pericyte-endothelial relationships in cardiac and skeletal muscle capillaries.* Microvasc Res, 1979. 18(3): p. 325-35.

105. Armulik, A., A. Abramsson, and C. Betsholtz, *Endothelial/pericyte interactions*. Circ Res, 2005. 97(6): p. 512-23.

106. Krause, D., J. Kunz, and R. Dermietzel, *Cerebral pericytes--a second line of defense in controlling blood-brain barrier peptide metabolism*. Adv Exp Med Biol, 1993. 331: p. 149-52.

107. Bandopadhyay, R., et al., *Contractile proteins in pericytes at the blood-brain and blood-retinal barriers*. J Neurocytol, 2001. 30(1): p. 35-44.

108. Haefliger, I.O. and D.R. Anderson, *Oxygen modulation of guanylate cyclase-mediated retinal pericyte relaxations with 3-morpholino-sydnonimine and atrial natriuretic peptide.* Invest Ophthalmol Vis Sci, 1997. 38(8): p. 1563-8.

109. Matsugi, T., Q. Chen, and D.R. Anderson, *Contractile responses of cultured bovine retinal pericytes to angiotensin II.* Arch Ophthalmol, 1997. 115(10): p. 1281-5.

110. Haefliger, I.O., A. Zschauer, and D.R. Anderson, *Relaxation of retinal pericyte contractile tone through the nitric oxide-cyclic guanosine monophosphate pathway*. Invest Ophthalmol Vis Sci, 1994. 35(3): p. 991-7.

111. Chen, Q. and D.R. Anderson, *Effect of CO_2 on intracellular pH and contraction of retinal capillary pericytes*. Invest Ophthalmol Vis Sci, 1997. 38(3): p. 643-51.

112. Matsugi, T., Q. Chen, and D.R. Anderson, *Adenosine-induced relaxation of cultured bovine retinal pericytes*. Invest Ophthalmol Vis Sci, 1997. 38(13): p. 2695-701.

113. Wang, Y.L., et al., *Strengthening tight junctions of retinal microvascular endothelial cells by pericytes under normoxia and hypoxia involving angiopoietin-1 signal way*. Eye (Lond), 2007. 21(12): p. 1501-10.

114. Darland, D.C., et al., *Pericyte production of cell-associated VEGF is differentiation-dependent and is associated with endothelial survival*. Dev Biol, 2003. 264(1): p. 275-88.

115. Enge, M., et al., *Endothelium-specific platelet-derived growth factor-B ablation mimics diabetic retinopathy*. EMBO J, 2002. 21(16): p. 4307-16.

116. Avolio, E. and P. Madeddu, *Discovering cardiac pericyte biology: From physiopathological mechanisms to potential therapeutic applications in ischemic heart disease.* Vascul Pharmacol, 2016. 86: p. 53-63.

117. Fuxe, J., et al., *Pericyte requirement for anti-leak action of angiopoietin-1 and vascular remodeling in sustained inflammation*. Am J Pathol, 2011. 178(6): p. 2897-909.

118. Goumans, M.J., et al., *Balancing the activation state of the endothelium via two distinct TGF-beta type I receptors*. EMBO J, 2002. 21(7): p. 1743-53.

119. Stratman, A.N., et al., *Endothelial-derived PDGF-BB and HB-EGF coordinately regulate pericyte recruitment during vasculogenic tube assembly and stabilization*. Blood, 2010. 116(22): p. 4720-30.

120. Chang, W.G., et al., *Pericytes modulate endothelial sprouting*. Cardiovasc Res, 2013. 100(3): p. 492-500.

121. Tillet, E., et al., *N-cadherin deficiency impairs pericyte recruitment, and not endothelial differentiation or sprouting, in embryonic stem cell-derived angiogenesis*. Exp Cell Res, 2005. 310(2): p. 392-400.

122. Tattersall, I.W., et al., *In vitro modeling of endothelial interaction with macrophages and pericytes demonstrates Notch signaling function in the vascular microenvironment*. Angiogenesis, 2016. 19(2): p. 201-15.

123. Yafai, Y., et al., *Retinal endothelial angiogenic activity: effects of hypoxia and glial (Muller) cells*. Microcirculation, 2004. 11(7): p. 577-86.

124. Bresnick, G.H., et al., *Patterns of ischemia in diabetic retinopathy.* Trans Sect Ophthalmol Am Acad Ophthalmol Otolaryngol, 1976. 81(4 Pt 1): p. OP694-709.

125. Kohner, E.M. and P. Henkind, *Correlation of fluorescein angiogram and retinal digest in diabetic retinopathy.* Am J Ophthalmol, 1970. 69(3): p. 403-14.

126. Fu, D., et al., *Mechanisms of modified LDL-induced pericyte loss and retinal injury in diabetic retinopathy*. Diabetologia, 2012. 55(11): p. 3128-40.

127. Romeo, G., et al., *Activation of nuclear factor-kappaB induced by diabetes and high glucose regulates a proapoptotic program in retinal pericytes.* Diabetes, 2002. 51(7): p. 2241-8.

128. Geraldes, P., et al., *Activation of PKC-delta and SHP-1 by hyperglycemia causes vascular cell apoptosis and diabetic retinopathy*. Nat Med, 2009. 15(11): p. 1298-306.

129. von Tell, D., A. Armulik, and C. Betsholtz*, Pericytes and vascular stability*. Exp Cell Res, 2006. 312(5): p. 623-9.

130. Davis, S., et al., *Angiopoietins have distinct modular domains essential for receptor binding, dimerization and superclustering*. Nat Struct Biol, 2003. 10(1): p. 38-44.

131. Maisonpierre, P.C., et al., *Angiopoietin-2, a natural antagonist for Tie2 that disrupts in vivo angiogenesis*. Science, 1997. 277(5322): p. 55-60.

132. Cai, J., et al., *The angiopoietin/Tie-2 system regulates pericyte survival and recruitment in diabetic retinopathy*. Invest Ophthalmol Vis Sci, 2008. 49(5): p. 2163-71.

133. Lemieux, C., et al., *Angiopoietins can directly activate endothelial cells and neutrophils to promote proinflammatory responses*. Blood, 2005. 105(4): p. 1523-30.

134. Asahara, T., et al., *Tie2 receptor ligands, angiopoietin-1 and angiopoietin-2, modulate VEGF-induced postnatal neovascularization*. Circ Res, 1998. 83(3): p. 233-40.

135. Takagi, H., et al., *Potential role of the angiopoietin/tie2 system in ischemia-induced retinal neovascularization*. Invest Ophthalmol Vis Sci, 2003. 44(1): p. 393-402.

136. Hammes, H.P., et al., *Angiopoietin-2 causes pericyte dropout in the normal retina: evidence for involvement in diabetic retinopathy*. Diabetes, 2004. 53(4): p. 1104-10.

137. Behl, Y., et al., *Diabetes-enhanced tumor necrosis factor-alpha production promotes apoptosis and the loss of retinal microvascular cells in type 1 and type 2 models of diabetic retinopathy*. Am J Pathol, 2008. 172(5): p. 1411-8.

138. Kowluru, R.A., Q. Zhong, and M. Kanwar, *Metabolic memory and diabetic retinopathy: role of inflammatory mediators in retinal pericytes*. Exp Eye Res, 2010. 90(5): p. 617-23.

139. Mathews, M.K., et al., *Vascular endothelial growth factor and vascular permeability changes in human diabetic retinopathy*. Invest Ophthalmol Vis Sci, 1997. 38(13): p. 2729-41.

140. Aiello, L.P., et al., *Vascular endothelial growth factor-induced retinal permeability is mediated by protein kinase C in vivo and suppressed by an orally effective beta-isoform-selective inhibitor.* Diabetes, 1997. 46(9): p. 1473-80.

141. Benjamin, L.E., et al., *Selective ablation of immature blood vessels in established human tumors follows vascular endothelial growth factor withdrawal*. J Clin Invest, 1999. 103(2): p. 159-65.

142. Gee, M.S., et al., *Tumor vessel development and maturation impose limits on the effectiveness of anti-vascular therapy*. Am J Pathol, 2003. 162(1): p. 183-93.

143. Durham, J.T., et al., *Pericyte chemomechanics and the angiogenic switch: insights into the pathogenesis of proliferative diabetic retinopathy?* Invest Ophthalmol Vis Sci, 2015. 56(6): p. 3441-59.

144. Trudeau, K., A.J. Molina, and S. Roy, *High glucose induces mitochondrial morphology and metabolic changes in retinal pericytes*. Invest Ophthalmol Vis Sci, 2011. 52(12): p. 8657-64.

145. Tian, X.Y., et al., *Uncoupling protein-2 protects endothelial function in diet-induced obese mice*. Circ Res, 2012. 110(9): p. 1211-6.

146. Trudeau, K., et al., *High glucose disrupts mitochondrial morphology in retinal endothelial cells: implications for diabetic retinopathy*. Am J Pathol, 2010. 177(1): p. 447-55.

147. Dymkowska, D., et al., *Hyperglycaemia modifies energy metabolism and reactive oxygen species formation in endothelial cells in vitro*. Arch Biochem Biophys, 2014. 542: p. 7-13.

148. Miyamoto, K., et al., *Prevention of leukostasis and vascular leakage in streptozotocin-induced diabetic retinopathy via intercellular adhesion molecule-1 inhibition.* Proc Natl Acad Sci U S A, 1999. 96(19): p. 10836-41.

149. Koziel, A., et al., *The influence of high glucose on the aerobic metabolism of endothelial EA.hy926 cells*. Pflugers Arch, 2012. 464(6): p. 657-69.

150. Karbach, S., et al., *Hyperglycemia and oxidative stress in cultured endothelial cells--a comparison of primary endothelial cells with an immortalized endothelial cell line*. J Diabetes Complications, 2012. 26(3): p. 155-62.

151. Akira, S. and K. Takeda, *Toll-like receptor signalling*. Nat Rev Immunol, 2004. 4(7): p. 499-511.

152. Beutler, B., *Inferences, questions and possibilities in Toll-like receptor signalling*. Nature, 2004. 430(6996): p. 257-63.

153. Rajamani, U. and I. Jialal, *Hyperglycemia induces Toll-like receptor-2 and -4 expression and activity in human microvascular retinal endothelial cells: implications for diabetic retinopathy.* J Diabetes Res, 2014. 2014: p. 790902.

154. Du, Y., V.P. Sarthy, and T.S. Kern, *Interaction between NO and COX pathways in retinal cells exposed to elevated glucose and retina of diabetic rats.* Am J Physiol Regul Integr Comp Physiol, 2004. 287(4): p. R735-41.

155. Li, A.F. and S. Roy, *High glucose-induced downregulation of connexin 43 expression promotes apoptosis in microvascular endothelial cells*. Invest Ophthalmol Vis Sci, 2009. 50(3): p. 1400-7.

156. Spoerri, P.E., et al., *Effects of VEGFR-1, VEGFR-2, and IGF-IR hammerhead ribozymes on glucose-mediated tight junction expression in cultured human retinal endothelial cells*. Mol Vis, 2006. 12: p. 32-42.

157. Bhattacharjee, P.S., et al., *High-glucose-induced endothelial cell injury is inhibited by a Peptide derived from human apolipoprotein E*. PLoS One, 2012. 7(12): p. e52152.

158. Miwa, K., et al., *The role of polyol pathway in glucose-induced apoptosis of cultured retinal pericytes*. Diabetes Res Clin Pract, 2003. 60(1): p. 1-9.

159. Murata, M., et al., *Selective pericyte degeneration in the retinal capillaries of galactose-fed dogs results from apoptosis linked to aldose reductase-catalyzed galactitol accumulation*. J Diabetes Complications, 2002. 16(5): p. 363-70.

160. Das Evcimen, N. and G.L. King, *The role of protein kinase C activation and the vascular complications of diabetes*. Pharmacol Res, 2007. 55(6): p. 498-510.

161. Galvez, M.I., *Protein kinase C inhibitors in the treatment of diabetic retinopathy. Review.* Curr Pharm Biotechnol, 2011. 12(3): p. 386-91.

162. Giacco, F. and M. Brownlee, *Oxidative stress and diabetic complications*. Circ Res, 2010. 107(9): p. 1058-70.

163. Brownlee, M., *Biochemistry and molecular cell biology of diabetic complications.* Nature, 2001. 414(6865): p. 813-20.

164. Cameron, N.E., et al., *Vascular factors and metabolic interactions in the pathogenesis of diabetic neuropathy*. Diabetologia, 2001. 44(11): p. 1973-88.

165. Denis, U., et al., *Advanced glycation end-products induce apoptosis of bovine retinal pericytes in culture: involvement of diacylglycerol/ceramide production and oxidative stress induction*. Free Radic Biol Med, 2002. 33(2): p. 236-47.

166. Yamagishi, S., et al., *Advanced glycation end products-induced apoptosis and overexpression of vascular endothelial growth factor in bovine retinal pericytes.* Biochem Biophys Res Commun, 2002. 290(3): p. 973-8.

167. Yang, Y., et al., *Retinal redox stress and remodeling in cardiometabolic syndrome and diabetes*. Oxid Med Cell Longev, 2010. 3(6): p. 392-403.

168. Brownlee, M., *The pathobiology of diabetic complications: a unifying mechanism*. Diabetes, 2005. 54(6): p. 1615-25.

169. Hattori, T., et al., *Aldose reductase inhibitor fidarestat attenuates leukocyte-endothelial interactions in experimental diabetic rat retina in vivo.* Curr Eye Res, 2010. 35(2): p. 146-54.

170. Obrosova, I.G., et al., *Aldose reductase inhibitor fidarestat prevents retinal oxidative stress and vascular endothelial growth factor overexpression in streptozotocin-diabetic rats.* Diabetes, 2003. 52(3): p. 864-71.

171. Nitti, M., et al., *PKC delta and NADPH oxidase in AGE-induced neuronal death.* Neurosci Lett, 2007. 416(3): p. 261-5.

172. Yamagishi, S., *Role of advanced glycation end products (AGEs) and receptor for AGEs (RAGE) in vascular damage in diabetes*. Exp Gerontol, 2011. 46(4): p. 217-24.

173. Yamagishi, S., et al*., Beraprost sodium, a prostaglandin I2 analogue, protects against advanced gycation end products-induced injury in cultured retinal pericytes*. Mol Med, 2002. 8(9): p. 546-50.

174. Pacher, P. and C. Szabo, *Role of poly(ADP-ribose) polymerase-1 activation in the pathogenesis of diabetic complications: endothelial dysfunction, as a common underlying theme*. Antioxid Redox Signal, 2005. 7(11-12): p. 1568-80.

175. Gologorsky, D., A. Thanos, and D. Vavvas, *Therapeutic interventions against inflammatory and angiogenic mediators in proliferative diabetic retinopathy.* Mediators Inflamm, 2012. 2012: p. 629452.

176. Rangasamy, S., P.G. McGuire, and A. Das, *Diabetic retinopathy and inflammation: novel therapeutic targets*. Middle East Afr J Ophthalmol, 2012. 19(1): p. 52-9.

177. Sickel, W., *Electrical and metabolic manifestations of receptor and higher-order neuron activity in vertebrate retina.* Adv Exp Med Biol, 1972. 24(0): p. 101-18.

178. Li, S.Y., Z.J. Fu, and A.C. Lo, *Hypoxia-induced oxidative stress in ischemic retinopathy.* Oxid Med Cell Longev, 2012. 2012: p. 426769.

179. Droge, W., *Free radicals in the physiological control of cell function*. Physiol Rev, 2002. 82(1): p. 47-95.

180. Osborne, N.N., et al., *Retinal ischemia: mechanisms of damage and potential therapeutic strategies*. Prog Retin Eye Res, 2004. 23(1): p. 91-147.

181. Squier, T.C., *Oxidative stress and protein aggregation during biological aging.* Exp Gerontol, 2001. 36(9): p. 1539-50.

182. Bodrova, M.E., et al., *Cyclosporin A-sensitive decrease in the transmembrane potential across the inner membrane of liver mitochondria induced by low concentrations of fatty acids and Ca2+.* Biochemistry (Mosc), 2003. 68(4): p. 391-8.

183. Greco, T., J. Shafer, and G. Fiskum, *Sulforaphane inhibits mitochondrial permeability transition and oxidative stress*. Free Radic Biol Med, 2011. 51(12): p. 2164-71.

184. Tsutsui, H., S. Kinugawa, and S. Matsushima, *Mitochondrial oxidative stress and dysfunction in myocardial remodelling*. Cardiovasc Res, 2009. 81(3): p. 449-56.

185. Kern, T.S., et al., Response of capillary cell death to aminoguanidine predicts the development of retinopathy: comparison of diabetes and galactosemia. Invest Ophthalmol Vis Sci, 2000. 41(12): p. 3972-8.

186. Madsen-Bouterse, S.A., et al., *Role of mitochondrial DNA damage in the development of diabetic retinopathy, and the metabolic memory phenomenon associated with its progression*. Antioxid Redox Signal, 2010. 13(6): p. 797-805.

187. Madsen-Bouterse, S.A., et al., *Oxidative damage of mitochondrial DNA in diabetes and its protection by manganese superoxide dismutase*. Free Radic Res, 2010. 44(3): p. 313-21.

188. Sesaki, H. and R.E. Jensen, *Division versus fusion: Dnm1p and Fzo1p antagonistically regulate mitochondrial shape*. J Cell Biol, 1999. 147(4): p. 699-706.

189. McBride, H.M., M. Neuspiel, and S. Wasiak, *Mitochondria: more than just a powerhouse*. Curr Biol, 2006. 16(14): p. R551-60.

190. Cassidy-Stone, A., et al., *Chemical inhibition of the mitochondrial division dynamin reveals its role in Bax/Bak-dependent mitochondrial outer membrane permeabilization*. Dev Cell, 2008. 14(2): p. 193-204.

191. Tanaka, A. and R.J. Youle, *A chemical inhibitor of DRP1 uncouples mitochondrial fission and apoptosis*. Mol Cell, 2008. 29(4): p. 409-10.

192. Jensen, P.K., *Antimycin-insensitive oxidation of succinate and reduced nicotinamide-adenine dinucleotide in electron-transport particles. I. pH dependency and hydrogen peroxide formation*. Biochim Biophys Acta, 1966. 122(2): p. 157-66.

193. Hansford, R.G., B.A. Hogue, and V. *Mildaziene, Dependence of H2O2 formation by rat heart mitochondria on substrate availability and donor age.* J Bioenerg Biomembr, 1997. 29(1): p. 89-95.

194. Kudin, A.P., et al., *Characterization of superoxide-producing sites in isolated brain mitochondria*. J Biol Chem, 2004. 279(6): p. 4127-35.

195. Kushnareva, Y., A.N. Murphy, and A. Andreyev, *Complex I-mediated reactive oxygen species generation: modulation by cytochrome c and NAD(P)+ oxidation-reduction state*. Biochem J, 2002. 368(Pt 2): p. 545-53.

196. Kussmaul, L. and J. Hirst, *The mechanism of superoxide production by NADH:ubiquinone oxidoreductase (complex I) from bovine heart mitochondria*. Proc Natl Acad Sci U S A, 2006. 103(20): p. 7607-12.

197. Trumpower, B.L., *The protonmotive Q cycle. Energy transduction by coupling of proton translocation to electron transfer by the cytochrome bc1 complex*. J Biol Chem, 1990. 265(20): p. 11409-12.

198. Kiritoshi, S., et al., *Reactive oxygen species from mitochondria induce cyclooxygenase-2 gene expression in human mesangial cells: potential role in diabetic nephropathy*. Diabetes, 2003. 52(10): p. 2570-7.

199. Nishikawa, T., et al., *Normalizing mitochondrial superoxide production blocks three pathways of hyperglycaemic damage*. Nature, 2000. 404(6779): p. 787-90.

200. Abdul-Ghani, M.A. and R.A. *DeFronzo, Mitochondrial dysfunction, insulin resistance, and type 2 diabetes mellitus*. Curr Diab Rep, 2008. 8(3): p. 173-8.

201. Petersen, K.F., et al., *Impaired mitochondrial activity in the insulin-resistant offspring of patients with type 2 diabetes*. N Engl J Med, 2004. 350(7): p. 664-71.

202. Petersen, K.F., S. Dufour, and G.I. Shulman, *Decreased insulin-stimulated ATP synthesis and phosphate transport in muscle of insulin-resistant offspring of type 2 diabetic parents.* PLoS Med, 2005. 2(9): p. e233.

203. Morino, K., et al., *Reduced mitochondrial density and increased IRS-1 serine phosphorylation in muscle of insulin-resistant offspring of type 2 diabetic parents*. J Clin Invest, 2005. 115(12): p. 3587-93.

204. Befroy, D.E., et al., *Impaired mitochondrial substrate oxidation in muscle of insulin-resistant offspring of type 2 diabetic patients*. Diabetes, 2007. 56(5): p. 1376-81.

205. Kowluru, R.A., J. Tang, and T.S. Kern, *Abnormalities of retinal metabolism in diabetes and experimental galactosemia. VII. Effect of long-term administration of antioxidants on the development of retinopathy*. Diabetes, 2001. 50(8): p. 1938-42.

206. Ford, E.S., et al., *The metabolic syndrome and antioxidant concentrations: findings from the Third National Health and Nutrition Examination Survey*. Diabetes, 2003. 52(9): p. 2346-52.

207. Kanwar, M., et al., *Oxidative damage in the retinal mitochondria of diabetic mice: possible protection by superoxide dismutase*. Invest Ophthalmol Vis Sci, 2007. 48(8): p. 3805-11.

208. Brooks, C., et al., *Regulation of mitochondrial dynamics in acute kidney injury in cell culture and rodent models*. J Clin Invest, 2009. 119(5): p. 1275-85.

209. Tan, A.L., et al., *Disparate effects on renal and oxidative parameters following RAGE deletion, AGE accumulation inhibition, or dietary AGE control in experimental diabetic nephropathy*. Am J Physiol Renal Physiol, 2010. 298(3): p. F763-70.

210. Fong, D.S., et al., *Diabetic retinopathy*. Diabetes Care, 2003. 26(1): p. 226-9.

211. Tang, J. and T.S. Kern, *Inflammation in diabetic retinopathy*. Prog Retin Eye Res, 2011. 30(5): p. 343-58.

212. Serhan, C.N., *Resolution phase of inflammation: novel endogenous anti-inflammatory and proresolving lipid mediators and pathways*. Annu Rev Immunol, 2007. 25: p. 101-37.

213. Joussen, A.M., et al., *A central role for inflammation in the pathogenesis of diabetic retinopathy.* FASEB J, 2004. 18(12): p. 1450-2.

214. Tellez Gil, L., et al., *Modulation of soluble phases of endothelial/leukocyte adhesion molecule 1, intercellular adhesion molecule 1, and vascular cell adhesion molecule 1 with interleukin-1beta after experimental endotoxic challenge.* Crit Care Med, 2001. 29(4): p. 776-81.

215. Hirano, Y., et al., *Suppression of ICAM-1 in retinal and choroidal endothelial cells by plasmid small-interfering RNAs in vivo*. Invest Ophthalmol Vis Sci, 2010. 51(1): p. 508-15.

216. Ishida, S., et al., *VEGF164 is proinflammatory in the diabetic retina*. Invest Ophthalmol Vis Sci, 2003. 44(5): p. 2155-62.

217. Mohr, S., et al., *Caspase activation in retinas of diabetic and galactosemic mice and diabetic patients*. Diabetes, 2002. 51(4): p. 1172-9.

218. Vincent, J.A. and S. Mohr, *Inhibition of caspase-1/interleukin-1beta signaling prevents degeneration of retinal capillaries in diabetes and galactosemia.* Diabetes, 2007. 56(1): p. 224-30.

219. Demircan, N., et al., *Determination of vitreous interleukin-1 (IL-1) and tumour necrosis factor (TNF) levels in proliferative diabetic retinopathy.* Eye (Lond), 2006. 20(12): p. 1366-9.

220. Kocak, N., et al., *Comparison of vitreous and plasma levels of vascular endothelial growth factor, interleukin-6 and hepatocyte growth factor in diabetic and non-diabetic retinal detachment cases*. Ann Ophthalmol (Skokie), 2010. 42 Spec No: p. 10-4.

221. Hernandez, C., et al., *Somatostatin molecular variants in the vitreous fluid: a comparative study between diabetic patients with proliferative diabetic retinopathy and nondiabetic control subjects*. Diabetes Care, 2005. 28(8): p. 1941-7.

222. Meleth, A.D., et al., *Serum inflammatory markers in diabetic retinopathy*. Invest Ophthalmol Vis Sci, 2005. 46(11): p. 4295-301.

223. Maier, R., et al., *Multiplex bead analysis of vitreous and serum concentrations of inflammatory and proangiogenic factors in diabetic patients.* Mol Vis, 2008. 14: p. 637-43.

224. Murugeswari, P., et al., *Proinflammatory cytokines and angiogenic and anti-angiogenic factors in vitreous of patients with proliferative diabetic retinopathy and eales' disease*. Retina, 2008. 28(6): p. 817-24.

225. Harada, C., et al., *Diverse NF-kappaB expression in epiretinal membranes after human diabetic retinopathy and proliferative vitreoretinopathy*. Mol Vis, 2004. 10: p. 31-6.

226. Stamatovic, S.M., et al., *Protein kinase Calpha-RhoA cross-talk in CCL2-induced alterations in brain endothelial permeability*. J Biol Chem, 2006. 281(13): p. 8379-88.

227. Gavard, J., et al., *A role for a CXCR2/phosphatidylinositol 3-kinase gamma signaling axis in acute and chronic vascular permeability*. Mol Cell Biol, 2009. 29(9): p. 2469-80.

228. Smyth, E.M., et al., *Prostanoids in health and disease*. J Lipid Res, 2009. 50 Suppl: p. S423-8.

229. Dubois, R.N., et al., *Cyclooxygenase in biology and disease*. FASEB J, 1998. 12(12): p. 1063-73.

230. El-Asrar, A.M., L. Missotten, and K. Geboes, *Expression of cyclo-oxygenase-2 and downstream enzymes in diabetic fibrovascular epiretinal membranes*. Br J Ophthalmol, 2008. 92(11): p. 1534-9.

231. Ayalasomayajula, S.P. and U.B. Kompella, *Retinal delivery of celecoxib is several-fold higher following subconjunctival administration compared to systemic administration.* Pharm Res, 2004. 21(10): p. 1797-804.

232. Kim, S.J., A.J. Flach, and L.M. Jampol, *Nonsteroidal anti-inflammatory drugs in ophthalmology.* Surv Ophthalmol, 2010. 55(2): p. 108-33.

233. Babaev, V.R., et al., *Macrophage EP4 deficiency increases apoptosis and suppresses early atherosclerosis.* Cell Metab, 2008. 8(6): p. 492-501.

234. Williams, C.S., M. Mann, and R.N. DuBois, *The role of cyclooxygenases in inflammation, cancer, and development.* Oncogene, 1999. 18(55): p. 7908-16.

235. Romagnani, P., et al., *CXC chemokines: the regulatory link between inflammation and angiogenesis.* Trends Immunol, 2004. 25(4): p. 201-9.

236. Leali, D., et al., *Osteopontin (Eta-1) and fibroblast growth factor-2 cross-talk in angiogenesis.* J Immunol, 2003. 171(2): p. 1085-93.

237. Naldini, A., et al., *Cutting edge: IL-1beta mediates the proangiogenic activity of osteopontin-activated human monocytes.* J Immunol, 2006. 177(7): p. 4267-70.

238. Voronov, E., et al., *IL-1 is required for tumor invasiveness and angiogenesis.* Proc Natl Acad Sci U S A, 2003. 100(5): p. 2645-50.

239. Zipori, D., *The nature of stem cells: state rather than entity.* Nat Rev Genet, 2004. 5(11): p. 873-8.

240. Tapp, H., et al., *Adipose-derived stem cells: characterization and current application in orthopaedic tissue repair.* Exp Biol Med (Maywood), 2009. 234(1): p. 1-9.

241. Bunnell, B.A., et al., *Adipose-derived stem cells: isolation, expansion and differentiation.* Methods, 2008. 45(2): p. 115-20.

242. Robertson, J.A., *Human embryonic stem cell research: ethical and legal issues.* Nat Rev Genet, 2001. 2(1): p. 74-8.

243. Thomson, J.A., et al., *Embryonic stem cell lines derived from human blastocysts.* Science, 1998. 282(5391): p. 1145-7.

244. Morrison, S.J. and I.L. Weissman, *The long-term repopulating subset of hematopoietic stem cells is deterministic and isolatable by phenotype.* Immunity, 1994. 1(8): p. 661-73.

245. Takahashi, K., et al., *Induction of pluripotent stem cells from adult human fibroblasts by defined factors.* Cell, 2007. 131(5): p. 861-72.

246. Yu, J., et al., *Induced pluripotent stem cell lines derived from human somatic cells.* Science, 2007. 318(5858): p. 1917-20.

247. Wei, G., et al., *Stem cell plasticity in mammals and transdetermination in Drosophila: common themes?* Stem Cells, 2000. 18(6): p. 409-14.

248. Li, L. and H. Clevers, *Coexistence of quiescent and active adult stem cells in mammals*. Science, 2010. 327(5965): p. 542-5.

249. Weissman, I.L., *Stem cells: units of development, units of regeneration, and units in evolution*. Cell, 2000. 100(1): p. 157-68.

250. Porada, C.D., E.D. Zanjani, and G. *Almeida-Porad, Adult mesenchymal stem cells: a pluripotent population with multiple applications*. Curr Stem Cell Res Ther, 2006. 1(3): p. 365-9.

251. Zuk, P.A., et al., *Human adipose tissue is a source of multipotent stem cells*. Mol Biol Cell, 2002. 13(12): p. 4279-95.

252. Romanov, Y.A., V.A. Svintsitskaya, and V.N. Smirnov, *Searching for alternative sources of postnatal human mesenchymal stem cells: candidate MSC-like cells from umbilical cord.* Stem Cells, 2003. 21(1): p. 105-10.

253. Petrie, C., et al., *Proliferative capacity and osteogenic potential of novel dura mater stem cells on poly-lactic-co-glycolic acid*. J Biomed Mater Res A, 2008. 85(1): p. 61-71.

254. Hiraoka, K., et al., *Mesenchymal progenitor cells in adult human articular cartilage.* Biorheology, 2006. 43(3,4): p. 447-54.

255. da Silva Meirelles, L., P.C. Chagastelles, and N.B. Nardi, *Mesenchymal stem cells reside in virtually all post-natal organs and tissues*. J Cell Sci, 2006. 119(Pt 11): p. 2204-13.

256. Janjanin, S., et al., *Human palatine tonsil: a new potential tissue source of multipotent mesenchymal progenitor cells*. Arthritis Res Ther, 2008. 10(4): p. R83.

257. De Bari, C., et al., *Multipotent mesenchymal stem cells from adult human synovial membrane.* Arthritis Rheum, 2001. 44(8): p. 1928-42.

258. Shih, D.T., et al., *Isolation and characterization of neurogenic mesenchymal stem cells in human scalp tissue*. Stem Cells, 2005. 23(7): p. 1012-20.

259. Sieber-Blum, M. and M. Grim, *The adult hair follicle: cradle for pluripotent neural crest stem cells.* Birth Defects Res C Embryo Today, 2004. 72(2): p. 162-72.

260. Fukuchi, Y., et al., *Human placenta-derived cells have mesenchymal stem/progenitor cell potential.* Stem Cells, 2004. 22(5): p. 649-58.

261. Gronthos, S., et al., *Postnatal human dental pulp stem cells (DPSCs) in vitro and in vivo.* Proc Natl Acad Sci U S A, 2000. 97(25): p. 13625-30.

262. Friedenstein, A.J., S. Piatetzky, II, and K.V. Petrakova, *Osteogenesis in transplants of bone marrow cells*. J Embryol Exp Morphol, 1966. 16(3): p. 381-90.

263. Dominici, M., et al., *Minimal criteria for defining multipotent mesenchymal stromal cells. The International Society for Cellular Therapy position statement*. Cytotherapy, 2006. 8(4): p. 315-7.

264. Chamberlain, G., et al., *Concise review: mesenchymal stem cells: their phenotype, differentiation capacity, immunological features, and potential for homing.* Stem Cells, 2007. 25(11): p. 2739-49.

265. Prockop, D.J., *Marrow stromal cells as stem cells for nonhematopoietic tissues.* Science, 1997. 276(5309): p. 71-4.

266. Kahan, B.D., *Individuality: the barrier to optimal immunosuppression.* Nat Rev Immunol, 2003. 3(10): p. 831-8.

267. Leto Barone, A.A., et al., *Immunomodulatory effects of adipose-derived stem cells: fact or fiction?* Biomed Res Int, 2013. 2013: p. 383685.

268. Yanez, R., et al., *Adipose tissue-derived mesenchymal stem cells have in vivo immunosuppressive properties applicable for the control of the graft-versus-host disease*. Stem Cells, 2006. 24(11): p. 2582-91.

269. Jiang, Y., et al., *Pluripotency of mesenchymal stem cells derived from adult marrow.* Nature, 2002. 418(6893): p. 41-9.

270. Pittenger, M.F., et al., *Multilineage potential of adult human mesenchymal stem cells.* Science, 1999. 284(5411): p. 143-7.

271. Gimble, J.M., et al., *Adipose-derived stromal/stem cells: a primer.* Organogenesis, 2013. 9(1): p. 3-10.

272. Horwitz, E.M., et al., *Clarification of the nomenclature for MSC: The International Society for Cellular Therapy position statement*. Cytotherapy, 2005. 7(5): p. 393-5.

273. Prockop, D.J. and J.Y. Oh, *Mesenchymal stem/stromal cells (MSCs): role as guardians of inflammation.* Mol Ther, 2012. 20(1): p. 14-20.

274. Krampera, M., et al., *Role for interferon-gamma in the immunomodulatory activity of human bone marrow mesenchymal stem cells.* Stem Cells, 2006. 24(2): p. 386-98.

275. Prasanna, S.J., et al., *Pro-inflammatory cytokines, IFNgamma and TNFalpha, influence immune properties of human bone marrow and Wharton jelly mesenchymal stem cells differentially*. PLoS One, 2010. 5(2): p. e9016.

276. Liotta, F., et al., *Toll-like receptors 3 and 4 are expressed by human bone marrow-derived mesenchymal stem cells and can inhibit their T-cell modulatory activity by impairing Notch signaling*. Stem Cells, 2008. 26(1): p. 279-89.

277. Meisel, R., et al., *Human bone marrow stromal cells inhibit allogeneic T-cell responses by indoleamine 2,3-dioxygenase-mediated tryptophan degradation.* Blood, 2004. 103(12): p. 4619-21.

278. Batten, P., et al., *Human mesenchymal stem cells induce T cell anergy and downregulate T cell allo-responses via the TH2 pathway: relevance to tissue engineering human heart valves*. Tissue Eng, 2006. 12(8): p. 2263-73.

279. Di Nicola, M., et al., *Human bone marrow stromal cells suppress T-lymphocyte proliferation induced by cellular or nonspecific mitogenic stimuli*. Blood, 2002. 99(10): p. 3838-43.

280. Aggarwal, S. and M.F. Pittenger, *Human mesenchymal stem cells modulate allogeneic immune cell responses*. Blood, 2005. 105(4): p. 1815-22.

281. Lee, R.H., et al., *Intravenous hMSCs improve myocardial infarction in mice because cells embolized in lung are activated to secrete the anti-inflammatory protein TSG-6.* Cell Stem Cell, 2009. 5(1): p. 54-63.

282. Sato, K., et al., *Nitric oxide plays a critical role in suppression of T-cell proliferation by mesenchymal stem cells*. Blood, 2007. 109(1): p. 228-34.

283. Doorn, J., et al., *Therapeutic applications of mesenchymal stromal cells: paracrine effects and potential improvements*. Tissue Eng Part B Rev, 2012. 18(2): p. 101-15.

284. Rasmusson, I., et al., *Mesenchymal stem cells inhibit lymphocyte proliferation by mitogens and alloantigens by different mechanisms*. Exp Cell Res, 2005. 305(1): p. 33-41.

285. Eggenhofer, E. and M.J. Hoogduijn, *Mesenchymal stem cell-educated macrophages*. Transplant Res, 2012. 1(1): p. 12.

286. Bernardo, M.E. and W.E. Fibbe, *Mesenchymal stromal cells: sensors and switchers of inflammation*. Cell Stem Cell, 2013. 13(4): p. 392-402.

287. Kim, J. and P. Hematti, *Mesenchymal stem cell-educated macrophages: a novel type of alternatively activated macrophages*. Exp Hematol, 2009. 37(12): p. 1445-53.

288. Maggini, J., et al., *Mouse bone marrow-derived mesenchymal stromal cells turn activated macrophages into a regulatory-like profile*. PLoS One, 2010. 5(2): p. e9252.

289. Brown, J.M., et al., *Bone marrow stromal cells inhibit mast cell function via a COX2-dependent mechanism*. Clin Exp Allergy, 2011. 41(4): p. 526-34.

290. Spaggiari, G.M., et al., *Mesenchymal stem cell-natural killer cell interactions: evidence that activated NK cells are capable of killing MSCs, whereas MSCs can inhibit IL-2-induced NK-cell proliferation*. Blood, 2006. 107(4): p. 1484-90.

291. Sotiropoulou, P.A., et al., *Interactions between human mesenchymal stem cells and natural killer cells*. Stem Cells, 2006. 24(1): p. 74-85.

292. Corcione, A., et al., *Human mesenchymal stem cells modulate B-cell functions.* Blood, 2006. 107(1): p. 367-72.

293. Franquesa, M., et al., *Immunomodulatory effect of mesenchymal stem cells on B cells.* Front Immunol, 2012. 3: p. 212.

294. Tabera, S., et al., *The effect of mesenchymal stem cells on the viability, proliferation and differentiation of B-lymphocytes*. Haematologica, 2008. 93(9): p. 1301-9.

295. Bartholomew, A., et al., *Mesenchymal stem cells suppress lymphocyte proliferation in vitro and prolong skin graft survival in vivo*. Exp Hematol, 2002. 30(1): p. 42-8.

296. Le Blanc, K., et al., *Treatment of severe acute graft-versus-host disease with third party haploidentical mesenchymal stem cells*. Lancet, 2004. 363(9419): p. 1439-41.

297. Zappia, E., et al., *Mesenchymal stem cells ameliorate experimental autoimmune encephalomyelitis inducing T-cell anergy*. Blood, 2005. 106(5): p. 1755-61.

298. Gonzalez, M.A., et al., *Treatment of experimental arthritis by inducing immune tolerance with human adipose-derived mesenchymal stem cells*. Arthritis Rheum, 2009. 60(4): p. 1006-19.

299. Nemeth, K., et al., *Bone marrow stromal cells attenuate sepsis via prostaglandin E(2)-dependent reprogramming of host macrophages to increase their interleukin-10 production*. Nat Med, 2009. 15(1): p. 42-9.

300. Gonzalez, M.A., et al., *Adipose-derived mesenchymal stem cells alleviate experimental colitis by inhibiting inflammatory and autoimmune responses.* Gastroenterology, 2009. 136(3): p. 978-89.

301. Gonzalez-Rey, E., et al., *Human adult stem cells derived from adipose tissue protect against experimental colitis and sepsis*. Gut, 2009. 58(7): p. 929-39.

302. Spiegelman, B.M. and J.S. Flier, *Obesity and the regulation of energy balance.* Cell, 2001. 104(4): p. 531-43.

303. Seale, P., *Transcriptional control of brown adipocyte development and thermogenesis*. Int J Obes (Lond), 2010. 34 Suppl 1: p. S17-22.

304. Seale, P., et al., *PRDM16 controls a brown fat/skeletal muscle switch.* Nature, 2008. 454(7207): p. 961-7.

305. Wu, J., et al., *Beige adipocytes are a distinct type of thermogenic fat cell in mouse and human*. Cell, 2012. 150(2): p. 366-76.

306. Hildebrand, S., J. Stumer, and A. Pfeifer, *PVAT and Its Relation to Brown, Beige, and White Adipose Tissue in Development and Function*. Front Physiol, 2018. 9: p. 70.

307. Gesta, S., Y.H. Tseng, and C.R. Kahn, *Developmental origin of fat: tracking obesity to its source.* Cell, 2007. 131(2): p. 242-56.

308. Tontonoz, P. and B.M. Spiegelman, *Fat and beyond: the diverse biology of PPARgamma*. Annu Rev Biochem, 2008. 77: p. 289-312.

309. Waki, H. and P. Tontonoz, *Endocrine functions of adipose tissue*. Annu Rev Pathol, 2007. 2: p. 31-56.

310. Gimble, J.M., A.J. Katz, and B.A. Bunnell, *Adipose-derived stem cells for regenerative medicine*. Circ Res, 2007. 100(9): p. 1249-60.

311. Locke, M., J. Windsor, and P.R. Dunbar, *Human adipose-derived stem cells: isolation, characterization and applications in surgery*. ANZ J Surg, 2009. 79(4): p. 235-44.

312. Zuk, P.A., et al., *Multilineage cells from human adipose tissue: implications for cell-based therapies*. Tissue Eng, 2001. 7(2): p. 211-28.

313. Cawthorn, W.P., E.L. Scheller, and O.A. MacDougald, *Adipose tissue stem cells: the great WAT hope.* Trends Endocrinol Metab, 2012. 23(6): p. 270-7.

314. Aust, L., et al., *Yield of human adipose-derived adult stem cells from liposuction aspirates.* Cytotherapy, 2004. 6(1): p. 7-14.

315. Boquest, A.C., et al., *Isolation of stromal stem cells from human adipose tissue*. Methods Mol Biol, 2006. 325: p. 35-46.

316. Mitchell, J.B., et al., *Immunophenotype of human adipose-derived cells: temporal changes in stromal-associated and stem cell-associated markers*. Stem Cells, 2006. 24(2): p. 376-85.

317. Ogawa, R., *The importance of adipose-derived stem cells and vascularized tissue regeneration in the field of tissue transplantation*. Curr Stem Cell Res Ther, 2006. 1(1): p. 13-20.

318. Puissant, B., et al., *Immunomodulatory effect of human adipose tissue-derived adult stem cells: comparison with bone marrow mesenchymal stem cells*. Br J Haematol, 2005. 129(1): p. 118-29.

319. Sackstein, R., et al., *Ex vivo glycan engineering of CD44 programs human multipotent mesenchymal stromal cell trafficking to bone*. Nat Med, 2008. 14(2): p. 181-7.

320. Zhu, H., et al., *The role of the hyaluronan receptor CD44 in mesenchymal stem cell migration in the extracellular matrix*. Stem Cells, 2006. 24(4): p. 928-35.

321. Zuk, P.A., et al., *Human adipose tissue is a source of multipotent stem cells.* Molecular Biology of the Cell, 2002. 13(12): p. 4279-4295.

322. Boquest, A.C., et al., *Isolation and transcription profiling of purified uncultured human stromal stem cells: alteration of gene expression after in vitro cell culture.* Mol Biol Cell, 2005. 16(3): p. 1131-41.

323. Gronthos, S., et al., *Surface protein characterization of human adipose tissue-derived stromal cells*. J Cell Physiol, 2001. 189(1): p. 54-63.

324. Katz, A.J., et al., *Cell surface and transcriptional characterization of human adipose-derived adherent stromal (hADAS) cells*. Stem Cells, 2005. 23(3): p. 412-23.

325. Rodbell, M., *Metabolism of isolated fat cells. II. The similar effects of phospholipase C (Clostridium perfringens alpha toxin) and of insulin on glucose and amino acid metabolism*. J Biol Chem, 1966. 241(1): p. 130-9.

326. Lalikos, J.F., et al., *Biochemical assessment of cellular damage after adipocyte harvest.* Journal of Surgical Research, 1997. 70(1): p. 95-100.

327. Moore, J.H., et al., *Viability of Fat Obtained by Syringe Suction Lipectomy - Effects of Focal Anesthesia with Lidocaine*. Aesthetic Plastic Surgery, 1995. 19(4): p. 335-339.

328. Oedayrajsingh-Varma, M.J., et al., *Adipose tissue-derived mesenchymal stem cell yield and growth characteristics are affected by the tissue-harvesting procedure*. Cytotherapy, 2006. 8(2): p. 166-77.

329. Maumus, M., et al., *Native human adipose stromal cells: localization, morphology and phenotype*. Int J Obes (Lond), 2011. 35(9): p. 1141-53.

330. Zimmerlin, L., et al., *Stromal vascular progenitors in adult human adipose tissue*. Cytometry A, 2010. 77(1): p. 22-30.

331. Crandall, D.L., G.J. Hausman, and J.G. Kral, *A review of the microcirculation of adipose tissue: anatomic, metabolic, and angiogenic perspectives*. Microcirculation, 1997. 4(2): p. 211-32.

332. Housman, T.S., et al., *The safety of liposuction: results of a national survey.* Dermatol Surg, 2002. 28(11): p. 971-8.

333. Strem, B.M., et al., *Multipotential differentiation of adipose tissue-derived stem cells*. Keio J Med, 2005. 54(3): p. 132-41.

334. Jurgens, W.J., et al., *Effect of tissue-harvesting site on yield of stem cells derived from adipose tissue: implications for cell-based therapies*. Cell Tissue Res, 2008. 332(3): p. 415-26.

335. Lee, R.H., et al., *Characterization and expression analysis of mesenchymal stem cells from human bone marrow and adipose tissue*. Cell Physiol Biochem, 2004. 14(4-6): p. 311-24.

336. Wagner, W., et al., *Comparative characteristics of mesenchymal stem cells from human bone marrow, adipose tissue, and umbilical cord blood*. Exp Hematol, 2005. 33(11): p. 1402-16.

337. De Ugarte, D.A., et al., *Comparison of multi-lineage cells from human adipose tissue and bone marrow.* Cells Tissues Organs, 2003. 174(3): p. 101-9.

338. von Heimburg, D., et al., *Comparison of viable cell yield from excised versus aspirated adipose tissue*. Cells Tissues Organs, 2004. 178(2): p. 87-92.

339. Tang, W., et al., *White fat progenitor cells reside in the adipose vasculature*. Science, 2008. 322(5901): p. 583-6.

340. Traktuev, D.O., et al., *A population of multipotent CD34-positive adipose stromal cells share pericyte and mesenchymal surface markers, reside in a periendothelial location, and stabilize endothelial networks*. Circ Res, 2008. 102(1): p. 77-85.

341. Case, J., et al., *Clonal multilineage differentiation of murine common pluripotent stem cells isolated from skeletal muscle and adipose stromal cells*. Ann N Y Acad Sci, 2005. 1044: p. 183-200.

342. Farrington-Rock, C., et al., *Chondrogenic and adipogenic potential of microvascular pericytes*. Circulation, 2004. 110(15): p. 2226-32.

343. Morgan, J. and F. Muntoni, *Mural cells paint a new picture of muscle stem cells*. Nat Cell Biol, 2007. 9(3): p. 249-51.

344. Traktuev, D.O., et al., *A population of multipotent CD34-positive adipose stromal cells share pericyte and mesenchymal surface markers, reside in a periendothelial location, and stabilize endothelial networks*. Circulation Research, 2008. 102(1): p. 77-85.

345. Hajmousa, G., et al., *Hyperglycemia Induces Bioenergetic Changes in Adipose-Derived Stromal Cells While Their Pericytic Function Is Retained*. Stem Cells Dev, 2016. 25(19): p. 1444-53.

346. Merfeld-Clauss, S., et al., *Adipose Tissue Progenitor Cells Directly Interact with Endothelial Cells to Induce Vascular Network Formation*. Tissue Engineering Part A, 2010. 16(9): p. 2953-2966.

347. Rajashekhar, G., et al., *Regenerative Therapeutic Potential of Adipose Stromal Cells in Early Stage Diabetic Retinopathy*. Plos One, 2014. 9(1).

348. Merfeld-Clauss, S., et al., *Adipose tissue progenitor cells directly interact with endothelial cells to induce vascular network formation*. Tissue Eng Part A, 2010. 16(9): p. 2953-66.

349. Mendel, T.A., et al., *Pericytes derived from adipose-derived stem cells protect against retinal vasculopathy*. PLoS One, 2013. 8(5): p. e65691.

350. Rajashekhar, G., et al., *Regenerative therapeutic potential of adipose stromal cells in early stage diabetic retinopathy*. PLoS One, 2014. 9(1): p. e84671.

351. Gir, P., et al., *Human adipose stem cells: current clinical applications*. Plast Reconstr Surg, 2012. 129(6): p. 1277-90.

352. Takahashi, M., et al., *Angiopoietin-1 mediates adipose tissue-derived stem cell-induced inhibition of neointimal formation in rat femoral artery.* Circ J, 2013. 77(6): p. 1574-84.

353. Feisst, V., S. Meidinger, and M.B. Locke, *From bench to bedside: use of human adipose-derived stem cells*. Stem Cells Cloning, 2015. 8: p. 149-62.

354. Kim, D.H., et al., *Effect of partial hepatectomy on in vivo engraftment after intravenous administration of human adipose tissue stromal cells in mouse*. Microsurgery, 2003. 23(5): p. 424-31.

355. Rombouts, W.J. and R.E. Ploemacher, *Primary murine MSC show highly efficient homing to the bone marrow but lose homing ability following culture*. Leukemia, 2003. 17(1): p. 160-70.

356. Shi, M., et al., *Regulation of CXCR4 expression in human mesenchymal stem cells by cytokine treatment: role in homing efficiency in NOD/SCID mice.* Haematologica, 2007. 92(7): p. 897-904.

357. Thangarajah, H., et al., *IFATS collection: Adipose stromal cells adopt a proangiogenic phenotype under the influence of hypoxia*. Stem Cells, 2009. 27(1): p. 266-74.

358. Prockop, D.J. and S.D. Olson, *Clinical trials with adult stem/progenitor cells for tissue repair: let's not overlook some essential precautions.* Blood, 2007. 109(8): p. 3147-51.

359. Naaijkens, B.A., et al., *Therapeutic application of adipose derived stem cells in acute myocardial infarction: lessons from animal models*. Stem Cell Rev, 2014. 10(3): p. 389-98.

360. Justesen, J., et al., *Subcutaneous adipocytes can differentiate into bone-forming cells in vitro and in vivo*. Tissue Engineering, 2004. 10(3-4): p. 381-391.

361. Lee, J.A., et al., *Biological alchemy: engineering bone and fat from fat-derived stem cells*. Ann Plast Surg, 2003. 50(6): p. 610-7.

362. Erickson, G.R., et al., *Chondrogenic potential of adipose tissue-derived stromal cells in vitro and in vivo*. Biochem Biophys Res Commun, 2002. 290(2): p. 763-9.

363. Huang, J.I., et al., *Chondrogenic potential of multipotential cells from human adipose tissue.* Plast Reconstr Surg, 2004. 113(2): p. 585-94.

364. Mizuno, H., et al., *Myogenic differentiation by human processed lipoaspirate cells*. Plast Reconstr Surg, 2002. 109(1): p. 199-209; discussion 210-1.

365. Bai, X.W., et al., *Spontaneous cardiomyogenic differentiation of human adipose tissue derived stem cells: Identification, isolation and characterization using lentiviral cardiac promoter/marker expression*. Circulation, 2005. 112(17): p. U155-U155.

366. Rangappa, S., et al., *Transformation of adult mesenchymal stem cells isolated from the fatty tissue into cardiomyocytes*. Ann Thorac Surg, 2003. 75(3): p. 775-9.

367. Planat-Benard, V., et al., *Plasticity of human adipose lineage cells toward endothelial cells: physiological and therapeutic perspectives*. Circulation, 2004. 109(5): p. 656-63.

368. Seo, M.J., et al., *Differentiation of human adipose stromal cells into hepatic lineage in vitro and in vivo*. Biochem Biophys Res Commun, 2005. 328(1): p. 258-64.

369. Ashjian, P.H., et al., *In vitro differentiation of human processed lipoaspirate cells into early neural progenitors*. Plast Reconstr Surg, 2003. 111(6): p. 1922-31.

370. Kang, S.K., et al., *Improvement of neurological deficits by intracerebral transplantation of human adipose tissue-derived stromal cells after cerebral ischemia in rats*. Exp Neurol, 2003. 183(2): p. 355-66.

371. Kang, S.K., et al., *Neurogenesis of Rhesus adipose stromal cells*. J Cell Sci, 2004. 117(Pt 18): p. 4289-99.

372. Safford, K.M., et al., *Neurogenic differentiation of murine and human adipose-derived stromal cells.* Biochem Biophys Res Commun, 2002. 294(2): p. 371-9.

373. Safford, K.M., et al., *Characterization of neuronal/glial differentiation of murine adipose-derived adult stromal cells*. Exp Neurol, 2004. 187(2): p. 319-28.

374. Brzoska, M., et al., *Epithelial differentiation of human adipose tissue-derived adult stem cells.* Biochem Biophys Res Commun, 2005. 330(1): p. 142-50.

375. Cousin, B., et al., *Reconstitution of lethally irradiated mice by cells isolated from adipose tissue.* Biochem Biophys Res Commun, 2003. 301(4): p. 1016-22.

376. Rodriguez, L.V., et al., *Clonogenic multipotent stem cells in human adipose tissue differentiate into functional smooth muscle cells.* Proc Natl Acad Sci U S A, 2006. 103(32): p. 12167-72.

377. Wong, J.Z., et al., *Smooth muscle actin and myosin expression in cultured airway smooth muscle cells*. Am J Physiol, 1998. 274(5 Pt 1): p. L786-92.

378. Kim, Y.M., et al., *Angiotensin II-induced differentiation of adipose tissue-derived mesenchymal stem cells to smooth muscle-like cells*. Int J Biochem Cell Biol, 2008. 40(11): p. 2482-91.

379. Yang, P., et al., *[Experiment of adipose derived stem cells induced into smooth muscle cells]*. Zhongguo Xiu Fu Chong Jian Wai Ke Za Zhi, 2008. 22(4): p. 481-6.

380. Lendeckel, S., et al., *Autologous stem cells (adipose) and fibrin glue used to treat widespread traumatic calvarial defects: case report*. J Craniomaxillofac Surg, 2004. 32(6): p. 370-3.

381. Elabd, C., et al., *Human adipose tissue-derived multipotent stem cells differentiate in vitro and in vivo into osteocyte-like cells*. Biochem Biophys Res Commun, 2007. 361(2): p. 342-8.

382. Lee, K., et al., *Systemic transplantation of human adipose-derived stem cells stimulates bone repair by promoting osteoblast and osteoclast function*. J Cell Mol Med, 2011. 15(10): p. 2082-94.

383. Kakudo, N., et al., *Effects of transforming growth factor-beta1 on cell motility, collagen gel contraction, myofibroblastic differentiation, and extracellular matrix expression of human adipose-derived stem cell*. Hum Cell, 2012. 25(4): p. 87-95.

384. Tomasek, J.J., et al., *Myofibroblasts and mechano-regulation of connective tissue remodelling.* Nat Rev Mol Cell Biol, 2002. 3(5): p. 349-63.

385. Yamada, Y., et al., *Cardiac progenitor cells in brown adipose tissue repaired damaged myocardium*. Biochem Biophys Res Commun, 2006. 342(2): p. 662-70.

386. Xu, Y., et al., *In vitro expansion of adipose-derived adult stromal cells in hypoxia enhances early chondrogenesis*. Tissue Eng, 2007. 13(12): p. 2981-93.

387. Carmeliet, P., *Angiogenesis in health and disease*. Nat Med, 2003. 9(6): p. 653-60.

388. Pugh, C.W. and P.J. Ratcliffe, *Regulation of angiogenesis by hypoxia: role of the HIF system*. Nat Med, 2003. 9(6): p. 677-84.

389. Folkman, J. and P.A. D'Amore, *Blood vessel formation: what is its molecular basis?* Cell, 1996. 87(7): p. 1153-5.

390. Rehman, J., et al., *Secretion of angiogenic and antiapoptotic factors by human adipose stromal cells*. Circulation, 2004. 109(10): p. 1292-8.

391. Cao, Y., et al., *Human adipose tissue-derived stem cells differentiate into endothelial cells in vitro and improve postnatal neovascularization in vivo.* Biochem Biophys Res Commun, 2005. 332(2): p. 370-9.

392. Miranville, A., et al., *Improvement of postnatal neovascularization by human adipose tissue-derived stem cells*. Circulation, 2004. 110(3): p. 349-55.

393. Amos, P.J., et al., *IFATS collection: The role of human adipose-derived stromal cells in inflammatory microvascular remodeling and evidence of a perivascular phenotype.* Stem Cells, 2008. 26(10): p. 2682-90.

394. Zannettino, A.C., et al., *Multipotential human adipose-derived stromal stem cells exhibit a perivascular phenotype in vitro and in vivo*. J Cell Physiol, 2008. 214(2): p. 413-21.

395. Terlizzi, V., et al., *The Pericytic Phenotype of Adipose Tissue-Derived Stromal Cells Is Promoted by NOTCH2*. Stem Cells, 2018. 36(2): p. 240-251.

396. Amos, P.J., et al., *Human adipose-derived stromal cells accelerate diabetic wound healing: impact of cell formulation and delivery*. Tissue Eng Part A, 2010. 16(5): p. 1595-606.

397. Nie, C., et al., *Locally administered adipose-derived stem cells accelerate wound healing through differentiation and vasculogenesis*. Cell Transplant, 2011. 20(2): p. 205-16.

398. Heo, S.C., et al., *Tumor necrosis factor-alpha-activated human adipose tissue-derived mesenchymal stem cells accelerate cutaneous wound healing through paracrine mechanisms*. J Invest Dermatol, 2011. 131(7): p. 1559-67.

399. Kim, W.S., B.S. Park, and J.H. Sung, *The wound-healing and antioxidant effects of adipose-derived stem cells.* Expert Opin Biol Ther, 2009. 9(7): p. 879-87.

400. Lee, E.Y., et al., *Hypoxia-enhanced wound-healing function of adipose-derived stem cells: increase in stem cell proliferation and up-regulation of VEGF and bFGF*. Wound Repair Regen, 2009. 17(4): p. 540-7.

401. Bai, X.W., et al., *Both cultured and freshly isolated adipose tissue-derived stem cells enhance cardiac function after acute myocardial infarction.* European Heart Journal, 2010. 31(4): p. 489-501.

402. Ii, M., et al., *Synergistic effect of adipose-derived stem cell therapy and bone marrow progenitor recruitment in ischemic heart*. Laboratory Investigation, 2011. 91(4): p. 539-552.

403. Bhang, S.H., et al., *Angiogenesis in ischemic tissue produced by spheroid grafting of human adipose-derived stromal cells*. Biomaterials, 2011. 32(11): p. 2734-2747.

404. Haque, N., et al., *Hypoxic Culture Conditions as a Solution for Mesenchymal Stem Cell Based Regenerative Therapy*. Scientific World Journal, 2013.

405. Feng, Y., et al., *Hypoxia-cultured human adipose-derived mesenchymal stem cells are non-oncogenic and have enhanced viability, motility, and tropism to brain cancer (vol 5, pg e1567, 2014).* Cell Death & Disease, 2015. 6.

406. Kim, J.H., et al., *The pivotal role of reactive oxygen species generation in the hypoxia-induced stimulation of adipose-derived stem cells*. Stem Cells Dev, 2011. 20(10): p. 1753-61.

407. Rehman, J., et al., *Secretion of angiogenic and antiapoptotic factors by human adipose stromal cells*. Circulation, 2004. 109(10): p. 1292-1298.

408. Bouacida, A., et al., *Pericyte-like progenitors show high immaturity and engraftment potential as compared with mesenchymal stem cells*. PLoS One, 2012. 7(11): p. e48648.

409. Loibl, M., et al., *Direct Cell-Cell Contact between Mesenchymal Stem Cells and Endothelial Progenitor Cells Induces a Pericyte-Like Phenotype In Vitro*. Biomed Research International, 2014.

410. Caplan, A.I. and J.E. Dennis, *Mesenchymal stem cells as trophic mediators*. Journal of Cellular Biochemistry, 2006. 98(5): p. 1076-1084.

411. Kinnaird, T., et al., *Marrow-derived stromal cells express genes encoding a broad spectrum of arteriogenic cytokines and promote in-vitro and in-vivo arteriogenesis through paracrine mechanisms* (vol 94, pg 678, 2004). Circulation Research, 2005. 97(3): p. E51-E51.

412. Oh, J.Y., et al., *The anti-inflammatory and anti-angiogenic role of mesenchymal stem cells in corneal wound healing following chemical injury.* Stem Cells, 2008. 26(4): p. 1047-55.

413. Valle-Prieto, A. and P.A. Conget, *Human mesenchymal stem cells efficiently manage oxidative stress*. Stem Cells Dev, 2010. 19(12): p. 1885-93.

414. Kim, W.S., et al., *Evidence supporting antioxidant action of adipose-derived stem cells: protection of human dermal fibroblasts from oxidative stress*. J Dermatol Sci, 2008. 49(2): p. 133-42.

415. Song, S.Y., H.M. Chung, and J.H. Sung, *The pivotal role of VEGF in adipose-derived-stem-cell-mediated regeneration.* Expert Opin Biol Ther, 2010. 10(11): p. 1529-37.

416. Hu, J.X., et al., *Effects of autologous adipose-derived stem cell infusion on type 2 diabetic rats*. Endocrine Journal, 2015. 62(4): p. 339-352.

417. Cramer, C., et al., *Persistent high glucose concentrations alter the regenerative potential of mesenchymal stem cells*. Stem Cells Dev, 2010. 19(12): p. 1875-84.

418. Cianfarani, F., et al., *Diabetes impairs adipose tissue-derived stem cell function and efficiency in promoting wound healing*. Wound Repair Regen, 2013. 21(4): p. 545-53.

419. Cronk, S.M., et al., *Adipose-Derived Stem Cells From Diabetic Mice Show Impaired Vascular Stabilization in a Murine Model of Diabetic Retinopathy*. Stem Cells Translational Medicine, 2015. 4(5): p. 459-467.

420. Cui, L., et al., *Expanded adipose-derived stem cells suppress mixed lymphocyte reaction by secretion of prostaglandin E2.* Tissue Eng, 2007. 13(6): p. 1185-95.

421. Gonzalez-Rey, E., et al., *Human adipose-derived mesenchymal stem cells reduce inflammatory and T cell responses and induce regulatory T cells in vitro in rheumatoid arthritis*. Ann Rheum Dis, 2010. 69(1): p. 241-8.

422. DelaRosa, O., et al., *Requirement of IFN-gamma-mediated indoleamine 2,3-dioxygenase expression in the modulation of lymphocyte proliferation by human adipose-derived stem cells*. Tissue Eng Part A, 2009. 15(10): p. 2795-806.

423. Keyser, K.A., K.E. Beagles, and H.P. Kiem, *Comparison of mesenchymal stem cells from different tissues to suppress T-Cell activation*. Cell Transplantation, 2007. 16(5): p. 555-562.

424. McIntosh, K., et al., *The immunogenicity of human adipose-derived cells: temporal changes in vitro*. Stem Cells, 2006. 24(5): p. 1246-53.

425. Yoo, K.H., et al., *Comparison of immunomodulatory properties of mesenchymal stem cells derived from adult human tissues*. Cellular Immunology, 2009. 259(2): p. 150-156.

426. Crop, M.J., et al., *Inflammatory conditions affect gene expression and function of human adipose tissue-derived mesenchymal stem cells*. Clin Exp Immunol, 2010. 162(3): p. 474-86.

427. Crop, M.J., et al., *Human adipose tissue-derived mesenchymal stem cells induce explosive T-cell proliferation*. Stem Cells Dev, 2010. 19(12): p. 1843-53.

428. Kronsteiner, B., et al., *Human Mesenchymal Stem Cells from Adipose Tissue and Amnion Influence T-Cells Depending on Stimulation Method and Presence of Other Immune Cells*. Stem Cells and Development, 2011. 20(12): p. 2115-2126.

429. Shi, D., et al., *Human adipose tissue-derived mesenchymal stem cells facilitate the immunosuppressive effect of cyclosporin A on T lymphocytes through Jagged-1-mediated inhibition of NF-kappa B signaling*. Experimental Hematology, 2011. 39(2): p. 214-224.

430. Yanez, R., et al., *Prostaglandin E2 plays a key role in the immunosuppressive properties of adipose and bone marrow tissue-derived mesenchymal stromal cells*. Experimental Cell Research, 2010. 316(19): p. 3109-3123.

431. Kang, J.W., et al., *Soluble factors-mediated immunomodulatory effects of canine adipose tissue-derived mesenchymal stem cells*. Stem Cells Dev, 2008. 17(4): p. 681-93.

432. Choi, E.W., et al., *Reversal of serologic, immunologic, and histologic dysfunction in mice with systemic lupus erythematosus by long-term serial adipose tissue-derived mesenchymal stem cell transplantation*. Arthritis Rheum, 2012. 64(1): p. 243-53.

433. Fumimoto, Y., et al., *Creation of a rich subcutaneous vascular network with implanted adipose tissue-derived stromal cells and adipose tissue enhances subcutaneous grafting of islets in diabetic mice*. Tissue Eng Part C Methods, 2009. 15(3): p. 437-44.

434. Ohmura, Y., et al., *Combined transplantation of pancreatic islets and adipose tissue-derived stem cells enhances the survival and insulin function of islet grafts in diabetic mice*. Transplantation, 2010. 90(12): p. 1366-73.

435. Manferdini, C., et al., *Adipose-derived mesenchymal stem cells exert antiinflammatory effects on chondrocytes and synoviocytes from osteoarthritis patients through prostaglandin E2.* Arthritis Rheum, 2013. 65(5): p. 1271-81.

436. Schelbergen, R.F., et al., *Treatment efficacy of adipose-derived stem cells in experimental osteoarthritis is driven by high synovial activation and reflected by S100A8/A9 serum levels*. Osteoarthritis and Cartilage, 2014. 22(8): p. 1158-1166.

437. Kim, W.S., et al., *Wound healing effect of adipose-derived stem cells: a critical role of secretory factors on human dermal fibroblasts*. J Dermatol Sci, 2007. 48(1): p. 15-24.

438. Patel, K.M., et al., *Mesenchymal stem cells attenuate hypoxic pulmonary vasoconstriction by a paracrine mechanism*. J Surg Res, 2007. 143(2): p. 281-5.

439. Kilroy, G.E., et al., *Cytokine profile of human adipose-derived stem cells: Expression of angiogenic, hematopoietic, and pro-inflammatory factors*. Journal of Cellular Physiology, 2007. 212(3): p. 702-709.

440. Salgado, A.J., et al., *Adipose Tissue Derived Stem Cells Secretome: Soluble Factors and Their Roles in Regenerative Medicine*. Current Stem Cell Research & Therapy, 2010. 5(2): p. 103-110.

441. Cai, L., et al., *IFATS collection: Human adipose tissue-derived stem cells induce angiogenesis and nerve sprouting following myocardial infarction, in conjunction with potent preservation of cardiac function.* Stem Cells, 2009. 27(1): p. 230-7.

442. Kondo, K., et al*., Implantation of adipose-derived regenerative cells enhances ischemia-induced angiogenesis*. Arterioscler Thromb Vasc Biol, 2009. 29(1): p. 61-6.

443. Platas, J., et al., *Paracrine effects of human adipose-derived mesenchymal stem cells in inflammatory stress-induced senescence features of osteoarthritic chondrocytes*. Aging (Albany NY), 2016. 8(8): p. 1703-17.

444. Iwashima, S., et al., *Novel Culture System of Mesenchymal Stromal Cells from Human Subcutaneous Adipose Tissue*. Stem Cells and Development, 2009. 18(4): p. 533-544.

445. Saka, Y., et al., *Adipose-derived stromal cells cultured in a low-serum medium, but not bone marrow-derived stromal cells, impede xenoantibody production*. Xenotransplantation, 2011. 18(3): p. 196-208.

446. Furuhashi, K., et al., *Serum-Starved Adipose-Derived Stromal Cells Ameliorate Crescentic GN by Promoting Immunoregulatory Macrophages*. Journal of the American Society of Nephrology, 2013. 24(4): p. 587-603.

447. Tarte, K., et al., *Clinical-grade production of human mesenchymal stromal cells: occurrence of aneuploidy without transformation*. Blood, 2010. 115(8): p. 1549-1553.

448. Prockop, D.J., et al., *Defining the risks of mesenchymal stromal cell therapy.* Cytotherapy, 2010. 12(5): p. 576-578.

449. Minonzio, G., et al., *Frozen adipose-derived mesenchymal stem cells maintain high capability to grow and differentiate*. Cryobiology, 2014. 69(2): p. 211-6.

450. Miyagi-Shiohira, C., et al., *Cryopreservation of Adipose-Derived Mesenchymal Stem Cells*. Cell Med, 2015. 8(1-2): p. 3-7.

Hyperglycemia Induces Bioenergetic Changes in Adipose-Derived Stromal Cells While Their Pericytic Function Is Retained

Ghazaleh Hajmousa[1], Alvaro A. Elorza[2,3], Vera J.M. Nies[4], Erik L. Jensen[3], Ruxandra A. Nagy[1], and Martin C. Harmsen[1]

[1] Department of Pathology and Medical Biology, University Medical Center Groningen , University of Groningen, Groningen, the Netherlands; [2] Millennium Institute of Immunology and Immunotherapy, Santiago, Chile; [3] Faculty of Biological Sciences and Faculty of Medicine, Center for Biomedical Research, Universidad Andres Bello, Santiago, Chile; [4] Department of Pediatrics and Laboratory Medicine, Center for Liver, Digestive and Metabolic Diseases, University Medical Center Groningen, Groningen, the Netherlands.

CHAPTER 02

Abstract

Diabetic retinopathy (DR) is a hyperglycemia (HG)-mediated microvascular complication. In DR, the loss of pericytes and subsequently endothelial cells leads to pathologic angiogenesis in retina. Adipose-derived stromal cells (ASC) are a promising source of therapeutic cells to replace lost pericytes in DR. To date, knowledge of the influence of HG on the bioenergetics and pericytic function of ASC is negligible. Human ASC were cultured in normoglycemia medium (5 mM d-glucose) or under HG (30 mM d-glucose) and assessed. Our data showed that HG increased the level of apoptosis and reactive oxygen species production in ASC, yet their proliferation rate was not affected. HG induced alterations in mitochondrial function and morphology in ASC. HG also strongly affected the bioenergetic status of ASC in which both the maximum oxygen consumption rate and extracellular acidification rate were decreased. This was corroborated by a reduced uptake of glucose under HG. In spite of these observations, in vitro, ASC promoted the formation of vascular-like networks of human umbilical vein endothelial cells on monolayers of ASC under HG with minimally affected.

Key words: Adipose tissue-derived stromal cells, Diabetic retinopathy, Hyperglycemia, Oxidative stress.

Introduction

The International Diabetes Federation estimates that there were 366 million people living with diabetes in 2011; by 2030 this will have increased to 552 million [1]. Diabetes enhances the risk of clinical ophthalmologic complications and particular of diabetic retinopathy (DR), which is the main cause of blindness in the working-age population of developed countries [2]. DR is the result of a disordered glucose metabolism and is characterized by the early loss of two main cell types of retinal capillaries: the pericyte, which wraps capillaries and the endothelial cell [3].

Pericytes are derived from the vascular smooth muscle lineage and exist in contact with endothelial cells. Pericytes provide a nourishing, anti-inflammatory and antiangiogenic environment for endothelial cells that makes them a potential mediator of the functional blood–retinal barrier, which is dependent on the interaction of the vascular endothelial cells with both glial cells and pericytes [4,5]. The onset of DR is caused by intracellular accumulation of reactive oxygen species (ROS) that are induced by hyperglycemia (HG). The ROS induces apoptosis of pericytes, which exacerbates capillary death. The formation of acellular capillaries and pericyte ghosts are typically the first abnormalities that are observed clinically in DR [6]. The capillary degeneration causes substantial ischemia and local hypoxia, which triggers massive neovascularization, typical for later stages of retinopathy [7].

In the absence of pericytes, these new vessels are not quiescent and do not mature, while the angiogenesis process continues. The resulting capillaries are morphologically and functionally abnormal. In particular, their high permeability causes leakage of serum and cellular components into the vitreous. If the condition is not

diagnosed and treated, the increased pressure can eventually lead to blindness [8,9]. Therefore, during DR the retina is in demand of a suitable cellular replacement for pericytes. It is well recognized that in HG the electron transport chain is overwhelmed with substrate and starts to produce oxygen radicals that is, ROS [10]. Exacerbated ROS may induce the opening of the permeability transition pore, creating swollen mitochondria. These swollen mitochondria may present rupture in the mitochondrial outer membrane and leak out cytochrome c, calcium ions to mention a few and cause both apoptosis and necrosis. Through these effects, oxidative stress together with the downregulation of antioxidative enzymes play an important role in the pathogenesis of DR [11,12].

The early stage of retinopathy (non-proliferative retinopathy) frequently goes unnoticed as it does not have significant pathological signs. However, advanced retinopathy (proliferative retinopathy) is in high demand of treatment, due to the existence of leaky, nonfunctional, and highly proliferative vessels that require normalization of blood glucose levels, laser treatment, vitrectomy, and injection of an anti-VEGF (vascular endothelial growth factor) medicine combined with anti-inflammatory medicine to name a few. All these methods no more than partially prevent or delay loss of vision.

More importantly, replacement pericytes are required to blunt the ongoing proliferative angiogenesis while normalizing the capillary function. This is not possible to date. Promising results from animal models and recent in vitro studies have been published that will impact DR via a regenerative medicine-based approach over the coming years [13,14]. Adipose tissue-derived stromal cells (ASC) are abundant, accessible multipotent mesenchymal stromal cells that can be easily isolated from human adipose tissue. ASC have been

recently shown to have functional and phenotypic overlap with pericytes covering micro-vessels in adipose tissues [15].

ASC and pericytes share the same surface markers including NG2, CD140a, and CD140b (PDGFR α and β). Also, human ASC cooperate with endothelial cells to form vascular-like networks in vitro [15,16]. It has been shown that in a rodent model for chronic diabetes, ASC acquired pericytic features, which rescued proliferative angiogenesis in the retina under hyperglycemic conditions [17].

Importantly, these studies suggested the direct role of ASC in providing retinal microvascular support and appear to migrate and integrate with the retinal microvasculature [17,18]. ASC features may allow a functional replacement, at least short term, pericytes loss in DR. While retinal pericytes readily undergo HG and ROS-driven apoptosis, it is unclear why ASC that engraft diabetic retinal vasculature appear refractory to HG.

In this study, we investigated the influence of HG on the mitochondrial function and metabolic activity of ASC and on their pericytic function in vitro. This information may help to delineate both their capabilities and limitations with respect to their potential clinical translation.

Materials and Methods

Cell isolation and culture Human subcutaneous adipose tissue samples from healthy human subjects with body mass index <30 were obtained after liposuction surgery (Bergman Clinics). All donors provided informed consent and all procedures were performed in accordance to national and institutional guidelines as well as with the ethical rules for human experimentation stated in the Declaration of Helsinki.

For ASC isolation, lipoaspirates were enzymatically digested with 0.1% collagenase A (Roche Diagnostic) in phosphate-buffered saline (PBS), containing 1% bovine serum albumin (Sigma-Aldrich) at 37°C for 90 mins. Centrifugation (300 g, 4°C, 10 mins) was used to separate adipocytes and lipid content from the stromal cell fraction. The stromal cell fraction was subjected to Lymphoprep (Axis-Shield PoC) density gradient centrifugation. The cells from the interface were seeded in culture flasks at 10,000 cells/cm^2.

The culture medium was normoglycemic RPMI-1640 (5 mM D-glucose, NG-RPMI) (Lonza Biowhittaker Verviers) supplemented with 10% fetal bovine serum (FBS) (Thermo Scientific), 100 U/mL penicillin, 100 μg/mL streptomycin (Gibco, Life Technologies), and 2 mM L-glutamine (Lonza Biowhittaker Verviers). It was sterilized by filtration (0.22 μm). Optimal culture conditions of 37°C, 5% CO2, and 95% humidity were maintained throughout the culture period.

ASC in passage 1–3 were harvested with Trypsin-EDTA in 0.9% NaCl (Sigma-Aldrich) and routinely checked for both mesenchymal cell surface and pericyte markers, including CD31-/ CD44+/ CD45-/ CD29+/ CD105+/ CD144-/ NG2+/ PDGFRβ + [19]. The cells were passaged at 70%–80% confluence until passage3 (P3) with three changes of medium per week. The cells from P3–6 were cultured in

normoglycemic and hyperglycemic (30 mM d-glucose, HG-RPMI) conditions. An osmotic control medium made of 5 mM D-glucose plus 25 mM mannitol (NG+Ma-RPMI) of RPMI-1640 was also used. Cell culture medium was changed daily during the 7 days of the experiment. The pooled ASC from three different donors were used for the experiments of this study.

Human Umbilical vein endothelial cells (HUVEC) were cultured on gelatin-coated culture flasks at 10,000 cells/cm^2 in endothelial culture medium (ECM) consisting of medium NG-RPMI medium supplemented with 10% FBS, 100 U/mL penicillin, 100 µg/mL streptomycin, 2 mM l-glutamine plus 5 U/mL heparin (Leo Pharma), and 50 µg/mL of endothelial cell growth factor [20].

For the co-cultures of ASC and HUVEC, ASC had to be cultured in RPMI-based medium, the influence of DMEM-based and RPMI-based medium on the expression of mesenchymal and pericytic markers in ASC was assessed (Supplementary Fig. S1, A). The expression of PDGFRβ, NG2 were marginally reduced in long-term cultures of ASC in ECM and considered of no influence to the experiments. (Supplementary Fig. S1, B)
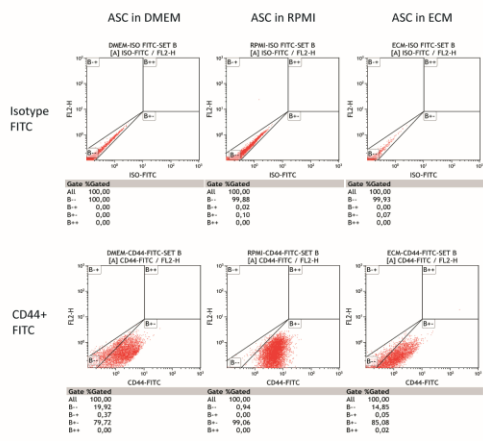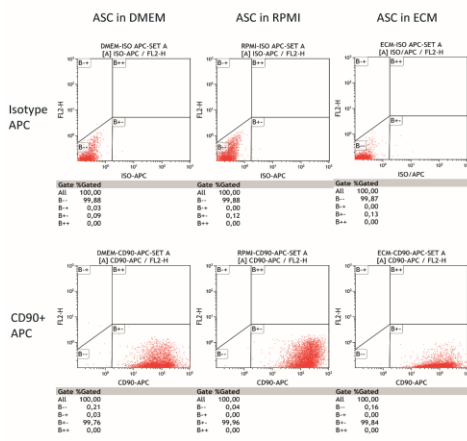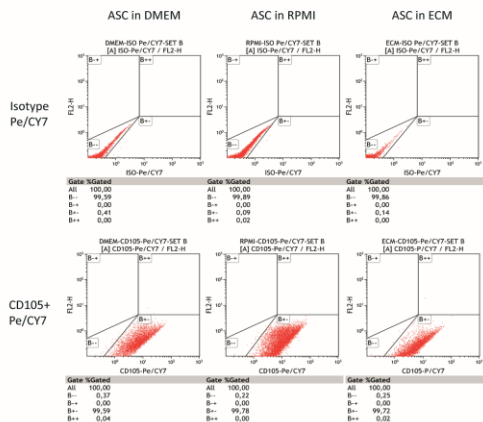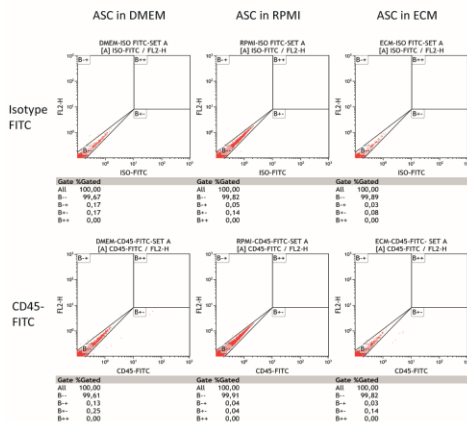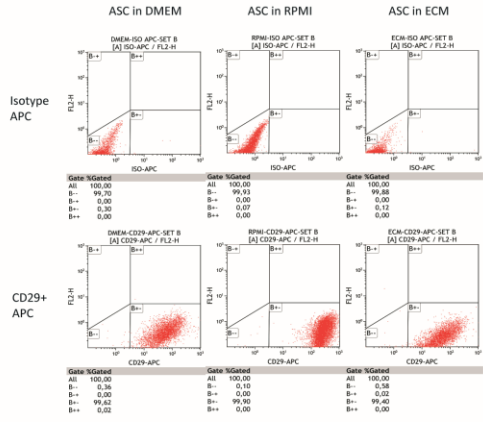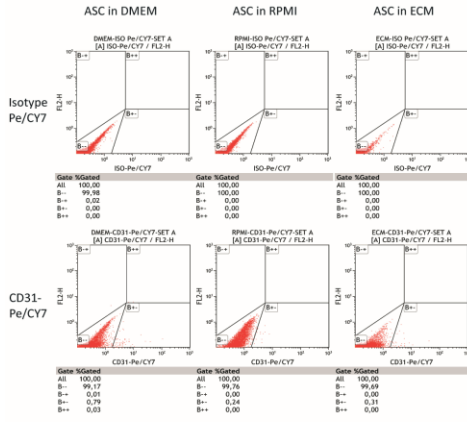
B
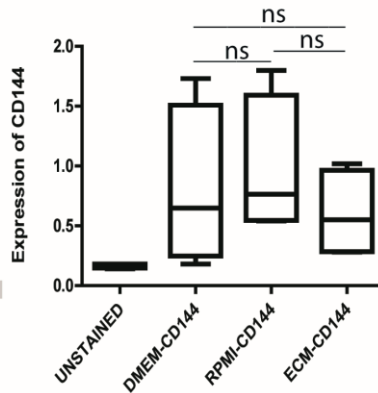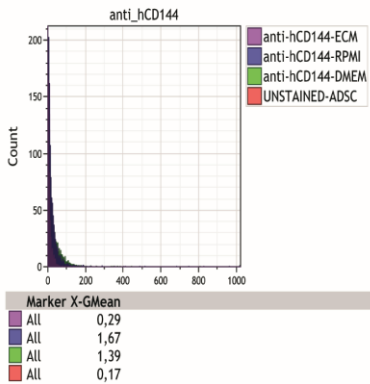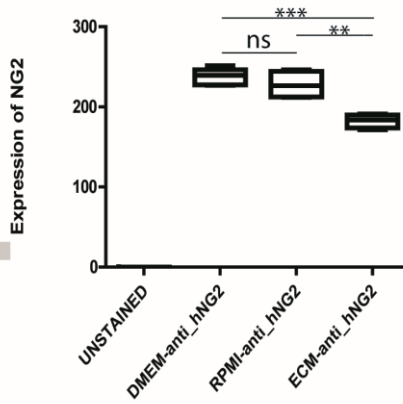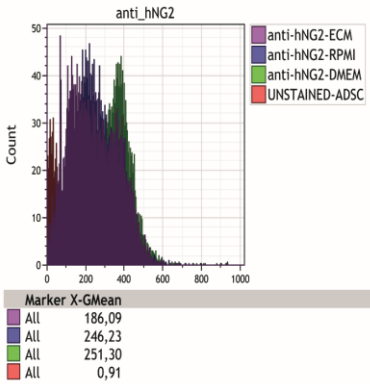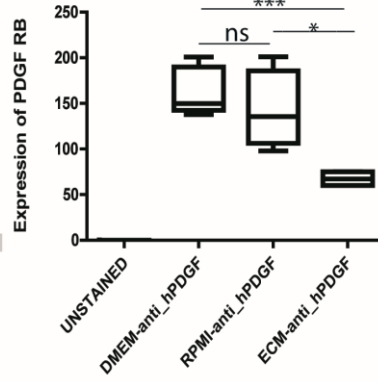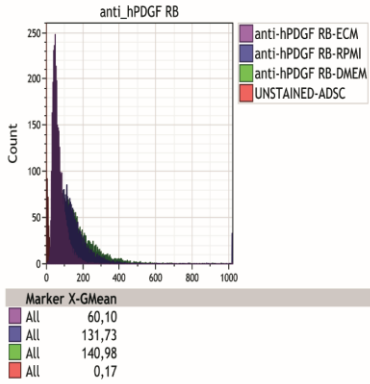
SUPPLEMENTARY Figure. S1. ASC were cultured in different medium (DMEM, RPMI, and ECM) under normoglycemic condition.

(A) ASC in passage 1–3 were routinely assessed for pericyte and mesenchymal cell surface markers, including CD31-/ CD44+/CD45-/CD29+/CD90+/CD105+/CD144-/NG2+/PDGFRb+ (*P< 0.01, **P< 0.001, ***P< 0.0001). Data are plotted as scatter graphs with relative frequencies below.

(B) The analyses indicate that medium has virtually no influence on these markers, with the exception of PDGFRb and NG2 upon culturing in ECM for three passages. ASC, adipose tissue-derived stromal cells; ECM, endothelial culture medium; NG, normoglycemia.

Immunofluorescence analysis of cocultured ASC and HUVEC ASC were plated in 24-well cell culture plates (Corning) at 10,000 cells/cm² in NG-RPMI medium for 5 days. HUVEC were seeded on top of ASC monolayers or as the control on gelatin-coated wells at 10,000 cells/cm² in NG-ECM or HG-ECM for 7 more days after which vascular networks had formed. Cells were washed with PBS and fixed in 2% paraformaldehyde in PBS at RT for 20 min. Cells were permeabilized with 0.5% Triton X-100 in PBS (Sigma-Aldrich) for 15 min. Subsequently, samples were incubated with goat-anti-human-RGS5 antibody (1:100; Santa Cruz)/rabbit anti-human-SM22α antibody (1:100; Abcam) and mouse-anti-human-CD31 antibody (1:100; Dako) for 90 min. Samples were washed with PBS and incubated with a cyanine3-conjugated-rabbit-antibody to goat-IgG for RGS5/cyanine3-conjugated-donkey-antibody to rabbit-IgG for SM22a (1:300; Life Technologies) and fluorescein-conjugated-donkey-antibody to mouse-IgG (for CD31, 1:300; Life Technologies) for 45 min. Stained samples were mounted with PBS. Imaging was performed with a high-end fully motorized Zeiss AxioObserver Z1 epifluorescent microscope (TissueGnosticsTissue Faxs). The coculture experiment was repeated with HUVEC that were lentivirally tagged to express EGFP (green) and ASC lentivirally tagged with dTomato (red) to monitor the origin cells irrespective of phenotypes changes during coculture.

Apoptosis and proliferation To estimate the influence of HG on cell survival, apoptosis was evaluated by fluorescence-activated cell sorting (FACS) analysis using an Apoptotic/Necrotic Cells Detection Kit (PromoKine). Briefly, ASC were treated with NG-RPMI, HG-RPMI, and NG+Ma-RPMI medium for 7 days and harvested by Trypsin-EDTA

in 0.9% NaCl right after treatment. Cells were washed with PBS once and resuspended in 500 µL kit binding buffer (100,000 cells/500 µL) and stained in the dark with 2.5 µL FITC-AnnexinV (marker for apoptosis) and 2.5 µL of Ethidium Homodimer lll (marker for necrosis) at RT for 15 min. Samples were analyzed using a FACS Calibur flow-cytometer (BD biosciences) within 1 h after staining and the results were analyzed with Kaluza 1.2 software. For measurement of proliferation, ASC from P3-6 were plated on 24-well cell culture plates (Corning) at 10,000 cells/cm^2 in NG-RPMI medium with 10% FBS for 24 h. The medium was changed for NG-RPMI, HG-RPMI, or osmotic control, all with 5% FBS for 7 days. Medium was changed daily. Cells were fixed and permeabilized as described above. Samples were incubated with rabbit-anti-human-ki67 (Monosan PSX1028) 1:250 in DAPI (5 mg/mL; Sigma-Aldrich) for 90 min. Samples were washed and subsequently stained by incubation with a cyanine3-conjugated-donkey-antibody to rabbit-IgG (1:100; Life Technologies) for 30 min. Stained samples were mounted with PBS. Imaging was performed with a high-end fully motorized Zeiss AxioObserver Z1 epifluorescent microscope.

Detection of ROS level Cellular ROS production was determined using the dye 2',7'-dichlorofluorescein diacetate (DCFH-DA; Sigma-Aldrich), a cell permeable nonfluorescent probe, which is de-esterified intracellularly by means of esterases (DCFH) and turns to highly fluorescent 2',7'-dichlorofluorescein (DCF) on oxidation [21]. Cells were harvested after 7 days culturing in NG, HG, and NG+Ma-RPMI medium and suspended in 1 mL of medium followed by incubation with 20 µM DCFH-DA in the dark at 37°C for 15 min. Samples were analyzed directly without washing using a FACS Calibur

flow cytometer (BD Biosciences) within 15 min after the staining and the results were analyzed with Kaluza 1.2 software.

Assessment of mitochondrial membrane potential and mitochondrial morphology analysis To specify the influence of HG on mitochondrial morphology and membrane potential, ASC cultured in NG-RPMI or HG-RPMI medium for 7 days were incubated at 37°C in a 5% CO_2 humidified chamber with 120 nM membrane potential–independent dye MitoTracker Green (MTG, Green, Life Technologies) and 10 nM tetramethylrhodamine, ethyl ester, perchlorate (TMRE, Red-orange; Life Technologies), a membrane potential-dependent fluorescent dye for 45 min, washed three times, and incubated in medium containing TMRE for 15 min before imaging to allow adequate equilibration of the membrane potential-sensitive TMRE dye within the mitochondria. TMRE was kept in the medium while imaging. All experiments were performed in triplicate with at least three technical replicates and normalized by the number of cells per sample.

Confocal microscopy Cells were imaged live by confocal microscope (Leica TCS SP8 Confocal Microscope) with a 63 × oil immersion objective. The cells were kept at 37°C in a 5% CO_2 humidified microscope stage chamber. MTG was subjected to 490 nm argon laser excitation and 516 nm filter emission. TMRE was recorded through a band-pass 573–607 nm filter. To observe individual mitochondria Z-stack images were acquired in series of six slices per cell ranging in thickness from 0.5 to 0.8 μm per slice [22].

Analysis of mitochondrial length and circularity Mitochondrial circularity of ASC was measured as described previously [23]. Mitochondrial circularity is a measure of "roundness" of mitochondria with 0 referring to a straight line and 1 as a perfect circle. Cells containing a majority of long interconnected mitochondrial networks were classified as cells with tubular mitochondria. Cells with a majority of short mitochondria were classified as fragmented and cells with mostly sparse small round mitochondria were classified as very fragmented [24]. Morphological aspects were measured by ImageJ software for individual mitochondria.

Oxygen consumption rate and extracellular acidification rate The oxygen consumption rate (OCR) and extracellular acidification rate (ECAR) of ASC grown in NG-RPMI or HG-RPMI medium were measured by a bioenergetic assay (XF24; Seahorse Bioscience). ASC were plated and grown on V7-PS plate (Seahorse Bioscience, Inc.) in NG-RPMI or HG-RPMI medium to reach a confluent monolayer for 7 days. Assays were initiated by removing growth medium, replacing with unbuffered RPMI-1640 medium and incubating at 37°C for 60 min in a CO2-free incubator to allow temperature equilibrium and CO2 degassing from plate. The microplate was then assayed (XF24 Extracellular Flux Analyzer; Seahorse Bioscience) to measure extracellular flux changes of oxygen and pH in the medium immediately surrounding the adherent cells. After steady state measurement, oxygen consumption and ECARs were obtained. Oligomycin (2 µM), which inhibits ATP synthase, and the proton ionophore FCCP [carbonyl cyanide 4-(trifluoromethoxy) phenylhydrazone; 5 µM], which uncouples mitochondria, were injected sequentially through reagent delivery chambers for each

well in the microplate, to obtain maximum OCRs. Finally, a mixture containing 2 µM rotenone (an inhibitor of mitochondrial complex I) and 2 µM antimycin A (an electron transport blocker) was injected to confirm that respiration changes were mainly due to mitochondrial respiration. The values of oxygen consumption and extracellular acidification were normalized to total cellular proteins in each sample well.

Assessment of glucose uptake by 2-deoxy D-glucose To determine the influence of HG on glucose uptake in ASC, cells from P3–6 were cultured in NG or HG for 7 days. After that cells were washed twice with PBS and serum deprived for 4 h, in either NG or HG medium supplemented with 100 U/mL penicillin, 100 µg/mL streptomycin, and 2 mM l-glutamine. Subsequently, the ASC were stimulated with 100 nM insulin (Novorapid; Novo Nordisk) for 20 min at 37°C or left untreated. The medium was removed, cells were washed twice with warm PBS, and 1 mL of PBS containing 0.1 µCi 2-deoxy-D-[14C]glucose (14C-2-DOG) (Perkin Elmer) and unlabeled 2-deoxy-d-glucose (2DG) (100 µM; Sigma-Aldrich) was added to each well. The uptake reaction was carried out at 37°C for 45 min. Glucose transport was terminated by washing twice with ice-cold PBS. Cells were harvested and lysed in 0.5 mL 0.05M NaOH. Of this, a 400 µL aliquot was used for β-scintillation determination by addition of scintillation cocktail and subsequent scintillation determination in a β-scintillation counter. The remaining 100 µL were used for the determination of protein concentration with the Pierce™ BCA Protein Assay Kit (Life Technologies). The results were analyzed as 2DG uptake in pmol/µg of protein. The data are plotted as the fold

change in 2DG uptake after culturing in HG compared to culturing in NG.

Statistics All the data are presented as a mean ± SEM and were analyzed by GraphPad Prism (GraphPad Software, Inc.). Statistical significance was determined using one-way ANOVA and unpaired t-test analysis. Values of $p < 0.05$ were considered statistically significant.

Results

HG reduces viability of ASC, but does not influence proliferation

After 7 days culture in HG medium ~25% ± 1.1% of the ASC were apoptotic and necrotic, while this was reduced in NG (16% ± 0.8%, P < 0.0001, Fig. 1A, B). Interestingly, the level of proliferation, as determined by the fraction of Ki-67-expressing ASC, did not differ between cells cultured in NG medium versus HG medium (Fig. 1C) or osmotic controls (data not shown) after 7 days culture.

A

B

C
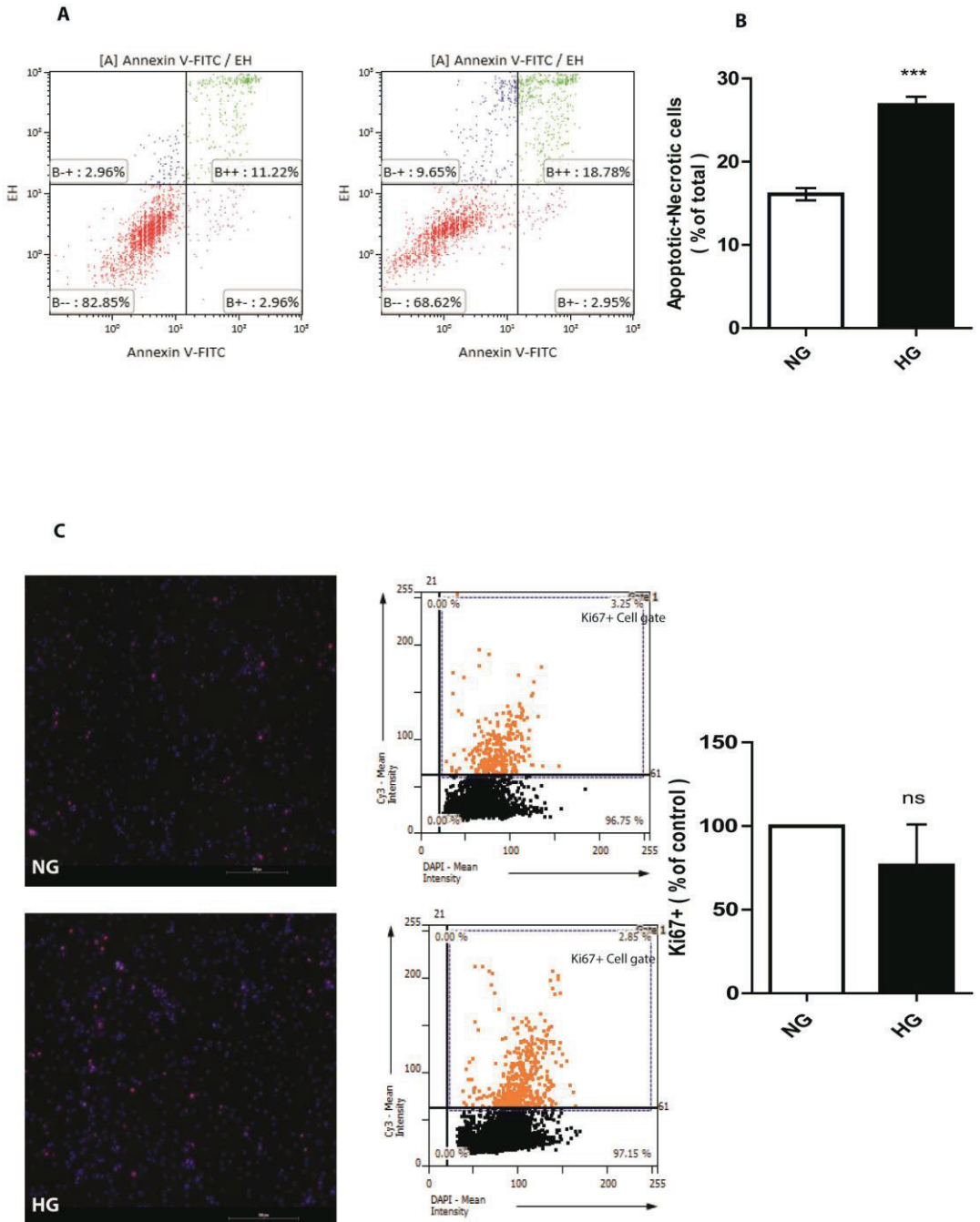
Figure. 1. ASC undergo apoptosis after exposure to HG for 7 days.

Apoptosis and necrosis were quantified by FACS after FITC-Annexin V and Ethidium Homodimer lll labeling.

(A) Representative FACS data for ASC in NG and HG. The abscissa and ordinate represent the fluorescence intensity of Annexin V and Ethidium Homodimer lll, respectively.

(B) Bar graph represents the mean percentage of the total apoptosis and necrosis rate – SEM. (n = 5). (***P < 0.0001)

(C) Proliferation of ASC is not influenced after exposure to HG for 7 days. Immunofluorescent staining of Ki67 (proliferation marker) after 7 days of culture in NG or HG medium. Images were analyzed with TissueGnostics tissue FAXS software. The bar graph shows the percentage of positive ki67 cells in HG-medium to the control (NG-medium culturing). The data are presented as the mean – SEM. Scale bar = 200 mm. ASC, adipose tissue-derived stromal cells; FACS, fluorescenceactivated cell sorting; NG, normoglycemia; HG, hyperglycemia.

HG induces ROS in ASC

ASC cultured in NG or control medium produced virtually no ROS, as determined by FACS analysis of converted DCFH-DA. However, 7 days culture of ASC in HG medium increased intracellular levels of ROS by more than threefold (P < 0.0001, Fig. 2A). In the positive control cells which were treated with 1 mM hydrogen peroxide (Merk) as a potent ROS inducer, ROS induced well beyond the levels induced by HG (Fig. 2B).
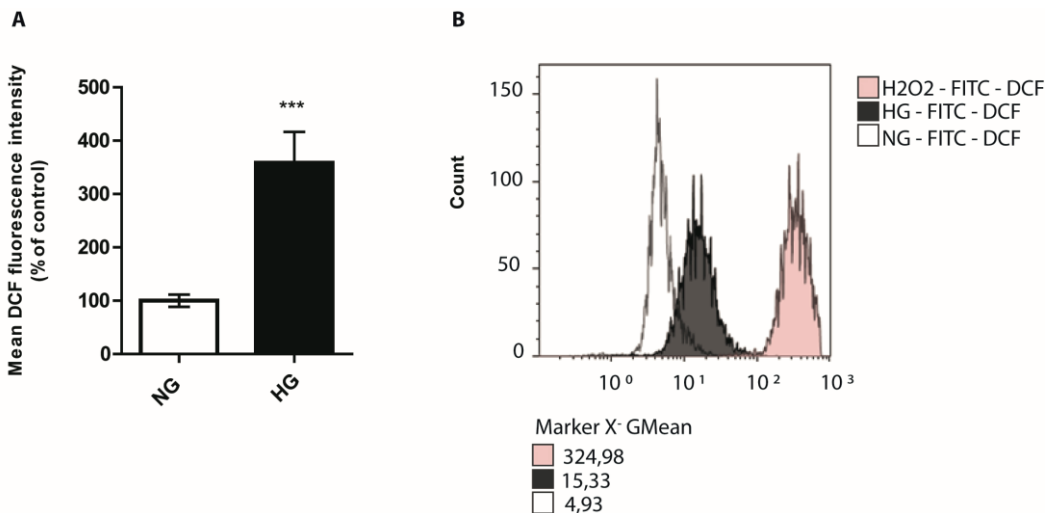

Figure. 2. HG induces production of total cellular ROS in ASC. ROS production was measured by conversion of DCF in ASC after exposure to HG for 7 days.

(A) The flow cytometric analysis shows a signifi- cantly higher mean fluorescence intensity (MFI) in HG compared to NG (***P< 0.0001). The graphs show the mean– SEM (n = 8).

(B) The histograms shows the representative increase of mean intensity after exposure to HG or H2O2 control compared to NG. ROS, reactive oxygen species.

HG alters the mitochondrial membrane potential and changes the mitochondrial phenotype of ASC

The continuous culture of ASC in HG medium decreased their mitochondrial membrane potential by ~31% ± 8% compared to NG medium as judged by TMRE fluorescence (P < 0.001, Fig. 3).
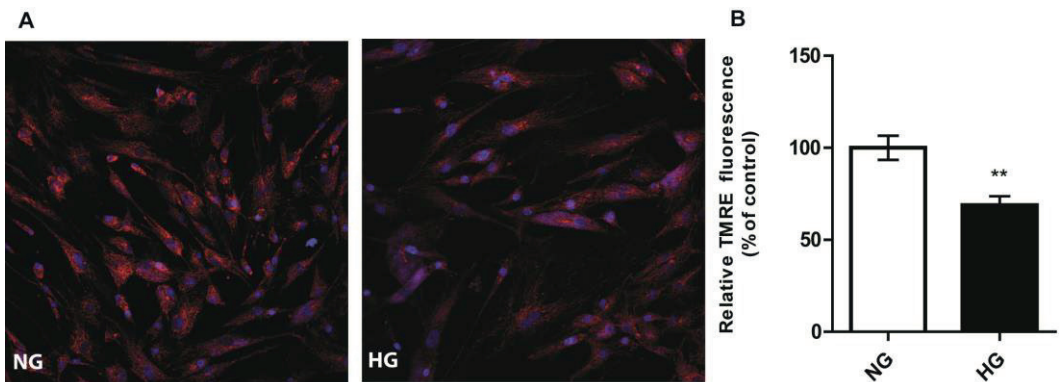

Figure. 3. HG effected mitochondrial membrane potential of ASC.

(A) Mitochondrial membrane potential of ASC grown for 7 days in NG or HG medium was detected and measured with mitochondrial membrane potential–sensitive TMRE (red) dye using confocal laser scanning microscopy.

(B) The results were plotted as MFI – SEM (**P< 0.001).

This apparent sign of a decreased mitochondrial membrane potential was corroborated by disturbances in the mitochondrial network of ASC cultured in HG medium for 7 days and assessed with MitoTracker dye. This showed a significant decrease of $23\% \pm 9.6\%$ compared to the NG control. ASC cultured in NG medium had an extensive network of mitochondria throughout the cell ($P < 0.01$, Fig. 4A).

Another relevant feature to determine mitochondrial dysfunction is mitochondrial shape and circularity. We observed a mainly tubular mitochondrial morphology in the ASC cultured in NG medium, which changed to a fragmented morphology when cultured in HG medium for 7 days. The mitochondrial fragmentation increased to virtually small fragments in nonphysiologically high (50 mM) glucose concentrations ($P < 0.0001$, Fig. 4B).
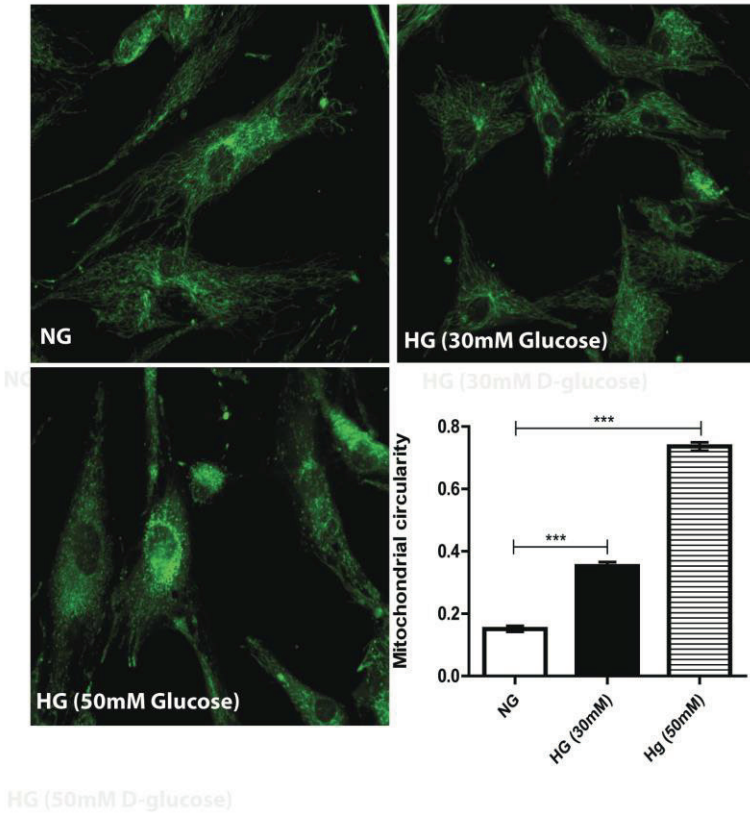
A
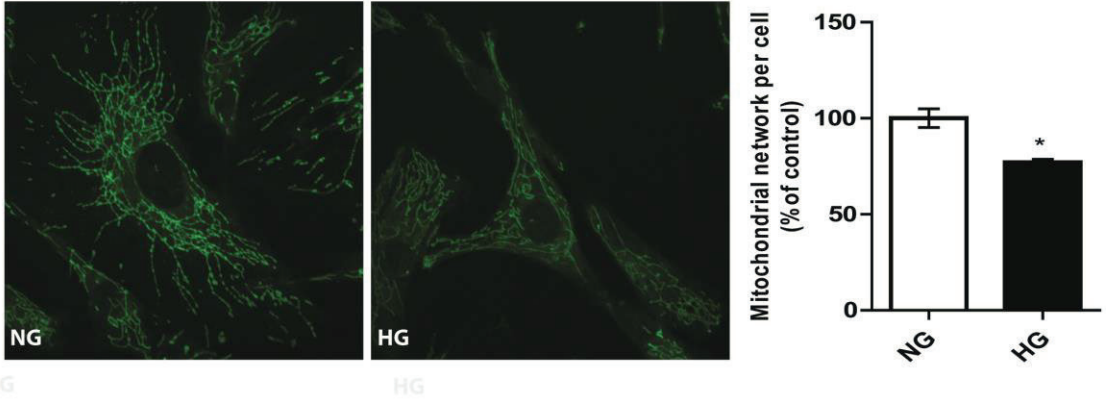
B

Figure. 4. Mitochondrial morphology of ASC changes after exposure to HG.

(A) Confocal images of ASC cultured in NG medium stained with membrane potential– independent dye MitoTracker Green FM show a network of interconnected, long and tubular mitochondria. HG significantly disrupts these mitochondrial networks. (*P < 0.01)

(B) HG induces mitochondrial fragmentation in ASC in a dose-dependent fashion. Compared to normoglycemic controls, the exposure of ASC to 30 mM glucose more than doubles the circularity (measure of fragmentation) of mitochondria, which increases another twofold when exposed to 50 mM glucose. – SEM (***P < 0.0001).

HG decreases the maximum OCR and the ECAR in ASC

ASC cultured in NG or HG conditions were simultaneously measured with a bioenergetic assay (XF24; Seahorse Bioscience) to determine the rates of cellular oxygen consumption and extracellular acidification. Steady state of oxygen consumption and extracellular acidification were measured at three time points (Fig. 5).

Oligomycin (Fig. 5A: injection vertical line A) was injected to inhibit ATP synthase, followed by the addition of FCCP (Fig. 5A: injection vertical line B) to uncouple mitochondria and obtain values for maximum oxygen consumption. Finally, mixture of rotenone and antimycin A were injected (Fig. 5A: injection vertical line C) to confirm that the respiration changes just could be attributed to mitochondrial respiration.

ASC grown in HG showed a significant decrease (29.54% ± 3%) in maximum oxygen consumption compared to ASC grown in NG medium (P < 0.0001, Fig. 5B). ECARs were examined simultaneously. Changes in the ECAR may indicate changes in the rate of glycolysis in these cells. Under HG, ASC showed significantly decreased extracellular acidification (Basal: 10%, oligomycin-induced: 34%, and FCCP-induced: 44%) as compared with ASC grown in NG medium (P < 0.01, Fig. 5C).

HG affects the glucose metabolism of ASC

Measuring uptake of 2DG is the gold standard to assess glucose uptake. ASC cultured in HG showed a 41% ± 0.17% decrease in glucose uptake compared to NG medium cultured ASC (P < 0.01, Fig. 5D), which is in line with the results from the extracellular acidification measurements. In mature adipocytes insulin stimulates the uptake of glucose into these cells. ASC can be regarded as the precursors of adipocytes. Interestingly, in our experiments insulin did not affect the glucose uptake into ASC. This shows that under these conditions ASC are not sensitive to insulin in terms of increased glucose uptake. Yet, GLUT4, the insulin-sensitive glucose transporter, was normally expressed (data not shown).
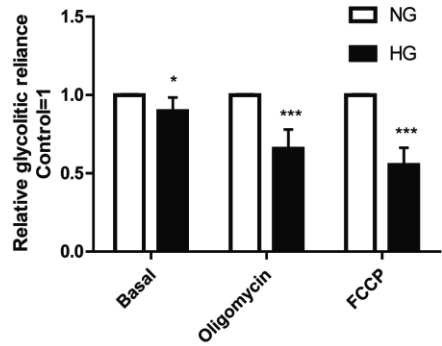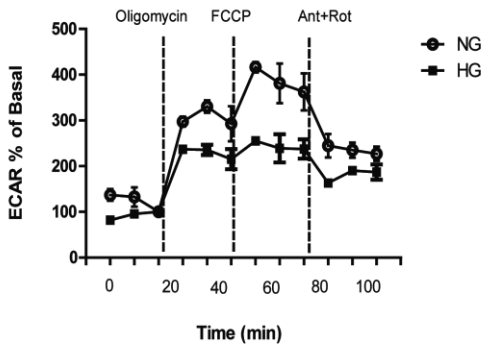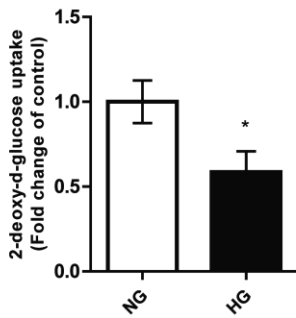
A
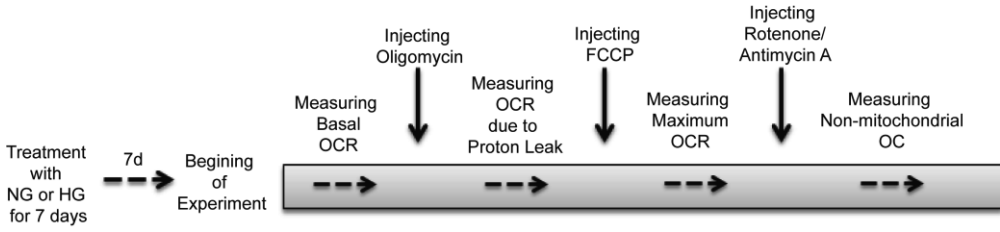
B
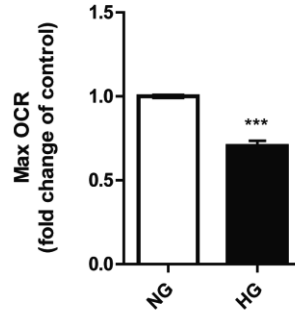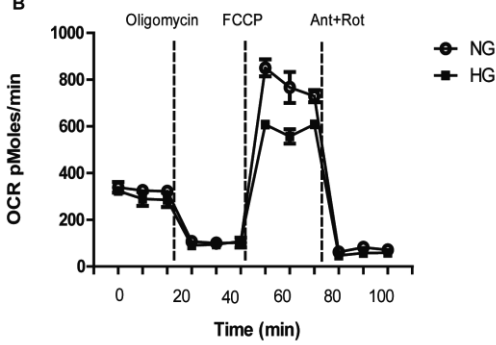
C

D

Figure. 5. HG affects mitochondrial maximum oxygen consumption rate (OCR) and extracellular acidification in ASC.

(A) Protocol for assessing mitochondrial function in ASC after exposure to HG. After measuring the basal respiration rate of cells, compounds modulating mitochondrial function are added sequentially. The effect on OCR and ECAR are measured after each compound addition.

(B) The line graph shows the experimental evaluation of steady state and maximum OCR for ASC grown in NG or HG 7 days (NG: open circles - B-, HG: black squares ---). Dotted lines (A–C) indicate injections of oligomycin, FCCP, and rotenone/antimycin A, respectively. The exposure of ASC to HG for 7 days results in reduced maximum OCRs compared to normoglycemic controls. (***P < 0.0001)

(C) HG reduces the extracellular acidification rate of ASC in basal state and also after inhibiting ATP synthase by oligomycin (after dotted line A) and injection of FCCP, which uncouples mitochondria (after dotted lineB). (*P< 0.01, ***P< 0.0001)

(D) HG significantly decreases the uptake of labeled 2-deoxyglucose by ASC. Figure shows the rate of glucose uptake, measured as pmol per mg protein and presented as the fold change compared to the control– SEM. (n = 9). In all cases the scored data were normalized for protein content (*P< 0.01).

The stimulation by ASC of vascular networks of HUVEC in vitro is affected by HG

In NG medium, preformed monolayers of ASC promoted the formation of vascular network-like structures by seeded HUVEC during 7 days coculture (Fig. 6A). These networks were absent in ASC or HUVEC controls (data not shown). The vascular-like networks comprise of interconnected multicellular tubes of endothelial cells with a lumen ranging from capillary size to multicellular structures to which ASC attach in a pericytic fashion as shown by their pericytic position and expression of SM22α (Fig. 6B, Supplementary Video S1). This is corroborated by the absence of SM22α expression by the ASC that are not involved in vascular stabilization that is, which remained bound to the tissue culture plate itself (Fig. 6B). In HG medium, the ASC still supported the formation of vascular networks by HUVEC, although at a 29% ± 3.5% reduced scale (P < 0.0001, Fig. 6C).
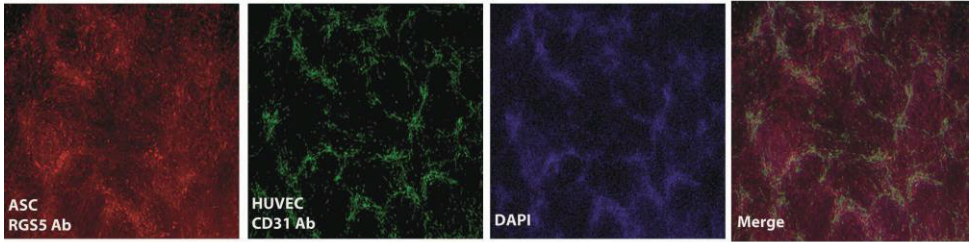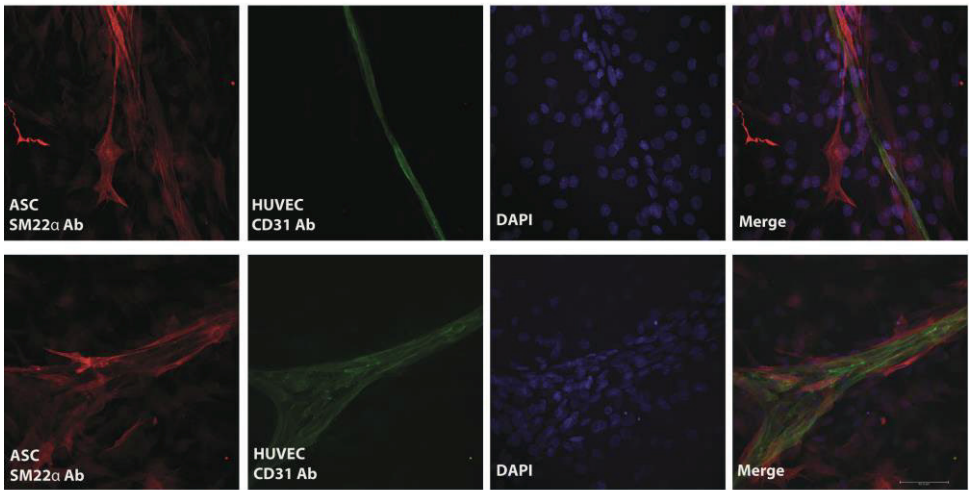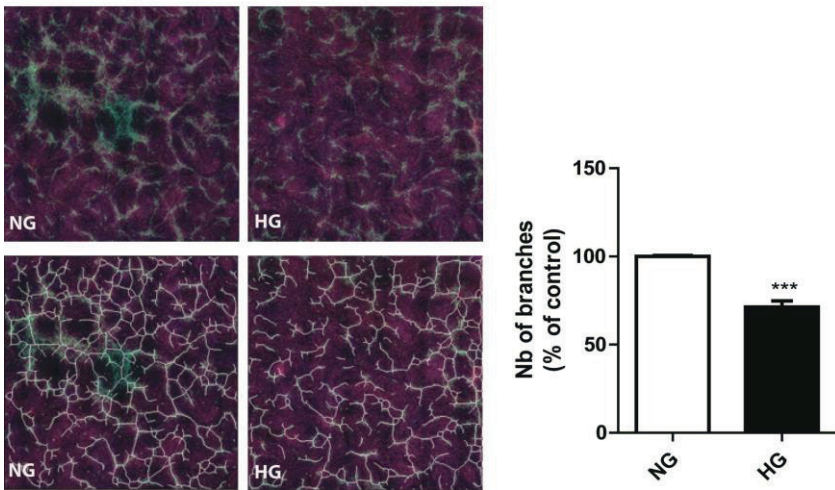
Figure. 6. (A) HUVEC (CD31, green) seeded on top of a monolayer of ASC (RGS5, red) for 7 days, results in the formation of vascular networklike structures, which does not occur in monolayers of HUVEC and ASC separately.

(B) High resolution (63 x) imaging using confocal laser scanning microscopy of interactions of ASC with vascular-like networks of HUVEC (green CD31). These vascular-like networks comprise of interconnected multicellular tubes of endothelial cells with a lumen ranging from capillary size to multicellular structures to which ASC attach in a pericytic fashion as shown by their pericytic position and expression of SM22a (red). Nuclei—blue (DAPI)

(C) HG decreases the number of branches in vascular networks on the monolayer of ASC. The network formation was analyzed with the ImageJ angiogenesis analyzer for each well (growth area 1.9 cm^2) and the number of branches were compared with the control condition (NG) (***P <0.0001). HUVEC, human umbilical vein endothelial cells.

Discussion

DR is characterized by progressive alterations in the retinal microvasculature, increasing vascular permeability caused by apoptosis in endothelial cells, and pericyte loss that leads to abnormal neovascularization in the late stage of the disease [25, 26]. Consequently, pericyte replacement would be an important step in the treatment or reversal of DR. Although, ASC are pericyte-like cells and they would be promising to stabilize the vessels in DR, more studies are necessary to show the mechanism of ASC in interaction with endothelial cells in DR in vivo. In this study we showed the influence of HG on these cells in vitro individually. HG has a remarkable influence on retinal pericyte and retinal endothelial cells including bioenergetics and metabolic dysfunction, reduced mitochondrial function, and induced mitochondrial fragmentation [22,27]. The detrimental effects of HG on mitochondrial function and cellular metabolism could play a role in the apoptosis associated with the retinal pericytes and endothelial cells in DR [28].

We showed ASC had increased intracellular ROS after a long-term (7 days) exposure to HG. Chronic HG caused mitochondrial dysfunction in ASC, which was observed both as a decreased membrane potential in HG and as structural changes as well. The increased ROS production correlated with increased apoptosis and necrosis of ASC. Interestingly, the proliferation capacity of ASC after exposure to HG for 7 days was not affected. This indicates that, with respect to function, ASC are largely refractory to the mitochondrial dysfunction that is induced by HG in vitro. It is well known that HG-induced overproduction of ROS can disrupt the mitochondrial membrane potential and damage appropriate functioning of the mitochondria [29].

This deviation in mitochondrial function is an early sign of apoptosis, which was confirmed by the apoptosis increased in treated cells [30,31]. We showed that ASC, similar to most mammalian cell types in NG, form long and tubular networks of mitochondria. These networks are critical for a normal function of the mitochondria by regulation of fusion and fission events that involve the formation or breaking of the mitochondria network, respectively [32]. A decrease in the rate of fusion and a simultaneous increase in the rate of fission cause fragmentation of the mitochondrial network, which results in shorter and rounder mitochondria [33].

Our results suggest that HG-induced mitochondrial fragmentation maybe involved in the increased ROS production in ASC. It remains unclear, however, why the proliferation rate of ASC was unaffected by ROS production under HG. While mitochondria are functional, they support cell proliferation. The fact that mitochondria under HG display similar basal respiration as NG, means that HG cells can deal with the stress condition. However, they are still suffering from HG according to the statement that maximal respiration is decreased and losing their capacity to make ATP.

Our results indicate that HG caused a decrease of the maximal OCR and the rate of extracellular acidification. The basal level of extracellular acidification in ASC decreased during HG exposure, and also after incubation with ATP synthase inhibitor (Oligomycin) and mitochondria uncoupler (FCCP). Corroborating the data obtained from the flux analyses, HG caused a significant decline in glucose uptake in ASC. Interestingly, this diminished rate of glycolysis was unresponsive to insulin stimulation. Our results indicate that ASC cultured in HG compensate the hyperglycemic environment by

changing the metabolic capacity, as displayed by decreased oxygen consumption and glycolysis.

In this study the question was addressed how the chronic diabetic microenvironment affects the ASC's therapeutic potential. This was investigated through continuous exposure of HG on ASC and their capacity to support the formation of vascular networks by HUVEC. Interestingly, the networks were still formed, although with a reduced number of branches. The ROS-induced mitochondrial dysfunction and apoptosis, only partly affected the pericytic function of ASC, because network formation by endothelial cells was only marginally affected.

Our in vitro results corroborate published data that ASC could functionally engraft in the retinal vasculature of hyperglycemic mice [17,18], while providing part of the protective measurements taken by HG-exposed ASC. Taken together, our results suggest ASC are largely resistant to long-term exposure to HG, which would explain why ASC can acquire a pericytic function in the diabetic retinal vasculature in mouse models for DR.

Our current research focuses on the paracrine and juxtacrine interactions between pericytic ASC and retinal microvascular endothelial cells under HG to understand how ASC protect microvascular endothelial cells and promote their vascular stabilization.

Author Disclosure Statement

No competing financial interests exist.

References

1. Whiting, D.R., et al., *IDF diabetes atlas: global estimates of the prevalence of diabetes for 2011 and 2030.* Diabetes Res Clin Pract, 2011. 94: p. 311-321.

2. Centers for Disease Control and Prevention (CDC)., *Blindness caused by diabetes--Massachusetts, 1987-1994,* 1996. MMWR Morb Mortal Wkly Rep 45: p. 937-941.

3. Hammes, H.P., et al., *Pericytes and the pathogenesis of diabetic retinopathy*, Diabetes. 2002. 51: p. 3107-3112.

4. Armulik, A., et al., *Endothelial/pericyte interactions*, 2005. Circ Res 97: p. 512-523.

5. Rajashekhar, G., *Mesenchymal stem cells: new players in retinopathy therapy.* Front Endocrinol (Lausanne), 2014. 5: p. 59.

6. Kowluru, R.A., J. Tang, and T.S. Kern, *Abnormalities of retinal metabolism in diabetes and experimental galactosemia. VII. Effect of long-term administration of antioxidants on the development of retinopathy*. Diabetes, 2001. 50: p. 1938-1942.

7. Cai, J., and M. Boulton, *The pathogenesis of diabetic retinopathy: old concepts and new questions*. Eye (Lond), 2002. 16: p. 242-260.

8. Henkind, P. and G.N. Wise, *Retinal neovascularization, collaterals, and vascular shunts*. Br J Ophthalmol, 1974. 58: p. 413-422.

9. Bergers, G. and S. Song, *The role of pericytes in blood-vessel formation and maintenance*. Neuro Oncol, 2005. 7: p. 452-464.

10. Green, K., M.D. Brand, and M.P. Murphy, *Prevention of mitochondrial oxidative damage as a therapeutic strategy in diabetes*. Diabetes, 2004. 53 Suppl 1: S110-8.

11. Kowluru, R.A. and P.S. Chan, *Oxidative stress and diabetic retinopathy*. Exp Diabetes Res, 2007: p. 43603.

12. Madsen-Bouterse, S.A. and R.A. Kowluru, *Oxidative stress and diabetic retinopathy: pathophysiological mechanisms and treatment perspectives.* Rev Endocr Metab Disord, 2008. 9: p. 315-327.

13. Huang, Y., V. Enzmann, and S.T. Ildstad, *Stem cell-based therapeutic applications in retinal degenerative diseases*. Stem Cell Rev, 2011. 7: p. 434-445.

14. Davey, G.C., et al., *Mesenchymal stem cell-based treatment for microvascular and secondary complications of diabetes mellitus*. Front Endocrinol (Lausanne), 2014. 5: p. 86.

15. Traktuev, D.O., et al., *A population of multipotent CD34-positive adipose stromal cells share pericyte and mesenchymal surface markers, reside in a periendothelial location, and stabilize endothelial networks*. Circ Res, 2008. 102: p. 77-85.

16. Merfeld-Clauss, S., et al., *Adipose tissue progenitor cells directly interact with endothelial cells to induce vascular network formation*. Tissue Eng Part A, 2010. 16: p. 2953-2966.

17. Rajashekhar, G., et al., *Regenerative therapeutic potential of adipose stromal cells in early stage diabetic retinopathy.* PLoS One, 2014. 9: e84671.

18. Mendel, T.A., et al., *Pericytes derived from adipose-derived stem cells protect against retinal vasculopathy*. PLoS One, 2013. 8: e65691.

19. Bourin, P., et al., *Stromal cells from the adipose tissue-derived stromal vascular fraction and culture expanded adipose tissue-derived stromal/stem cells: a joint statement of the International Federation for Adipose Therapeutics and Science (IFATS) and the International Society for Cellular Therapy (ISCT).* Cytotherapy, 2013. 15: p. 641-648.

20. Burgess, W.H., et al., *Multiple forms of endothelial cell growth factor. Rapid isolation and biological and chemical characterization*. J Biol Chem, 1985. 260: p. 11389-11392.

21. Eruslanov, E. and S. Kusmartsev, *Identification of ROS using oxidized DCFDA and flow-cytometry.* Methods Mol Biol, 2010. 594: p. 57-72.

22. Trudeau, K., A.J. Molina, and S. Roy, *High glucose induces mitochondrial morphology and metabolic changes in retinal pericytes*. Invest Ophthalmol Vis Sci, 2011. 52: p. 8657-8664.

23. Lu, Y., S.G. Rolland, and B. Conradt, *A molecular switch that governs mitochondrial fusion and fission mediated by the BCL2-like protein CED-9 of Caenorhabditis elegans*. Proc Natl Acad Sci U S A, 2011. 108: E813-22.

24. Regmi, S.G., S.G. Rolland, and B. Conradt, *Age-dependent changes in mitochondrial morphology and volume are not predictors of lifespan*. Aging (Albany NY), 2014. 6: p. 118-130.

25. Gariano, R.F., *Special features of human retinal angiogenesis*. Eye (Lond), 2010. 24: p. 401-407.

26. Calcutt, N.A., M.E. Cooper, T.S. Kern, and A.M. Schmidt, *Therapies for hyperglycaemia-induced diabetic complications: from animal models to clinical trials*. Nat Rev Drug Discov, 2009. 8: p. 417-429.

27. Trudeau, K., A.J. Molina, W. Guo, and S. Roy, *High glucose disrupts mitochondrial morphology in retinal endothelial cells: implications for diabetic retinopathy*. Am J Pathol, 2010. 177: p. 447-455.

28. Kroemer, G., *Mitochondrial implication in apoptosis. Towards an endosymbiont hypothesis of apoptosis evolution*. Cell Death Differ, 1997. 4: p. 443-456.

29. Xie, L., et al., *Mitochondrial DNA oxidative damage triggering mitochondrial dysfunction and apoptosis in high glucose-induced HRECs*. Invest Ophthalmol Vis Sci, 2008. 49: p. 4203-4209.

30. Rego, A.C. and C.R. Oliveira, *Mitochondrial dysfunction and reactive oxygen species in excitotoxicity and apoptosis: implications for the pathogenesis of neurodegenerative diseases.* Neurochem Res, 2003. 28: p. 1563-1574.

31. Kowluru, R.A., *Diabetic retinopathy: mitochondrial dysfunction and retinal capillary cell death*. Antioxid Redox Signal, 2005. 7: p. 1581-1587.

32. Karbowski, M. and R.J. Youle, *Dynamics of mitochondrial morphology in healthy cells and during apoptosis*. Cell Death Differ, 2003. 10: p. 870-880.

33. Scorrano, L., *Multiple functions of mitochondria-shaping proteins*. Novartis Found Symp, 2007. 287: p. 47-55; discussion 55-9.

Assessment of Energy Metabolic Changes in Adipose Tissue-Derived Stromal Cells

Ghazaleh Hajmousa[1], Martin C. Harmsen[1]

[1] Department of Pathology and Medical Biology, University Medical Center Groningen , University of Groningen, Groningen, the Netherlands.

CHAPTER 03

Abstract

Adipose tissue-derived stromal cells (ASC) are promising candidates for therapeutic applications in cardiovascular regenerative medicine. By definition, the phenotype ASCs *e.g.* the ubiquitous secretion of growth factors, cytokines and extracellular matrix components is not met *in vivo*, which renders ASC a culture 'artefact'. The medium constituents therefore impact the efficacy of ASC. Little attention has been paid to the energy source in medium *i.e.* glucose, which feeds the cell's power plants: mitochondria. The role of mitochondria in stromal cell biology goes beyond their function in ATP synthesis, because it includes cell signaling, reactive oxygen species (ROS) production, regulation of apoptosis and aging. Appropriate application of ASC for stromal cells therapy of cardiovascular disease warrants knowledge of their mitochondrial phenotype and function. We discuss several methodologies for assessing ASC mitochondrial function and structural changes under environmental cues in particular increased ROS caused by hyperglycemia.

Keywords: ASC, Mitochondria,   Hyperglycemia,   ROS, Energy Metabolism.

1. Introduction

Adipose tissue-derived stromal cells (ASC) are a promising source of white adipose tissue stromal cells for use in cardiovascular regenerative medicine; for their differentiation potential, their ease of isolation and their secretion of therapeutically relevant trophic factors [1,2]. The therapeutic potential of ASC has been assessed in various animal models with specific disorders such as Parkinson's disease [3] and Alzheimer's disease [4,5], bone and cartilage defects [6,7], skin wound healing [8], myocardial infarction [9,10] and diabetic retinopathy [11,12].

There is new evidence that, in addition to growth factors and extracellular matrix cues, the (energy) metabolism of stromal cell directs self-renewal and differentiation [13-15].

Recent studies have revealed limitations in the therapeutic efficacy of ASC derived from patients that were compromised by diabetes or aging or obesity. It has been demonstrated that ASC from these patients have impaired differentiation and migration [16-19]. Recently, we also showed *in vitro,* that ASC respond to chronic hyperglycemic exposure by increased apoptosis caused by amplified ROS. In addition, hyperglycemically cultured ASC showed an altered mitochondrial membrane potential and changes in mitochondrial network morphology. Interestingly, we found an altered glycolysis and glucose uptake potential in ASC upon culture under hyperglycemic conditions (30mM D-glucose) compared to normaglycemically (5mM D-glucose) cultured ASC.

These data confirm the well-established fact that mitochondrial disorders have a key role in apoptosis [20] and it contributes to a wide number of diseases, including mitochondrial myopathies [21],

mitochondrial neuropathies [22] and diabetes [23]. Mitochondria are a main source of reactive oxygen species (ROS) in the cell [24]. In healthy cells, the inner membrane of mitochondria is impermeable to ions [25] which allows the electrons transport chain (ETC) to build up the proton gradient required to generate energy. The mitochondrial membrane potential ($\Delta\Psi$m) results from the difference in electrical potential generated by the electrochemical gradient across the inner membrane [26].

Mitochondria are the source for ROS, but also the major target of their damaging effects, demonstrating the trigger for several mitochondrial dysfunctions. Chronic increases in ROS production cause the accumulation of ROS-associated damage in DNA, proteins, and lipids, and is headed by severe perturbations in mitochondrial function detected as a decrease in $\Delta\Psi_m$. This reduction in $\Delta\Psi_m$ is accompanied by the production of ROS contributing to cell apoptosis [27]. Alterations of the glucose metabolism may cause mitochondrial dysfunction, i.e. affect the energy metabolism, and may be responsible for further cellular damage and disease pathogenesis. The failure to manage cellular energy pathways either the aerobic respiration or glycolysis via mitochondria may result in serious complications in diseases such as diabetes [28]. Detecting mitochondrial dysfunction in therapeutic used ASC is a prerequisite in the development of novel stromal cell therapies for diseases such as diabetes.

2. Materials

2.1. Isolation of ASC

1. Human subcutaneous fat tissue or liposuction-derived fat
2. Phosphate-buffered saline (PBS)
3. PBS/1% Bovine serum albumin (BSA)
4. 0.1% Collagenase dissolved in PBS/1%BSA, freshly prepared prior to use (Dissociation medium)

5. Dulbecco's Modified Eagle Medium (DMEM) supplemented with 10% fetal bovine serum (FBS) and 100U/ml Penicillin, 100µg/ml Streptomycin, 2mM L-glutamine and 1 (gr/L) D-glucose (control medium). Store at 4°C.

6. 50-ml Centrifuge tube
7. 40-µm Nylon mesh
8. Lymphoprep
9. Lysis buffer
10. Trypan blue

2.2. ASC Culture

1. DMEM supplemented with 10% fetal bovine serum (FBS) and 100U/ml Penicillin, 100µg/ml Streptomycin, 2mM L-glutamine and 1 (gr/L) D-glucose (control medium) or 4.5 (gr/L) D-glucose (hyperglycemic medium). Store at 4°C.
2. Trypsin (0.25%) and ethylenediaminetetraacetic acid (EDTA, 1 mM)

2.3. Apoptosis detection of ASC (using FACS Calibur flow-cytometer)

1. Annexin V- Ethidium Homodimer lll (EthD-III): Apoptotic/Necrotic Cells Detection Kit (#PK-CA707-30018-Promokine)
2. Trypsin (0.25%) and ethylenediaminetetraacetic acid (EDTA, 1 mM).
3. FACS tubes

2.4. Intracellular ROS and mitochondrial ROS measurement in ASC (using FACS Calibur flow-cytometer)

1. 2',7'-Dichlorofluorescin diacetate: H_2DCFDA (#D399-Thermo Fisher)
2. MitoSOX™ Red: Mitochondrial superoxide indicator (#M36008-Thermo Fisher)
3. Trypsin (0.25%) and ethylenediaminetetraacetic acid (EDTA, 1 mM).
4. Control medium/PBS

2.5.   Monitoring mitochondrial health
2.5.1. Assessment of mitochondrial membrane potential

1. MitoProb ™ JC1 (5',6,6'-tetrachloro-1,1',3,3'tetraethylbenzimidazolylcarbocyanine iodide (#M34152-Thermo Fisher)
2. CCCP (carbonyl cyanide 3-chlorophenylhydrazone)
3. Trypsin (0.25%) and ethylenediaminetetraacetic acid (EDTA, 1 mM).
4. Control medium/PBS

2.5.2. Mitochondrial Morphology Analysis

1. Mito-Tracker Green [MTG] (#M7514-Thermo Fisher)
2. Trypsin (0.25%) and ethylenediaminetetraacetic acid (EDTA, 1 mM).
3. Control medium/PBS

2.6.   ASC bioenergetics profiling

1. V7-PS XF24 cell culture microplates (#11915-Seahorse Bioscience), XF24 extracellular flux assay kits (#Q09015-Seahorse Bioscience)
2. DMEM-XF containing, 1 mM glutamine, 1% FBS, 1 (gr/L) D-glucose (control medium) or 4.5 (gr/L) D-glucose (hyperglycemic medium) and pyruvate-free (Unbuffered medium)
3. Oligomycin (#103015-Seahorse Bioscience)
4. FCCP (carbonyl cyanide 4-(trifluoromethoxy) phenylhydrazone (#103015-Seahorse Bioscience)

5. Rotenone and Antimycin A (#103015-Seahorse Bioscience)
6. 2-deoxy-D-glucose (#D8375-Sigma Aldrich)
7. Pierce™ BCA Protein Assay Kit (#23225-Thermo Fisher)

2.7.   Assessment of Glucose uptake

1. 2-deoxy D-glucose (#D8375-Sigma Aldrich)
2. PBS
3. DMEM supplemented with 10% fetal bovine serum (FBS) and 100U/ml Penicillin, 100µg/ml Streptomycin, 2mM L-glutamine and 1 (gr/L) D-glucose (control medium) or 4.5 (gr/L) D-glucose (hyperglycemic medium). Store at 4°C. (serum-free medium)
4. Insulin
5. 2-deoxy-D-[^{14}C]glucose (^{14}C- 2-DOG) (#NEC495-Perkin Elmer)
6. NaOH
7. β-scintillation cocktail and β-scintillation counter
8. Pierce™ BCA Protein Assay Kit (#23225-Thermo Fisher)

3. Methods

3.1.   Isolation of ASC

1. Mince the fat tissue with fine scissors in culture dishes, and transfer the material into a 50ml centrifuge tube. Alternatively, lipoaspirated fat can be transferred to centrifuge tubes directly.
2. Wash the fat 3 times with PBS, centrifuge at 300xg for 3 min each time.
3. Add an equal volume of dissociation medium with the fat, stir for 90 min in 37°C water bath.
4. Filter the digested fat through 40-µm Nylon mesh; collect the flow-through in 50 ml tubes.
5. Centrifuge the cell suspension at 600×g for 10 min to obtain a high-density ASC pellet.
6. Aspirate the supernatant, being careful not to disturb the cell pellets.
7. Resuspend the cell pellets in 30 ml PBS/1%BSA and add the cell-suspension gently on top of 15 ml Lymphoprep.
8. Centrifuge at 4°C, 1,000×g for 20 min.
9. Carefully aspirate the cells from the interphase.
10. Resuspend cells in lysis buffer and place on ice for 5 min, centrifuge at 600×g for 10 min.
11. Count the cells using Trypan blue and seed at a concentration of 1.25×10^5 cells/cm^2 in culture flasks.

3.2. ASC Culture

1. Maintain the primary ASC in control medium at 37°C in 5% carbon dioxide. Change the culture medium every 3 days.

2. Once adherent cells become confluent, aspirate the culture medium and wash the cells with 5 ml of PBS. Add 1-3 ml of trypsin–EDTA at 37°C for 5 min to detach the cells.

3. Resuspend the ASC with an equal volume of control medium.

4. Centrifuge the cell suspension at 300×g for 10 min at 4°C and split the cells 1:3 in control medium.

5. Use the cells from passage 2-7 for the experiments (*e.g.* to expose the cells to an apoptotic condition such as hyperglycemia)

3.3. Apoptosis detection of ASC (using FACS Calibur flow cytometer)

1. Harvest ASC from control/ treated group: aspirate the culture medium and wash the cells with 5 ml of PBS. Add 1-3 ml of trypsin–EDTA at 37°C for 5 min to detach the cells.
2. Wash the cells, centrifuge at 300×g for 10 min at 4°C and resuspend the cells in 500μl binding buffer (100,000 cells/500μl) in FACS tubes.
3. Stain the cells with 2.5μl FITC-AnnexinV (marker for apoptosis) and 2.5μl of Ethidium Homodimer lll (marker for necrosis) in the dark at room temperature for 15min
4. Analyze the samples (FITC-AnnexinV -Ex/Em= ~492/514 nm and EthD-III-Ex/Em= ~528/617 nm) using a FACS Calibur flow cytometer within 1 hour after staining.

3.4. Intracellular ROS and mitochondrial ROS measurement in ASC (using FACS Calibur flow-cytometer)

1. Harvest ASC from control/ treated groups: aspirate the culture medium and wash the cells with 5 ml of PBS. Add 1-3 ml of trypsin–EDTA at 37°C for 5 min to detach the cells.
2. Wash the cells, centrifuge at 300×g for 10 min at 4°C and resuspend the cells in FACS tubes with 1ml of warm control medium followed by incubation with 20µM H_2DCFDA or 5 µM MitoSOX™ Red in the dark at 37 °C for 15min.
3. Analyze the samples (DCF: Ex/Em= ~492/527 nm and oxidized MitoSOX: Ex/Em= ~510/580 nm) directly without washing, using a FACS Calibur flow-cytometer within 30 min after the staining.

3.5.   Monitoring mitochondrial health

3.5.1.   Assessment of mitochondrial membrane potential

1. Harvest ASC from control/ treated groups: aspirate the culture medium and wash the cells with 5 ml of PBS. Add 1-3 ml of trypsin–EDTA at 37°C for 5 min to detach the cells.
2. Wash the cells, centrifuge at 300×g for 10 min at 4°C and resuspend the cells in 1 mL warm control medium at 1×10^6 cells/mL, followed by adding 2 µM MitoProbe JC-1 and 50 µM CCCP as control.
3. Incubate the samples at 37°C for 15 minutes.
4. Determine the mitochondrial accumulation of the probe by fluorescence emission shift from green (~529 nm) to red (~590 nm) by FACS Calibur flow-cytometer within 15 min after staining.

3.5.2. Mitochondrial Morphology Analysis

1. Once ASC cultures from control/ treated group become confluent, aspirate the culture medium and wash the cells with PBS twice.
2. Incubate the ASC at 37°C in a 5% CO2 humidified chamber with 120 nM membrane potential–independent dye: Mito- Tracker Green [MTG] in culture medium for 45 min.
3. Wash the cells three times with PBS and refresh the medium.
4. Keep the cells at 37°C in a 5% CO_2 humidified microscope stage chamber and image the cells live by confocal microscope with a 60x oil immersion objective (MTG: Ex/Em= ~488/550 nm)
5. Acquire in series of 6 slices per cell ranging in thickness from 0.5 to 0.8 µm per slice to visualize individual mitochondria as well as their inter-connective network or disturbances.
6. Analyze the mitochondrial length and circularity of ASC with ImageJ software.

3.6. ASC bioenergetics profiling

1. Plate the ASC on V7-PS microplate under control or treatment condition to reach a confluent monolayer.
2. Wash the cells three times with PBS.
3. Replace the unbuffered medium and incubate cell at 37°C in a CO_2-free incubator for 60min.
4. For oxygen consumption rate (OCR): pipet 2µM oligomycin in port A, 5µM FCCP in port B and a mixture containing 2µM rotenone and 2 µM antimycin A in port C. For extracellular acidification rate (ECAR): pipet the saturating concentration of glucose (10 *mM)* in port A, 2µM oligomycin in port B and 100µM 2-deoxy-D-glucose in port C.
5. Place the microplate in XF24 Extracellular Flux Analyzer; Seahorse Bioscience to measure extracellular flux changes (Follow the protocol in Fig. 2C)
6. Normalize the results from the measurement to total cellular proteins in each well.

3.7.   Assessment of Glucose uptake

1. Once ASC cultures from control/ treated group reach confluency, aspirate the culture medium and wash the cells twice with PBS.
2. Incubate the cells in serum-free medium at 37°C for 4 hours.
3. Stimulate the ASC with 100nM insulin for 20 min at 37°C or leave untreated.
4. Remove the medium; wash the cells twice with warm PBS.
5. Add 1ml of PBS containing 0.1µCi 2-deoxy-D-[^{14}C]glucose (^{14}C-2-DOG) and unlabeled 100µM 2-deoxy-D-glucose to each well.
6. Incubate the cells at 37°C for 45min.
7. Terminate the glucose transport by washing twice with ice-cold PBS.
8. Lyse the cells in 500µl 0.05M NaOH.
9. Use 400µl of the aliquot for β-scintillation determination.
10. Use the remained 100µl for the determination of protein concentration with the Pierce™ BCA Protein Assay Kit.

4. Notes

- MitoSOX is considered a superoxide-specific probe to visualize superoxide ions inside mitochondria [29]. The MitoSox specify for hydrogen peroxide or reactive nitrogen species is quite low [30].

- DCF formation is reflected to H_2O_2 production but it cannot be used to measure H_2O_2 production exclusively inside mitochondria. For imaging mitochondrial H_2O_2 in living cells we recommend peroxy-yellow-1 (MitoPY1), a new type of fluorophore [31], although advanced studies have to be performed to stablish its efficacy.

- Mitochondrial circularity is a measure of the "roundness" of mitochondria with 0 referring to a straight line and 1 as a perfect circle. Cells containing a majority of long interconnected mitochondrial networks were classified as cells with tubular mitochondria. Cells with a majority of short mitochondria were classified as fragmented and cells with mostly sparse small round mitochondria were classified as very fragmented [32].

  As an example we showed a mainly long and tubular mitochondrial network morphology in the healthy ASC cultured in 5mM D-glucose medium, which changed to a very fragmented morphology when cultured in medium with a non-physiologically high (50mM) concentration of D-glucose (Fig. 1A, B).
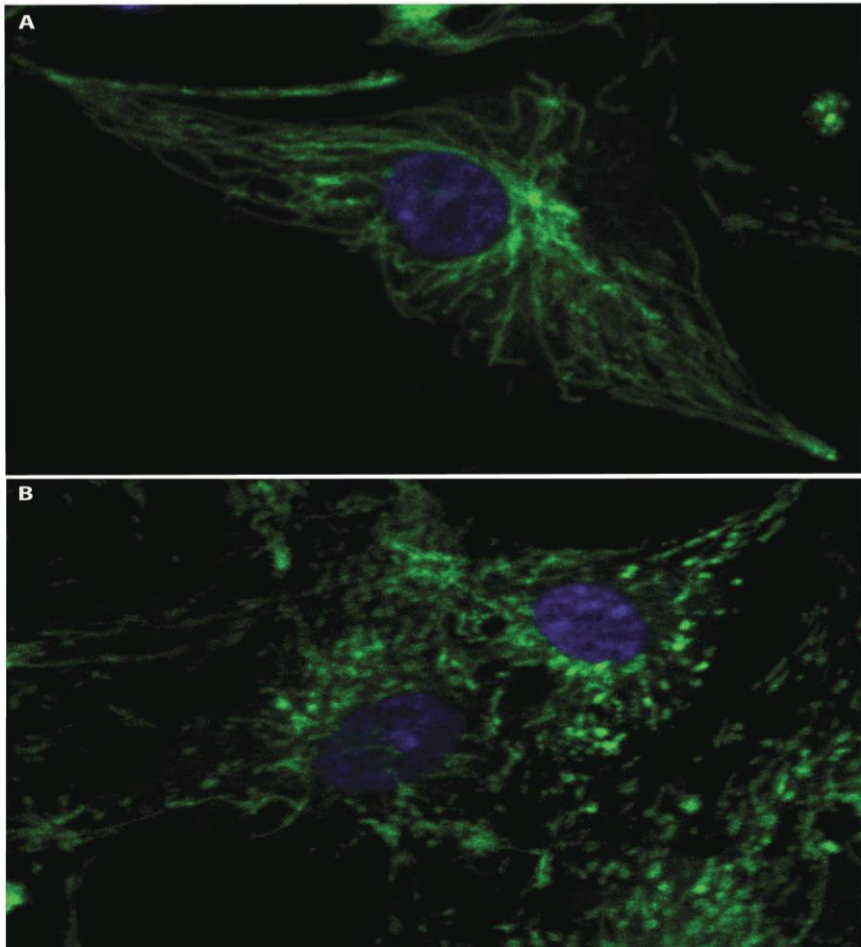
Figure. 1. Confocal analysis of ASC using staining with Mitotracker Green FM. Long and tubular mitochondrial network morphology in healthy ASC cultured in 5mM D-glucose medium (A). Very fragmented mitochondrial morphology of ASC after culturing in non-physiologically high (50mM) D-glucose concentration medium (B). Blue pseudocolor = DAPI, nucleus staining.
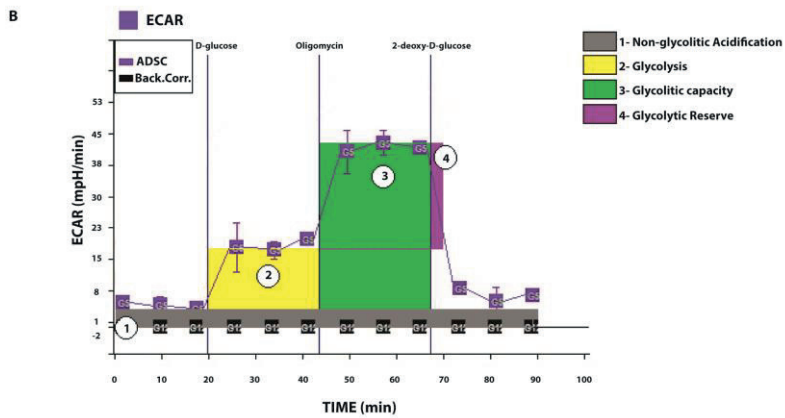
The tubular mitochondria networks are desired for a normal function of the mitochondria by regulation of fusion and fission events that involve the formation or breaking of the mitochondria network, respectively. A decrease in the rate of fusion and a simultaneous increase in the rate of fission cause fragmentation of the mitochondrial network which results in shorter and rounder mitochondria [33, 34].

- OCR measurement steps:

  1. Measuring the basal OCR.

  2. Inhibitory analysis using injections of oligomycin (Olig) at $2\,\mu M$ which inhibits ATP synthase [ATP-linked respiration $=OCR_{pre-Olig} - OCR_{post-Olig}$], [proton leak $=OCR_{post-Olig} - OCR_{post-AntA/R}$].

  3. Applying proton ionophore FCCP at $5\,\mu M$, which uncouples mitochondria to obtain the maximum oxygen consumption rates [maximal respiration $=OCR_{post-FCCP} - OCR_{post-AntA/R}$], [respiratory capacity $=OCR_{post-FCCP} - OCR_{pre-Olig}$].

  4. Adding a mixture of an electron transport blocker, antimycin A (AntA) at $2\,\mu M$ and rotenone at $2\,\mu M$ as an inhibitor of mitochondrial complex to confirm that respiration changes were due mainly to mitochondrial respiration.

- ECAR measurement steps:
    1. Measuring the basal ECAR in a medium without glucose or pyruvate.
    2. Measuring glycolysis rate of cells in saturating concentration of glucose [basic glycolysis $=ECAR_{pre-Olig}$].
    3. Inhibitory analysis using injections of oligomycin (Olig) at 2 µM which inhibits ATP synthase and shifts the energy production pathway to glycolysis to reach to the cellular maximum glycolytic capacity [glycolytic capacity $=ECAR_{post-Olig}$], [glycolytic reserve $=ECAR_{post-Olig} - ECAR_{pre-Olig}$].
    4. Inhibiting the glycolysis by using 100µM 2-deoxy-glucose, a glucose analog.

    After normalization and analyzing the data, the mentioned mitochondrial respiration and glycolytic indexes can be calculated (Fig. 2A, B).

A

● OCR

■ ADSC
■ Back.Corr.

Oligomycin   FCCP   Antimycin A & Rotenone

OCR (pMoles/min)

774
675
577
478
379
280
181
82
-17

1- Non-mitochondrial Respiration
2- Basal Respiration
3- proton Leak
4- ATP Production
5- Maximal Respiration
6- Spare Respiratory Capacity

0   10   20   30   40   50   60   70   80   90   100

TIME (min)

B

■ ECAR

■ ADSC
■ Back.Corr.

D-glucose   Oligomycin   2-deoxy-D-glucose

ECAR (mpH/min)

53
45
38
30
23
15
8
1
-2

1- Non-glycolitic Acidification
2- Glycolysis
3- Glycolitic capacity
4- Glycolytic Reserve

0   10   20   30   40   50   60   70   80   90   100

TIME (min)

C   ADSC XF-analyzing protocol commands

EVENT	TIME	REPEAT
Start		
Loading Cartridge		
Calibration		
Equilibration		
Mixing	2 min	
Waiting	2 min	x3
Measuring	4 min	
Injecting From Port A		
Mixing	2 min	
Waiting	2 min	x3
Measuring	4 min	
Injecting From Port B		
Mixing	2 min	
Waiting	2 min	x3
Measuring	4 min	
Injecting From Port C		
Mixing	2 min	
Waiting	2 min	x3
Measuring	4 min	
End		

Figure. 2. Mitochondrial respiration graph of ASC : Basal respiration, ATP production and proton leak after injecting oligomycin, maximal respiration after exposure the ASC to FCCP and spare respiratory capacity of the cells were measured by using a Seahorse XF-analyzer and plotted (A). The glycolytic function of ASC: glycolysis, glycolytic capacity after injecting oligomycin and glycolytic reserve are shown (B). Protocol commands for ASC extracellular flux analyzing by Seahorse XF-analyzer (C).

References

1. Gimble, J. and F. Guilak, *Adipose-derived adult stem cells: isolation, characterization, and differentiation potential*. Cytotherapy. 2003. 5:p. 362-369.

2. Parker, A.M. and A.J. Katz, *Adipose-derived stem cells for the regeneration of damaged tissues*. Expert Opin.Biol.Ther, 2006. 6: p.567-578.

3. Choi, H.S., et al., *Therapeutic potentials of human adipose-derived stem cells on the mouse model of Parkinson's disease*. Neurobiol.Aging, 2015. 36:p.2885-2892.

4. Chang, K.A., J.H. Lee, and Y.H. Suh, *Therapeutic potential of human adipose-derived stem cells in neurological disorders*. J.Pharmacol.Sci, 2014. 126: p. 293-301.

5. Chang, K.A., et al., *The therapeutic effects of human adipose-derived stem cells in Alzheimer's disease mouse models*. Neurodegener Dis, 2014. 13: p. 99-102.

6. Mehrabani, D., et al., *The Healing Effect of Adipose-Derived Mesenchymal Stem Cells in Full-thickness Femoral Articular Cartilage Defects of Rabbi. Int.J.Organ.Transplant.Med*, 2015. 6: p. 165-175.

7. Wu, L., X. Cai, S. Zhang, M. Karperien, and Y. Lin, *Regeneration of articular cartilage by adipose tissue derived mesenchymal stem cells: perspectives from stem cell biology and molecular medicine*. J.Cell.Physiol, 2013. 228: p. 938-944.

8. Spiekman, M., et al., *Adipose tissue-derived stromal cells inhibit TGF-beta1-induced differentiation of human dermal fibroblasts and keloid scar-derived fibroblasts in a paracrine fashion*. Plast.Reconstr.Surg, 2014. 134: p. 699-712.

9. Chen, L., F. Qin, M. Ge, Q. Shu, and J. Xu, *Application of adipose-derived stem cells in heart disease*. J.Cardiovasc.Transl.Res, 2014. 7: p. 651-663.

10. Naaijkens, B.A., et al., *Therapeutic application of adipose derived stem cells in acute myocardial infarction: lessons from animal models*. Stem Cell.Rev, 2014. 10: p. 389-398.

11. Rajashekhar, G., et al., *Regenerative therapeutic potential of adipose stromal cells in early stage diabetic retinopathy*. PLoS One, 2014. 9: e84671.

12. Mendel, T.A., et al., *Pericytes derived from adipose-derived stem cells protect against retinal vasculopathy*. PLoS One, 2013. 8: e65691.

13. Rehman, J., *Empowering self-renewal and differentiation: the role of mitochondria in stem cells*. J.Mol.Med.(Berl), 2010. 88: p. 981-986.

14. Xu, X., et al., *Mitochondrial regulation in pluripotent stem cells*. Cell.Metab, 2013. 18: p. 325-332.

15. Zhang, J., et al., *Metabolic regulation in pluripotent stem cells during reprogramming and self-renewal.* Cell.Stem Cell, 2012. 11: p. 589-595.

16. Ferrer-Lorente, R., et al., *Systems biology approach to identify alterations in the stem cell reservoir of subcutaneous adipose tissue in a rat model of diabetes: effects on differentiation potential and function*. Diabetologia, 2014. 57: p. 246-256.

17. Efimenko, A., et al., *Angiogenic properties of aged adipose derived mesenchymal stem cells after hypoxic conditioning*. J.Transl.Med, 2011. 9: p. 10-5876-9-10.

18. Perez, L.M., et al., *Metabolic rescue of obese adipose-derived stem cells by Lin28/Let7 pathway*. Diabetes, 2013. 62: p. 2368-2379.

19. Cronk, S.M., et al., *Adipose-derived stem cells from diabetic mice show impaired vascular stabilization in a murine model of diabetic retinopathy*. Stem Cells Transl.Med, 2015. 4: p. 459-467.

20. Suen, D.F., K.L. Norris, and R.J. Youle, *Mitochondrial dynamics and apoptosis*. Genes Dev, 2008. 22: p. 1577-1590.

21. DiMauro, S., *Mitochondrial myopathies*. Curr.Opin.Rheumatol, 2006. 18: p. 636-641.

22. DiMauro, S., and E.A. Schon, *Mitochondrial disorders in the nervous system*. Annu.Rev.Neurosci, 2008. 31: p. 91-123.

23. Sivitz, W.I., and M.A. Yorek, *Mitochondrial dysfunction in diabetes: from molecular mechanisms to functional significance and therapeutic opportunities.* Antioxid.Redox Signal, 2010. 12: p. 537-577.

24. Suski, J.M., et al., *Relation between mitochondrial membrane potential and ROS formation*. Methods Mol.Biol, 2012. 810: p. 183-205.

25. Fulda, S., L. Galluzzi, and G. Kroemer, *Targeting mitochondria for cancer therapy*. Nat.Rev.Drug Discov, 2010. 9: p. 447-464.

26. Marchi, S., et al., *Mitochondria-ros crosstalk in the control of cell death and aging*. J.Signal.Transduct, 2012. 2012: p. 329635.

27. Kroemer, V., *Mitochondrial implication in apoptosis. Towards an endosymbiont hypothesis of apoptosis evolution*. Cell Death Differ, 1997. 4: p. 443-456.

28. Patti, M.E., and S. Corvera, *The role of mitochondria in the pathogenesis of type 2 diabetes.* Endocr.Rev, 2010. 31: p. 364-395.

29. Robinson, K.M., M.S. Janes, and J.S. Beckman, *The selective detection of mitochondrial superoxide by live cell imaging*. Nat.Protoc, 2008. 3: p. 941-947.

30. Zielonka, J., and B. Kalyanaraman, *Hydroethidine- and MitoSOX-derived red fluorescence is not a reliable indicator of intracellular superoxide formation: another inconvenient truth*. Free Radic.Biol.Med, 2010. 48: p. 983-1001.

31. Dickinson, B.C., and C.J. Chang, *A targetable fluorescent probe for imaging hydrogen peroxide in the mitochondria of living cells.* J.Am.Chem.Soc, 2008. 130: p. 9638-9639.

32. Regmi, S.G., S.G. Rolland, and B. Conradt, *Age-dependent changes in mitochondrial morphology and volume are not predictors of lifespan*. Aging (Albany NY), 2014. 6: p. 118-130.

33. Karbowski, M., and R.J. Youle, *Dynamics of mitochondrial morphology in healthy cells and during apoptosis*. Cell Death Differ, 2003. 10: p. 870-880.

34. Scorrano, L., *Multiple functions of mitochondria-shaping proteins*. Novartis Found.Symp, 2007. 287: p. 47-55; discussion 55-9.

Chapter 3

Human adipose tissue-derived stromal cells act as functional pericytes in mice and suppress high-glucose-induced proinflammatory activation of bovine retinal endothelial cells

Ghazaleh Hajmousa[1], Ewa Przybyt[1], Frederick Pfister[2], Genaro A. Paredes-Juarez[1], Kondaiah Moganti[3], Stephanie Busch[2], Jeroen Kuipers[4], Ingeborg Klaassen[5], Marja J.A. van Luyn[1], Guido Krenning[1], Hans-Peter Hammes[2], Martin C. Harmsen[1*]

[1]   Department of Pathology and Medical Biology, University Medical Center Groningen, University of Groningen, Hanzeplein 1 (EA11), 9713 GZ Groningen, the Netherlands

[2]   5th Medical Department, Medical Faculty Mannheim, University of Heidelberg, Mannheim, Germany

[3]   Institute of Transfusion Medicine and Immunology, Medical Faculty Mannheim, University of Heidelberg, Mannheim, Germany

[4]   Department of Cell Biology, Molecular Imaging and Electron Microscopy, University Medical Center Groningen, University of Groningen, Groningen, the Netherlands

[5]   Ocular Angiogenesis Group, Departments of Ophthalmology and Medical Biology, Academic Medical Center, University of Amsterdam, Amsterdam, the Netherlands

CHAPTER 04

Abstract

The immunomodulatory capacity of adipose tissue-derived stromal cells (ASCs) is relevant for next-generation cell therapies that aim to reverse tissue dysfunction such as that caused by diabetes. Pericyte dropout from retinal capillaries underlies diabetic retinopathy and the subsequent aberrant angiogenesis.

We investigated the pericytic function of ASCs after intravitreal injection of ASCs in mice with retinopathy of prematurity (ROP) as a model for clinical diabetic retinopathy. In addition, ASCs influence their environment by paracrine signalling. For this, we assessed the immunomodulatory capacity of conditioned medium from cultured ASCs (ASC-Cme) on high glucose (HG)-stimulated bovine retinal endothelial cells (BRECs).

ASCs augmented and stabilised retinal angiogenesis and co-localised with capillaries at a pericyte-specific position. This indicates that cultured ASCs exert juxtacrine signalling in retinal microvessels. ASC-Cme alleviated HG-induced oxidative stress and its subsequent upregulation of downstream targets in an NF-κB dependent fashion in cultured BRECs. Functionally, monocyte adhesion to the monolayers of activated BRECs was also decreased by treatment with ASC-Cme and correlated with a decline in expression of adhesion-related genes such as *SELE*, *ICAM1* and *VCAM1*.

The ability of ASC-Cme to immunomodulate HG-challenged BRECs is related to the length of time for which ASCs were preconditioned in HG medium. Conditioned medium from ASCs that had been chronically exposed to HG medium was able to normalise the HG-challenged BRECs to NG levels. In contrast, conditioned medium from ASCs that had been exposed to HG medium for a shorter time did not have this effect.

Our results show that the manner of HG preconditioning of ASCs dictates their immunoregulatory properties and thus the potential outcome of treatment of diabetic retinopathy.

Keywords

Introduction

Diabetic retinopathy is the most common microvascular complication of diabetes and remains a leading cause of blindness worldwide [1]. The prevalence of diabetic retinopathy increases with diabetes duration and develops from non-proliferative diabetic retinopathy to proliferative diabetic retinopathy (PDR) and macular oedema [2]. Hyperglycaemia in the retina activates four main biochemical pathway-related changes: (1) polyol pathway flux; (2) accumulation of advanced glycation end-products (AGEs); (3) activation of protein kinase C (PKC); (4) activation of hexosamine pathway flux [3]. Together, these molecular changes induce formation of reactive oxygen species (ROS), which induces impaired retinal blood flow and increased vascular permeability [4].

Retinas or vitreous from diabetic individuals with PDR contain increased levels of proinflammatory mediators including TNF-α, IL-1β [5], IL-6 [6], IL-8 [7] and chemokine (C-C motif) ligand 2 (CCL2) [8, 9]. NF-κB is the main transcription factor that regulates expression of proinflammatory genes. Activation and nuclear translocation of NF-κB promotes forward feedback that augments the proinflammatory state of activated cells [10]. Diabetes is related to the upregulation of cyclooxygenase-2 (COX2) encoded by the prostaglandin-endoperoxide synthase 2 gene (*PTGS2*), both in macro- and microvessels [11]. In retinas of diabetic animals, increased COX2 is followed by increased production of prostaglandin E_2 (PGE2) [12].

At the onset of diabetic retinopathy, pericyte dropout and the subsequent loss of retinal endothelial cells through apoptosis causes vasoregression. This is the driving force for the pathological angiogenesis of PDR [13].

In the normal retina, pericytes protect and regulate endothelial cell survival and proliferation, vessel integrity and the susceptibility of vascular cells to environmental stimuli [14]. Cell therapy with adipose tissue-derived stromal cells (ASCs) were promising in diabetic animal models. Adipose tissue is easy to acquire and is rich in ASCs. These ASCs are the endogenous mesenchymal stem cells in fat and they harbour a multipotent capacity to differentiate, for example, into adipocytes, chondrocytes and osteoblasts [15].

Recent studies suggested a direct role for ASCs in retinal microvascular support [16]. In rodent models of diabetic retinopathy, ASCs acquired pericytic features, which dampened proliferative angiogenesis [17, 18]. Recently, we showed that the pericytic nature of ASCs depends on neurogenic locus notch homolog protein 2 (NOTCH2)-based juxtacrine interaction between ASCs and endothelial cells [18]. Moreover, ASCs may home in on sites of inflammation [19]. The prime immunosuppressive factors produced by mesenchymal stem cells and ASCs include indoleamine 2,3-dioxygenase [20], PGE2 [21], nitric oxide (NO) [22], IL-10 [23] and antioxidant enzymes such as haem oxygenase-1 [24].

Individually or in combination, these factors also reduce oxidative stress in target cells [25, 26]. We hypothesised that ASCs preconditioned in high glucose (HG) can rescue a dysfunctional retinal endothelium through suppression of the inflammation that was caused by glucose-induced oxidative stress.

The aim of this study was to investigate the immunomodulatory paracrine function of ASCs in decreasing the production of endothelial ROS and in the normalisation of dysfunctional endothelial cells in diabetic retinopathy.

Materials and Methods

Cell isolation and culture Human subcutaneous adipose tissue samples from healthy individuals (white females aged 25 to <75 years and BMI < 30 kg/m^2) were obtained after liposuction surgery (Bergman Clinics, Zwolle, the Netherlands). Anonymously donated samples were obtained with informed consent as approved by the ethical board of the University Medical Center Groningen, following the guidelines for 'waste materials'. Lipoaspirates were enzymatically digested to obtain the ASCs, as described in our previous study [27]. The pooled ASCs from passages 3 to 6 were used for experiments. The ASCs were cultured in DMEM (Lonza, Basel, Switzerland) either with normal glucose (NG; 5 mmol/l D-glucose) or HG (30 mmol/l D-glucose) at normoxia (21% O$_2$). Continuous HG maintenance of ASCs (more than three passages; ≥ 21 days) was considered to be chronic HG, while short-term exposure to HG (7 days) was considered to be acute HG. Conditioned medium from ASCs (ASC-Cme) was collected from confluent monolayers after culturing for more than three passages in HG-DMEM. The percentage of FBS was reduced from 10% to 2% (vol./vol.) for 24 h prior to collection [28].

For the co-culture of ASCs and HUVECs, single-cell suspensions of HUVECs were seeded on top of confluent ASCs monolayers or, as a control, on gelatin-coated wells at 10,000 cells/cm^2 and vascular networks were allowed to form for at least 7 days [29]. Bovine retinal endothelial cells (BRECs) were isolated from freshly-enucleated cow eyes obtained from the slaughterhouse as described previously [30]. First-passage BRECs were used in all experiments. A purity of >99% was routinely achieved in BREC culture, which was

checked microscopically, and by immunofluorescence staining of von Willebrand factor (not shown). Confluent monolayers of BRECs were incubated in three different groups (NG-DMEM, HG-DMEM and ASC-Cme) for 7 days to study the effects of each set of conditions.

Ultrastructural analyses Co-cultures were fixed in 2% (wt/vol.) glutaraldehyde (Polysciences, Eppelheim, Germany) for 24 h. Samples were post-fixed using osmium tetroxide (Sigma-Aldrich, St. Louis*,* MO, USA) / potassium ferrocyanide (Sigma-Aldrich) for 30 min. Next, samples were embedded in Epon 812 (SERVA, Heidelberg, Germany) and polymerised at 37°C for 16 h followed by 56°C for 24 h. Thick sections (0.5 μm) were stained with toluidine blue (Sigma-Aldrich). Ultrathin sections (60 nm) were stained with uranyl-acetate (Sigma-Aldrich) in methanol and lead citrate (Sigma-Aldrich). Imaging was performed using a CM100 Biotwin transmission electron microscope (FEI, Eindhoven, the Netherlands).

Animals and the retinopathy of prematurity model All animal experiments in this study adhered to the association for research in vision and ophthalmology (ARVO) Statement for the use of animals in ophthalmic and vision research. Male C57BL/6J mice (Charles River, Frankfurt, Germany) were housed with free access to standard chow and water under a 12 h light-dark rhythm. To study the effect of ASCs on hypoxia-driven angiogenesis, newborn mice were subjected to the model of retinopathy of prematurity (ROP) [31]. Mice at postnatal (P) day 7 (P7) were exposed to an atmosphere of 75% oxygen with their nursing mother for 5 days and then returned to room air at P12. Directly after their return to room air, randomly selected mice were intravitreally injected under anaesthesia with either 1 μl of PBS containing approximately 10,000 ASCs (passage 1) or 1 μl of PBS as a control. Eyes were enucleated under deep

anaesthesia at P13 for immunofluorescence analysis; at P13 and P19 for quantitative real-time PCR (qPCR) analysis; and at P17 for quantification of neovascularisation. After collection, eyes were immediately fixed in buffered formalin or stored at −80°C for the following analysis.

Quantification of hypoxia-driven neovascularisation Neovascularisation in retinas was assessed in paraffin sections of P17 animals injected at P12 with ASCs or a control. To this end, sections (6 μm) were stained with periodic acid–Schiff's reagent (Sigma-Aldrich). Nuclei of neovessels at the vitreous side of the inner limiting membrane of the retinas were counted as described previously [32].

Assessment of ASCs in vivo Whole-mount retinas from P13 animals were permeabilised with 0.5% (wt/vol.) Triton-X100 at room temperature for 1 h. Overnight staining was with FITC/TRITC-labelled isolectin-B4 (1:50; Sigma-Aldrich) at 4°C. After PBS washes, retinas were flat-mounted in glycerol and micrographs were obtained with a fluorescence microscope (Lectin-FITC/ASC-Dil red staining; Leica BMR, Bensheim, Germany) or a confocal microscope (Lectin-TRITC/ASC-EGFP staining; Leica TCS SP2 confocal microscope, Leica, Wetzlar, Germany). ASCs presence was revealed through their preinjection label, which was either CM-DiI-red (ThermoFisher, Waltham, MA, USA) or enhanced green fluorescent protein (EGFP) lentiviral tag.

Gene expression analysis Total RNA was extracted from ASCs and BRECs in TRIzol reagent (Life Technologies, Carlsbad, CA, USA) following the manufacturer's protocol. Retinas were isolated from frozen eyes of ROP and control mice at P13 (n=5) and ROP mice at

P19 in the presence of ASC injection or PBS (*n*=5). Afterwards, 1 μg of total RNA from each sample was reverse transcribed using the First Strand cDNA Synthesis Kit (Fermentas, Vilnius, Lithuania) according to the manufacturer's instructions. The cDNA equivalent of 10 ng RNA was used for amplification in 384-well plates in a TaqMan ABI 7900HT thermal cycler (Applied Biosystems, Foster City, CA, USA) in a final reaction volume of 10 μl containing 5 μl SYBR Green Universal PCR Master Mix (BioRad, Hercules, CA, USA) and 6 μmol/l primer mix (forward and reverse). The cycle threshold (C_t) values were normalised to *GAPDH/ACTB* as a reference gene using the ΔΔCt method [33].

Assessment of cell viability Viability was assessed using the Apoptosis & Necrosis Kit (Promokine, Heidelberg, Germany) as recommended in the manufacturer's instructions. In short, BRECs were incubated with 5 μl fluorescein-conjugated annexin V (a marker of apoptosis) and 5 μl ethidium homodimer III (at a concentration of 2×10^6 cells/ml) at room temperature for 15 min. Fluorescence was recorded on a BD FACSCalibur (BD Biosciences, Franklin Lakes, NJ, USA) within 1 h of staining.

Quantification of ROS Cellular ROS production was determined using the dye 2',7'-dichlorofluorescin diacetate (DCFH-DA, Sigma-Aldrich). Two-electron oxidation of DCFH-DA results in the formation of a fluorescent product, dichlorofluorescein (DCF) [34]. Experimental cells were suspended in 20 μmol/l DCFH-DA in the dark at 37°C for 15 min. The general ROS scavenger *N*-acetyl-L-cysteine (NAC, 10 mmol/l, Sigma-Aldrich) and H_2O_2 (3 μmol/l, Merck Millipore, Darmstadt, Germany) were used as negative and positive controls, respectively. Samples were analysed directly using a FACSCalibur within 15 min of staining.

Screening for immune stimulation The supernatant of HG-stimulated BRECs cultured with or without ASC-Cme and the control group (BRECs in NG) were collected after 7 days. To assess the immunogenicity of these samples, THP1-XBlue-MD2-CD14 cells (InvivoGen, Toulouse, France) were used as described previously [35]. THP1-XBlue-MD2-CD14 cells were plated, then each well was stimulated with samples of supernatants and cultured overnight at 37°C in 5% CO_2. Lipopolysaccharide (LPS,10 μg/ml, Sigma-Aldrich) was used as a positive control. Production of SEAP in the supernatant was quantified using QUANTI-Blue (InvivoGen). An aliquot of QUANTI-Blue (200 μl) was dispensed into a new flat-bottomed 96-well plate with 20 μl of supernatant from the stimulated cell-lines for 45 min at 37°C. SEAP activity, representing activation of NF-κB, was then measured at a wavelength of 650 nm on a VersaMax microplate reader (Molecular Devices, Biberach an der Riss, Germany) [35].

ELISA Culture medium was collected from different experimental conditions. The concentrations of PGE2 and CCL2 in the medium were quantified, respectively, with the Prostaglandin E2 Human ELISA Kit (ThermoFisher) and the Human CCL2/MCP-1 DuoSet ELISA (R&D Systems, Minneapolis, MN, USA) according to the manufacturer's protocol. LPS (200 ng/ml) and TNF-α (50 ng/ml, Sigma-Aldrich) were used as positive controls. The COX2 inhibitor celecoxib (10 mmol/l , Sigma-Aldrich) was used to inhibit PGE2 production. Results were normalised to the number of cells in each experimental condition and presented in pg/ml as fold change relative to their respective experimental controls.

Monocyte adhesion assay One of the cardinal steps of inflammation is the infiltration of immune cells such as monocytes across the endothelial cell layer [36]. THP-1 monocytes were stained using the Vybrant CFDA SE Cell Tracer Kit (ThermoFisher) according to the manufacturer's instructions. Treated groups of BRECs (under HG with or without ASC-Cme), a positive-control group (pre-incubated with medium containing TNF-α [10 ng/ml] for 8 h) and a control group (NG) were plated at a density of 5×10^3 cells/cm^2 in standard 96-well culture plates and allowed to adhere at 37°C for 4 h. Labelled THP-1 cells (2×10^5 cells/ml) were added to each well. After incubation for 1 h, wells were washed to remove non-adhered cells. Fluorescence of adherent cells was recorded on a Varioskan spectrofluorometer (Thermo Scientific, Waltham, MA, USA) at excitation/emission = 492/520 nm [37].

Scratch wound healing assay BRECs in three different groups (NG, HG and ASC-Cme) were cultured until they reached confluency. The straight, width-limited scratch was made in all the wells, simulating a wound. The recovery of both wound edges was recorded simultaneously using the Solamere Nipkow confocal live cell imaging microscope (Solamere Technology Group, Salt Lake City, UT, USA) for 30 h. The percentage of covered area between the edges was analysed by imageJ 1.8.0-172 software (imagej.nih.gov/ij/download/).

Statistical analysis Data are expressed as average ± SEM and relative to vehicle controls of at least three independent experiments in triplicate. Statistical evaluation was performed using unpaired t tests and ANOVA followed by Bonferroni post hoc analysis. p values <0.05 were considered statistically significant.

Results

Ultrastructure of ASC-induced vascular networks

The 0.5 μm cross-sections showed that interconnected laminar structures had been formed by co-cultures of endothelial cells on ASC monolayers at day 5 and subsequent days (Fig. 1a).

Transmission electron micrographs of longitudinal sections showed the build-up of 3D structures that comprised endothelial-cell-derived (Fig. 1c) vessel-like structures with a lumen (Fig. 1a–c), surrounded and tightly aligned by ASCs (Fig. 1c). At high magnification, these vessel-like structures appeared as intermittent structures between the ASCs (Fig. 1d).

The vascular networks formed were reminiscent of genuine vessels with respect to the slanted intercellular junctions between endothelial cells (Fig. 1e,h,i). Peg-and-socket processes [38, 39] that extended from ASC-derived pericytes to endothelial cells had also formed (Fig. 1f,g), as well as an extracellular matrix-based membrane between pericytes and endothelial cells (Fig. 1f,i).

ASC-derived pericytes, i.e. those cells in close contact with endothelial cells, had lost their typically abundant vesicular contents compared with more distal ASCs (Fig. 1d).

These ultrastructural results indicate that ASCs promoted formation of vascular networks by endothelial cells and that ASCs had acquired a functional pericytic phenotype in vitro (Fig. 1g).
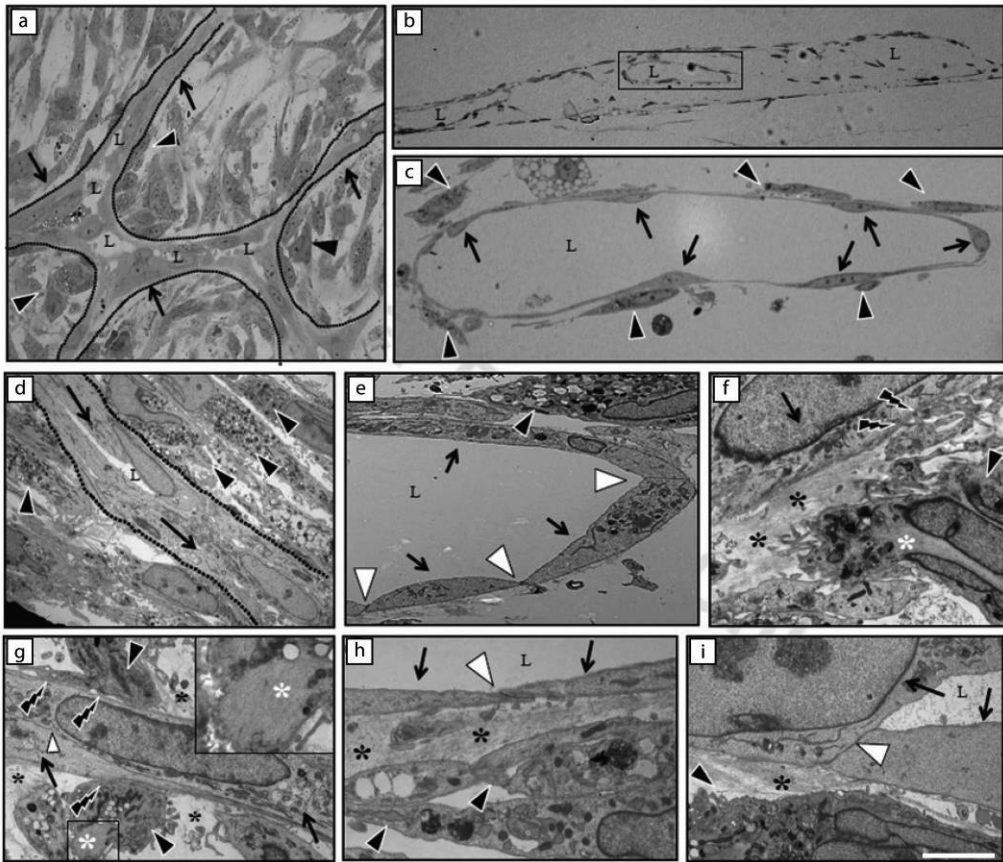
Fig. 1 **Ultrastructure of ASC-induced vascular network. HUVECs were seeded on confluent monolayers of ASCs.** After 5 days, 0.5 µm sections were stained with toluidine blue and analysed by light microscopy, and 60 nm sections of glutaraldehyde-fixed and plastic-embedded co-cultures were analysed by transmission electron microscopy.

(**a–c**) Representative light micrographs: (**a**) Planar, parallel section (i.e. the top view of the culture) showing the formation of a vascular network (arrows, endothelial cells) demarcated by the dotted lines. Lumens (L) have

formed, which are aligned by ASCs (black arrowheads) in close contact. (**b**) Cross section of the lumen-containing 3D vascular structures in between (interrupted) layers of ASCs. (**c**) Enlargement of a vascular structure with several aligned ASCs (arrows, endothelial cells; black arrowheads, ASCs).

(**d–i**) Transmission electron micrographs of the vascular structures: (**d**) a vascular structure consisting of endothelial cells (arrows) and lumen is depicted by the dotted lines with surrounding ASCs (black arrowheads).

(**e**) Specific cell–cell connections with tight junctions between endothelial cells (white arrowheads), with lumen formation on top of the ASCs.

(**f**) ASCs deposited extracellular matrix (black asterisks), which forms a basement membrane-like structure between the endothelial cells and the ASCs.

(**f**, **g**) Peg-and-socket connections are shown by the lightning symbols, and the inset in (**g**) shows intracellular filaments (white asterisks), indicative of contractility, similar to smooth muscle cells, i.e. hinting at the maturation of ASCs to pericytes.

(**h**, **i**) Details of the endothelial cell–cell connections and basal membrane formation around the endothelial cells, i.e. the vascular structure with connected ASCs. Scale bar, 5 µm.

Lumen (L); endothelial cells (arrows); ASCs (black arrowheads); endothelial cell–cell connections (white arrowheads); extracellular matrix formation (black asterisks); intracellular filaments representative for smooth muscle cell phenotype (white asterisks); peg-and-socket connections of ASCs with endothelial cells (lightning symbols)

ASCs stabilise hypoxia-driven angiogenesis but also engraft at pericytic sites in the animal model of ROP

ASCs were injected intravitreally at P12 in the eyes of ROP-model mice (Fig. 2a). At P13, injected ASCs were present in angiogenic sprouts and had attached to endothelial cells of maturating capillaries at a pericyte-like position (arrows, Fig. 2b,c). Further analyses showed that dye-labelled-ASCs (green, Fig. 2d–f) had aligned and attached to maturing intraretinal capillaries (red, Fig. 2d–f) at pericyte-specific perivascular positions and in contact with the endothelium.

Quantification of hypoxia-induced retinal neovascularisation at P17 showed that injection of ASCs in the animal models of ROP increased neovascularisation by 54% (Fig. 2g–i; PBS vs ASCs, 8.3±0.62 vs 12.8±0.96).

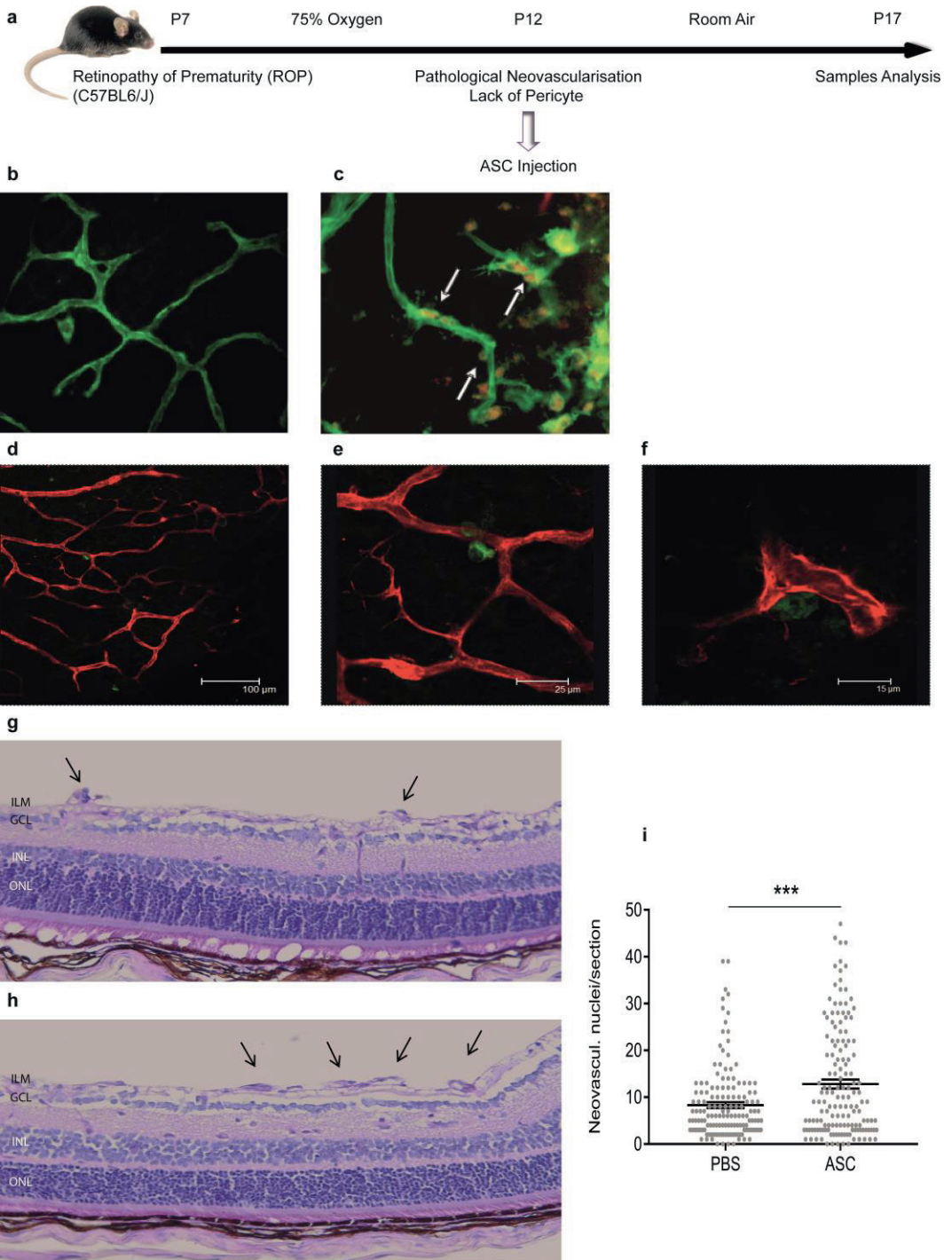a — P7 · 75% Oxygen · P12 · Room Air · P17

Retinopathy of Prematurity (ROP) (C57BL6/J) | Pathological Neovascularisation Lack of Pericyte | Samples Analysis

ASC Injection

Fig. 2   ASCs enhance hypoxia-driven angiogenesis in the ROP mouse model.

(**a**) Scheme of the ROP model. Mouse pups were exposed to hyperoxia (75% O_2) from P7 to P12 and subsequently transferred to room air (21% O_2). This causes hypoxia at room air that results in extensive retinal neovascularisation at P17. ASCs were injected into the vitreous at P12 to evaluate their influence on hypoxia-driven neovascularisation.

(**b**, **c**) Representative micrographs of CM-DiI-labelled ASCs (red, white arrows) co-localising with the endothelial layer (lectin, green); magnification ×20.

 (**d–f**) Micrographs of EGFP-tagged ASCs (green) co-localising with the endothelial layer (lectin, red) in the pericytic position. The scale bars in (**d–f**) are 100 μm, 25 μm and 15 μm, respectively.

(**g, h**) Histological analysis of the effects of ASC injection on hypoxia-induced retinal neovascularisation; magnification ×20. Neovascularisation was assessed histologically by counting the endothelial cell nuclei anterior to the inner limiting membrane. (**g**) Histological features of retinal neovascularisation in the control group. (**h**) Histological features of retinal neovascularisation in ASC-injected mice. Intravitreal injection of ASCs in the ROP mouse model increased the number of neovascular tufts extending into the vitreous (black arrows).

 (**i**) Hypoxia-driven neovascularisation in the retinas was enhanced by 54% in animals injected with ASCs (PBS vs ASC, 8.3±0.62 vs 12.8±0.96). The graph shows the mean number of neovascularisation nuclei per section per animal, ***p<0.001. GCL, ganglion cell layer; ILM, inner limiting membrane; INL, inner nuclear layer; neovascul., neovascularised; ONL, outer nuclear layer

ASCs modulate the inflamed ROP microenvironment

ROP and control retinas (P13) were assessed by qPCR. At P13, i.e. 24 h after returning the animals from hyperoxia to ambient oxygen, *Angpt1* (encoding angiopoietin [ANGPT] 1) expression had slightly decreased in ROP retinas, while *Angpt2* had slightly increased (although neither significantly) compared with the non-ROP controls (Fig. 3a). This was accompanied by increased expression of angiogenesis-related genes i.e. *Vegfa* (encoding vascular endothelial growth factor [VEGF] A; 2.0-fold change), *Fgf2* (3.2-fold change), and *Col4a1* (1.4-fold change) (Fig. 3a). The analysis showed increased expression of proinflammatory genes i.e. *Il1b* (2.0-fold change) and *Ccl2* (2.1-fold change) compared with P13 controls. *Cxcl15* (mouse orthologue of human *CXCL8*) and *Tnf* changed non-significantly (Fig. 3a). Comparison of ROP retinas with and without ASC intervention showed that injection of ASCs at P12 caused a 1.5-fold increase of *Angpt1* and a 0.6-fold decrease of *Angpt2*, suggesting induction of vascular quiescence. Injection of ASCs into the ROP eyes caused increased expression of inflammatory genes such as *Tnf*, *Cxcl15* and *Ccl2* by 2.2-, 1.8- and 2.5-fold, respectively. A slight decrease was observed in the expression of proangiogenic *Vegfa* and a 1.3-fold increase of *Fgf2* was observed in ROP at P19 with ASCs, compared with the control ROP at P19 without ASCs (Fig. 3b). No differences in the expression of *Pdgfb*, *Col4a1* and *Il1b* were detected.
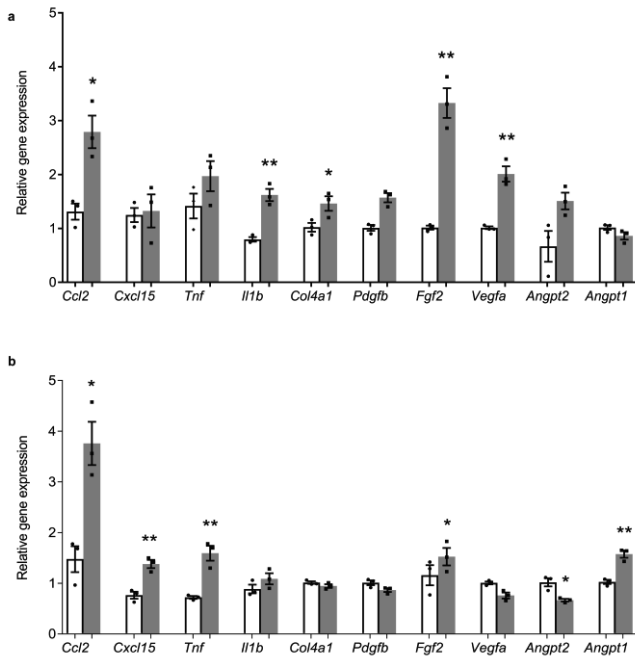
Fig. 3   ASCs modulate the ROP micro-environment. Gene expression analyses normalised to Gapdh of (**a**) dissected ROP retinas at P13 (grey bars) compared with the control retinas at P13 (white bars). The expression levels of Vegfa, Fgf2, and Col4a1 were increased. In addition, an inflammatory response was induced, as measured by increased expression of Il1b and Ccl2. (**b**) To assess the ASC-guided changes to the ROP micro-environment at P19, ROP retinas of eyes with ASC injection (grey bars) and controls (white bars) showed increased expression of Angpt1 and Fgf2, and decreased expression of Angpt2. The expression of Vegfa, Pdgfb and Col4a1 was similar to controls. The inflammatory response was modulated by normalised Il1b expression, while the expression of Tnf, Cxcl15 and Ccl2 was increased. *p<0.05, **p<0.01 vs control retinas. Graphs represent means ± SEM from retinas of five animals in each group, performed in triplicate

Chronic or acute exposure to HG influences ASC gene expression

The expression of 36 relevant genes was measured in ASCs after acute exposure to HG (i.e. maintained in NG medium, followed by 7 days in HG medium) or chronic exposure to HG (i.e. always maintained in HG medium and for more than 21 days). Data are presented as the fold change compared with (chronic) maintenance in NG medium (Fig. 4a,b). The acute exposure of ASCs to HG upregulated the proinflammatory genes *TNF* (1.8-fold change)*, IL1A* (6.0-fold change)*, IL6* (4.5-fold change), *CCL2* (4.3-fold change) and *CXCL8* (6.0-fold change); as well as the proangiogenic genes *VEGFA* (4.8-fold change), *ANGPT2* (1.8-fold change) and *MMP1* (4.2-fold change). Expression of the angiopoietin receptors *TIE1* and TEK (also known as *TIE2*) was downregulated (0.52-fold and 0.47-fold change, respectively). The glucose transporter *SLC2A1* (encoding GLUT1) was upregulated 2.5-fold.

Interestingly, acute HG exposure induced a 4.9-fold change in the mesenchymal pericyte marker *RGS5*, while expression of other mesenchymal markers such as *ACTA1, TAGLN* and *PDGFRB* changed only marginally. Endothelial marker *PECAM1* was also upregulated (1.3-fold change). The expression of two immunoregulatory genes, *PTGS2* (encoding COX2) and *IDO1,* were upregulated (3.4-fold and 3.6-fold change, respectively).

The expression of all genes in ASCs was similar upon culture under chronic HG and chronic NG conditions, which indicated that ASCs adapt to different glucose concentrations in the culture medium during log-term culture. The inflammatory response after acute exposure to HG resulted in an increased release of PGE2 (11.0-fold change) and CCL2 (1.6-fold change) by ASCs, compared with chronic exposure to HG (Fig. 4c,d). Interestingly, chronic exposure to HG medium slightly decreased PGE2 secretion (0.3-fold change) and

secretion of CCL2 (0.8-fold change) compared with controls maintained in NG. LPS and TNF-α both induced the secretion of PGE2 and CCL2, while celecoxib inhibited the production of PGE2 completely and had less effect on secretion of CCL2 in acute-HG-stimulated ASCs.
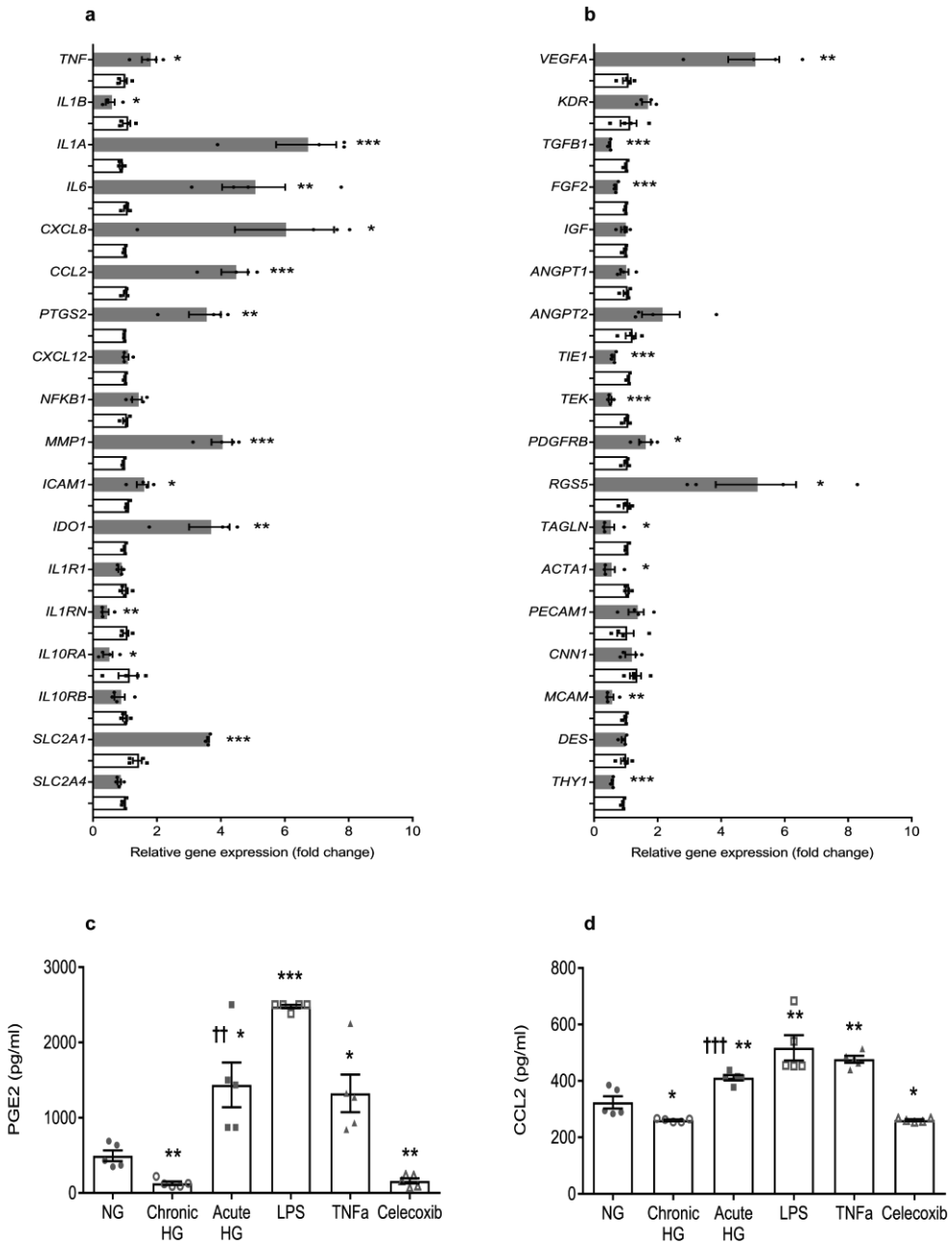
Fig. 4   Anti-inflammatory and anti-apoptotic effects of ASCs depend on chronic HG preconditioning.

(**a**, **b**) Expression of 36 genes, normalised to ACTB, in ASCs after acute exposure to HG (7 days) or chronic HG (more than 21 days maintenance in HG) compared with NG-exposed controls. Grey bars, acute HG exposure; white bars, chronic HG exposure. Graphs represent data ± SEM from n=4 independent experiments. *p<0.05, **p<0.01, ***p<0.001 vs NG-exposed control. (**c**, **d**) The inflammatory response in HG conditions was induced in ASCs and measured by ELISA to detect PGE2 and CCL2 in ASC-Cme. LPS and TNF-α were used as positive-stimulated controls. Celecoxib (10 mmol/l) was used as an inhibitor of COX2 in acute-HG-treated ASCs. Graphs show mean ± SEM from n=5 independent experiments. *p<0.05, **p<0.01, ***p<0.001 vs NG control; ††p<0.01, †††p<0.001 vs chronic HG. Genes encode the following proteins: TNF, tumor necrosis factor; IL1B, IL-1β; IL1A, IL-1α; IL6, IL-6; CXCL8, C-X-C motif chemokine ligand 8 (also known as IL-8); CCL2, chemokine (C-C motif) ligand 2; PTGS2, prostaglandin-endoperoxide synthase 2; CXCL12, C-X-C motif chemokine 12; NFKB1, NF-κB subunit 1; MMP1, matrix metallopeptidase 1; ICAM1, intercellular adhesion molecule 1; IDO1, indoleamine 2,3-dioxygenase 1; IL1R1, IL-1 receptor type 1; IL1RN, IL-1 receptor antagonist; IL10RA, IL-10 receptor subunit α; IL10RB, IL-10 receptor subunit β; SLC2A1, solute carrier family 2 member 1 (also known as GLUT1); SLC2A4, solute carrier family 2 member 4 (also known as GLUT4); VEGFA, vascular endothelial growth factor A; KDR, kinase insert domain receptor/VEGF receptor 2; TGFB1, TGF-β1; FGF2, fibroblast growth factor 2; IGF, IGF; ANGPT1, angiopoietin 1; ANGPT2, angiopoietin 2; TIE1, tyrosine kinase with immunoglobulin like and EGF like domains 1; TEK, TEK receptor tyrosine kinase (also known as Tie2); PDGFRB, platelet derived growth factor receptor β; RGS5, regulator of G-protein signaling 5; TAGLN, transgelin; ACTA1, actin α1; PECAM1, platelet/endothelial cell adhesion molecule 1 (skeletal muscle); CNN1, calponin 1; MCAM, melanoma cell adhesion molecule (also known as CD146); DES, desmin; THY1, Thy-1 cell surface antigen (also known as CD90)

The antioxidant role of ASC-Cme abrogates NF-κB activation and promotes cell viability of BRECs

Culture of BRECs under HG conditions for 7 days induced cell death (viability ~88% vs 94.6% for HG vs NG, Fig. 5a). Apoptosis was increased (annexin V-positive cells ~11.2% vs 4.6% for HG vs NG, Fig. 5b), while necrosis had also increased (ethidium homodimer III-positive cells ~0.73% vs 0.45% for HG vs NG, Fig. 5c). Simultaneous treatment of HG-stimulated BRECs with ASC-Cme (i.e. conditioned medium from ASCs chronically cultured in HG medium) normalised viability (~93.9% vs 88% for ASC-Cme vs HG, Fig. 5a) and suppressed apoptosis (~4.8% vs 11.2% for ASC-Cme vs HG, Fig. 5b) and necrosis (~0.25% vs 0.73% for ASC-Cme vs HG, Fig. 5c) of the BRECs.

Exposure of BRECs to HG increased intracellular ROS production (4.6-fold change compared with NG controls, Fig. 5e), while ASC-Cme abrogated this (0.4-fold change, Fig. 5e). This was comparable to the NAC effect on HG induced BRECs (0.25-fold change, Fig. 5e).

The monocytic NF-κB reporter (SEAP) cell line THP1-XBlue-MD2-CD14 was used to assess the proinflammatory capacity of conditioned medium obtained from BRECs that were co-treated with HG and ASC-Cme. The strongest activation of NF-κB occurred after stimulation with LPS (29.0-fold change, Fig. 5f), while neither NG nor HG medium (DMEM) had any influence. Compared with NG controls, the activation of monocyte-expressed NF-κB increased (1.4-fold change) upon exposure to conditioned medium from HG-stimulated BRECs. In contrast, NF-κB activation was normalised to NG control levels (0.6-fold change) by conditioned medium from BRECs that were HG induced and simultaneously treated with ASC-Cme.
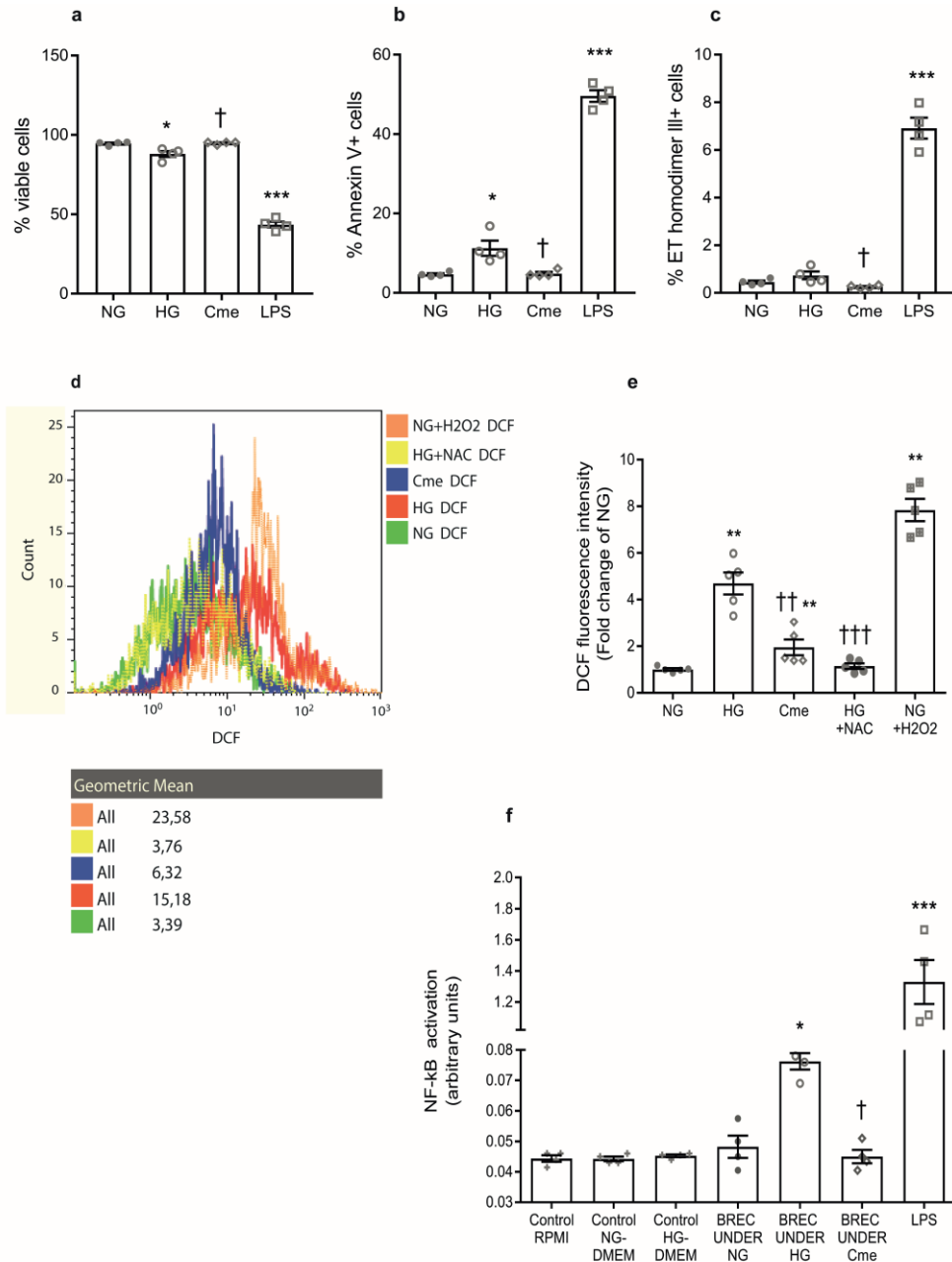
Fig. 5   The antioxidant role of ASC-Cme, combined with declining NF-κB activation, promotes cell viability of HG-challenged BRECs.

(**a**) ASC-Cme promotes BREC viability following HG-induced apoptosis (viability ~88% vs 94.6%, HG vs NG; 88% vs 93.9%, HG vs Cme).

(**b**) HG-induced apoptosis was normalised by ASC-Cme (annexin V-positive cells ~11.2% vs 4.6%, HG vs NG; 11.2% vs 4.8% for HG vs Cme).

(**c**) Necrosis (ethidium [ET] homodimer lll-positive cells ~0.73% vs 0.45%, HG vs NG; 0.73% vs 0.25% for HG vs Cme). (**a–c**) LPS was used as a positive control.

(**d**) The histogram shows the representative increase of fluorescence intensity (by DCF) after exposure to HG or H_2O_2 control compared with NG or ASC-Cme and NAC treatment.

(**e**) HG induces ROS in BRECs. Total cellular ROS production was measured by DCF. ASC-Cme suppressed ROS production in the presence of HG, compared with HG alone. The ROS inhibitor NAC and H_2O_2 were used as negative and positive controls, respectively.

(**f**) NF-κB activation by conditioned BREC medium in THP1-XBlue-MD2-CD14 cells, and mediated by ASC-Cme. NF-κB activation was significantly higher in cells treated with BREC conditioned medium under HG conditions (BREC under HG), compared with unstimulated control. This response was almost absent when cells were treated with ASC-Cme alongside BREC conditioned medium under HG conditions (BREC under Cme). LPS was used as a positive control for THP1-XBlue-MD2-CD14 cells and induced NF-κB activation. RPMI-1640 medium, NG-DMEM and HG-DMEM were used as controls, which had no effect on activation of THP1-XBlue-MD2-CD14 cells. Absorbance values were plotted to express NF-κB activation with arbitrary units. *p<0.05, **p<0.01, ***p<0.001 vs NG control**;** †p<0.05, ††p<0.01, †††p<0.001 vs HG. Values are mean ± SEM (n=4 in **a–c**, **f** and n=5 in **e**). Cme, ASC-Cme

ASC-Cme downregulates principal inflammatory factors in HG-challenged BRECs

HG stimulation of BRECs for 7 days upregulated the gene expression of the relevant proinflammatory genes *TNF, IL1B, IL1A, IL6, CXCL8* and *CCL2,* as well as leucocyte adhesion-related genes *SELE, ICAM1* and *VCAM1*. In addition, the proangiogenic genes *ANGPT1, ANGPT2, VEGFA, VEGFB* and *PDGFB,* and the endothelial NO synthases, *NOS2* and *NOS3*, were upregulated, as well as *PTGS2*. The upregulation of these genes was normalised to NG control level in ASC-Cme-treated HG-challenged BRECs. Only *KLF4* did not change after HG challenge of BRECs. Interestingly, expression of both *KLF4* and *NOS2* were upregulated in ASC-Cme-treated HG-challenged BRECs. The expression of *ANGPT1*, a vessel quiescence-associated factor, remained increased upon ASC-Cme treatment of HG-challenged BRECs (Fig. 6a–r).

As expected, the proinflammatory condition of HG-challenged BRECs (Fig. 6a–r) also increased their adhesiveness to THP-1 monocytes (2.4-fold change, Fig. 7a), while treatment with ASC-Cme normalised monocytic adhesion to NG levels (0.6-fold change). Treatment of BRECs with TNF-α promoted the strongest adhesion of monocytes (4.5-fold change, Fig. 7a).

Wound closure of BRECs cultured in NG medium, after HG challenge or treatment with ASC-Cme during HG challenge, was similar over a measurement period of 30 h, after which time full closure occurred (Fig. 7b).
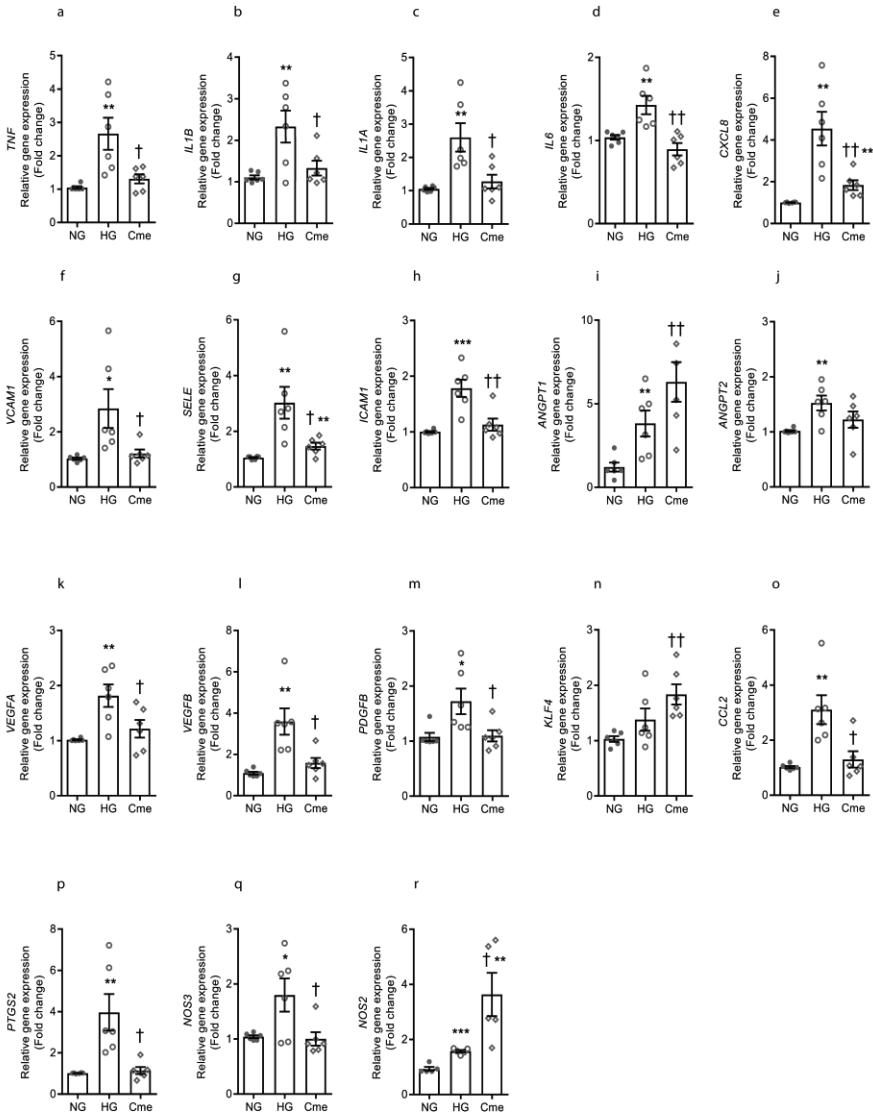
Fig. 6 ASC-Cme downmodulates the main inflammatory genes in HG-challenged BRECs, compared with NG-treated controls. (a–r) HG upregulated the expression of the main genes related to inflammation. This upregulation of TNF, IL1B, IL1A, IL6, CXCL8, VCAM1, SELE, ICAM1, VEGFA, VEGFB, PDGFB, CCL2, PTGS2, and NOS3 is significantly modulated by ASC-Cme. ASC-Cme upregulated the gene expression of ANGPT1, KL4 and NOS2. Values are mean ± SEM (n=6). *p<0.05, **p<0.01, ***p<0.001 vs NG control; †p<0.05, ††p<0.01, †††p<0.001 vs HG
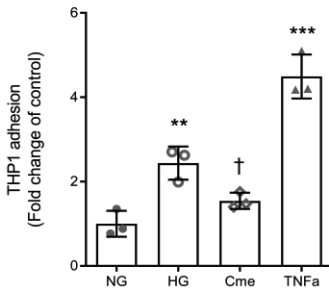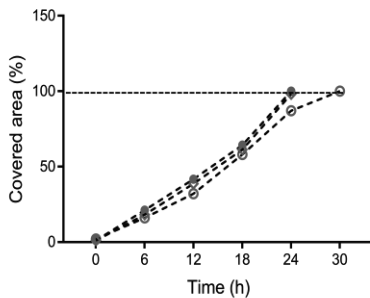
Fig. 7 (**a**) THP-1 cell adhesion to BRECs exposed to HG, with and without ASC-Cme. The intensity of fluorescence of adherent THP-1 cells (mean ± SEM, n=3, fold change of NG-treated control) in resting or activated BRECs was measured. A significant decrease in adhered THP-1 cells occurred after treatment of HG-challenged BRECs with ASC-Cme, compared with HG treatment alone.

(**b**) Scratch wound healing assay to study interaction in the BREC monolayer under NG, HG and ASC-Cme conditions. The percentage of covered area between the edges was analysed. The percentage signifies the remaining gap size 30 h after making the scratches, compared with the initial gap size. The gap width decreased in a similar pattern in all three groups (NG, closed circles; HG, open circles; ASC-Cme, open diamond) and was not significantly delayed in HG conditions. Values are mean ± SEM. **p<0.01, ***p<0.001 vs NG control; †p<0.05 vs HG

Discussion

The main results of our studies are that human ASCs stimulate retinal angiogenesis in ROP mice via acquisition of a pericytic position and function. This was confirmed by ultrastructural analyses showing that in vitro ASCs promote vascular network formation of endothelial cells and stabilise these networks via a pericytic function. Extracellular matrix was deposited between ASC-derived pericytes and endothelial cells in vitro, while typical peg-and-socket connections were also formed [38, 39]. Acute exposure of ASCs to HG caused a proinflammatory and proangiogenic activation compared with ASCs that were propagated chronically in HG. In fact, conditioned medium from ASCs that had been chronically exposed to HG reduced ROS and proinflammatory activation of BRECs challenged with HG. Activated genes were reduced to normal expression levels, while endothelial protective genes such as *KLF4* were upregulated. The immunomodulatory properties of ASCs [40-42] may vary upon passaging in culture [41]. Early passages of ASCs express markers, e.g. ligands that stimulate cells of the adaptive immune system such as MHCII, CD80 and CD86, which are lost upon passaging [41, 43]. Our results show that ASC injection into ROP mice, a model of pathological angiogenesis in PDR [44], led to an increased expression of inflammatory genes such as *Tnf*, *Cxcl15* and *Ccl2,* which might relate to the early passaging of ASCs. The balance of *ANGPT1* and *ANGPT2* and the expression of *VEGFA* are among the most important regulators of vascular development, maturation and maintenance [45]. Reduced expression of pericyte-derived ANGPT1, and concomitant upregulation of its antagonist ANGPT2 and increased VEGFA levels induce pericyte dropout, vessel destabilisation and sprouting angiogenesis [46]. In ROP retinas of ASC-treated mice, expression of *Angpt1* and *Fgf2* were increased,

while levels of *Angpt2* and *Vegfa* were reduced. Injected ASCs adhered to neovessels at a pericytic position. This corroborates the role of NOTCH2 in the juxtracrine function of ASCs [18]. Earlier work from our group showed that under acute HG culturing, ASCs largely maintain their pericytic role as an endothelial supporting cell, despite an upregulated ROS production accompanied by increased apoptosis in ASCs [29].

In general, most papers use DMEM as constitutive culture medium to propagate ASCs. This medium contains 25 mmol/l D-glucose, which is, in fact, similar to hyperglycaemic conditions in vivo. A main finding of our study was that chronic exposure of ASCs to HG medium normalised gene expression to levels seen under NG conditions. Interestingly, in comparison to chronic propagation in HG, ASCs that were shifted from NG-DMEM to HG-DMEM for 7 days had upregulated gene expression of proinflammatory cytokines and chemokines, but also of proangiogenic factors. Moreover, secretion of PGE2 and CCL2 were also strongly increased. COX2 is responsible for the diabetes-induced retinal PGE2 production, and inhibition of COX2 inhibited the diabetes-induced upregulation of retinal VEGF, which links COX2 expression to angiogenesis in diabetic retinopathy [12, 47, 48]. PGE2 activates the extracellular signal-regulated kinases 1 and 2 (ERK1/2) and thus promotes angiogenesis through endothelial upregulation of the secretion of e.g. VEGF, chemokines and activation of cell cycle genes [49, 50]. Thus, the acute HG exposure of ASCs likely renders these cells in a proangiogenic state. Their upregulated expression of proinflammatory genes likely also activates endothelial cells. Yet the exposure of retinal endothelial cells to HG alone activated NF-κB and increased expression of downstream *IL1B, VEGFA, TNF and ICAM1* to name a few of the upregulated main proinflammatory genes. ASC-Cme suppressed these proinflammatory genes such as *PTGS2* in BRECs plus *VEGFA* as

a proangiogenic gene. Acute HG exposure of ASCs would induce endothelial dysfunction rather than counteract it. However, the continuous propagation of ASCs in HG medium not only suppresses their proinflammatory status, but also augments their capacity to normalise endothelial cell function. This was corroborated in HG-activated BRECs by the suppression, by ASC-Cme, of ROS production, the reduction of monocyte adhesion and improved cell survival (Fig. 8). Part of the immunosuppression resides in the suppression of endothelial ROS production by ASC-secreted factors, because ROS functions, via activation of TAK1, as an activator of NF-κB. Taken together, our results show that HG preconditioning of ASCs potentially improves their therapeutic efficacy as compared with short-term exposure to environmental conditions such as HG.

References

1. Fong, D.S., et al*., Diabetic retinopathy.* Diabetes Care, 2003. 26(1): p. 226-229.

2. Kempen, J.H., et al., *The prevalence of diabetic retinopathy among adults in the United States*. Archives of Ophthalmology, 2004. 122(4): p. 552-563.

3. Brownlee, M., *The pathobiology of diabetic complications - A unifying mechanism.* Diabetes, 2005. 54(6): p. 1615-1625.

4. Chen, Y., et al., *Photoreceptor degeneration and retinal inflammation induced by very low-density lipoprotein receptor deficiency*. Microvascular Research, 2009. 78(1): p. 119-127.

5. Demircan, N., et al., *Determination of vitreous interleukin-1 (IL-1) and tumour necrosis factor (TNF) levels in proliferative diabetic retinopathy.* Eye, 2006. 20(12): p. 1366-1369.

6. Elasrar, A.M., et al., *Cytokines in the Vitreous of Patients with Proliferative Diabetic-Retinopathy*. American Journal of Ophthalmology, 1992. 114(6): p. 731-736.

7. Elner, S.G., et al., *Cytokines in Proliferative Diabetic-Retinopathy and Proliferative Vitreoretinopathy*. Current Eye Research, 1995. 14(11): p. 1045-1053.

8. Abu El-Asrar, A.M., et al., *Chemokines in proliferative diabetic retinopathy and proliferative vitreoretinopathy*. European Cytokine Network, 2006. 17(3): p. 155-165.

9. AbuElAsrar, A.M., et al., *Monocyte chemotactic protein-1 in proliferative vitreoretinal disorders.* American Journal of Ophthalmology, 1997. 123(5): p. 599-606.

10. Kern, T.S., *Contributions of Inflammatory Processes to the Development of the Early Stages of Diabetic Retinopathy*. Experimental Diabetes Research, 2007.

11. Szerafin, T., et al., *Increased cyclooxygenase-2 expression and prostaglandin-mediated dilation in coronary arterioles of patients with diabetes mellitus*. Circulation Research, 2006. 99(5): p. E12-E17.

12. Ayalasomayajula, S.P., A.C. Amrite, and U.B. Kompella, *Inhibition of cyclooxygenase-2, but not cyclooxygenase-1, reduces prostaglandin E-2 secretion from diabetic rat retinas*. European Journal of Pharmacology, 2004. 498(1-3): p. 275-278.

13. Hammes, H.P., et al., *Diabetic Retinopathy: Targeting Vasoregression.* Diabetes, 2011. 60(1): p. 9-16.

14. Armulik, A., A. Abramsson, and C. Betsholtz, *Endothelial/pericyte interactions*. Circulation Research, 2005. 97(6): p. 512-523.

15. Gimble, J.M. and F. Guilak, *Adipose-derived adult stem cells: isolation, characterization, and differentiation potential*. Cytotherapy, 2003. 5(5): p. 362-369.

16. Rajashekhar, G., et al., *Regenerative Therapeutic Potential of Adipose Stromal Cells in Early Stage Diabetic Retinopathy*. Plos One, 2014. 9(1).

17. Mendel, T.A., et al., *Pericytes Derived from Adipose-Derived Stem Cells Protect against Retinal Vasculopathy*. Plos One, 2013. 8(5).

18. Terlizzi, V., et al., *The Pericytic Phenotype of Adipose Tissue-Derived Stromal Cells Is Promoted by NOTCH2*. Stem Cells, 2018. 36(2): p. 240-251.

19. Fiori A, Terlizzi V, Kremer H, et al*., Mesenchymal stromal/stem cells as potential therapy in diabetic retinopathy.* Immunobiology, 2018 doi: 10.1016/j.imbio.2018.01.001

20. DelaRosa, O., et al., *Requirement of IFN-gamma-Mediated Indoleamine 2,3-Dioxygenase Expression in the Modulation of Lymphocyte Proliferation by Human Adipose-Derived Stem Cells*. Tissue Engineering Part A, 2009. 15(10): p. 2795-2806.

21. Aggarwal, S. and M.F. Pittenger, *Human mesenchymal stem cells modulate allogeneic immune cell responses.* Blood, 2005. 105(4): p. 1815-1822.

22. Ren, G.W., et al., *Mesenchymal stem cell-mediated immunosuppression occurs via concerted action of chemokines and nitric oxide.* Cell Stem Cell, 2008. 2(2): p. 141-150.

23. Gao, F., et al., *In vitro cultivation of islet-like cell clusters from human umbilical cord blood-derived mesenchymal stem cells*. Translational Research, 2008. 151(6): p. 293-302.

24. Chabannes, D., et al., *A role for heme oxygenase-1 in the immunosuppressive effect of adult rat and human mesenchymal stem cells.* Blood, 2007. 110(10): p. 3691-3694.

25. Kadekar, D., et al., *Conditioned Medium from Placental Mesenchymal Stem Cells Reduces Oxidative Stress during the Cryopreservation of Ex Vivo Expanded Umbilical Cord Blood Cells*. Plos One, 2016. 11(10).

26. Li, M.R., et al., *Mesenchymal Stem Cell-Conditioned Medium Improves the Proliferation and Migration of Keratinocytes in a Diabetes-Like Microenvironment*. International Journal of Lower Extremity Wounds, 2015. 14(1): p. 73-86.

27. Hajmousa, G., et al., *The 6-chromanol derivate SUL-109 enables prolonged hypothermic storage of adipose tissue-derived stem cells*. Biomaterials, 2017. 119: p. 43-52.

28. Iwashima, S., et al., *Novel culture system of mesenchymal stromal cells from human subcutaneous adipose tissue*. Stem Cells Dev, 2009. 18(4): p. 533-43.

29. Hajmousa, G., et al., *Hyperglycemia Induces Bioenergetic Changes in Adipose-Derived Stromal Cells While Their Pericytic Function Is Retained*. Stem Cells and Development, 2016. 25(19): p. 1444-1453.

30. Wisniewska-Kruk, J., et al., *A novel co-culture model of the blood-retinal barrier based on primary retinal endothelial cells, pericytes and astrocytes.* Experimental Eye Research, 2012. 96(1): p. 181-190.

31. Smith, L.E.H., et al., *Oxygen-Induced Retinopathy in the Mouse*. Investigative Ophthalmology & Visual Science, 1994. 35(1): p. 101-111.

32. Hammes, H.P., et al., *Subcutaneous injection of a cyclic peptide antagonist of vitronectin receptor-type integrins inhibits retinal neovascularization.* Nature Medicine, 1996. 2(5): p. 529-533.

33. Livak KJ, Schmittgen TD., et al., *Analysis of relative gene expression data using real-time quantitative PCR and the* $2^{-\Delta\Delta C_t}$ *method*. Methods, 2001. 25: 402-408

34. Eruslanov, E. and S. Kusmartsev, *Identification of ROS using oxidized DCFDA and flow-cytometry*. Methods Mol Biol, 2010. 594: p. 57-72.

35. Paredes-Juarez, G.A., et al., *DAMP production by human islets under low oxygen and nutrients in the presence or absence of an immunoisolating-capsule and necrostatin-1*. Scientific Reports, 2015. 5.

36. Ortega-Gomez A, Perretti M, Soehnlein O, *Resolution of inflammation: an integrated view*. EMBO Mol Med, 2013. 5: 661-674

37. Dicorleto, P.E. and C.A. Delamotte, *Characterization of the Adhesion of the Human Monocytic Cell-Line U937 to Cultured Endothelial-Cells*. Journal of Clinical Investigation, 1985. 75(4): p. 1153-1161.

38. Caruso, R.A., et al., *Ultrastructural descriptions of pericyte/endothelium peg-socket interdigitations in the microvasculature of human gastric carcinomas.* Anticancer Res, 2009. 29(1): p. 449-53.

39. Diaz-Flores, L., Jr., et al., *Peg-and-socket junctions between smooth muscle cells and endothelial cells in femoral veins are stimulated to angiogenesis by prostaglandin E(2) and glycerols*. Histol Histopathol, 2011. 26(5): p. 623-30.

40. Keyser, K.A., K.E. Beagles, and H.P. Kiem, *Comparison of mesenchymal stem cells from different tissues to suppress T-Cell activation.* Cell Transplantation, 2007. 16(5): p. 555-562.

41. McIntosh, K., et al., *The immunogenicity of human adipose-derived cells: Temporal changes in vitro*. Stem Cells, 2006. 24(5): p. 1246-1253.

42. Yoo, K.H., et al., *Comparison of immunomodulatory properties of mesenchymal stem cells derived from adult human tissues*. Cellular Immunology, 2009. 259(2): p. 150-156.

43. Lindroos, B., R. Suuronen, and S. Miettinen, *The Potential of Adipose Stem Cells in Regenerative Medicine*. Stem Cell Reviews and Reports, 2011. 7(2): p. 269-291.

44. Stahl A, Connor KM, Sapieha P, et al., *The mouse retina as an angiogenesis model*. Invest Ophth Vis Sci, 2010. 51: 2813-2826

45. Cai, J., et al., *The angiopoietin/tie-2 system regulates pericyte survival and recruitment in diabetic retinopathy*. Investigative Ophthalmology & Visual Science, 2008. 49(5): p. 2163-2171.

46. Armulik, A., G. Genove, and C. Betsholtz, *Pericytes: Developmental, Physiological, and Pathological Perspectives, Problems, and Promises*. Developmental Cell, 2011. 21(2): p. 193-215.

47. Ayalasomayajula, S.P. and U.B. Kompella, *Celecoxib, a selective cyclooxygenase-2 inhibitor, inhibits retinal vascular endothelial growth factor expression and vascular leakage in a streptozotocin-induced diabetic rat model.* European Journal of Pharmacology, 2003. 458(3): p. 283-289.

48. Sennlaub, F., et al., *Cyclooxygenase-2 in human and experimental ischemic proliferative retinopathy*. Circulation, 2003. 108(2): p. 198-204.

49. Finetti, F., et al., *Prostaglandin E2 regulates angiogenesis via activation of fibroblast growth factor receptor-1*. J Biol Chem, 2008. 283(4): p. 2139-46.

50. Gomez, I., et al., *The role of prostaglandin E2 in human vascular inflammation.* Prostaglandins Leukot Essent Fatty Acids, 2013. 89(2-3): p. 55-63.

The 6-chromanol derivate SUL-109 enables prolonged hypothermic storage of adipose tissue-derived stromal cells.

Ghazaleh Hajmousa [1], Pieter Vogelaar [2], Linda. A. Brouwer[1],
Adrianus. C. van der Graaf[2], Robert. H. Henning[3], Guido Krenning[1,2,*].

[1] Cardiovascular Regenerative Medicine, Dept. Pathology and Medical Biology, University Medical Center Groningen, University of Groningen, Hanzeplein 1 (EA11), 9713GZ Groningen, The Netherlands. [2] Sulfateq B.V., Admiraal de Ruyterlaan 5, 9726GN Groningen, The Netherlands. [3] Dept. Clinical Pharmacy and Pharmacology, University Medical Center Groningen, University of Groningen, Hanzeplein 1 (EB71), 9713GZ Groningen, The Netherlands.

CHAPTER 05

Abstract

Encouraging advances in cell therapy research with adipose derived stromal cells (ASC) require an effective short-term preservation method that provides time for quality control and transport of cells from their manufacturing facility to their clinical destination.

Hypothermic storage of cells in their specific growth media offers an alternative and simple preservation method to liquid nitrogen cryopreservation or commercial preservation fluids for short-term storage and transport. However, accumulation of cell damage during hypothermia may result in cell injury and death upon rewarming through the production of excess reactive oxygen species (ROS). Here, the ability of the cell culture medium additive SUL-109, a modified 6-chromanol, to protect ASC from hypothermia and rewarming damage is examined. SUL-109 conveys protective effects against cold-induced damage in ASC as is observed by preservation of cell viability, adhesion properties and growth potential. SUL-109 does not reduce the multilineage differentiation capacity of ASC. SUL-109 conveys its protection against hypothermic damage by the preservation of the mitochondrial membrane potential through the activation of mitochondrial membrane complexes I and IV, and increases maximal oxygen consumption in FCCP uncoupled mitochondria. Consequently, SUL-109 alleviates mitochondrial ROS production and preserves ATP production. In summary, here we describe the generation of a single molecule cell preservation agent that protects ASC from hypothermic damage associated with short-term cell preservation that does not affect the differentiation capacity of ASC.

Keywords: Adipose tissue-derived stromal cells (ASC), hypothermia, cold storage, mitochondrial damage, chromanol

Introduction

Adipose derived Stromal Cells (ASC) hold great promise in regenerative medicine. ASC are multipotent mesenchymal-like stem cells that reside in the perivascular niche as pericytes or periadventitial cells [1] in white adipose tissue throughout the body [2-4]. ASC secrete a plethora of trophic factors [5] that suppress inflammation and apoptosis, yet promote angiogenesis and mitosis of parenchymal cells [6]. Moreover, ASC have the ability to differentiate into several cell types, including adipocytes, chondrocytes, osteoblasts and muscle cells under lineage-specific culture conditions [2-4].

Encouraging advances in cell therapy research using ASC or ASC-derived tissue engineered constructs demonstrated their ability in the regeneration of bone and cartilage defects [7,8], ischemic limb disease [9], skin wound healing [5], and myocardial infarction [10]. However, the clinical application of ASC requires an effective short-term preservation method, thus providing time for quality control and transport of cells from their manufacturing facility to their clinical destination.

Hypothermic storage of cells in their normal culture media offers an accessible, logistically easy and cost-effective alternative to cryopreservation, vitrification and protocols using preservation fluids (e.g. ViaSpan or HypoThermosol) for short-term storage and transport [11]. In contrast to cryopreservation, which is a complicated cell type-specific process hampered by cell loss and mutagenesis [12,13], hypothermic storage should be a simplified process that voids these complications at low costs. Hypothermia slows metabolic activity and cell cycle progression, thereby maintaining the ASC in their current state. However, hypothermia

207

may produce significant cell injury and death, particularly upon rewarming when excess reactive oxygen species (ROS) are produced [14,15]. Current hypothermic preservation fluids suffer from this rewarming damage; whilst effective at low temperature, they do not prevent severe cell damage upon rewarming [16]. Additionally, the chemical composition of commercially available hypothermic preservation fluids differs vastly from the chemical composition of culture media, which might induce undesirable dedifferentiation of cells or failure of a tissue engineered construct [17,18]. Consequently, hypothermic storage warrants strategies to alleviate these deleterious effects of hypothermia and rewarming, while reliably and consistently maintaining the key characteristics of cells, including viability, phenotype, and, in the case of ASC, differentiation potential.

Substituted 6-chromanols represent a novel class of pharmacological compounds that preserve cell viability under a number of conditions [19-21]. Here, we describe the identification of a 6-chromanol derivate (SUL-109), a single molecule cell culture additive, as a preservation agent that protects human ASC from hypothermia and rewarming damage without affecting their subsequent differentiation capacity.

Materials and Methods

ASC isolation and culture   Human subcutaneous adipose tissue samples from healthy human subjects with (BMI< 30) were obtained after liposuction surgery (Bergman Clinics, The Netherlands). All donors provided informed consent and all procedures were performed in accordance to national and institutional guidelines as well as with the ethical rules for human experimentation as stated in the Declaration of Helsinki.

Lipoaspirates were enzymatically digested with 0.1% Collagenase A (Roche Diagnostic, Mannheim, Germany) in PBS, containing 1% bovine serum albumin (BSA; Sigma-Aldrich, St. Louis, MI) at 37°C for 90 mins. Centrifugation (300g, 4°C, 20 mins) separated adipocytes and lipid content from the stromal cell fraction. The stromal cell fraction was subjected to Lymphoprep (Axis-Shield PoC, Oslo, Norway) density gradient centrifugation (300g, 20°C, 30 mins). The cells from the interface were collected and cultured in DMEM (Lonza #707F, Breda, The Netherlands) containing 10% Fetal Bovine Serum (FBS, GE LifeSciences #SH30071, Pittsburg, PA), 1% Penicillin/Streptomycin (Sigma-Aldrich #P4333, St. Louis, MI) and 2 mM L-glutamine (Life Technologies #25030, Carlsbad, CA). ASC at passage 1 were routinely checked for the expression of pericyte and mesenchymal cell markers according to [22] and had the following phenotype: CD10+, CD13+, CD31-, CD34-, CD44+, CD45-, CD73+, CD90+ and CD105+. At 80% confluence, ASC were dissociated using 0.12% Trypsin, 0.02% EDTA solution in PBS (#59430, Sigma-Aldrich, St. Louis, MI) pelleted by centrifugation (300g, 4°C, 5 mins), and re-seeded at a density of 10.000 cells/cm2. ASC at passage 3 were used for experiments described below.

Cell viability, adherence and proliferation   Alpha-Tocopherol (10 µM, #T1539 Sigma-Aldrich, St. Louis, MI), TROLOX (10 µM, # 10011659, Cayman Chemical, Ann Arbor, MI) or SUL-109 (10 µM; #Rokepie-01, Sulfateq BV, Groningen, The Netherlands) were added to the ASC culture medium. After 2 hours culturing at 37°C, ASC cultures were placed under hypothermic conditions (4°C) in a standard laboratory refrigerator for 48 hours. Thereafter, ASC were re-warmed for 2 hours under normal cell culture conditions (37°C and 5% CO_2). Viability was assessed using the Apoptosis & Necrosis Kit (Promokine #PK-CA707-30018, Heidelberg, Germany) as by manufacturer's instructions. In short, ASC were dissociated using Trypsin-EDTA solution and suspended in 1X AnnexinV-binding buffer at a concentration of $2 \cdot 10^6$ cells/ml. Next, ASC were incubated with 5 µl fluorescein-conjugated AnnexinV and 5 µl Ethidium Homeodimer III in the dark at room temperature for 15 min. Fluorescence was recorded on a BD FACSCalibur (BD Bioscience, Franklin Lakes, NJ) by a skilled operator at the UMCG Flow Cytometry Core Facility within 1 hour of staining.

To assess the adherence capacity of ASC, hypothermic preserved ASC were dissociated using Trypsin-EDTA in 0.9% NaCl and fluorescently labeled with the CFDA SE Cell Tracer (ThermoFisher #V12883, Waltham, MA) according to manufacturer's instructions. Next, fluorescently-labeled ASC were plated at a density of $5 \cdot 10^3$ cells/cm2 in standard 96-well culture plates (Corning #CLS3596, St. Louis, MI) and allowed to adhere under standard culture conditions (37°C and 5% CO_2) for 15-240 min. Following extensive washing with PBS to remove non-adhered cells, fluorescence of adherent cells was recorded on a Varioskan spectrofluorometer at Ex/Em 492/520 nm.

To assess cell proliferation, ASC were fixed using 2% paraformaldehyde (Sigma-Aldrich #P6148, St. Louis, MI) in PBS for 20

min. Next, samples were permeabilized using 0.5% Triton X100 (Life Technologies #85112, Carlsbad, CA) in PBS and incubated in 5% rabbit normal goat serum (Jackson Immunoresearch #005-000-121, Suffolk, UK) at room temperature to block non-specific antibody binding for 10 min. Samples were incubated with polyclonal antibodies to Ki67 (Monosan #PSX1028, San Diego, CA) at a concentration of 2.5 µg/ml. After extensive washing in PBS/Tween-20 (0.1%), samples were incubated with AlexaFluor555-conjugated antibodies to rabbit IgG (Life Technologies #A-21428, Carlsbad, CA) at a dilution of 1:300 in PBS containing 5 µM DAPI (4',6-Diamidino-2-Phenylindole, Life Technologies #D1306, Carlsbad, CA) at room temperature for 30 min. Samples were mounted in citifluor (Citifluor Ltd #AP-1, London, UK) and visualized on a Zeiss AxioObserver Z1 microscope. Total cell number and Ki67-positive cells were quantified using automated fluorescence microscopy software (TissueFaxs, TissueGnostics, Vienna, Austria).

Multipotency of ASC   ASC were subjected to hypothermia and rewarming as described above, after which the culture media was changed for differentiation media. To induce multi-lineage differentiation of ASC, cells were cultured in adipogenic medium (DMEM containing 10% FBS, 1% Penicillin/Streptomycin, 2 mM L-glutamine, Dexamethasone (0.1 µM, Sigma-Aldrich #D4903, St. Louis, MI), Insulin (1 nM, Sigma-Aldrich #I2643, St. Louis, MI) and IBMX (0.5 mM, Sigma-Aldrich #I7018, St. Louis, MI)), osteogenic medium (DMEM containing 10% FBS, 1% Penicillin/Streptomycin and 2 mM L-glutamine, Dexamethasone (0.1 µM), β-glycerophosphate (10 mM, Sigma-Aldrich #G9422, St. Louis, MI) and L-ascorbic acid (0.5 mM, Sigma-Aldrich #A5960, St. Louis, MI)), or myogenic medium (DMEM

containing 10% FBS, 1% Penicillin/Streptomycin and 2 mM L-glutamine and TGF-β1 (10 ng/ml, Peprotech #100-21, Rocky Hill, NJ)) for 21 days. To assess differentiation, ASC were fixed using 2% paraformaldehyde (Sigma-Aldrich, #P6148) in PBS for 20 min and phenotyped using (immuno)histological stains. For adipogenesis, ASC were rinsed with 60% isopropanol and stained with Oil Red O (0.5%, Sigma-Aldrich #O0625, St. Louis, MI) at room temperature for 15 mins. For osteogenesis, samples were stained in Alizarin Red (0.5%, Sigma-Aldrich #A5533, St. Louis, MI) at room temperature for 10 mins. Samples were counterstained using hematoxylin and mounted in Kaisers Glycerin.

To assess myogenic differentiation, ASC were permeabilized with 0.5% Triton X100 (Life Technologies #85112, Carlsbad, CA) in PBS and incubated with polyclonal antibodies to SM22 alpha (2.5 µg/ml, #ab14106, Abcam, Cambridge, UK) for 60 mins. After extensive washing in PBS/Tween-20 (0.1%), samples were incubated with AlexaFluor555-conjugated antibodies to rabbit IgG (2.0 µg/ml, Life Technologies #A-21428, Carlsbad, CA) in PBS containing 5 µM DAPI (4',6-Diamidino-2-Phenylindole, Life Technologies #D1306, Carlsbad, CA) at room temperature for 30 min. Samples were mounted in citifluor (Citifluor Ltd #AP-1, London, UK) and visualized on a Zeiss AxioObserver Z1 microscope in fluorescence mode.

Antioxidant assays   5 µM 2'7'-dichlorodihydrofluorescein diacetate (DCF, Sigma-Aldrich #D6883, St. Louis, MI) was dissolved in Hanks Balanced Salt Solution (#H1641, Sigma-Aldrich, St. Louis, MI) and supplemented with α-tocopherol, TROLOX, or SUL-109 at concentrations ranging from 10^{-9} to 10^{-3} M. 3 µM hydrogen peroxide (H_2O_2, MerckMillipore #107209, Darmstadt, Germany) was added as reactive oxygen donor and samples were incubated at room

temperature for 1 hour. Fluorescence was recorded on a Varioskan spectrofluorometer (ThermoScientific, Waltham, MA) at 488/525 nm (Ex/Em).

Metabolic state, mitochondrial structure and mitochondrial membrane potential analyses The oxygen consumption rate (OCR) and extracellular acidification rate (ECAR) of hypothermically preserved ASC were determined after rewarming in the presence or absence of SUL-109 for 2 hours, using the Seahorse Bioscience Extracellular Flux analyzer (Seahorse Bioscience, Billerica, MA). In short, changes in extracellular oxygen tension and pH were determined on the XF24 Extracellular Flux Analyzer (Seahorse Bioscience, Billerica, MA).

 After steady state oxygen consumption and basal extracellular acidification rates were obtained, 2 µM Oligomycin (ATP Synthase inhibitor, Seahorse Bioscience #9634398, Billerica, MA) and 5 µM carbonyl cyanide 4-(trifluoromethoxy) phenylhydrazone (FCCP, mitochondrial uncoupler, Seahorse Bioscience #9634398, Billerica, MA) were sequentially added through the reagent delivery chambers of the flux analyzer to measure the maximum oxygen consumption rates and maximum acidification rates. Finally, a mixture of 2 µM Rotenone and 2 µM Antimycin A was used to block mitochondrial electron transport. As OCR and ECAR reflect the metabolic activity of cells and are influenced by cell number, OCR and ECAR values were normalized to total protein content in a sample.

Mitochondrial morphology was assessed using a mitochondrial membrane potential-independent dye (*i.e.* MitoTracker-Green, ThermoFisher Scientific #M7514, Waltham, MA). In short, ASC were incubated with 120 nM MitoTracker-Green at 37°C in a 5% CO_2

humidified chamber for 45 min. Next, cells were analyzed by live cell imaging on a confocal microscope (Leica TCS SP2 Confocal Microscope, Wetzlar, Germany) with a 63x oil immersion objective using an excitation wavelength of 488 nm and emission was recorded through a band pass 500 to 550 nm filters. ASC were kept at 37°C in a 5% CO_2 humidified microscope stage chamber throughout the analysis. The mitochondrial membrane potential was assessed using the JC-1 MitoProbe (ThermoFisher Scientific #M34152, Waltham, MA). ASC were dissociated using Trypsin-EDTA in 0.9% NaCl and suspended at $1\cdot10^6$ cells/mL in warm medium containing 2 µM JC-1. Membrane potential-dependent JC-1 accumulation in the mitochondria (indicated by a fluorescence emission shift from green (~529 nm) to red (~590 nm)) was recorded by flow cytometry on a FACS Calibur (BD Biosciences, Franklin Lakes, NJ). To depolarize the mitochondrial membrane, 50 µM carbonyl cyanide 3-chlorophenylhydrazone (CCCP) was added for 15 mins prior to JC-1 loading.

Mitochondrial Complex I-V activity measurements ASC-derived mitochondria were isolated using density gradient centrifugation using the MitoCheck® Mitochondrial Isolation Kit (Cayman Chemical #701010, Ann Arbor, MI) according to manufacturer's instructions and assessed for the activities of mitochondrial complex I-V. In all activity measurements, isolated ASC-derived mitochondria were pre-incubated with a concentration series of SUL-109 (10-9-10-4M) at room temperature for 15 mins. Mitochondrial complex I (NADH oxidase/co-enzyme Q reductase) activity was determined by measuring the decrease in NADH oxidation, which is reflected by a decreased in absorbance at 340nm (Cayman Chemical #700930, Ann

Arbor, MI) in the presence of 2mM potassium cyanide (KCN) to prevent the oxidation of Q.

Activity of mitochondrial complex II (Succinate dehydrogenase/co-enzyme Q reductase) was assessed by the rate of reduction of DCPIP, which is protonated by reduced co-enzyme Q (Cayman Chemical #700940, Ann Arbor, MI), and is reflected by a decrease in absorbance at 600nm. To prevent interference of mitochondrial complexes I, III and IV, complex II activity measurements were performed in the presence of 1µM Rotenone, 10µM Antimycin A and 2mM KCN (all Sigma-Aldrich (#R8875, #A8674, #60178), St. Louis, MI), respectively. Mitochondrial Complex III (Co-enzyme Q cytochrome c oxidoreductase) activity was determined by the rate of cytochrome c reduction, which is reflected by increased absorbance at 550nm (Cayman Chemical #700950, Ann Arbor, MI). To prevent backflow of electrons through complex I and the reduction of cytochrome c by complex IV, activity measurements were performed in the presence of 1µM Rotenone and 2mM KCN. The activity of Mitochondrial Complex IV (cytochrome c oxidase) was determined by measuring the rate of oxidation of cytochrome c, which is reflected by a decrease in absorbance at 550nm (Cayman Chemical #700990, Ann Arbor, MI). The activity of Mitochondrial Complex V (F1F0 ATP Synthase) was determined by the rate of NADH oxidation, which can be monitored at 340nm (Cayman Chemical #701000, Ann Arbor, MI). Under physiologic conditions, mitochondrial complex V uses the proton gradient generated by complexes I-IV to generate ATP from ADP in the presence of Pi. However, complex V can also run in reverse [23]. In the determination of complex V activity, ATP is converted in ADP by complex V, which is used for the conversion of phosphoenolpyruvate into pyruvate by pyruvate kinase. Pyruvate is subsequently reduced to lactate in the presence of lactate dehydrogenase and NADH. Hence, complex V activity is reflected by

the rate of NADH oxidation, which can be measured by a change in absorption at 340nm. To prevent interference of mitochondrial complex I, which also oxidizes NADH, all complex V activity measurements were performed in the presence of 1µM Rotenone.

Measurement of ATP and ROS production To assess the ATP production of human ASC, we used the ATP Determination Kit (ThermoFisher Scientific #A22066, Carlsbad, CA). In short, ASC were treated with SUL-109 (10^{-9}-10^{-4}M), 0.1µM Rotenone, 1µM KCN or a combination of SUL-109 and the Mitochondrial Complex I or IV inhibitors for 1 hour. Next, cells were lysed in a Tris/Glycine buffer (25mM, pH 7.8, 5mM $MgSO_4$, 0.1mM EDTA and 0.1mM sodium azide) that contained 0.5mM D-luciferin, 1.25µg/ml firefly luciferase and 1mM DTT. ATP production was assessed as luminescence measured on a Luminoskan (ThermoFisher Scientific, Carlsbad, CA) set to an integration time of 500ms at 1200mV. To assess ROS production, ASC were treated with SUL-109 (10^{-9}-10^{-4}M), 0.1µM Rotenone, 1µM KCN or a combination of SUL-109 and the Mitochondrial Complex I or IV inhibitors for 1 hour. Next, cells were incubated with the fluorescent ROS-indicator DHE (1µM, Life technologies #D11347, Carlsbad, CA) for 30 mins. Fluorescence was recorded on a Varioskan spectrofluorometer (TheroScientific, Waltham, MA) at Ex/Em 518/605.

Statistical analysis Data are expressed as average ± SEM and relative to vehicle controls of at least 3 independent experiments. Statistical evaluation was performed using ANOVA followed by Bonferroni *post hoc* analysis. P-values <0.05 were considered statistically significant.

Results

(Modified) 6-chromanols are water soluble α-tocopherol derivatives. Alpha-tocopherol, TROLOX and SUL-109 (fig.1) belong to chemical class of 6-chromanols. SUL-109 and TROLOX differ from α-tocopherol by the absence of the large hydrophobic side chain. In contrast to the hydrophobic α-tocopherol (logP = 9.98), TROLOX and SUL-109 are hydrophilic compounds (logP=3.19 and 2.25, respectively). Consequently, the water solubility at room temperature ranges from α-tocopherol (S=63.1 nM) < TROLOX (S= 2.75 mM) < SUL-109 (S= 4.90 mM).

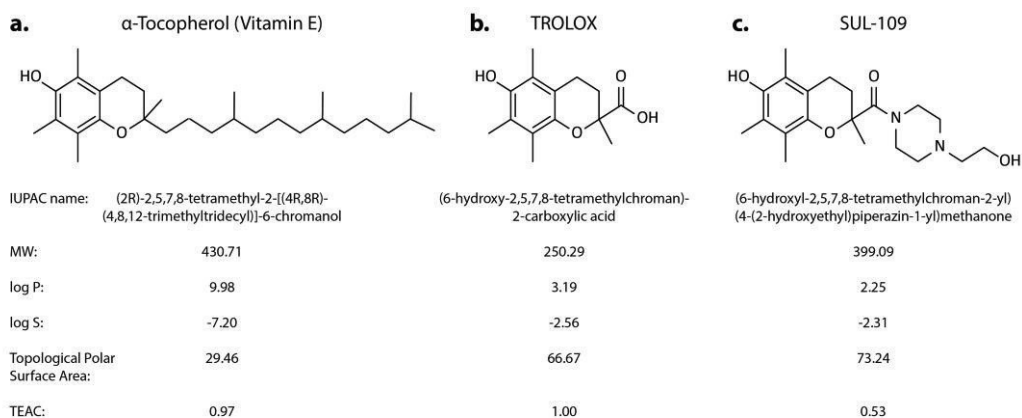| IUPAC name:	a. α-Tocopherol (Vitamin E)	b. TROLOX	c. SUL-109
	(2R)-2,5,7,8-tetramethyl-2-[(4R,8R)-(4,8,12-trimethyltridecyl)]-6-chromanol	(6-hydroxy-2,5,7,8-tetramethylchroman)-2-carboxylic acid	(6-hydroxyl-2,5,7,8-tetramethylchroman-2-yl)(4-(2-hydroxyethyl)piperazin-1-yl)methanone
MW:	430.71	250.29	399.09
log P:	9.98	3.19	2.25
log S:	-7.20	-2.56	-2.31
Topological Polar Surface Area:	29.46	66.67	73.24
TEAC:	0.97	1.00	0.53

Figure 1. (Modified) 6-chromanols are water soluble α-tocopherol derivatives. Structural and chemical properties of the compounds under investigation; (a) α-tocopherol (vitamin E), (b) TROLOX, and (c) SUL-109.

SUL-109 improves ASC viability, adhesion and proliferation after hypothermic damage.

A hypothermic challenge (4°C, 48h) reduced ASC viability to ~7% (p<0.001, fig.2a). Pretreatment of ASC with α-tocopherol marginally increased cell viability (viability ~16%, p<0.05) whereas SUL-109 completely rescued cell viability (viability ~84%, p<0.001, fig.2a).

Moreover, viability of ASC that received a hypothermic challenge in the presence of SUL-109 did not differ from ASC that were maintained at 37°C under standard cell culture conditions or ASC that were preserved using cryopreservation (fig.2a).

Cell death resulting from hypothermia was primarily induced by necrosis (~66%, p<0.001 compared to ASC maintained at 37°C, fig.2c) and to a lesser extent by apoptosis (~27%, p<0.001, fig.2b). Consistent with the improved cell viability, SUL-109 completely blocked the initiation of apoptosis and necrosis following the hypothermia (figs.2b,c), whereas α-tocopherol did not reduce apoptosis and necrosis (maximum ~10% reduction, p=0.10, fig.2b,c). Further, hypothermic preservation of ASC using SUL-109 was effective with full preservation of viability (~88%, fig.2d) over a period of four days.

As tissue engineering and regenerative medicine strategies require ASC to readily adhere and grow at the treatment site following injection or implantation, we assessed the effects of 6-chromanols on their adhesion capacity and growth potential after hypothermic treatment (figs.2e-g).

Hypothermia challenged ASC had a decreased adherence capacity (~4-fold, p<0.001) compared to ASC that were maintained under standard culture conditions over a period of 4 hours post-seeding (fig.2d).

Pretreatment with the 6-chromanols α-tocopherol and TROLOX did not attenuate the loss in adherence capacity (fig.2d). In contrast, ASC that were treated with SUL-109 prior to the hypothermic preservation, adhered to the same extent as ASC maintained at 37°C throughout the experiment (fig.2d).

The growth potential of ASC that underwent hypothermic preservation was investigated by Ki67 expression. ASC that were exposed to hypothermia were devoid of Ki67 expression (fig.2f) for as long as 48h after rewarming (fig.2f), indicating prolonged growth arrest. Pretreatment with the 6-chromanols increased ASC proliferation to 25% (α-tocopherol, $p < 0.05$), 40% (TROLOX, $p < 0.001$) and 62% (SUL-109, $p < 0.001$, fig.2g). Notably, ASC pretreated with SUL-109 had a growth potential equal to cryopreserved and normothermic ASC (figs.2f,g).

Thus, pretreatment of ASC with SUL-109 fully preserves cell viability, adherence capacity and proliferative capacity following hypothermic storage.
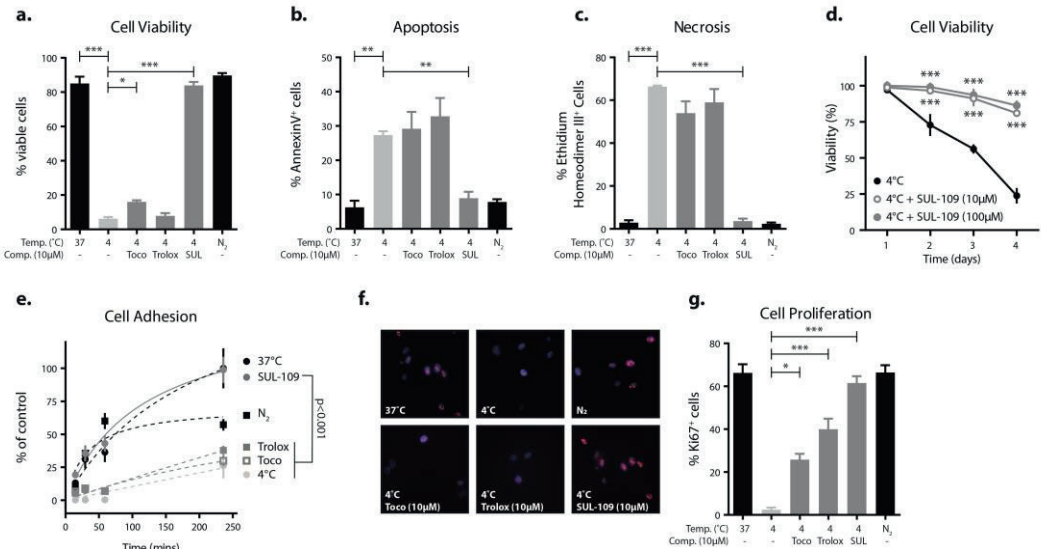
Figure 2. SUL-109 protects ASC from hypothermic damage. Hypothermia strongly reduces cell viability (a). Hypothermia-induced cell death was both caused by apoptosis (~27% Annexin V-positive cells; b) and necrosis (~66% Ethidium Homeodimer III-positive cells; c). Alpha-tocopherol and TROLOX do not inhibit hypothermia-induced cell death, but SUL-109 abrogates both the apoptotic and necrotic cell death responses of ASC during hypothermic preservation (b,c). SUL-109 maintains ASC viability during hypothermic preservation for 4 days (d). Cells that encountered hypothermic damage for 48h followed by 2h re-warming show poor adherence during 240mins post-seeding (e), whereas ASC treated with SUL-109 prior to hypothermia adhered at a similar rate as ASC that were maintained at 37°C (e). Hypothermia slows metabolic activity and cell cycle progression resulting in failure to undergo the G2/M transition after cooling from 37°C to 4°C (g). ASC show cell cycle arrest (absence of Ki67; f) after hypothermic preservation despite 48h of rewarming (f). In contrast, hypothermically stored ASC that were treated with α-tocopherol, TROLOX or SUL-109 (e,f) maintained their cycling activity and SUL-109-treated ASC proliferated at a similar rate to control cells (g) that were maintained at 37°C . TOCO = α-tocopherol, N$_2$ = liquid nitrogen cryopreservation, * $p<0.05$, ** $p<0.01$, *** $p<0.001$, N$_2$ = liquid nitrogen cryopreservation.

ASC maintain their multipotent differentiation capacity after hypothermic damage.

The ability of ASC to differentiate into multiple cell types under lineage-specific culture conditions holds promise for tissue engineering and regenerative medicine.

Hence, preservation protocols should have minimal interference with these characteristics and must maintain the multipotency of ASC. Hypothermic preserved ASC readily differentiated along the adipogenic (Oil Red O), osteogenic (Alizarin Red) or myogenic (SM22α) lineage (fig.3). Although hypothermia causes a large decrease in available cell numbers, ASC exposed to hypothermia did not display any signs of decreased multilineage specialization (fig.3).

Moreover, the adipogenic, osteogenic and myogenic differentiation capacity of ASC treated with α-tocopherol, TROLOX or SUL-109 prior to hypothermia did not differ from ASC that were maintained under standard culture conditions (fig.3).
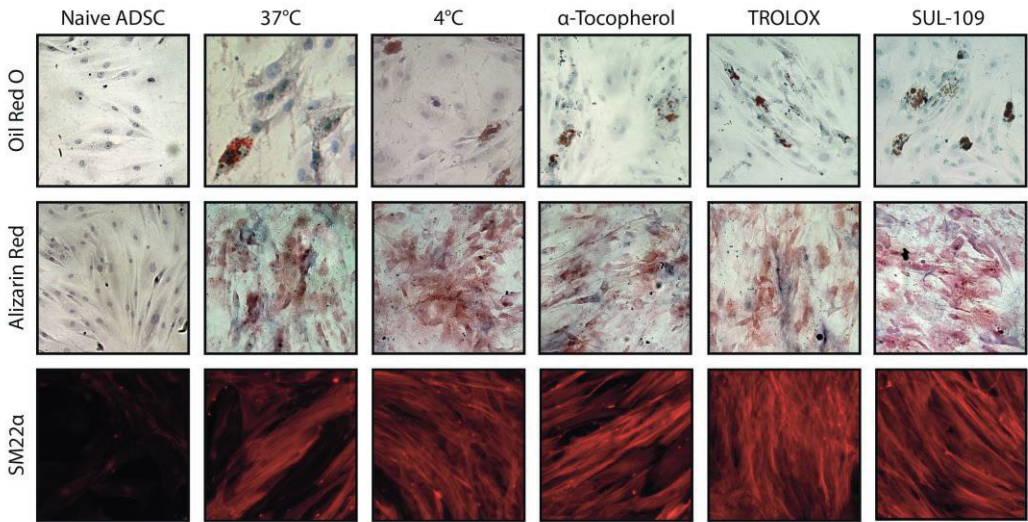
Figure 3. Hypothermia does not reduce the multipotency of ASC. ASC differentiation into the adipogenic (Oil Red O-positive cells), osteogenic (Alizarin Red-positive cells) and myogenic (SM22α-positive cells) lineage. Naive ASC differentiate efficiently into the three lineages when treated with the appropriate stimuli. ASC that survived the hypothermic challenge maintained their differentiation capacity and treatment with the 6-chromanols did not affect multilineage differentiation.

Cell survival is not associated with the antioxidant capacity of (modified) 6-chromanols.

Hypothermic damage is associated with a drastic increase in reactive oxygen species (ROS) and can be reduced by antioxidants [24]. Therefore we investigated in a test-tube setting if the 6-chromanol derivate SUL-109 (fig.1a) possessed antioxidant properties [19, 20] using the fluorescent ROS sensor 2'7'-dichlorodihydrofuorecein diacetate (DCF).

The oxidation of DCF by H2O2 was strongly inhibited by the co-incubation with α-tocopherol (IC50=0.40 μM, TROLOX-equivalent antioxidant capacity (TEAC)=0.98±0.05) and TROLOX (IC50=0.32 μM, TEAC=1.0±0.11), whereas SUL-109 only inhibited DCF oxidation at concentration above 10-5M (IC50=229 μM, TEAC=0.53±0.06, fig.4a). ASC survival during hypothermia increased dose-dependently with the addition of (modified) 6-chromanols (fig.4b). Alpha-tocopherol provided protection against hypothermia at concentrations above 10-3 M (EC50= 5.40 mM), whereas the modified 6-chromanols TROLOX (EC50=306.20 μM) and SUL-109 (EC50=2.65 μM) showed a higher potency (fig.4b) with effective concentrations in the micromole range.

These data imply that the protective effects of 6-chromanols are not derived from their antioxidant capacity, but from their interference with specific cellular processes. Indeed, the TEAC of α-tocopherol, TROLOX and SUL-109 shows a positive correlation with ASC viability, whereas a negative correlation would be expected if antioxidant capacity was the driving force (r2=0.952,p=0.003, fig.4c).
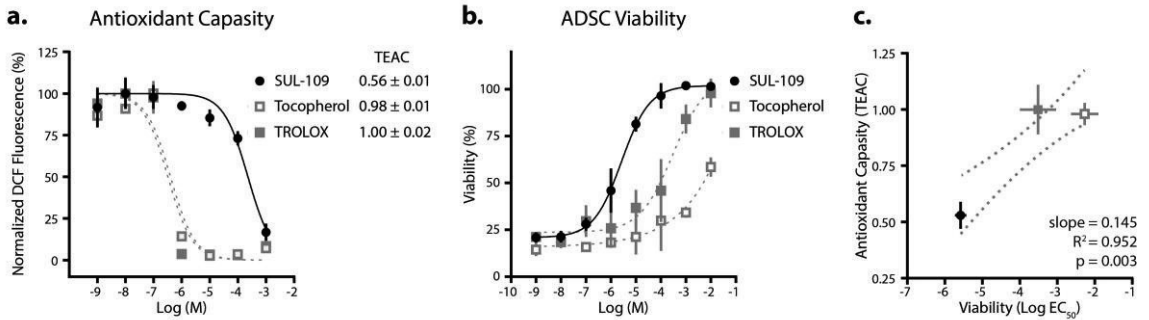
Figure 4. ROS-scavenging by 6-chromanols does not associate with cell survival. Dose-response of the antioxidant capacities of α-tocopherol, TROLOX and SUL-109 (a). Alpha-tocopherol and TROLOX are strong antioxidants with and IC_{50} for H_2O_2-induced DCF fluorescence of 0.40 μM and 0.32 μM, respectively. SUL-109 is a weak antioxidant (TEAC 0.56) with an IC_{50} of 229 μM for H_2O_2-induced DCF fluorescence. Dose-response of 6-chromanols on the viability of hypothermia-challenged ASC (b). Alpha-tocopherol and TROLOX increase cell viability after hypothermia only at high concentrations. Alpha-tocopherol had an EC_{50} of 2.2 mM, TROLOX had an EC_{50} of 0.3 mM. In comparison, SUL-109 readily increases cell viability with an EC_{50} of 2.6 μM. Association between antioxidant capacity and cell viability (c). TOCO = α-tocopherol, TEAC = TROLOX-equivalent antioxidant capacity.

SUL-109 maintains mitochondrial integrity, mitochondrial membrane potential and ATP production by activation of mitochondrial complexes I and IV.

As cell death and the induction of growth arrest are both highly influenced by cellular redox state and mitochondrial function [25, 26], we investigated if 6-chromanols influenced the mitochondrial function of hypothermically preserved ASC (fig.5).

Hypothermia induces a drastic decrease in mitochondrial respiration through oxidative phosphorylation as observed by the decrease in basal oxygen consumption rate (OCR, ~2.6-fold, p<0.001, fig.5a,c), without changing the extracellular acidification rate (ECAR, fig.5b,c).

TROLOX and SUL-109 pretreatment maintained basal mitochondrial respiration, normalizing the OCR to the level of normothermic controls (fig.5a,c). Further, in contrast to α-tocopherol and TROLOX, SUL-109 fully prevented the drop in FCCP-induced maximal OCR of hypothermically preserved ASC (figs.5a,d), indicative of increased mitochondrial reserve capacity and increased mitochondrial coupling [27] compared to hypothermia-treated ASC and ASC pretreated with α-tocopherol or TROLOX (Fig.5a,d).

Notably, the SUL-109-induced increase in mitochondrial respiration was only observed for oxidative phosphorylation (OCR, fig.5d) and not for glycolysis (ECAR), indicating that SUL-109 preserves mitochondrial coupling.

Indeed, the dense network of fused mitochondria observed in normothermic ASC became fragmented following hypothermia (fig.5e). Pretreatment of ASC with α-tocopherol did not prevent mitochondrial fragmentation, whereas TROLOX only partially inhibited the fission of the mitochondrial networks. SUL-109

pretreatment fully blocked the hypothermia-induced fragmentation, as ASC maintained a dense network of fused mitochondria (fig.5e).

Corroboratively, hypothermic storage for 48h induced a complete loss of the mitochondrial membrane potential, whereas α-tocopherol and TROLOX only partially prevented the collapse in mitochondrial membrane potential (fig.5f).

ASC that received SUL-109 treatment prior to hypothermic preservation maintained their mitochondrial membrane potential at the level of normothermic ASC (fig.5f). Concurrent with the loss in mitochondrial membrane potential, hypothermic ASC, as well as α-tocopherol and TROLOX-treated ASC showed an increase in mitochondrial superoxide production (fig.5g), which is associated with cell death [28]. SUL-109-treated ASC did not show excessive mitochondrial superoxide formation (fig.5g).

a. Oxidative Phosphorylation

b. Glycolysis

c. Basal Mitochondrial Respiration

d. Forced Mitochondrial Respiration

e.

f. Membrane Potential

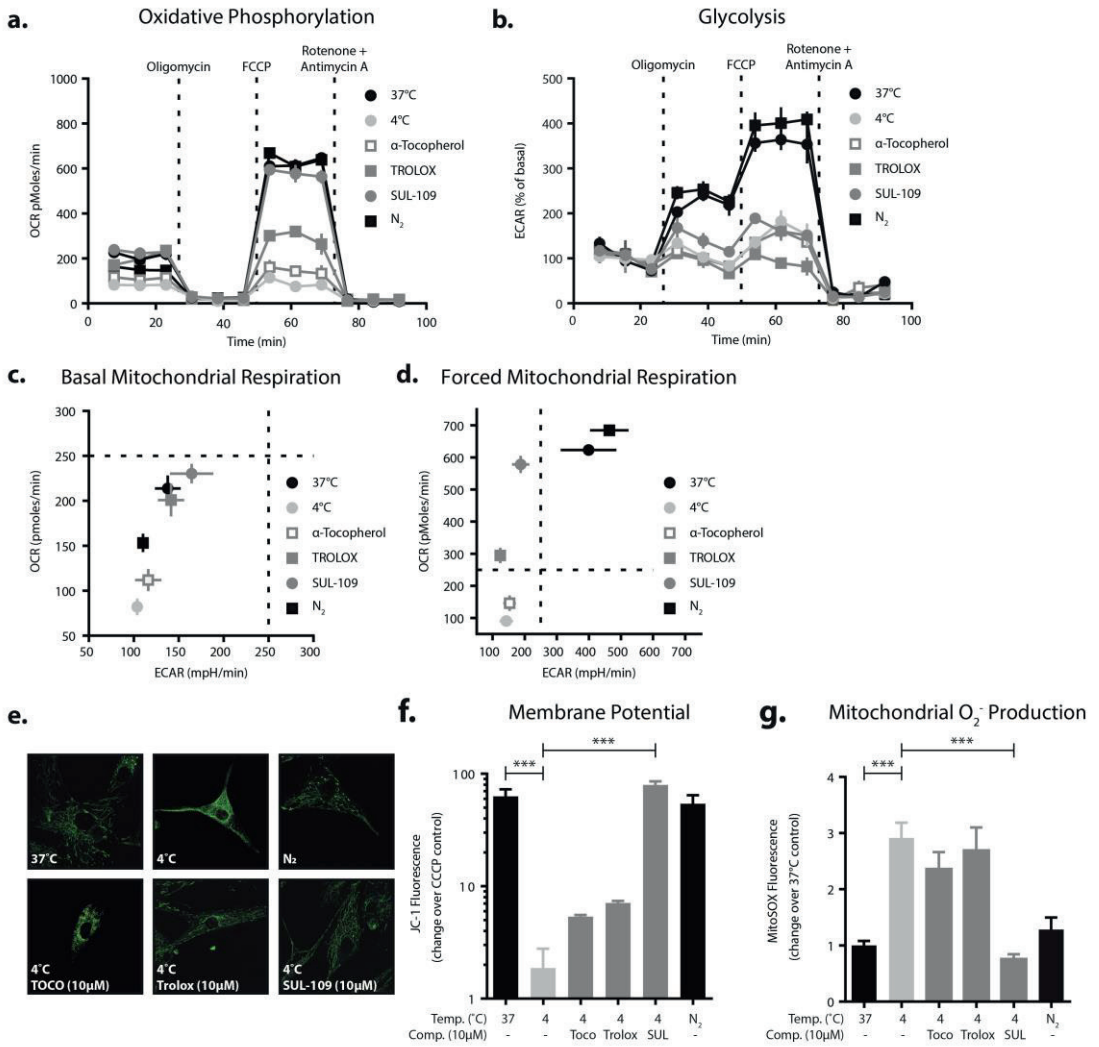**g.** Mitochondrial O_2^- Production

Figure 5. SUL-109 maintains mitochondrial function and integrity and function during hypothermic damage. Assessment of mitochondrial oxidative phosphorylation

(a) and glycolysis (b) in hypothermia challenged ASC. Hypothermia reduces the basal oxygen consumption rate (OCR) of ASC, which is normalized by treatment with TROLOX or SUL-109 (c). During forced respiration, SUL-109 maintains the mitochondrial OCR, but does not affect glycolysis (d). 6-chromanols protect against hypothermia-induced fission of mitochondria with different efficacies (e) and maintain the mitochondrial membrane potential (f). Concurrently, mitochondrial Superoxide production is reduced (g). TOCO = α-tocopherol, OCR = Oxygen Consumption Rate, ECAR = Extracellular Acidification Rate, FCCP = Carbonyl cyanide-4-(trifluoromethoxy)phenylhydrazone, CCCP = Carbonyl cyanide m-chlorophenyl hydrazone, N_2 = liquid nitrogen cryopreservation, *** $p < 0.001$.

As SUL-109 maintained mitochondrial spare capacity in ASC following hypothermia/rewarming, we questioned at what level SUL-109 influenced mitochondrial respiration and performed activity measurements for mitochondrial complexes I-V on isolated ASC-derived mitochondria (fig.6). SUL-109 dose-dependently increased the activity of mitochondrial complexes I and IV (1.1-fold and 2.1-fold ($p<0.05$), respectively, figs.6a,e) but did not affect the activity of mitochondrial complexes II, III and V (suppl.fig.1).

Concurrently, SUL-109 at a concentration of 1 µM inhibited the rotenone-induced reduction of complex I activity (fig.6b) and the potassium cyanide (KCN)-induced reduction of complex IV activity (fig.6f).

Given the maintenance of mitochondrial function by SUL-109, we next investigated whether it also preserved ATP production and inhibited mitochondrial ROS production in ASC following damage. To this end we treated mitochondria isolated from ASC with either rotenone or KCN to inhibit ATP production and induce ROS generation. Indeed, SUL-109 treatment almost completely restored ATP production in rotenone-treated ASC (fig.6c) and normalized their mitochondrial ROS production (fig.6d) to baseline levels.

Likewise, SUL-109 treatment dose-dependently restored ATP production (fig.6g) and inhibited ROS generation (fig.6h) in KCN-treated ASC. These data imply that SUL-109 protects cells from oxidative stress by maintenance of the mitochondrial function through the specific activation of mitochondrial complexes I and IV.
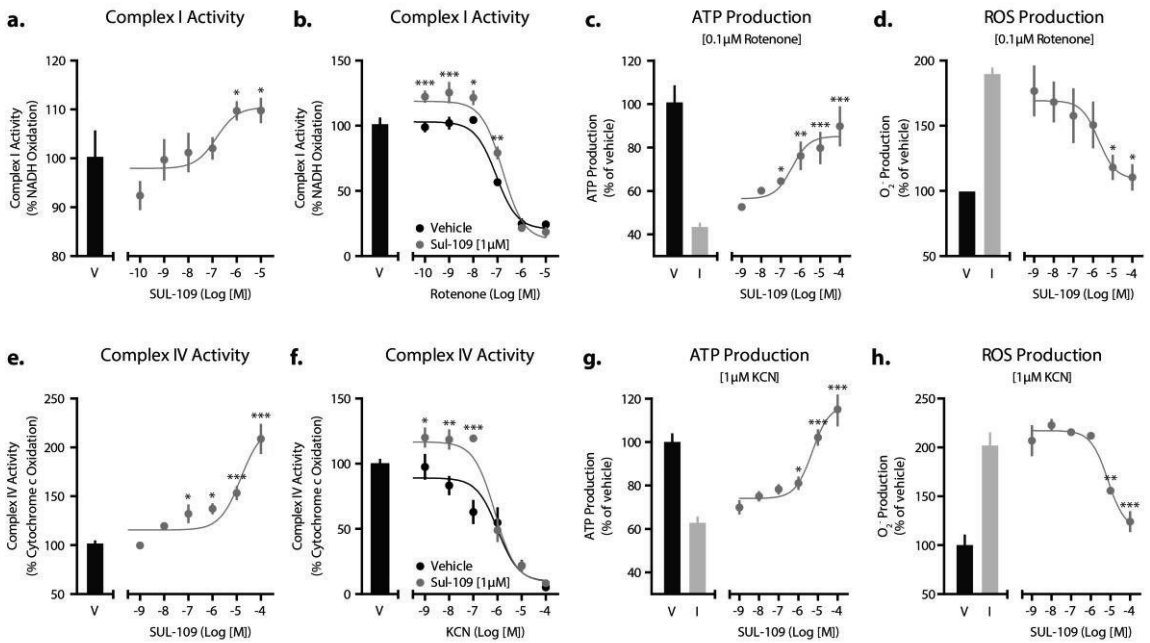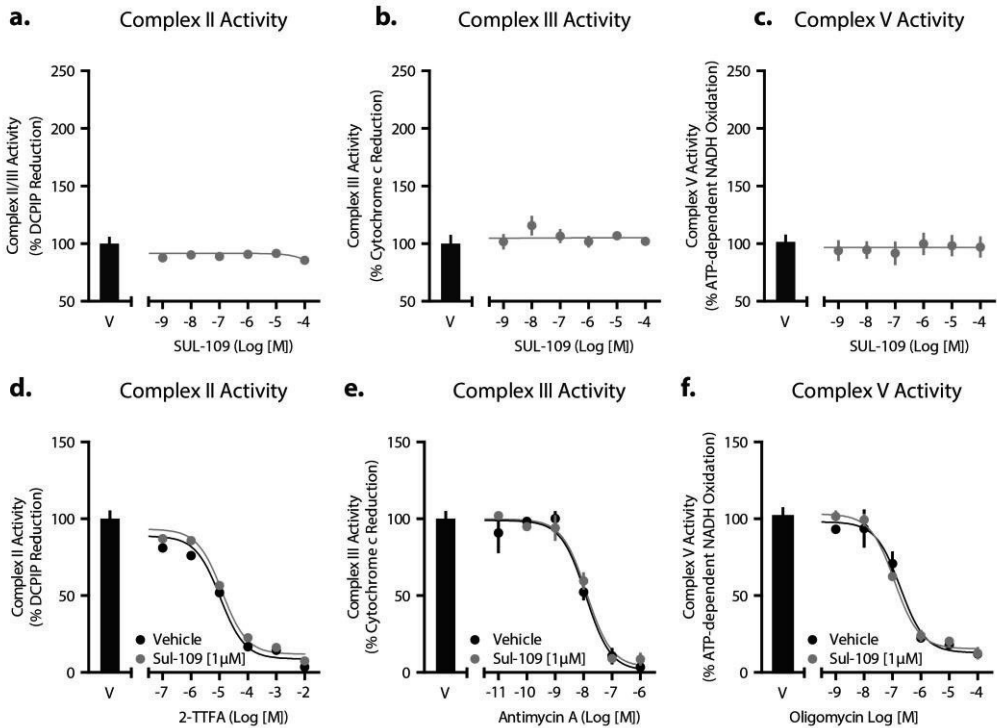
Figure 6. SUL-109 activates mitochondrial complex I and IV to maintain ATP production and inhibit ROS formation. SUL-109 activates mitochondrial complex I (a) and dose-dependently limits the rotenone-induced inhibition of complex I activity (b) in isolated ASC-derived mitochondria. Resulting from its effects on complex I, SUL-109 dose-dependently increases ATP production in rotenone-treated ASC (c) and reduces mitochondrial ROS formation (d). Besides, SUL-109 activates mitochondrial complex IV (e) and dose-dependently limits the KCN-induced inhibition of complex IV activity (f) in isolated ASC-derived mitochondria. Resulting from its effects on complex IV, SUL-109 dose-dependently increases ATP production in KCN-treated ASC (g) and reduces mitochondrial ROS formation (h). * $p < 0.05$, ** $p < 0.01$, *** $p < 0.001$, KCN = potassium cyanide.

Supplemental figure 1. SUL-109 does not affect the activity of mitochondrial complexes II, III and V. SUL-109 does not alter the activity of mitochondrial complex II (a), III (b) and V (c) activity, nor does it limit the reduction of complex II, III and IV activity by 2-TTFA (d), Antimycin A (e) and Oligomycin A (f), respectively. 2-TTFA = 2-thenoyltrifluoroacetone.

Discussion

Here we describe the efficacy of the novel pharmacologic compound, (6-hydroxyl-2,5,7,8-tetramethylchroman-2-yl)(4-(2-hydroxyethyl)piperazin-1-yl)methanone (SUL-109), that protects ASC from hypothermic damage and cell death during cell preservation without affecting their multipotency.

SUL-109 conveys its protective effect by preserving the mitochondrial network structure and activating mitochondrial complexes I and IV, therefore maintaining ATP production and preventing ROS formation. SUL-109 protects ASC from damage associated with hypothermic cell preservation and simplifies the application of ASC in cell therapy and tissue engineering by removing the major limitations of cell death and dysfunction encountered during the manufacturing process.

Despite the encouraging progress in experimental regenerative medicine applications of stem cells for the treatment of chronic diseases [3, 4, 8, 9], clinically acceptable methods of cell preservation are poorly developed [11, 29-31].

Current advances in cell therapy and tissue engineering thus create the need for standardized procedures for short term cell preservation that void the necessity of using expensive cryopreservation or vitrification equipment and laborious protocols [11] or the usage of cell preservation reagents that are toxic to cells at ambient temperatures (e.g. dimethyl sulfoxide) [32-34], to allow for proper quality control and transport of cells from their manufacturing facility to their clinical destination. Low- temperature cell pausing, or hypothermic preservation of cells in their specialized culture media, holds great potential as short-term cell storage in these respects [11, 35].

Low temperatures have a wide range of beneficial effects in the context of cell preservation, i.e. a reduction of energy-dependent processes such as cell cycle progression and protein synthesis [36-39], but may also induce cell damage. The hypothermia-induced reduction in ATP production causes an influx of sodium ions that is no longer counteracted by the Na+-K+-ATPase, which is followed by an influx of water and the concomitant cell swelling results in necrotic cell damage [40, 41].

Additionally, the generation of ROS during the rewarming phase causes a significant apoptotic response [42-44], wherein only slight changes in temperature (~5°C) can have detrimental effects on stem cell survival [45]. The addition of antioxidants to cell preservation media is reported to reduce the hypothermia-induced apoptosis [14, 46], but fails to limit the necrosis induction as ATP production is limited during hypothermia. Moreover, some cell preservation solutions are reported to be toxic to ASC [REF], stressing the urgency of developing a cell culture additive that can void the hypothermic damage. Notably, SUL-109 maintained ATP production under hypothermic conditions and inhibited the generation of ROS upon rewarming. Concurrently, SUL-109 inhibited both the hypothermia-induced apoptosis and necrosis. Hypothermic cell preservation induces cell cycle arrest due to the reduction of available ATP in the cold phase and the accumulation of ROS-induced DNA damage during the rewarming phase [25, 36, 37]. We show hypothermia to induce growth arrest which is maintained in ASC 48h post-rewarming. Alpha-tocopherol, TROLOX and SUL-109 maintained cell cycle activity, whereas proliferation of SUL-109-treaded cells was similar to ASC that had not encountered a hypothermia challenge.

Hypothermia and cryopreservation protocols can also limit the multipotency or induce differentiation of stem cells [47, 48]. Therefore, we investigated the multilineage differentiation of ASC that were subjected to a hypothermic challenge for 48h. ASC that survived the hypothermic challenge maintained their differentiation capacity towards adipocytes, osteoblasts and muscle cells regardless of their treatment.

We explored the mechanisms-of-action by which SUL-109 could protect the ASC from damage encountered during hypothermic preservation and rewarming and found that the protective effects were not derived from the ROS-scavenging capability of 6-chromanols [19, 20, 49], as antioxidant capacity did not associate with cell survival. Rather, SUL-109 increases the activity of mitochondrial complexes I and IV, thereby maintaining the mitochondrial membrane potential, ATP production and minimalizing ROS generation. 6-chromanols might form Quinones [49, 50], the electron acceptor substrate for mitochondrial complexes I and II, upon oxidation. Therefore, it seems conceivable that such mechanism underlies the increase in mitochondrial complex I activity by SUL-109 following hypothermia [51-53]. Notably, short-chain Quinones are able to bypass a deficiency in complex I by shuttling electrons directly from the cytoplasm to complex III of the mitochondrial respiratory chain to maintain ATP production [54].

Cytochrome c-mediated lipid peroxidation, resulting in a decreased mitochondrial membrane potential and decreased ATP production, is highly influenced by ROS and hypothermia [55-57]. Cytochrome c acts as an electron shuttle between mitochondrial complexes III and IV [58], which facilitates oxidative phosphorylation and thus ATP production. ROS or hypothermia-induced conformational changes in

cytochrome c, facilitate its binding to cardiolipin and the resulting partial unfolding of cytochrome c [59], enable its lipid peroxidation activity while decreasing the amount of cytochrome c available for oxidative phosphorylation [60-62]. Hence, this conformational change in cytochrome c might contribute to the mitochondrial dysfunction observed during hypothermia. Pentamethyl-6-chromanol (PMC), another vitamin E analogue with structural similarity to SUL-109, reduces cytochrome c-mediated lipid peroxidation [62] by a mechanism that is currently not elucidated. Therefore, we postulate that SUL-109 also preserves the conformational state of cytochrome c, which thereby remains available for oxidative phosphorylation and ATP production. Although this mechanism might explain how SUL-109 maintains the mitochondrial membrane potential and ATP production by complex IV following hypothermia, it does not clarify why SUL-109 raises the activity of mitochondrial complex IV in normothermic cells. Shuttling of electrons from the cytoplasm to mitochondrial complex III [54] and the concomitant increase in oxidized cytochrome c represent potential mechanisms, but this effect of SUL-109 needs further biochemical exploration.

In conclusion, here we describe the efficacy of SUL-109, a 6-chromanol derivate that protects ASC against hypothermic cell damage during preservation. The protective effects of SUL-109 against hypothermia are twofold; (1) SUL-109 has an antioxidant capacity, and (2) SUL-109 maintains the integrity of the mitochondria and activates mitochondrial complexes I and IV, which conserved ATP production and mitigates ROS production. Therefore, SUL-109 represents a single molecule cell preservation agent that protects ASC from hypothermic damage associated with short-term cell preservation that does not affect the stemness of ASC.

Conflicts of interest

A.C.G. is stock holder and the chief executive officer, G.K. is chief scientific officer and P.V. is chief of operations at Sulfateq B.V. (Groningen, the Netherlands), a company that owns patents on SUL-109, and produces and markets similar compounds.

References

1. Corselli, M., et al., *The Tunica Adventitia of Human Arteries and Veins as a Source of Mesenchymal Stem Cells*. Stem Cells Dev, 2012. 21: p. 1299-308.

2. Mizuno, H., M. Tobita, and A.C. Uysal, *Concise Review: Adipose-Derived Stem Cells as a Novel Tool for Future Regenerative Medicine*. STEM CELLS, 2012. 30: p. 804-10.

3. Philips, B.J., K.G. Marra, and J.P. Rubin, *Adipose Stem Cell-Based Soft Tissue Regeneration*. Expert Opin Biol Ther, 2012. 12: p. 155-63.

4. Wilson, A., P.E. Butler, and A.M. Seifalian, *Adipose-Derived Stem Cells for Clinical Applications: A Review*. Cell Prolif, 2011. 44: p. 86-98.

5. Spiekman, M., et al., *Adipose Tissue-Derived Stromal Cells Inhibit Tgf-Beta1-Induced Differentiation of Human Dermal Fibroblasts and Keloid Scar-Derived Fibroblasts in a Paracrine Fashion*. Plast Reconstr Surg, 2014. 134: p. 699-712.

6. Hong, S.J., D.O. Traktuev, and K.L. March, *Therapeutic Potential of Adipose-Derived Stem Cells in Vascular Growth and Tissue Repair*. Curr Opin Organ Transplant, 2010. 15: p. 86-91.

7. Shi, Y., et al., *Adipose-Derived Stem Cells Combined with a Demineralized Cancellous Bone Substrate for Bone Regeneration*. Tissue Eng, 2012. 18: p. 1313-21.

8. Zhang, K., et al., *Repair of an Articular Cartilage Defect Using Adipose-Derived Stem Cells Loaded on a Polyelectrolyte Complex Scaffold Based on Poly(L-Glutamic Acid) and Chitosan*. Acta Biomaterialia, 2013. 9: p. 7276-88.

9. Nakagami, H., et al., *Novel Autologous Cell Therapy in Ischemic Limb Disease through Growth Factor Secretion by Cultured Adipose Tissue–Derived Stromal Cells*. Arterioscler Thromb Vasc Biol, 2005. 25: p. 2542-7.

10. Houtgraaf, J.H., et al., *First Experience in Humans Using Adipose Tissue–Derived Regenerative Cells in the Treatment of Patients with St-Segment Elevation Myocardial Infarction*. J Am Coll Cardiol, 2012. 59: p. 539-40.

11. Robinson, N.J., A. Picken, and K. Coopman, *Low Temperature Cell Pausing: An Alternative Short-Term Preservation Method for Use in Cell Therapies Including Stem Cell Applications*. Biotechnol Lett, 2014. 36: p. 201-9.

12. Kopeika, J., A. Thornhill, and Y. Khalaf, *The Effect of Cryopreservation on the Genome of Gametes and Embryos: Principles of Cryobiology and Critical Appraisal of the Evidence*. Hum Reprod Update, 2014.

13. Todorova, T., et al., *Mutagenic Effect of Freezing on Nuclear DNA of Saccharomyces Cerevisiae*. Yeast, 2012. 29: p. 191-9.

14. Mathew, A.J., R.G. Van Buskirk, and J.G. Baust, *Improved Hypothermic Preservation of Human Renal Cells through Suppression of Both Apoptosis and Necrosis*. Cell Preserv Technol, 2003. 1: p. 239-53.

15. Stier, A., et al., *Mitochondrial Uncoupling Prevents Cold-Induced Oxidative Stress: A Case Study Using Ucp1 Knockout Mice*. J Exp Biol, 2014. 217: p. 624-30.

16. Abrahamse, S.L., et al., *Induction of Necrosis and DNA Fragmentation During Hypothermic Preservation of Hepatocytes in Uw, Htk, and Celsior Solutions*. Cell Transplant, 2003. 12: p. 59-68.

17. Sohn, H.S., et al., *Duration of in Vitro Storage Affects the Key Stem Cell Features of Human Bone Marrow-Derived Mesenchymal Stromal Cells for Clinical Transplantation*. Cytotherapy, 2013. 15: p. 460-6.

18. Lane, T.A., D. Garls, E. Mackintosh, S. Kohli, and S.C. Cramer, *Liquid Storage of Marrow Stromal Cells.* Transfusion, 2009. 49: p. 1471-81.

19. Gregor, W., et al*., Antioxidant Properties of Natural and Synthetic Chromanol Derivatives: Study by Fast Kinetics and Electron Spin Resonance Spectroscopy.* J Org Chem, 2005. 70: p. 3472-83.

20. Inami, K., et al., *Chlorine Atom Substitution Influences Radical Scavenging Activity of 6-Chromanol*. Bioorg Med Chem, 2012. 20: p. 4049-55.

21. Van Der Graaf, A.C., A. Heeres, and J.P.G. Seerden, *Compounds for the Protection of Cells*. 2013. PCT/NL2013/050915.

22. Bourin, P., et al., *Stromal Cells from the Adipose Tissue-Derived Stromal Vascular Fraction and Culture Expanded Adipose Tissue-Derived Stromal/Stem*

Cells: A Joint Statement of the International Federation for Adipose Therapeutics and Science (Ifats) and the International Society for Cellular Therapy (Isct). Cytotherapy, 2013. 15: p. 641-8.

23. Hong, S., P.L. Pedersen, *ATP Synthase and the Actions of Inhibitors Utilized to Study Its Roles in Human Health, Disease, and Other Scientific Areas*. Microbiol Mol Biol Rev, 2008. 72: p. 590-641.

24. Bilzer, M., G. Paumgartner, and A.L. Gerbes, *Glutathione Protects the Rat Liver against Reperfusion Injury after Hypothermic Preservation*. Gastroenterology, 1999. 117: p. 200-10.

25. Menon, S.G., and P.C. Goswami, *A Redox Cycle within the Cell Cycle: Ring in the Old with the New*. Oncogene, 2006. 26: p. 1101-9.

26. Fleury, C., B. Mignotte, and J.L. Vayssière, *Mitochondrial Reactive Oxygen Species in Cell Death Signaling*. Biochimie, 2002. 84: p. 131-41.

27. Brand Martin, D., et al., *Assessing Mitochondrial Dysfunction in Cells*. Biochem J, 2011. 435: p. 297-312.

28. Suski, J.M., et al., *Relation between Mitochondrial Membrane Potential and Ros Formation.* Methods Mol Biol, 2012. 810: p. 183-205.

29. Asghar, W., et al., *Preserving Human Cells for Regenerative, Reproductive, and Transfusion Medicine.* Biotechnol J, 2014. 9: p. 895-903.

30. Coopman, K., *Large-Scale Compatible Methods for the Preservation of Human Embryonic Stem Cells: Current Perspectives*. Biotechnol Prog, 2011. 27: p. 1511-21.

31. Pegg, D.E., *The Current Status of Tissue Cryopreservation*. Cryo Letters, 2001. 22: p. 105-14.

32. Hebling, J., et al., *Cytotoxicity of Dimethyl Sulfoxide (Dmso) in Direct Contact with Odontoblast-Like Cells.* Dent Mater, 2015. 31: p. 399-405.

33. Galvao, J., et al., *Unexpected Low-Dose Toxicity of the Universal Solvent Dmso*. FASEB J, 2014. 28: p. 1317-30.

34. Almansoori, K.A., et al., *Cryoprotective Agent Toxicity Interactions in Human Articular Chondrocytes.* Cryobiology, 2012. 64: p. 185-91.

35. Storey, K., *7. Lessons in Organ Preservation from Nature*. Cryobiology,2015. 71: p. 166.

36. Matijasevic, Z., J.E. Snyder, and D.B. Ludlum, *Hypothermia Causes a Reversible, P53-Mediated Cell Cycle Arrest in Cultured Fibroblasts*. Oncology Res, 1998. 10: p. 605-10.

37. Rieder, C.L., and R.W. Cole, *Cold-Shock and the Mammalian Cell Cycle*. Cell Cycle, 2002. 1: p. 168-74.

38. Tanaka, T., et al., *Persisting Mild Hypothermia Suppresses Hypoxia-Inducible Factor-1α Protein Synthesis and Hypoxia-Inducible Factor-1-Mediated Gene Expression.* Am J Physiol Regul Integr Comp Physiol 2010;298:R661-R71.

39. Vreugdenhil, P.K., et al., *Biphasic Mechanism for Hypothermic Induced Loss of Protein Synthesis in Hepatocytes1*. Transplantation, 1999. 67: p. 1468-73.

40. Pchejetski, D., et al., *Inhibition of Na+,K+-Atpase by Ouabain Triggers Epithelial Cell Death Independently of Inversion of the [Na+]I/[K+]I Ratio*. Biochem Biophys Res Commun, 2003. 301: p. 735-44.

41. Yu, S.P., *Na+, K+-Atpase: The New Face of an Old Player in Pathogenesis and Apoptotic/Hybrid Cell Death*. Biochem Pharmacol, 2003. 66: p. 1601-9.

42. Alva, N., J. Palomeque, and T. Carbonell, *Oxidative Stress and Antioxidant Activity in Hypothermia and Rewarming: Can Rons Modulate the Beneficial Effects of Therapeutic Hypothermia?* Oxid Med Cell Longev, 2013. 2013: p. 10.

43. Carey, H.V., M.T. Andrews, and S.L. Martin, *Mammalian Hibernation: Cellular and Molecular Responses to Depressed Metabolism and Low Temperature*. Physiol Rev, 2003. 83: p. 1153-81.

44. Polderman, K.H., *Mechanisms of Action, Physiological Effects, and Complications of Hypothermia*. Crit Care Med, 2009. 37: p. 186-202.

45. Stolzing, A., S. Sethe, and A.M. Scutt, *Stressed Stem Cells: Temperature Response in Aged Mesenchymal Stem Cells*. Stem Cells Dev, 2006. 15: p. 478-87.

46. Ginis, I., B. Grinblat, and M.H. Shirvan, *Evaluation of Bone Marrow-Derived Mesenchymal Stem Cells after Cryopreservation and Hypothermic Storage in Clinically Safe Medium*. Tissue Eng, 2011. 18: p. 453-63.

47. Pogozhykh, D., et al., *Influence of Factors of Cryopreservation and Hypothermic Storage on Survival and Functional Parameters of Multipotent Stromal Cells of Placental Origin*. PLoS One, 2015. 10: e0139834.

48. François, M., et al., *Cryopreserved Mesenchymal Stromal Cells Display Impaired Immunosuppressive Properties as a Result of Heat-Shock Response and Impaired Interferon-Γ Licensing*. Cytotherapy, 2012. 14: p. 147-52.

49. Jameson, V.J.A., et al., *Synthesis of Triphenylphosphonium Vitamin E Derivatives as Mitochondria-Targeted Antioxidants*. Tetrahedron, 2015. 71: p. 8444-53.

50. Vasilchenko, L.G., et al., *Phenolic Antioxidants and Their Role in Quenching of Reactive Molecular Species in the Human Skin Injury*. Lipid Technology, 2015. 27: p. 36-9.

51. Karuppagounder, S.S., et al., *Quercetin up-Regulates Mitochondrial Complex-I Activity to Protect against Programmed Cell Death in Rotenone Model of Parkinson's Disease in Rats*. Neuroscience, 2013. 236: p. 136-48.

52. Erb M., et al., *Features of Idebenone and Related Short-Chain Quinones That Rescue Atp Levels under Conditions of Impaired Mitochondrial Complex I*. PLoS One, 2012. 7: e36153.

53. Bongard, R.D., M.I. Townsley, and M.P. Merker, *The Effects of Mitochondrial Complex I Blockade on Atp and Permeability in Rat Pulmonary Microvascular Endothelial Cells in Culture (Pmvec) Are Overcome by Coenzyme Q1 (Coq1).* Free Radic Biol Med, 2015. 79: p. 69-77.

54. Haefeli, R.H., et al., *Nqo1-Dependent Redox Cycling of Idebenone: Effects on Cellular Redox Potential and Energy Levels.* PLoS One, 2011. 6: e17963.

55. Kuznetsov, A.V., et al., *Mitochondrial Defects and Heterogeneous Cytochrome C Release after Cardiac Cold Ischemia and Reperfusion.* Am J Physiol Heart Circ Physiol, 2004. 286: H1633-H41.

56. Green, C.J., et al., *Evidence of Free-Radical-Induced Damage in Rabbit Kidneys after Simple Hypothermic Preservation and Autotransplantation*. Transplantation, 1986. 41: p. 161-5.

57. Sanderson, T., et al., *Molecular Mechanisms of Ischemia–Reperfusion Injury in Brain: Pivotal Role of the Mitochondrial Membrane Potential in Reactive Oxygen Species Generation*. Mol Neurobiol, 2013. 47: p. 9-23.

58. Errede, B., and M.D. Kamen, *Comparative Kinetic Studies of Cytochromes C in Reactions with Mitochondrial Cytochrome C Oxidase and Reductase.* Biochemistry, 1978. 17: p. 1015-27.

59. Godoy, L.C., et al., *Disruption of the M80-Fe Ligation Stimulates the Translocation of Cytochrome C to the Cytoplasm and Nucleus in Nonapoptotic Cells.* Proc Natl Acad Sci U S A, 2009. 106: p. 2653-8.

60. Musatov, A., and N.C. Robinson, *Susceptibility of Mitochondrial Electron-Transport Complexes to Oxidative Damage. Focus on Cytochrome C Oxidase.* Free Radic Res, 2012. 46: p. 1313-26.

61. Srinivasan, S., and N.G. Avadhani, *Cytochrome C Oxidase Dysfunction in Oxidative Stress.* Free Radic Biol Med, 2012. 53: p. 1252-63.

62. Samhan-Arias, A.K., Y.Y. Tyurina, and V.E. Kagan, *Lipid Antioxidants: Free Radical Scavenging Versus Regulation of Enzymatic Lipid Peroxidation.* J Clin Biochem Nutr, 2011. 48: p. 91-5.

GENERAL DISCUSSION

Adipose tissue derived stromal cells-based therapy for diabetic retinopathy to state both retinal capillary support and inflammatory regulation

CHAPTER 06

Diabetes mellitus (DM) is one of the world's fastest growing diseases. In fact, it is a heterogeneous set of metabolic disorders that all feature hyperglycemia [1]. Diabetic retinopathy (DR) influences one third of individuals who experience the effects of DM [2]. In the early phases of DR, hyperglycemia causes pericyte demise and thickening of the basement membrane, which compromises the integrity of retinal vessels and the increases the permeability of the blood-retinal barrier [3]. The subsequent collapse of retinal vessels is unequivocally connected with the consequence of ischemia and results in the release of angiogenic factors in the affected area. This advances the DR to the proliferative phase (PDR) where adverse and aberrant neovascularization occurs. Accumulation of liquid follows due to fragile dysfunctional vessels inside the retina, named macular edema, and strongly contributes the loss of vision. PDR is the main source of visual impairment among adults in the working age [4-6]. The retinal vessels are excessively covered with pericytes. As a matter of fact, the EC to pericyte ratio is the highest in the body i.e. 1: 1. This also means that loss of pericytes not only is an early pathological marker for developing DR but also that the ramifications are expectedly serious and warrant the development of pericyte replacement therapy to treat DR [7]. A great part of the work from our research lab and others brings forward that the retinal restorative angiovasculogenesis process should include pericyte replacement to stabilize and normalize the function of the retinal vasculature [8-11].

This approach is intended to target early phases of DR to improve vascular regeneration, diminish inflammatory stimulations, adjust hypoxia and ischemia and anticipate advancement to the late phases of DR. Adipose tissue-derived stromal cells (ASC) belong to mesenchymal stem/stromal cells which are characterized by (a) their

plastic adherent capacity; (b) their expression panel of certain cell surface markers (i.e. +CD73, +CD90, +CD105, -CD34, -CD45); and (c) their ability to differentiate into osteocytes, chondrocytes and adipocytes [12, 13]. These parameters make ASC an alluring choice for cell therapy. In co-culture with endothelial cells (EC), ASC prompt vascular network formation. The particular confinement of ASC on the abluminal side of EC enhances the stability of vascular network [8, 10, 11, 14]. Cultured ASC have phenotypic and functional similarities with perivascular pericytes and either share the similar surface markers including NG2, CD140a, and CD140b (PDGFR α and β) [14, 15]. Injected ASC into diabetic rat model procured pericytic features. ASC incorporated with the retinal microvasculature and could protect retinal proliferative angiogenesis [10, 11]. Therefore, ASC-derived pericyte replacement would be an effective development in treatment of DR. Type 2 diabetes is clinically portrayed by hyperglycemia (HG) combined by relative insulin inadequacy [16].

Although, diabetic retinal pericytes experience hyperglycemic condition and oxidative stress-induced apoptosis, ASC-derived pericytes onto the diabetic retinal vasculature remains unclear. **In chapter 2**, we showed the impact of HG on ASC in vitro. HG stimulates generation of mitochondrial reactive oxygen species (ROS), which significantly contributes to the pathogenesis of vascular complications of diabetes [17]. HG has impact on retinal EC and pericytes, instigated mitochondrial fragmentation which decreased mitochondrial function [18, 19].

HG actuate oxidative stress damage in the inner membrane of mitochondria and causes the disability of mitochondria, which prompts imbalance in the electron transport chain and therefore

overproduction of ROS [20]. We indicated ASC had extensive production of intracellular ROS following 7 days culture in HG. HG actuates mitochondrial dysfunction in ASC, as shown by a diminished mitochondrial membrane potential in HG and adverse morphological structural changes of the mitochondrial network. The observed ROS overproduction augmented apoptosis and necrosis in ASC. We demonstrated that ASC somehow resist this HG-induced mitochondrial dysfunction because the proliferation of ASC after exposure to HG was not influenced. We demonstrated that mitochondrial ASC, in normoglycemia (NG), harbor an extensive and extensively branched mitochondrial tubular network. This network is essential for mitochondrial function and regulated by fusion and fission events [21].

Interruption of mitochondrial fusion and fission causes fragmentation of the mitochondrial network, which brings about shorter and rounder mitochondria [22]. Our outcomes indicate that HG-induced mitochondrial fragmentation is associated with the formation of ROS in HG-challenged ASC. The fact that mitochondria under HG show the same basal respiration as under NG, demonstrates that ASC manage the HG condition. However, we showed that HG caused a reduction of the maximal oxygen consumption rate (OCR) and diminished the basal level of extracellular acidification. The latter suggest that HG dampens the glycolysis rate in ASC. Remarkably, HG caused a huge decrease in glucose take-up in ASC.

We propose that ASC under HG compensate the hyperglycemic condition by changing the metabolic limit, as shown by reduced glucose uptake, diminished OCR and glycolysis. In spite of these bioenergetics changes in ASC under HG, we showed that ASCs' ability to support vascular network formation by endothelial cells is

maintained. The ROS-incited mitochondrial fragmentation and apoptosis only partially influenced the pericytic capacity of ASC. This data may depict both their capacities and restrictions regarding ASCs' potential to treat the vasculopathy component of DR. In spite of the fact that mitochondria vary in structure and capacity in different cell types, they share some basic features.

Mitochondria are closely confined organelles that comprise a complex system of two membranes that are required for the majority of energy generation, i.e. generation of ATP and GRP by the oxidative phosphorylation [23]. Mitochondria are also the major source of cellular ROS and likewise are relevant targets for the negative impacts of these oxidants. Prolonged oxidative damage to the mitochondrial inner membrane imbalances the electron transport chain. This could bring about overproduction of ROS and disturb mitochondrial membrane proteins additionally [24]. When cytochrome-c is discharged from mitochondria, it serves to activate apoptosis via the intracellular, intrinsic, route. Cytochrome-c binds to caspase-9, which activates caspase-3 which further upregulates and executes apoptosis. Mitochondrial oxidative stress increased in ASC under HG [25].

The retina is highly demanding with regard to energy production and consumption. Therefore chronic exposure to oxidative stress renders the retina one of the body's most sensitive organs to mitochondrial dysfunction [26]. Mitochondrial inability to accomplish energy pathways may cause more severe complications in diabetes [27]. Identifying mitochondrial dysfunction is essential for the advancement of novel stem cell therapies. In regard to this point, **in chapter 3**, we presented the assessment of energy metabolic changes in ASC in details. Our reproducible methods included:

isolation of ASC from subcutaneous fat tissue, ASC culturing, measuring of apoptosis and necrosis in ASC, detecting intracellular and mitochondrial ROS, monitoring mitochondrial health via mitochondrial morphology and measuring the mitochondrial membrane potential, evaluating ASC bioenergetics profiling using Extracellular Flux Analyzer (Seahorse Bioscience) and detecting the glucose uptake from ASC as a detector of glycolysis.

Our methods provided extensive information to evaluate bioenergetical changes in ASC cultured under HG condition and more upcoming in vitro studies. Above and beyond hyperglycemia, there is proof that low level inflammation triggers the vascular complexities of DR. Undoubtedly, chronic inflammation is a trademark seen at DR which is detectable by elevated TNF-α, IL-1β and activated leukocytes [28]. Immunosuppressive capability is imparted to ASC, which appear to be extremely efficient in various studies [29-32]. Mesenchymal stem/stromal cells (MSC) demonstrate their immunomodulatory capacities by direct cell-cell contact and indirect paracrine effect via indoleamine-2,3-dioxygenase (IDO), nitric oxide (NO), prostaglandin-E2 (PGE-2), IL-10 to mention a few [33-35].

In chapter 4, we showed the dual efficacy of ASC in promoting the vascular network formation in contact with EC in vivo and its paracrine immunomodulatory effect on retinal endothelial cells under HG-induced inflammatory status. Ultrastructure analysis of our ASC-EC coculture underlined the juxtacrine i.e. pericytic role of ASC in the maintenance of the vascular architecture. One of the working definitions of pericytes is that these are 'matrix-embedded' cells in contact with endothelial cells. This is corroborated by our investigations which show that ASC deposited extracellular matrix components that separated the ASC from the EC.

To confirm our in vitro results, ASC injected intravitreally into retinopathy of prematurity (ROP) mouse models. The injected ASC are found on angiogenic sprouts and in pericyte-specific extra-luminal positions in the immature vascular tree. Attachment of ASC to EC resulted in increased retinal neovascularization, suggesting that ASC also in vivo increased the stability of the vessels. Reduced expression of pericyte-derived angiopoietin-1, upregulation of angiopoietin-2 alongside with increased VEGFA levels prompts vessel destabilization and initiates pathological angiogenesis in the eye [36]. The mRNA analysis of ROP retinas which were injected with ASC revealed that the total mRNA levels of *Angpt1* and *Fgf2* were increased, while levels of *Angpt2* and *Vegfa* were reduced. In this study, ASC injection into the ROP promotes expression of inflammatory genes like *Tnf, Cxcl15* and *Ccl2* in retina which was expected due to the applying of early-passage of ASC. ASC in early passages express MHCII, CD80, and CD86 which may stimulate APCs and trigger the immune reaction. However, by passaging the ASC, these APC-related markers are lost [37, 38].

MSC should be activated by inflammatory mediators (i.e. cytokines) to apply their immunomodulatory properties [39]. In this way, the inflammatory status at the time of ASC injection is important to get the best clinical advantages. In general, HG is considered as a pro-inflammatory environment which causes upregulation of pro-inflammatory cytokines in retinal cells [40]. Comparison between ASC in acute (seven days) and chronic (several passages) hyperglycemic condition showed high upregulation of *TNF, IL1A, IL6, CXCL8, CCL2, PTGS2, CXCL12, MMP1, IDO1, VEGFA, ANGPT1, SLC2A1, RGS5* genes only after acute exposure to HG. In contrast, chronic exposure to HG led to decreased levels, even lower than under chronic NG mainenance, of secreted PGE2. The action of PGE2 is

paradoxal: known as immunosuppressor of macrophage and T cell function, it is an important pro-inflammatory activator of EC and fibroblasts. The secretion of the chemoattractant CCL2 is also normalized under chronic hyperglycemic maintenance of ASC. Therefore, we suggest that for vascularization therapy, the preculturing of ASC under hyperglycemia should be chronic i.e for more than 3 passages, before injecting into hyperglycemic environment. ASC conditioned medium (ASC-Cme) produced under standardized and reproducible conditions could be an alternative to transplantation of (autologous) ASC in cell therapy. We showed that ASC-Cme rescues bovine retinal endothelial cells (BREC) from hyperglycemia-induced apoptosis and inflammatory activation. This impact on BREC was evoked by the ROS-inhibiting ability of ASC-Cme as it could decrease the hyperglycemia-induced ROS in culture.

The antioxidant capacity of ASC-Cme correlated to the reduced NF-κB activation in the BREC. The BREC under HG activate NF-κB pathway followed by pro-inflammatory genes upregulation. ASC-Cme in HG-treated BREC suppressed main pro-inflammatory pathways like COX2/PGE2 and *VEGFA* as a proangiogenic gene.

We show that adhesion of adherent THP-1 cells to HG-activated BREC was suppressed by ASC-Cme and coincided with the downregulation of related genes as *VCAM-1, ICAM-1* and *SELE*. We suggest that inhibiting ROS by ASC-Cme can decrease the expression of upregulated pro-inflammatory genes besides their production.

Our findings show a strong therapeutic potential of ASC in DR. Presently, all the treatment strategies which are based on temporary or permanently cell replacement called cell therapy. Replaced cells may use as immunomodulatory mediator or as a new functional regenerated cells to substitute the damaged cells [41].

The field of cell therapy is quickly developing, thusthere are numerous challenges that should be tackled before cell therapy is broadly embraced. Whereas a significant part of the studies focuses on how cells should be adequately isolated, expanded and transplanted, only minor consideration has been given to how these cells can be well-maintained and transported to their clinical destination. Hypothermic storing of cells in their own culture medium proposes an interesting option to skip the difficulties of liquid nitrogen cryopreservation or commercial preservation methods. Anyhow, post-thawing cell death or during the rewarming period is likely to occur through the overproduction of ROS. **In chapter 5,** We tested the efficacy of a new pharmacologic compound, (6-hydroxyl-2,5,7,8-tetramethylchroman-2-yl)(4-(2-hydroxyethyl)piperazin-1-yl) methanone (SUL-109), that shields ASC during cell preservation from hypothermic cell death without influencing their multi-potency capacity.

We showed that the protective effect of SUL-109 is through maintenance of the mitochondrial membrane potential and promoting the activation of mitochondrial complexes I and IV, consequently sustaining ATP production and preventing the overproduction of ROS under hypothermic conditions. In this way, SUL-109 inhibited hypothermia-induced apoptosis and necrosis. This impact was retained during the rewarming phase as well. We showed proliferation of ASC under SUL-109 treatment was comparable to ASC that had not been challenged with hypothermia. Cryopreservation and hypothermia may constrain the multi-potency capacity of stem cells and can actuate the stem cells to differentiate [42].

SUL-109-treated ASC maintained their differentiation capacity into adipocytes, osteocytes and smooth muscle cells. We proposed that 6-chromanols derivate SUL-109 may form quinones, the electron acceptor for mitochondrial complexes I and II [43, 44] so, it is possible that this mechanism activates mitochondrial complex I following hypothermia. Cytochrome-c enables oxidative phosphorylation and consequently ATP production via transporting electrons among mitochondrial complexes III and IV [45]. We assume that SUL-109 decreases cytochrome-c-mediated lipid peroxidation and can preserve the conformational state of cytochrome-c, which is remained accessible for oxidative phosphorylation and ATP production. The protective impact of SUL-109 through its antioxidant capacity and mitochondrial function and integrity maintenance, effectively eliminating the cell death and dysfunction challenges of ASC during hypothermic preservation processes.

Nonetheless, this is an exciting area of future studies that would speak to a genuine advance change in how ASC can be delivered.

References

1. Alam, U., et al., *General aspects of diabetes mellitus.* Handb Clin Neurol, 2014. 126: p. 211-22.

2. Kempen, J.H., et al., *The prevalence of diabetic retinopathy among adults in the United States.* Arch Ophthalmol, 2004. 122(4): p. 552-63.

3. Frank, R.N., *Diabetic retinopathy*. N Engl J Med, 2004. 350(1): p. 48-58.

4. Klein, R., et al., *The Wisconsin epidemiologic study of diabetic retinopathy. III. Prevalence and risk of diabetic retinopathy when age at diagnosis is 30 or more years.* Arch Ophthalmol, 1984. 102(4): p. 527-32.

5. Moss, S.E., R. Klein, and B.E. Klein, *Ten-year incidence of visual loss in a diabetic population*. Ophthalmology, 1994. 101(6): p. 1061-70.

6. Thylefors, B., et al., *Global data on blindness*. Bull World Health Organ, 1995. 73(1): p. 115-21.

7. Armulik, A., A. Abramsson, and C. Betsholtz, *Endothelial/pericyte interactions.* Circ Res, 2005. 97(6): p. 512-23.

8. Hajmousa, G., et al., *Hyperglycemia Induces Bioenergetic Changes in Adipose-Derived Stromal Cells While Their Pericytic Function Is Retained*. Stem Cells Dev, 2016. 25(19): p. 1444-53.

9. Loffredo, F. and R.T. Lee, *Therapeutic vasculogenesis: it takes two.* Circ Res, 2008. 103(2): p. 128-30.

10. Mendel, T.A., et al., *Pericytes derived from adipose-derived stem cells protect against retinal vasculopathy*. PLoS One, 2013. 8(5): p. e65691.

11. Rajashekhar, G., et al., *Regenerative therapeutic potential of adipose stromal cells in early stage diabetic retinopathy*. PLoS One, 2014. 9(1): p. e84671.

12. Bunnell, B.A., et al., *Adipose-derived stem cells: isolation, expansion and differentiation*. Methods, 2008. 45(2): p. 115-20.

13. Dominici, M., et al., *Minimal criteria for defining multipotent mesenchymal stromal cells. The International Society for Cellular Therapy position statement*. Cytotherapy, 2006. 8(4): p. 315-7.

14. Traktuev, D.O., et al., *A population of multipotent CD34-positive adipose stromal cells share pericyte and mesenchymal surface markers, reside in a periendothelial location, and stabilize endothelial networks*. Circ Res, 2008. 102(1): p. 77-85.

15. Merfeld-Clauss, S., et al., *Adipose tissue progenitor cells directly interact with endothelial cells to induce vascular network formation*. Tissue Eng Part A, 2010. 16(9): p. 2953-66.

16. Mathis, D., L. Vence, and C. Benoist, *beta-Cell death during progression to diabetes*. Nature, 2001. 414(6865): p. 792-8.

17. Kroemer, G., *Mitochondrial implication in apoptosis. Towards an endosymbiont hypothesis of apoptosis evolution*. Cell Death Differ, 1997. 4(6): p. 443-56.

18. Trudeau, K., et al., *High glucose disrupts mitochondrial morphology in retinal endothelial cells: implications for diabetic retinopathy*. Am J Pathol, 2010. 177(1): p. 447-55.

19. Trudeau, K., A.J. Molina, and S. Roy, *High glucose induces mitochondrial morphology and metabolic changes in retinal pericytes*. Invest Ophthalmol Vis Sci, 2011. 52(12): p. 8657-64.

20. Li, S.Y., Z.J. Fu, and A.C. Lo, *Hypoxia-induced oxidative stress in ischemic retinopathy*. Oxid Med Cell Longev, 2012. 2012: p. 426769.

21. Karbowski, M. and R.J. Youle, *Dynamics of mitochondrial morphology in healthy cells and during apoptosis.* Cell Death and Differentiation, 2003. 10(8): p. 870-880.

22. Scorrano, L., *Multiple functions of mitochondria-shaping proteins.* Novartis Found Symp, 2007. 287: p. 47-55; discussion 55-9.

23. Scheffler, I.E., *A century of mitochondrial research: achievements and perspectives*. Mitochondrion, 2001. 1(1): p. 3-31.

24. Kowluru, R.A., *Diabetic retinopathy: mitochondrial dysfunction and retinal capillary cell death.* Antioxid Redox Signal, 2005. 7(11-12): p. 1581-87.

25. Kristal, B.S., et al., *Oxidant-mediated repression of mitochondrial transcription in diabetic rats.* Free Radical Biology and Medicine, 1997. 22(5): p. 813-822.

26. D'Amico, A. and E. *Bertini, Metabolic neuropathies and myopathies*. Handb Clin Neurol, 2013. 113: p. 1437-55.

27. Patti, M.E. and S. *Corvera, The role of mitochondria in the pathogenesis of type 2 diabetes*. Endocr Rev, 2010. 31(3): p. 364-95.

28. Lutty, G.A., *Effects of diabetes on the eye*. Invest Ophthalmol Vis Sci, 2013. 54(14): p. ORSF81-7.

29. Constantin, G., et al., *Adipose-derived mesenchymal stem cells ameliorate chronic experimental autoimmune encephalomyelitis*. Stem Cells, 2009. 27(10): p. 2624-35.

30. Gonzalez, M.A., et al., *Treatment of experimental arthritis by inducing immune tolerance with human adipose-derived mesenchymal stem cells.* Arthritis Rheum, 2009. 60(4): p. 1006-19.

31. Puissant, B., et al., *Immunomodulatory effect of human adipose tissue-derived adult stem cells: comparison with bone marrow mesenchymal stem cells*. Br J Haematol, 2005. 129(1): p. 118-29.

32. Yanez, R., et al., *Adipose tissue-derived mesenchymal stem cells have in vivo immunosuppressive properties applicable for the control of the graft-versus-host disease.* Stem Cells, 2006. 24(11): p. 2582-91.

33. Franquesa, M., M.J. Hoogduijn, and C.C. Baan, *The impact of mesenchymal stem cell therapy in transplant rejection and tolerance*. Curr Opin Organ Transplant, 2012. 17(4): p. 355-61.

34. Pourgholaminejad, A., et al., *The effect of pro-inflammatory cytokines on immunophenotype, differentiation capacity and immunomodulatory functions of human mesenchymal stem cells*. Cytokine, 2016. 85: p. 51-60.

35. Ringden, O., et al., *Mesenchymal stem cells for treatment of therapy-resistant graft-versus-host disease*. Transplantation, 2006. 81(10): p. 1390-7.

36. Cai, J., et al., *The angiopoietin/Tie-2 system regulates pericyte survival and recruitment in diabetic retinopathy*. Invest Ophthalmol Vis Sci, 2008. 49(5): p. 2163-71.

37. Lindroos, B., R. Suuronen, and S. Miettinen, *The potential of adipose stem cells in regenerative medicine*. Stem Cell Rev, 2011. 7(2): p. 269-91.

38. McIntosh, K., et al., *The immunogenicity of human adipose-derived cells: temporal changes in vitro*. Stem Cells, 2006. 24(5): p. 1246-53.

39. Krampera, M., *Mesenchymal stromal cell 'licensing': a multistep process.* Leukemia, 2011. 25(9): p. 1408-14.

40. Tang, J. and T.S. Kern, *Inflammation in diabetic retinopathy*. Prog Retin Eye Res, 2011. 30(5): p. 343-58.

41. Mason, C., et al., *Cell therapy industry: billion dollar global business with unlimited potential.* Regen Med, 2011. 6(3): p. 265-72.

42. Pogozhykh, D., et al., *Influence of Factors of Cryopreservation and Hypothermic Storage on Survival and Functional Parameters of Multipotent Stromal Cells of Placental Origin.* PLoS One, 2015. 10(10): p. e0139834.

43. Erb, M., et al., *Features of Idebenone and Related Short-Chain Quinones that Rescue ATP Levels under Conditions of Impaired Mitochondrial Complex I*. Plos One, 2012. 7(4).

44. Karuppagounder, S.S., et al., *Quercetin up-Regulates Mitochondrial Complex-I Activity to Protect against Programmed Cell Death in Rotenone Model of Parkinson's Disease in Rats*. Neuroscience, 2013. 236: p. 136-148.

45. Errede, B. and M.D. Kamen, *Comparative kinetic studies of cytochromes c in reactions with mitochondrial cytochrome c oxidase and reductase*. Biochemistry, 1978. 17(6): p. 1015-27.

Therapeutic actions of ASC in the normalization of hyperglycemically challenged retinal endothelial cells: a roadmap to the treatment of diabetic retinopathy.
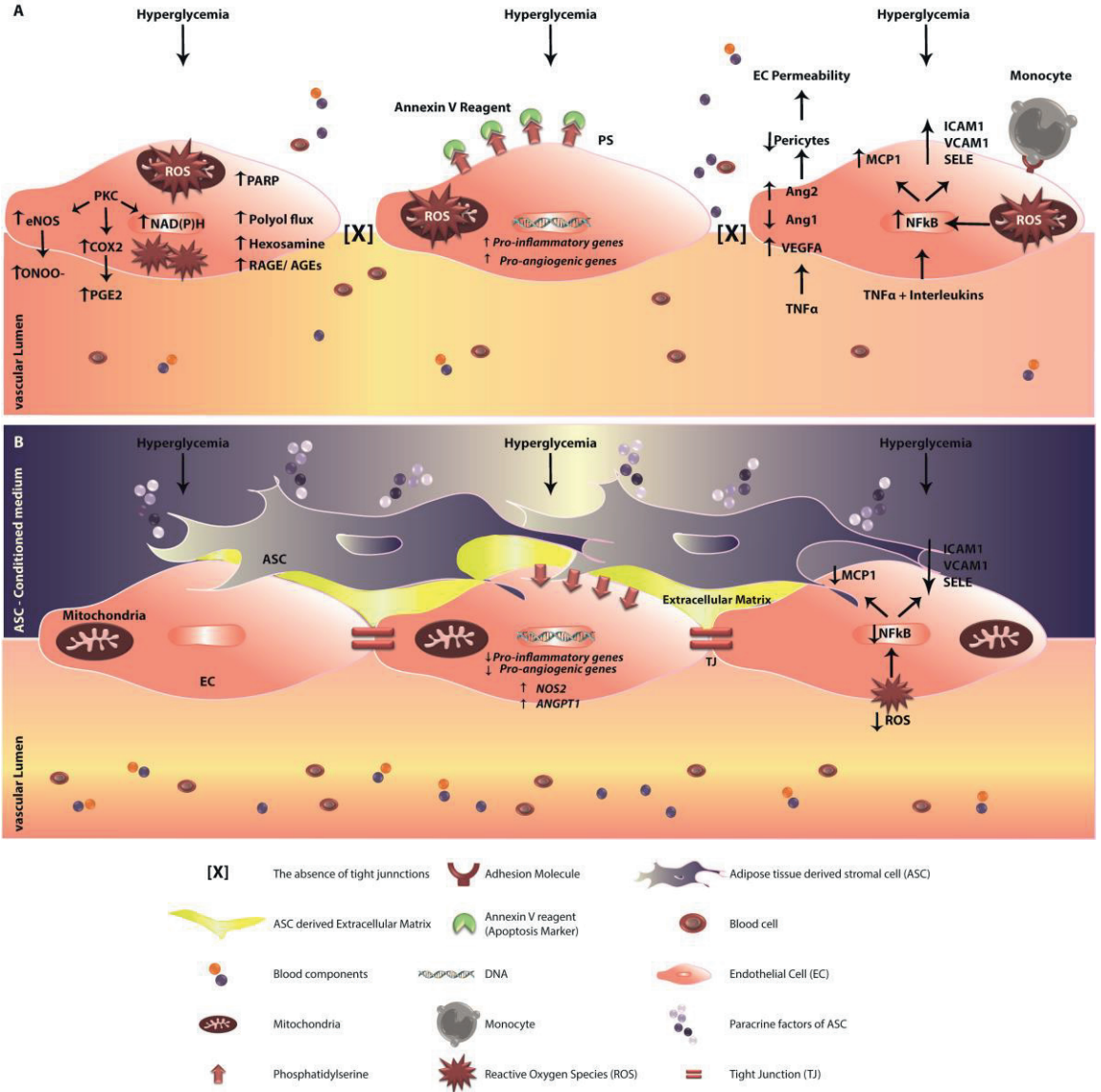
SUMMARY

CHAPTER 07

Towards adipose tissue derived stromal cells-based therapy for diabetic retinopathy

In this thesis we investigated the impact of hyperglycemia as a model for diabetes on adipose tissue-derived stromal cells (ASC) as a prelude to their use in future therapeutic treatment of diabetic retinopathy (DR). DR is a multifactorial complexity characterized by incessant and fluctuating hyperglycemia, mild chronic inflammation and vascular as well as neuronal dysfunction. Hyperglycemia-initiated overproduction of reactive oxygen species (ROS) causes mitochondrial dysfunction in retinal vascular cells and leads to fragile and defective vessels. Hypoxia causes non-perfused vessels and brings about the proliferative phase of DR that is associated with increased secretion of proangiogenic factors and propelling the pathological neovascularization in parallel with the chronic inflammation in diabetic retina. Considering the absence of effective treatments for DR, cell-based therapy may offer novel strategies by supplanting of the lost cells to forestall advanced DR and adjust the inflammatory state by means of their anti-inflammatory and anti-angiogenic paracrine factors as well as juxtacrine interactions between stem cells and dysfunctional vessels.

We showed that ASC may indeed impact progression of DR in multiple ways. As indicated by their phenotypic and functional similarities with perivascular pericytes, ASC offer suitable swap for the pericyte lost in the early phases of DR. Ultrastructure analysis of co-cultured ASC-endothelial cells (EC) featured the juxtacrine i.e. pericytic role of ASC in the maintenance of the vascular architecture

combined by deposition of extracellular matrix components that separated the ASC from the EC. ASC-derived pericytes under hyperglycemic condition still support new formed vascular networks by endothelial cells in culture. The ROS-incited mitochondrial dysfunction and hyperglycemia-induced apoptosis only partially influenced the pericytic ability of ASC. Despite of the diminished level of maximal oxygen consumption rate (OCR) and glycolysis, ASC under HG showed the same basal respiration as under NG which proves that ASC resist the HG condition by changing the metabolic limit deprived of altering the proliferation rate. Injected ASC into retinopathy of prematurity (ROP) mouse models are found in pericytic positions on angiogenic new formed vessels. ASC administration upregulated the mRNA level of *Angpt1* and *Fgf2* and reduced the expression of *Angpt2* and *Vegfa* in ROP retinas. Preculturing of ASC under hyperglycemia should be 'chronic', before injecting into hyperglycemic environment. Comparison between ASC in acute (seven days) and chronic (several passages) hyperglycemic condition showed high upregulation of pro-inflammatory and pro-angiogenic genes only after acute exposure to HG. Interestingly, chronic HG diminished secretion of PGE2 and the chemoattractant CCL2 in ASC.

ASC-conditioned medium (ASC-Cme) delivered from ASC cultured in chronically HG protected bovine retinal endothelial cells (BREC) from hyperglycemia-induced apoptosis and inflammatory activation. This effect on BREC was evoked by the ROS-neutralizing capacity of ASC-Cme in culture. The antioxidant capacity of ASC-Cme was associated with a reduced NF-κB activation in the BREC. We demonstrated that inhibition of ROS by ASC-Cme can downmodulate upregulated pro-inflammatory genes. ASC-Cme in HG-treated BREC suppressed principle inflammatory pathways like COX2/PGE2 and prevented the

adhesion of adherent THP-1 cells to HG-activated BREC. Our results demonstrate a solid restorative capability of ASC in several processes associated with DR.

Towards using the ASC for treatment of DR, we present a new hypothermic storing technique of cells in their own culture medium to well-maintain and transport the prepared cells to their clinical destination. The new pharmacologic compound, (6-hydroxyl-2,5,7,8-tetramethylchroman-2-yl)(4-(2-hydroxyethyl)piperazin-1-yl) methanone (SUL-109) shields ASC during cell preservation from hypothermic cell death without influencing their multi-potency capacity and proliferation. We showed that the protective effect of SUL-109 is through maintenance of the mitochondrial membrane potential and promoting the activation of mitochondrial complexes I and IV, consequently sustaining ATP production and preventing the overproduction of ROS under hypothermic conditions. In this way, SUL-109 inhibited hypothermia-induced apoptosis and necrosis in ASC. This impact was retained during the rewarming phase as well. Our pre-clinical study endorses the medical translational expansion of adipose tissue derived stromal cells-based therapy for diabetic retinopathy to state both retinal capillary support and inflammatory regulation.

Op weg naar het gebruik van de uit vetweefsel afkomstige stromale cellenals voor therapie van diabetische retinopathie

In dit proefschrift hebben we de impact van hyperglycemie op van vetweefsel afgeleide stromale cellen (ASC) onderzocht als een model voor diabetes en hun gebruik in toekomstige therapeutische behandelingen van diabetische retinopathie (DR). DR is een multifactoriële complexe ziekte die wordt gekenmerkt door onophoudelijke en fluctuerende hyperglycemie, milde chronische ontsteking en vasculaire als mede neuronale disfunctie. Hyperglycemie-geïnitieerde overproductie van reactieve zuurstofverbindingen (ROS) veroorzaakt mitochondriale disfunctie in retinale vasculaire cellen en leidt tot fragiele en defecte bloedvaten. Hypoxie veroorzaakt geblokkeerde vaten en brengt de proliferatieve fase van DR tot stand die geassocieerd is met verhoogde uitscheiding van pro-angiogene factoren die de pathologische neovascularisatie voortduwt en is parallel aan de chronische ontsteking in de diabetische retina. Gezien de afwezigheid van effectieve behandelingen voor DR, kan een cel gebaseerde therapie nieuwe strategieën bieden door de verloren cellen te vervangen om gevorderde DR te voorkomen en de inflammatoire toestand te verminderen. Stamcellen hebben ontstekingsremmende en anti-angiogene paracriene factoren en juxtacrine interacties tussen stamcellen en de disfunctionele vaten.

We hebben aangetoond dat ASC de progressie van DR inderdaad op meerdere manieren kunnen beïnvloeden. Zoals aangegeven, bieden ASC een mogelijkheid verloren perivasculaire pericyten te vervangen

in de vroege fasen van DR door hun fenotypische en functionele overeenkomsten. Ultrastructuuranalyse van ASC in kweek samen met endotheelcellen (EC) bevestigde de juxtacrine, dat wil zeggen dat de pericytische rol van ASC in het onderhoud van de vasculaire architectuur gecombineerd door afzetting van extracellulaire matrixcomponenten die het ASC van de EC scheiden. ASC-afgeleide pericyten onder hyperglycemische toestand ondersteunen nog steeds nieuw gevormde vasculaire netwerken door endotheelcellen in kweek. De ROS-geïnduceerde mitochondriale disfunctie en hyperglycemie-geïnduceerde apoptose beïnvloedden slechts gedeeltelijk het pericytische vermogen van de ASC. Ondanks het verminderde niveau van maximale zuurstofconsumptie (OCR) en glycolyse, vertoonden ASC onder HG dezelfde basale ademhaling als onder NG. Dit bewijst dat ASC de HG-toestand weerstaan door de metabole limiet aan te passen zonder de proliferatiesnelheid te veranderen. Geïnjecteerde ASC in retinopathie muismodellen (ROP) werden teruggevonden in pericytische posities op angiogene nieuw gevormde bloedvaten. ASC-toediening reguleerde het mRNA-niveau van Angpt 1 en Fgf2 op en verminderde de expressie van Angpt2 en Vegfa in ROP-retina's. ASC moeten onder hyperglycemische condities worden geweekt voordat ze in een hyperglycemische omgeving worden geïnjecteerd. Vergelijking tussen ASC in acute (zeven dagen) en chronische (verschillende passages) hyperglycemische toestand toonde een verhoogde expressie van pro-inflammatoire en pro-angiogene genen na acute blootstelling aan HG. Interessant is dat chronische HG de secretie van PGE2 en de chemoattractant CCL2 in ASC verminderde.

ASC-geconditioneerd medium (ASC-Cme) afgeleid van ASC gekweekt in chronische HG beschermde endotheelcellen van runderen (BREC) van hyperglycemie-geïnduceerde apoptose en inflammatoire activering. Dit effect op BREC werd verklaard door de ROS-

neutraliserende capaciteit van het ASC-Cme in kweek. Het antioxiderende vermogen van ASC-Cme was geassocieerd met een verminderde NF-KB-activering in de BREC. We hebben aangetoond dat remming van ROS door ASC-Cme verhoogde expressie van pro-inflammatoire genen kan verminderen. In met HG behandelde BREC onderdrukte het ASC-Cme principiële inflammatoire routes zoals COX2 / PGE2 en voorkwam het de adhesie van aanhangende THP-1-cellen aan HG-geactiveerde BREC. Onze resultaten tonen een solide herstellend vermogen van ASC in verschillende processen geassocieerd met DR.

Op weg naar het gebruik van de ASC voor de behandeling van DR presenteren we een nieuwe hypotherme opslagtechniek van cellen in hun eigen kweekmedium om de geprepareerde cellen goed te onderhouden en naar hun klinische bestemming te transporteren. De nieuwe farmacologische verbinding (6-hydroxyl-2,5,7,8-tetramethylchroman-2-yl) (4- (2-hydroxyethyl) piperazin-1-yl) methanon (SUL-109) beschermt ASC tijdens cel behoud van hypo thermische celdood zonder hun vermogen tot multipotentie en proliferatie te beïnvloeden. We toonden aan dat het beschermende effect van SUL-109 verklaard kan worden door het behoud van het mitochondriale membraanpotentieel en het bevorderen van de activering van mitochondriale complexen I en IV, waardoor de ATP-productie wordt ondersteund en de overproductie van ROS onder hypotherme omstandigheden wordt voorkomen. Op deze manier remde SUL-109 hypothermie-geïnduceerde apoptose en necrose in ASC. Deze impact werd ook behouden tijdens de opwarmfase. Onze pre-klinische studie onderschrijft de medische translationele expansie van uit vetweefsel afkomstige stromale cellenals therapie voor diabetische retinopathie om zowel de retinale capillaire ondersteuning als de ontstekingsregulatie te vermelden.

Appendix

Word of Thanks

I would like to seize this opportunity to acknowledge those who have been of great assistance to me to finalize this thesis.

It is great pleasure to express my sincere gratitude to my supervisor Prof. Dr. M.C. Harmsen. Marco, it has been an honor to be your Ph.D. student. I appreciate all your contribution of time, ideas, and funding to let me do research and make my Ph.D. Experience productive and stimulating. You have created an amazing space to develop myself as a researcher in the best atmosphere in your country.

I express my deepest regards to my co-supervisor Dr. Guido Krenning. Guido, I have always been benefited from your professional character, fine ideas, and excellent critics. I am very thankful to you for the opportunities and all the support you have provided me to carry out my research work. You have been great help. Many thanks!

I would like to thank the Reading committee: Prof. J.L. Hillebrands, Prof. R.O. Schlingemann and Prof. M. Schmidt for taking their time, evaluating my dissertation. I truly appreciate it.

Words of thanks are due to Prof. Dr. Han Moshage. Thank you very much for the opportunity given me in the first step. I will never forget your role in my life.

Dear Linda and Azizam Ena, a bunch of thanks to you both to be my paranymphs.

I give my gratitude to all from graduate school (GUIDE). You have always been big favor in all administrative and financial issues.

I am grateful to the members of the CAVAREM group who have contributed immensely to my personal life and professional task at Groningen.

My sincere appreciation to colleagues and friends in the department of Medical Biology and University Medical Center of Groningen.

I give my gratitude to my colleagues from Andres Bello University in Santiago, Chile to have me in their lab kindly.

No words can express how grateful I am for my family. Thank you for all your love and encouragement. Maman Azaram va baba Majidam, merci.

I am grateful to all my friends and colleagues with whom I have shared wonderful moments and moral support for the completion of this long journey.

I did not mention the names on this page as your place is in my heart.

Ghazal

Curriculum Vitae

Ghazaleh Hajmousa (Tehran, 1983) graduated as a Doctor of Veterinary Medicine at the Veterinary University, Iran. She conducted her Ph.D. research at the University Medical Center of Groningen, under the supervision of Prof. M. C. Harmsen. Ghazaleh is currently working as a postdoctoral researcher in the Clinical genetics department in the AMC, Amsterdam, The Netherlands.

PUBLICATIONS

Hajmousa G, Elorza A, Nies V, Jansen E, Harmsen M. Hyperglycemia induces bioenergetic changes in adipose-derived stromal cells while their pericytic function is retained. Stem Cells Dev. 2016; 25(19):1444-53.

Hajmousa G, Vogelaar P, Brouwer LA, van der Graaf AC, Henning RH, Krenning G. The 6-chromanol derivate SUL-109 enables prolonged hypothermic storage of adipose tissue-derived stem cells. Biomaterials. 2017; 119:43-52.

Hajmousa G, Harmsen M. Assessment of Energy Metabolic Changes in Adipose tissue-Derived Stem Cells. Methods in MolecularBiology. 2017; 1553:55-65

Hajmousa G, Przybyt E, Pfister F, Paredes-Juarez G, Moganti K, Busch S, Kuipers J, Klaassen I, van Luyn M, Krenning G, Hammes HP, Harmsen MC. Human adipose tissue-derived stromal cells act as functional pericytes in

mice and suppress high-glucose-induced proinflammatory activation of bovine retinal endothelial cells. Diabetologia. 2018; 10.1007

van Dijk T, Rudnik-Schöneborn S, Senderek J, **Hajmousa G**, Mei H, Dusl M, Aronica E, Barth P, Baas F. Pontocerebellar hypoplasia with spinal muscular atrophy (PCH1): identification of SLC25A46 mutations in the original Dutch PCH1 family. Brain. 2017; 1;140(8):e46.

Nies VJM, Struik D, Wolfs MGM, Rensen SS, Szalowska E, Unmehopa UA, Fluiter K, van der Meer TP, **Hajmousa G**, Buurman WA, Greve JW, Rezaee F, Shiri-Sverdlov R, Vonk RJ, Swaab DF, Wolffenbuttel BHR, Jonker JW, van Vliet-Ostaptchouk JV. TUB gene expression in hypothalamus and adipose tissue and its association with obesity in humans. Int J Obes. 2017.

Tahaei LS, Eimani H, **Hajmusa G**, Fathi R, Rezazadeh Valojerdi M, Shahverdi A, Eftekhari-Yazdi P. Follicle Development of Xenotransplanted Sheep Ovarian Tissue into Male and Female Immunodeficient Rats. Int J Fertil Steril. 2015; 9(3):354-60.

Hajmousa G, Asghari Vosta M, Nemati A. *(2013).* The Basis of Laboratory Animal Science. ISBN: 978-600-92587-8-9.